

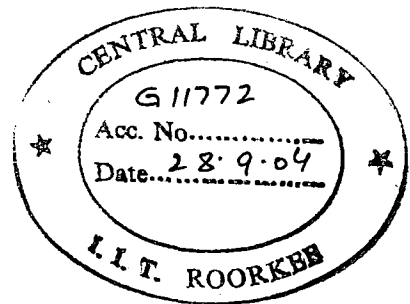
**STRESS AND DEFORMATION ANALYSIS
OF UNDERGROUND POWERHOUSE
CAVERN USING 2-D FEM:
A CASE STUDY**

A DISSERTATION

*Submitted in partial fulfillment of the
requirements for the award of the degree*
of
MASTER OF TECHNOLOGY
in
**WATER RESOURCES DEVELOPMENT
(CIVIL)**

By

TONNY SUAK



**WATER RESOURCES DEVELOPMENT TRAINING CENTRE
INDIAN INSTITUTE OF TECHNOLOGY ROORKEE
ROORKEE - 247 667 (INDIA)
JUNE, 2004**

A handwritten signature in black ink, appearing to be the initials "TS" or similar, located in the bottom left corner of the page.

CANDIDATE'S DECLARATION

I hereby certify that the work which is being presented in the dissertation entitled **STRESS AND DEFORMATION ANALYSIS OF UNDERGROUND POWERHOUSE CAVERN USING 2-D FEM: A CASE STUDY** in partial fulfillment of the requirement for the award of the Degree of Master of Technology in WRD (CIVIL) submitted in the **WATER RESOURCES DEVELOPMENT TRAINING CENTER (WRDTC)** of the **Indian Institute of Technology of Roorkee** is an authentic record of my own work carried out during a period from August, 2003 to June 2004 under the supervision of **Prof. Ram Pal Singh, Prof. BN Asthana, and Dr. N.K. Samadhiya.**

The matter presented in this dissertation has not been submitted by me for the award of any other degree.

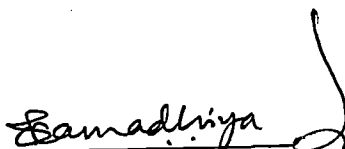


Date: June 08, 2004



(TONNY SUAK)

This is to certify that the above statement made by the candidate is correct to the best of our knowledge.

Date: 07/06/04

| | | |
|--|--|---|
|  Dr. N.K. Samadhiya Associate Professor Civil Eng. Dept. IIT Roorkee Roorkee, India |  Dr. B.N. Asthana Professor Design WRDTC IIT Roorkee Roorkee, India |  Dr. Ram Pal Singh Professor Design WRDTC IIT Roorkee Roorkee, India |
|--|--|---|

The M. Tech Viva-Voce examination of **Tonny Suak**, Trainee Officer, has been held on _____

ACKNOWLEDGEMENT

Thanks God for so kind to me.

I found dearth of words to express my tributes & deep sense of gratitude to **Dr. Ram Pal Singh**, Professor of WRDTC, **Dr. BN Asthana**,^{Visitor} Professor of WRDTC, and **Dr. NK Samadhiya**, Associates Professor of CED, for their meticulous guidance, keen interest, continuous encouragement and valuable suggestion throughout my work, and especially their help at time when I need to finish my work earlier.

I am very much grateful to **Dr. UC Chaube**, Head & Professor, WRDTC, for extending various facilities for this work.

I am thankful to my company **PT. Istaka Karya (Persero)** which give the opportunity to pursue higher study at WRDTC and full support during this two years study periods.

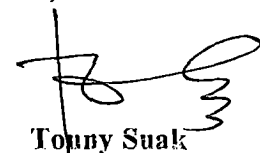
I am also thankful to **TCS-Colombo Plan** which gives scholarship so I am able to study here.

The author gratefully acknowledges **PT. PLN-Jasa Engineering – Indonesia** which provide the valuable data for this work.

Thanks also due to all faculty members, all my friends and colleagues for their help and support towards the improvement of this work and during my stay here, especially at the end of the study time when I needed most. The author sincerely thanks and appreciates to those who helped directly and indirectly for the work presented herein.

At last thanks to my mother and brother/sisters who support and pray always for me, also to my beloved wife, Ayu and son, Jordy who through the last six month being here, sacrificed all their comforts and pleasures, to support me and to be my inspiration.

Roorkee, June 2004



Tony Suak
47th Batch WRD Civil

ABSTRACTS

Design and analysis of underground structure such as cavern has always been regarded as one of the most difficult job for engineer. The main reason is that such problems as determination of the surrounding rock load, the force distribution and the deformation behaviour of the rock mass around cavern have not been thoroughly understood. Nevertheless, the engineers have been striving to get some empirical formulas or approximate results by way of observation, statistical analysis and numerical methods. In recent years, as the development in computer technology is advancing, numerical methods are increasingly becoming a popular engineering tool for design & analysis of underground structures and out of the available numerical methods, Finite Element Method has emerged as the most popular due to its flexibility in handling material inhomogeneity and anisotropy, complex boundary conditions and dynamic problems, together with moderate efficiency in dealing with complex constitutive models.

Review of literature reveals that a number of analytical studies have been carried out to investigate the behaviour (stress and deformation) of rock medium around cavern is identified. However, most analysis of underground cavern is elastic or employs Mohr-Coulomb or Hoek-Brown criteria for elastoplastic. Hence the present study aims at providing a better understanding of the behaviour of rock mass around cavern using finite element code ANSYS in elastic and elasto-plastic with Drucker-Prager criteria approach and also to address some issues regarding the capabilities of ANSYS in modeling rock mass.

In the present study, two types of rock mass domain (in elastic and elasto-plastic material approach) from 2-D nonsymmetrical vertical cross section of powerhouse cavern of Cirata (Indonesia) have been analyzed. The cavern is 35 m wide, 49.6 m high and 280 m long. It is located in dominantly laharic breccia. The rock mass properties from previous study have been used in the analysis. The rock support system i.e., shotcrete and rock bolts/prestressed anchor has also been modeled. The time-dependent behaviour, anisotropy of the material and the joints or other discontinuities those materially influence the behaviour of rock mass have not been

considered to simplify the problem. The same cavern previously studied by Reik (1986) & Kamemura (1986) using finite element analysis and LAPI ITB (1995) employ both finite element and distinct element through UDEC code. The results of the present study, in term of the deformation around periphery of cavern, then compare with the previous study and insitu measurement's data.

The results of present study reveals that elastoplastic model, both of Model I & Model II, always give magnitude of horizontal stress lesser than elastic model, but not always in term of vertical stress. All maximum and minimum, horizontal and vertical stress always occurs on lower part of cavern. The analysis recognize that minimum horizontal stress is very high which seem to be unreasonable (- 6.6 Mpa tensile stress), and probably exceeds the tensile strength of rock mass.

In term of rock deformation, the maximum horizontal deformation occur at lower part of cavern e.g. wall of the bench, whereas the maximum vertical deformation occur as expected, at roof of cavern.

From comparison with previous study generally there is similar evolution of deformation on nodal investigated with slightly anomalies, and elasto-plastic model in present study show the results comparing well with record measurement. Overall, from deformation field Model I gives results closer to the previous study and instrumented data.

On the basis of the above observation, it may be concluded that Model I and elasto-plastic material approach are better for represent the problem domain. Such a study is found to be very helpful for evaluating stress and deformation behaviour of the rock surrounding underground cavern in elastic model as well as elastoplastic model.

Regarding the capabilities of ANSYS, there is main difficulty, which arise when user wants to simulate the horizontal ground pressure for pre-existing stress state since no option in the code for that purpose. However, with the techniques such like applying the horizontal ground pressure at far-field boundary or at periphery of opening, the simulation can be done although not so representing the actual stress state of rock mass.

TABLE OF CONTENTS

| | Page No. |
|--|-----------|
| CANDIDATE'S DECLARATION | |
| ACKNOWLEDGEMENT | i |
| ABSTRACT | ii |
| TABLE OF CONTENTS | iii |
| LIST OF NOTATIONS & SYMBOLS | v |
| LIST OF FIGURES | vi |
| LIST OF TABLES | viii |
| | |
| I. INTRODUCTION | 1 |
| I.1 GENERAL | 1 |
| I.2 IDENTIFICATION OF THE PROBLEM AND OBJECTIVES OF STUDY | 1 |
| I.3 OUTLINE OF DISSERTATION | 2 |
| | |
| II. GENERAL CONSIDERATION FOR DESIGN & ANALYSIS OF CAVERN | 5 |
| II.1 METHODS FOR DESIGN & ANALYSIS OF UNDERGROUND STRUCTURES | 5 |
| II.1 i) Empirical methods | 5 |
| II.1 ii) Analytical and Computational methods | 6 |
| II.2 GENERAL CONSIDERATION FOR DESIGN AND ANALYSIS OF POWERHOUSE CAVERN IN ROCK | 7 |
| II.2 i) Geometry of Cavern | 9 |
| II.2 ii) Choice of Cavern Shapes | 9 |
| II.2 iii) Influence of Joints and Bedding Planes | 10 |
| II.2 iv) Sidewall and Roof Support System | 10 |
| II.2 v) Cavern Instrumentation | 11 |
| II.3 LITERATURES REVIEW | 13 |
| II.3 i) Numerical Modeling for analysis of Underground Cavern | 14 |
| II.3 ii) FEM Analysis for Underground Cavern | 16 |
| | |
| III. NUMERICAL MODELING FOR LARGE UNDERGROUND CAVERN | 19 |
| III.1 GEOMECHANICAL ANALYSIS FOR MODELING UNDERGROUND OPENING | 19 |
| III.1 i) Exact Solution using Elastic Stress-Strain Relationships | 19 |
| III.1 ii) Inelastic Stress-Strain Relationships | 21 |
| III.1 iii) Insitu Stresses State | 25 |
| III.2 NUMERICAL METHODS FOR UNDERGROUND CAVERN | 27 |
| III.2 i) Rock mass Modeling | 28 |
| III.2 ii) Modeling Rock Supports and Construction Sequences | 32 |
| III.2 ii (1) Rock Support | 32 |
| III.2 ii (2) Construction Sequences | 34 |
| III.2 ii (3) Civil Engineering Structures | 34 |

| | | |
|---|--|-----------|
| III.2 iii) | Finite Element Analysis for Rock mass | 35 |
| III.3 | ANSYS | 39 |
| III.3 i) | Building a Model | 40 |
| III.3 ii) | Apply Load and Obtain the Solution | 41 |
| III.3 iii) | Review the Results | 42 |
| IV. | CASE STUDY: CAVERN HPP CIRATA INDONESIA | 43 |
| IV.1 | SALIENT FEATURES OF CIRATA HYDROELECTRIC POWER PLANT (INDONESIA) | 43 |
| IV.2 | POWERHOUSE TYPE AND BASIC LAYOUT | 44 |
| IV.3 | SUPPORT ARRANGEMENT | 45 |
| IV.4 | EXCAVATION STAGES AND MONITORING PROGRAMME | 47 |
| V. | ANALYTICAL PROGRAM | 53 |
| V.1 | INTRODUCTION | 53 |
| V.2 | MODEL PREPARATION | 53 |
| V.2 i) | General | 53 |
| V.2 ii) | Finite Element Model | 54 |
| V.2 iii) | Model Calibration | 55 |
| VI. | RESULTS & DISCUSSION | 65 |
| VI.1 | INTRODUCTION | 65 |
| VI.2 | RESULTS | 65 |
| VI.2 i) | Stress Field Study | 65 |
| VI.2 i (1) | General | 85 |
| VI.2 i (2) | Stresses in X – Direction | 85 |
| VI.2 i (3) | Stresses in Y – Direction | 87 |
| VI.2 i (4) | Plastic Zone | 88 |
| VI.2 ii) | Deformation Field Study | 91 |
| VI.2 ii (1) | Comparison with previous studies and field measurement record | 112 |
| VII. | CONCLUSIONS | |
| VII.1 | SUMMARY OF PRESENT STUDY | 117 |
| VII.2 | CONCLUSIONS | 117 |
| VII.3 | SCOPE OF FURTHER STUDY | 120 |
| APPENDIX A: Derivation of some elastic and elasto plastic equation for underground opening | | |
| APPENDIX B: Derivation of basic structural matrices in finite element analysis | | |
| APPENDIX C: Stepwise procedure for calculation in ANSYS | | |
| APPENDIX D: Explanation of element types chosen | | |
| REFERENCES | | |

LIST OF NOTATIONS & SYMBOLS

ROCK MATERIAL

| | |
|----------------------|---|
| ϵ^e | = elastic strain |
| ϵ^p | = plastic strain |
| γ | = density of rock mass |
| ν | = Poisson's ratio of rock material |
| σ_1 | = major principal stress |
| σ_2, σ_3 | = minor principal stress |
| σ_v | = insitu overburden pressure or vertical ground stress |
| σ_h | = insitu horizontal ground pressure |
| σ_r | = radial stress around opening (in polar coordinate) |
| σ_θ | = tangential stress around opening (in polar coordinate) |
| $\tau_{r\theta}$ | = shear stress around opening (in polar coordinate) |
| C | = cohesion of the rock mass |
| ϕ | = angle of internal friction |
| E_m | = modulus of deformation |
| S_h | = horizontal applied stress |
| S_v | = vertical applied stress |
| a | = opening radius |
| r | = radial distance from center of opening |
| θ | = polar coordinate; horizontal axis represents $\theta=0^\circ$ |
| RMR | = Rock Mass Rating |

FINITE ELEMENT MATRIX

| | |
|----------------|------------------------------|
| [B] | = strain-displacement matrix |
| [D] | = elasticity matrix |
| [K] | = stiffness matrix |
| [N] | = shape function matrix |
| {u} | = nodal displacement vector |
| { ϵ } | = strain vector |
| { σ } | = stress vector |

ANSYS COMMANDS

| | |
|--------|--|
| UX | = magnitude of displacement in x-direction |
| UY | = magnitude of displacement in y-direction |
| SX | = magnitude of stress in x-direction |
| SY | = magnitude of stress in y-direction |
| EPPL X | = magnitude of plastic strain in x-direction |
| EPPL Y | = magnitude of plastic strain in y-direction |
| SEPL | = magnitude of equivalent stress plastic |

LIST OF FIGURES

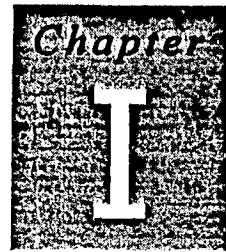
| Fig. | Description | Page No. |
|--------------|---|----------|
| II-1 | Important parameter for design of cavern | 8 |
| II-2 | Cross section shapes of cavern | 9 |
| II-3 | Typical support-arrangement of cavern (in HPP Cirata) | 11 |
| II-4 | Typical main monitoring cross-section for cavern (in Cirata HPP) | 13 |
| II-5 | Shaped studied (after Liu, 1988) | 14 |
| III-1 | Plotting σ_r and σ_θ in term of stress concentration for circular opening | 21 |
| III-2 | Stress-strain curve in plane for elasto-plastic material | 22 |
| III-3 | Some of Yield Criterion surface (from <i>DIANA</i> ® Manual) | 25 |
| III-4 | Insitu Stresses state in plane (after Hudson, 1989) | 26 |
| III-5 | Suitability of different rock mass modeling (after Jing, 2003) | 30 |
| III-6 | Example of Hybrid model (DEM for near field region and BEM for the far field) (after Jing, 2003) | 31 |
| III-7 | Representation of a jointed rock mass in each method | 31 |
| III-8 | Example of Modeling Roof support | 32 |
| III-9 | Modeling Rock Bolts | 33 |
| III-10 | Comparison between actual excavation stages and models | 34 |
| III-11 | Concrete structure typically not considered in numerical analysis of Cavern | 35 |
| IV-1 | Location of HPP Cirata in Java Island, Indonesia | 43 |
| IV-2 | Sketch map of extensive discontinuities exposed at the cavern wall | 44 |
| IV-3 | Layout of cavern and adjacent tunnels | 46 |
| IV-4 | Design Support Arrangement of rock bolts (tensioning 100 kN) and prestressed rock anchors (1000 kN) | 47 |
| IV-5 | Sequences of Excavation and support installation (After Reik, 1986) | 47 |
| IV-6(a) | Typical main monitoring cross-section (After Reik, 1986) | 48 |
| IV-6(b) | Location of measuring points (after Kamemura, 1986) | 49 |
| V-1 | Illustration of typical elements used | 55 |
| V-2 | Model I: Geometry, Loading condition, and coordinate system | 57 |
| V-3 | Model II: Geometry, Loading condition, and coordinate system | 57 |
| V-4 | Meshing Pattern of Preliminary Model I | 59 |
| V-5 | Meshing Pattern of Preliminary Model II | 59 |
| V-6 | Meshing Pattern for Model I with opening | 60 |
| V-7 | Meshing Pattern for Model II with opening | 60 |
| V-8 | Support Modeling | 61 |
| V-9 | Meshing pattern for additional model (circular shaped) | 61 |
| VI-1 | Vertical stress concentration around periphery for Model I | 67 |
| VI-2 | Horizontal stress concentration around periphery for Model I | 68 |
| VI-3 | Vertical stress concentration around periphery for Model II (a) & (b) | 71-72 |
| VI-4 | Horizontal stress concentration around periphery for Model II (a) & (b) | 73-74 |
| VI-5 (a) | Contour plot in ANSYS -SX and SY- for elastic behaviour Model I | 79 |
| VI-5 (b) | Contour plot in ANSYS -SX and SY- for elastoplastic behaviour Model I | 80 |
| VI-6 (a) | Contour plot in ANSYS -SX and SY- for elastic behaviour Model II | 81 |
| VI-6 (b) | Contour plot in ANSYS -SX and SY- for elastoplastic behaviour Model II | 82 |
| VI-7 | Vector principal stress cavern with/without support for Model I&II | 83-84 |
| VI-8 (a) | Plastic Zone on Model I & Model II | 89 |
| VI-8 (b) | Stress path on Side-walls Elastoplastic model –Model I | 90 |
| VI-9 | Deformed shape for Model I | 93 |
| VI-10(a)/(b) | Horizontal & Vertical deformation around periphery for Model I | 94-95 |
| VI-11 | Deformed shape for Model II | 96 |
| VI-12 | Horizontal deformation around periphery for Model II (a) & (b) | 97 |
| VI-13 | Vertical deformation around periphery for Model II (a) & (b) | 98 |

Cont.

| <u>Fig.</u> | <u>Description</u> | <u>Page No.</u> |
|-------------|--|-----------------|
| VI-14 (a) | Contour plot in ANSYS -UX - for elastic & elastoplastic behaviour Model I | 103 |
| VI-14 (b) | Contour plot in ANSYS -UY - for elastic & elastoplastic behaviour Model I | 104 |
| VI-15 | Plastic Zone Model I | 105 |
| VI-16 | Displacement Vector Model I | 106 |
| VI-17 (a) | Contour plot in ANSYS -UX - for elastic & elastoplastic behaviour Model II | 107 |
| VI-17 (b) | Contour plot in ANSYS -UY - for elastic & elastoplastic behaviour Model II | 108 |
| VI-18 | Plastic Zone Model II | 109 |
| VI-19 | Displacement Vector Model II | 110 |
| VII-1 | Comparison of actual cross section and its model geometry | 118 |

LIST OF TABLES

| Table. | Description | Page No. |
|---------------|--|-----------------|
| IV-1 | Rock support arrangement | 45 |
| IV-2 | Main Features of the Cirata Hydro Power Complex | 50 |
| V-1 | Data Model | 58 |
| V-2 | Sidewall Stress Concentration for calibration model | 62-63 |
| VI-1 | Magnitude of stresses around periphery for Model I | 69-70 |
| VI-2 | Magnitude of stresses around periphery for Model II | 75-78 |
| VI-3 | Resume results of SX | 87 |
| VI-4 | Resume results of SY | 88 |
| VI-5 | Deformation at some critical point around periphery of cavern | 92 |
| VI-6 (a) | Resume results of max UX & max UY | 111 |
| VI-6 (b) | Resume results of UY at crown | 112 |
| VI-7 (a) | Calculated maximum displacement on Periphery Cavern, FEA Results | 112 |
| VI-7 (b) | Calculated maximum displacement on Periphery Cavern, UDEC Results | 113 |
| VI-7 (c) | Calculated maximum displacement on crown, UDEC Results | 113 |
| VI-8 | Comparison between present study's result with previous study in term of Rock deformation | 115 |
| VI-9 | Magnitude of deformation around periphery for Model I | 115a-115b |
| VI-10 (a) | Magnitude of horizontal deformation around periphery for Model II | 115c-115d |
| VI-10 (b) | Magnitude of vertical deformation around periphery for Model II | 115e-115f |



INTRODUCTION

I.1 GENERAL

Underground structures such as tunnels, shafts, cavern and their appurtenances are structure completely built and housed into the existing ground medium, mostly in rock masses. To accommodate an underground structure, an opening is made by excavation which influences equilibrium of the host medium. The influence of these changed characteristics of host ground is difficult to ascertain in a quantitative manner due to the fact that: (1) ground is usually nonhomogeneous and thus its characteristics cannot be predicted from point wise observation and (2) uncertainties persist in the properties of the rock materials and in the way the rock mass and the groundwater will behave. Design and construction of underground structures in rock require thought processes and procedures that are in many ways different from other design and construction projects, because the principal construction material is the rock mass itself rather than an engineered material. Hence the behaviour of rock mass subjected to excavation is of interest and a better understanding of behaviour of disturbed rockmass is very important for design of underground structure.

I.2 IDENTIFICATION OF THE PROBLEM AND OBJECTIVES OF STUDY

Extensive research work has been done in the area of finite element modeling of rock engineering, and numerous reports have been published which deal with both 2D and 3D finite element models. Most of the finite element analyses dealing with the behaviour of rock masses subjected to stress induced by excavation of large cavern seem to be concentrated in the area of statical analysis wherein a number of fundamental analysis have been conducted to understand the behaviour of rock mass medium under different condition of opening as parametric studies. Review of the earlier works which are relevant to the present study is discussed in Chapter II in section *Literature review*. A number of analytical studies carried out to investigate the behaviour (stress and displacement) of rock medium

around cavern are identified. However a major portion of these studies utilized elastic analysis or employ *Mohr-Coulomb* or *Hoek-Brown* criteria for elastoplastic analysis.

The present study aims at providing a better understanding of the behaviour of rock mass around cavern using FEM (ANSYS code) in elastic and elasto-plastic approach using *Drucker-Prager* criteria and also to address some issues regarding the capabilities of finite element modeling of rock mass in ANSYS. Two aspects have been investigated in this study. The first is the stress and deformation analysis of the cavern and comparison with the deformation results from previous study of same cavern and with insitu measurement data. Two types of rock model (elastic and elastoplastic) have been developed to investigate the deformational behaviour of rock medium around cavern, which can deal with different horizontal ground load application methods, different upper far-field boundary condition, and also taking into account insitu stress field as the basic reference for the deformation prediction. The second part of this study has been to verify the validity and capability of ANSYS ver. 5.4 as FEM commercial code for application in underground cavern. Due to time and resource constraint the study is limited only to two-dimensional analysis.

1.3 OUTLINE OF DISSERTATION

Chapter 1 presents the introduction followed by an identification of the problem and objective of the present study, then an overview of outline of the dissertation is presented.

Chapter 2 consists of general overview of the state of the art of design and analysis methods available for underground cavern, as well as general concept for designing powerhouse cavern. This chapter also includes the literature review regarding the current state-of-the art in the numerical modeling of rock mass and also regarding the behaviour of rock mass subjected to stress induced due to an opening by finite element analysis.

Chapter 3 deals with the numerical methods for analysis of the underground rock cavern. Within this chapter the first section gives a short introduction as well as an overview of two basic factors that affect the modeling of rock mass, *elastic & inelastic stress strain relationship* and *in-situ stresses*. Section 3.2 forms the central part of the chapter, where the approach available for modeling the rock mass and simulation of underground excavation is discussed, it also subsequently gives a short overview of application of FEM in modeling rock mass, including the advantage and disadvantage of the methods followed by an

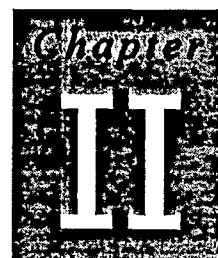
introduction to ANSYS, computer code which is employed for present study, describing the capabilities and the analysis procedure as well as background theory briefly.

Chapter 4 deals with the case study: Underground Powerhouse of Cirata (Indonesia) Project. After brief salient features, it gives a concise overview of the site geological data, the layout & type of the powerhouse, cavern support arrangement & monitoring program.

In Chapter 5 analytical program to model the case study, the model developed and the model data, the assumption for simulating the loading condition and calculation procedure are presented. The analyses with ANSYS performed on rock model are also discussed along with the model calibrated.

Chapter 6 discusses the results of the study.

Chapter 7 gives a short overview of the main conclusions and recommendations regarding the analysis. It also provides some insight into various aspects of finite element modeling of rock masses through ANSYS ver. 5.4. On the basis of these conclusions suggestions for further work are presented.



GENERAL CONSIDERATION FOR DESIGN & ANALYSIS OF CAVERN

II.1 METHODS FOR DESIGN & ANALYSIS OF UNDERGROUND STRUCTURES

The design of an underground structure in rock is one important step from planning to its construction. It will result in a description of the geometry and shape and also an estimation of the rock support measures applicable to the rock conditions and of the observation and controlling measures. The design is based on the geological and geomechanical investigations as well as the layout of the project. The choice of the design method depends on the type of the project and of the state of the project. Large caverns with complicated layout and geometry require beside experiences more sophisticated methods as advanced calculations with computer in order to get the preliminary design. The design strategy for underground structure is therefore divided in two steps; first a preliminary design based on experience and calculations and after that a follow-up with measurement during construction in order to get the final design. In that framework, the design & analysis methods which are available for underground structures can be categorized as follows:

II.1.i) Empirical methods

Due to the difficulty in predicting or modeling the behaviour of a complex system of rock in response to the excavation and despite the development of many new design tools -in the form of faster, cheaper and more versatile software-, the adoption of the design approach based on precedent practice and experience by means of general assessment of the characteristics of the rock mass or empirical approach is still adopted as a primary method to a wide range of rock engineering design problems. The empirical approach is based on the rock mass classification systems in which the rock mass is rated according to the values of a variety of input parameters. Such classifications are useful when they are applied to

projects similar to those for which the classification techniques were derived, but can be very misleading when inappropriately applied -especially when there is no precedent practice-. The problem with classifying rock mass is the apparent uniqueness of each rock formation, which makes generalizations inappropriate. In fact, on many major rock engineering projects, the individual classification approach is developed (or adapted from existing schemes) and serves as the only practical basis for the design of underground structures. These classification schemes are thus empirical and project specific. Starting from the Terzaghi's rock load theory, there are number of rock mass classifications. To name a few as follows:

- (1) Terzaghi's rock load theory (1946)
- (2) Classification of Deere & Miller (1969)
- (3) Rock Structure Rating (RSR) system of Wickham et. Al. (1972)
- (4) Rock Mass Rating (RMR) system of Bieniawski (1973-1984)
- (5) Rock Mass Quality (Q) system of Barton et al. (1974)

Out of all above classifications, the RMR and Q systems of rock mass classification are the two most popular and widely used. However, it is to be expected that classification schemes will gradually be phased out, as rock mechanics principles are directly applied to the engineering problems in hands (*Hudson, 1989*).

II.1.ii) Analytical and Computational methods

The principle of this method is to simplify underground structure to a mathematical model, representing the structure by tractable -partial differential- equations, and solving those equations, in the terms of stress and displacement. A number of assumptions are made in the approach for the constitutive law for material involved (elastic-inelastic, continuous-discontinuous, isotropic-anisotropic and homogeneous-nonhomogeneous). For a simple geometry (circular, elliptical, rectangular, etc) there are available solutions for distribution of elastic stress and displacement induced around opening using Airy stress functions or complex variable theory (*Obert & Duvall, 1967*). But it is very rare that analytical solutions can be found to 'real world' rock mechanics problem. This may be because the boundary conditions cannot be described by simple mathematical functions, the governing partial differential equations are non-linear, the problem domain is nonhomogeneous, or the constitutive relations for rock mass are non-linear or otherwise insufficiently simple

mathematically. In these cases, approximate solutions may be found using computer-based numerical methods, which has been described briefly in Chapter III. As a note, beside mathematical model described above, physical models can be developed and used in the analysis. The photoelastic models were very popular from 1950 to the early 1980's for making quantitative assessment of stress analysis in both two and three dimension approach of analysis. Other types of model are rock model (scale 1:1 or less) using synthetic material having mechanical properties satisfying model-prototype requirements, and rock model in centrifugal testing for simulating the loading condition effect of body force in rock i.e. underground structures at shallow depth.

II.2 GENERAL CONSIDERATION FOR DESIGN AND ANALYSIS OF POWERHOUSE CAVERN IN ROCK

An underground opening having a cross sectional area of 120 sq.m or more and an axial dimension of not exceeding 15 times the lateral dimension is classified as a 'cavern' according to *Einstein (Sinha, 1989)*. It is a large opening and always requires a special analysis & design by empirical, analytical or numerical methods. In general sense a cavern design should accommodate different demands and conditions - i.e. geology, rock stresses, construction technique, construction cost and operational demands- into a comprehensive solution. From civil engineering regards, the cavern is designed to maintain the smallest possible width and to provide a self-supporting structure with respect to the average quality of the rock. Due to these reasons presently caverns are limited in width to about 35 m. (*Sinha, 1989*). From standpoint of geomechanical, the objective of the cavern design is to guarantee that there is sufficient stability and serviceability with respect to the planned usage as long as it is expected to function. Basically, the stability of an underground cavern are influenced by the following factors and these shall be accounted for in cavern design:

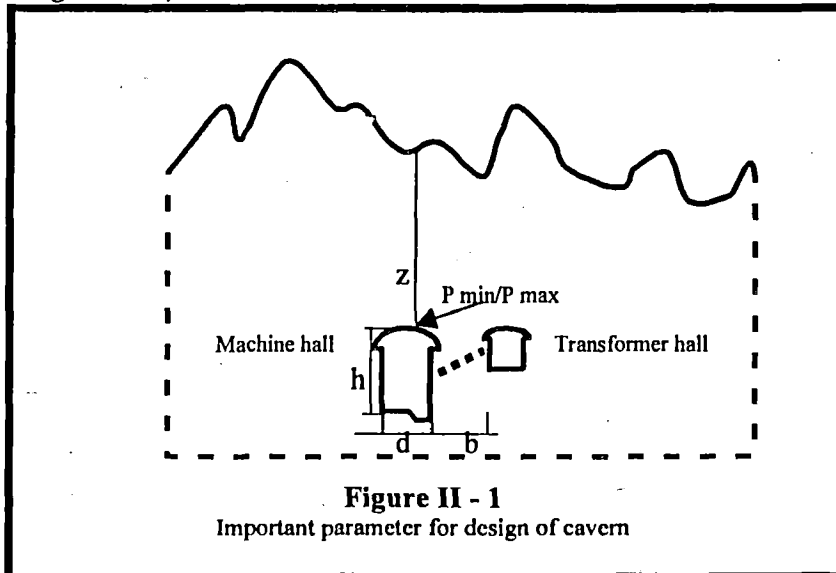
- physical effects (*initial rock stresses, internal pressure, temperature*),
- rock stresses, theoretically determined from insitu measurement or with the help of a calculation model,
- resistance (strength) of the rock that acts against the physical effects,
- influence of geological structures such as faults, shear zones, joints, etc.

In a specific cavern layout, for example a powerhouse cavern, the variables to be taken for consideration predominantly based on the final use to which the cavern is to be put, e.g.

machine hall, transformer hall and it will be different and unique for each scheme. Issues which are common to all schemes are:

- (1) The choice of the geometry (*size, shape and orientation*) of cavern;
- (2) The location of the cavern relative to adjacent and to the ground surface;
- (3) The influence of joints and bedding planes on the stability of the excavations;
- (4) The choice of the most appropriate support systems; and
- (5) Monitoring and instrumentation.

Each site will have its own set of rock mass properties, in-situ stress conditions and design constraints imposed by mechanical, electrical and hydraulic considerations. Consequently, the general design concepts have to be modified to suit each location. The important parameters to be taken into consideration in the design of a powerhouse cavern are as follows (see Figure II-1):



- depth of rock cover over the cavern (z),
- cavern geometry (diameter/width (d), height (h), orientation, roof/vault shape),
- distance (b) of the caverns from one another, (if machine hall and transformer hall have to be built separately or for multiple cavern)
- the stress state due to opening and its distribution along the periphery (p_{min} ; p_{max}).

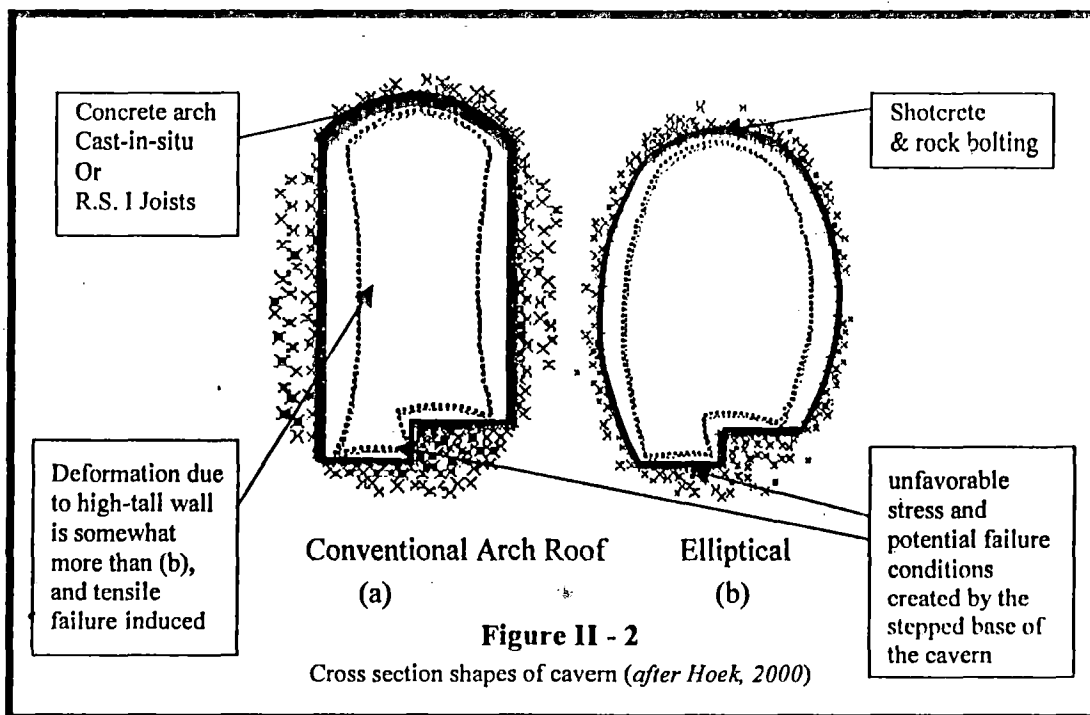
Detail concept for design of underground large cavern for powerhouse is beyond the scope of this dissertation; only some points will be highlighted below.

II.2.i) Geometry of cavern

The geometry of a cavern is influenced by the following factors (*Sinha, 1989*):

The size is determined mainly by the functional requirements of its capacity, geological setting, host media characteristics, and the selected construction methodology, while the orientation is chosen by considering the insitu principal stresses.

The Shape is influenced by the geologic setting, magnitude and orientation of in-situ existing rock stress, selected construction methods, estimated rock load including its distribution, and existing structural instability such like shear zones, faults, and joint. The common shapes are shown in **Figure II – 2**.



II.2.ii) Choice of cavern shapes

Based on geotechnical consideration, the conventional shape similar to that illustrated in **Figure II -2 (a)** can be chosen for strong rock masses, for which rock mass failure is not a problem, (*Hoek, 2000*). The arched roof provides stability in the rock above the cavern roof and also provides convenient headroom for an overhead crane. The sidewalls are simple to excavate and provide clean uncomplicated walls for crane column location and the accommodation of services. The problem with this cavern shape when used in weak rock

masses, particularly with high horizontal insitu stresses, is that tall straight sidewalls are deflected inwards and tensile failure is induced as shown in **Figure II - 2**. An alternative cavern shape is illustrated in **Figure II - 2 (b)**. This elliptical/egg-shaped has been used on schemes such as *HPP Cirata (8x125MW)* & *HPP Singkarak (4x37.5MW)* in Indonesia (where author has posted as site engineer during 1995-1997). As shown in **Figure II - 2**, the deformation as a sign of the failure zones in the sidewalls has been reduced as compared to that in the conventional cavern. This results in a more stable overall cavern and a reduced support requirement. The disadvantage for the elliptic cavern is that the construction has to be more carefully executed than the conventional straight-walled cavern and the cranes and services etc. have to be designed to suit the cavern shape.

II.2.iii) Influence of joints and bedding planes

In rock masses, joints and bedding planes are usually present but cannot make dominant weakness directions in the rock mass (*Hoek, 2000*). While faults or shear zones can introduce a directional pattern of weakness in the rock mass and this should be taken into account in the cavern design. The joints have influence as they have low shear strength as compared with that of the rock material such that failure takes place on the joints. The inclination of the joints with respect to the principal stress directions is also important. Joints inclined to the direction of the maximum principal stress will tend to slide more easily than those parallel and normal to this direction.

II.2.iv) Sidewall and roof support system

Safety during construction and long-term stability are factors which have to be considered in design of excavations for sidewalls in rock. It is usual for these requirements to lead to a need for the installation of some form of rock support. The rock supports somewhat controls the deformation of the rock mass toward the excavation opening, counteracts the loosening of the strata and, in form of rock bolts, introduce the confining effect to rock mass. Rock support design traditionally is based on Terzaghi's rock load theory way back in 50's, then followed more approaches, such as empirical design by rock mass classification, or by limit equilibrium, key block theory that support should penetrate through block, or design by observation as in NATM, or even by finite element study to find the extent of tensile/plastic zone then length of support is designed to reach beyond that zone. Despite extensive theoretical and model studies of the behaviour of a single bolt or anchor when embedded in

rock or of the behaviour of a system of such reinforcing elements, the practical design of rock reinforcement continues to involve application of empirical rules generated from experience (Hoek, 2000). Some theoretical models, which provide a very clear understanding of the mechanics of rock support in tunnels, based upon very simple assumptions, have been developed in recent years (Sinha, 1989, Brady and Brown, 1993) but rock mass conditions may vary from these assumptions. With the development of powerful numerical models such as PLAXIS®, UDEC/3DEC®, SIGMA/W®, FLAC®, more realistic and reliable support designs will eventually become possible and can be used as design tools. In case of cavern, the support systems for roof, sidewalls, and invert are normally a system of rock bolts, prestressed anchor and shotcrete as temporary or permanent support. Roof of cavern have special supporting treatment since it is a critical area. Shotcrete (flexible) or cast-in-place concrete (rigid) are typical roof cover support. Typical support arrangement of cavern is shown in Figure II – 3.

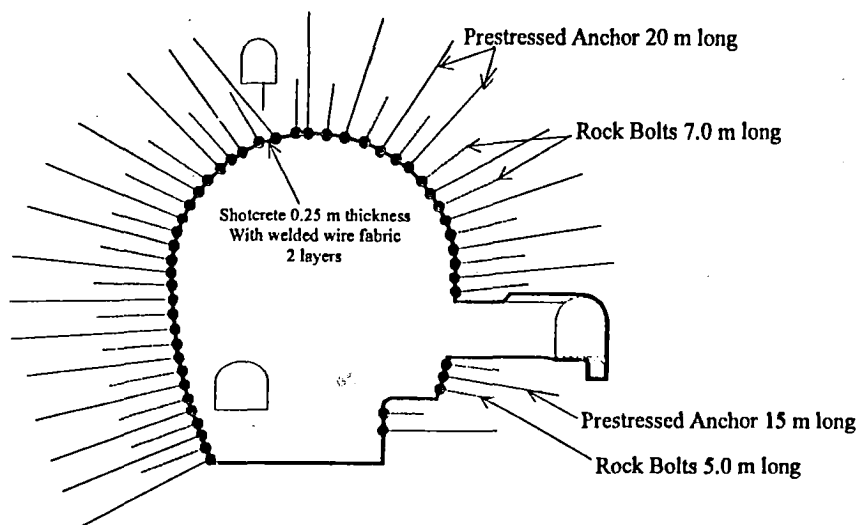


Figure II - 3
Typical support-arrangement of cavern (in HPP Cirata)
(after Reik G. 1986)

II.2.v) Cavern instrumentation

During the excavation and for utilization period it has become necessary to monitor the behaviour of the rock mass surrounding the cavern. For this purpose a control and readout system is built in the cavern designed to ensure the systematic control of the stress and deformation condition of the rock mass and the permanent shield. These direct

measurements in natural conditions and after construction are used for timely detection of the signs indicating impaired stability. The monitoring of these signs is the safest way of preventing serious damage to the installations.

The simplest, most direct and most relevant measurement that can be made of rock behaviour around cavern is the displacement between two reference points, wall-wall and roof-floor convergence for example (see **Figure II – 4**). There is variety of methods for measuring displacement, ranging from a measuring tape, through multi-rod borehole extensometers, to electronic techniques. There are also a variety of scales over which the displacement can be measured, from a few millimeters (using strain gauge), to many meters (using tapes and electronic measuring device). On the design side, displacement measurement can form the basis for support systems as in NATM during excavation. On the research side, displacement/ deformation is probably the best parameter for verifying the validity of analytical techniques which model stresses and displacements in rocks. Displacement monitoring may be relative or absolute, relative if the installation of a multipoint extensometer in the sidewall of a cavern with the deepest anchor inside the zone of rock where movement may be expected. Movements beyond the deepest anchor will not be registered by the extensometer. An example of absolute movement monitoring is the measurement of the horizontal convergence of the two sidewalls of the cavern by means of a tape extensometer stretched between the walls. However deep the movement, it will all be registered by the tape extensometer. By comparison, measurements of stress change in the rock cavern by load meter can only be conducted at isolated points which may not be representative of the average condition due to highly localized strains and load changes may occur where the bolt/cable crosses a specific joint, by then stress changes in the rock can be calculated from monitored displacements by the assumption of a value for the rock mass modulus. It is also important to assessing the groundwater conditions in the rock mass surrounding the cavern. Where groundwater discharges into a cavern, piezometer installations are advisable to check that build up of excessive pressure in the roof or behind the sidewalls. Typical main monitoring cross-section for cavern is shown in **Figure II – 4**.

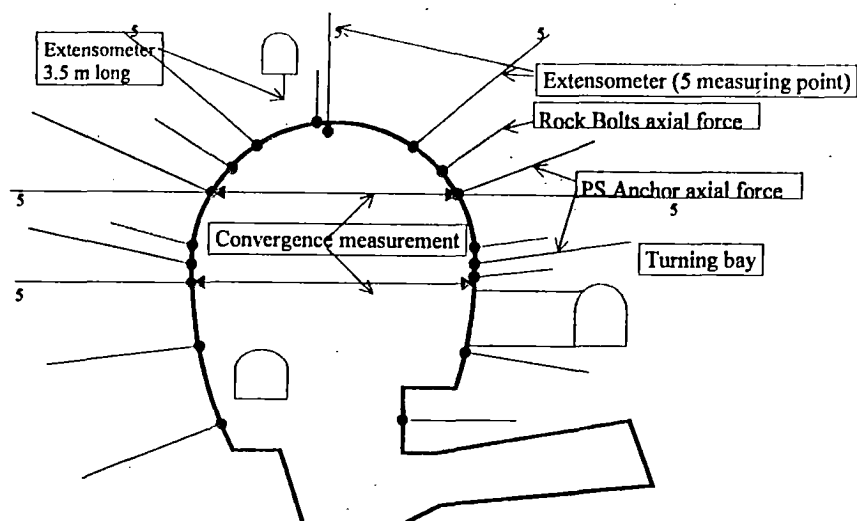


Figure II - 4
 Typical main monitoring cross-section for cavern (in Cirata HPP)
 (after Reik, 1986)

II.3 LITERATURES REVIEW

There is extensive information available regarding the behaviour of rockmass around large opening as rock mechanics modeling has developed for the design of rock engineering structures with widely different purposes (published papers in '*International Journal of Rock Mechanic and Mining Science*', International journal of '*Tunneling and Underground Space Technology*', journal of '*Computers and Geotechnics*', and proceeding of *ISRM Symposium* and proceeding of seminars/conferences/symposium on related topic in India and worldwide, as well as numerous outstanding textbooks on rock engineering). There is a wide spectrum of modeling approaches as the results of worldwide studies and research. Most of these studies incorporate the effect of stress distribution induced by opening in analysis and are focused on continuum/discontinuum approach. Only limited research has been performed which analyzes the dynamic loading such as seismic effect, thermo-hydro-mechanical behaviour of rock masses, rock fracture model, or neural networks and probabilistic design. Out of these works, only a few which are relevant to present study are briefly described below, i.e.:

II.3.i) Numerical Modeling for Analysis of Underground Cavern

A number of studies have been carried out since 80's to analyze the possible shape, stability concerns, and rock supports design of large cavern and its interaction with adjacent cavern using numerical model. Liu et al. (1988) performed study for possible shape of cavern of Mingtan hydropower complex (Taiwan) using a Boundary Element Program (BEM) and the Finite Element Program EXCA for two-dimensional plane strain analysis. BEM treated the rock mass as an isotropic elastic material, whilst FEM treated the rock mass as non-linear material and took construction staging into consideration. Both methods predicted approximately the similar extent of relaxed zone due to excavation which were used to evaluate the optimum shape of the cavern. Three different shapes, i.e., the egg shape, the mushroom shape and the horseshoe shape have been studied, as shown in Figure II - 5.

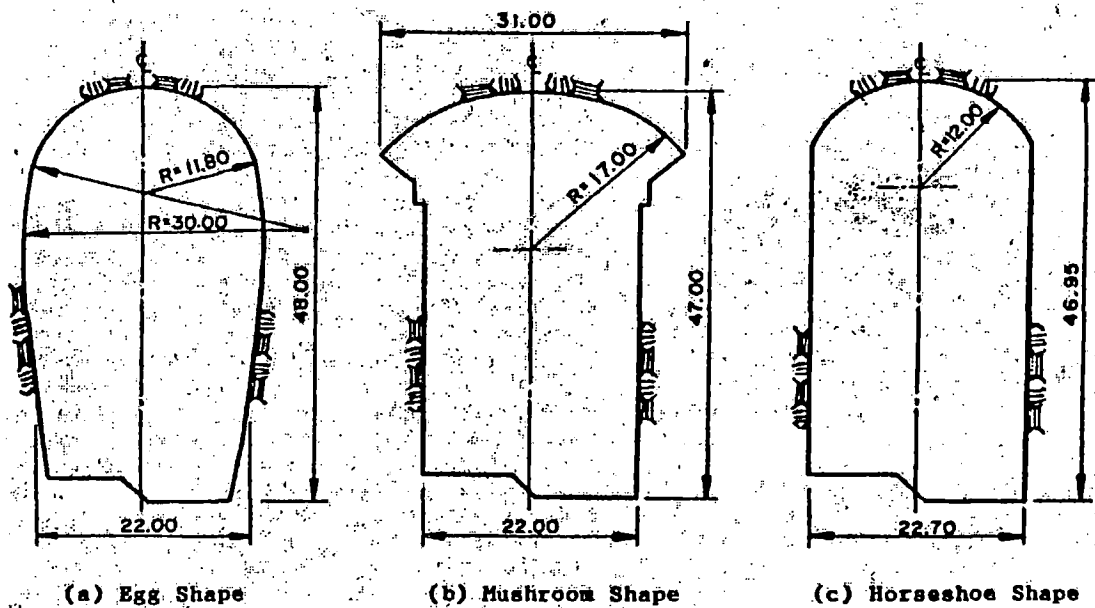


Figure II - 5
Shape studied (after Liu, 1988)

In their FEM analysis, cross-sections were studied incorporating fault zones at different elevations in the sidewall. The conclusion of their study which is relevant to present study is from the standpoint of cavern stability and stress distribution, the horseshoe shape and the egg shape are similar to each other, both being superior to the mushroom shape.

Parametric studies related to various cavern stability affecting parameters were carried out by Huang (1988) using numerical methods. His studies aimed at determining deformational law in high in-situ stress region in China and trying out forwarding some suggestions about designing multiple caverns. He concluded that one factor to be considered for the selection of the plane stress-plane strain condition of two-dimensional analysis is to take into account the elasto-plastic material properties approach, due to reason that at plastic stage the stress of model plane stress will not be equal to that of model plane strain and this condition is very harsh for rock mass (in elastic exact solution the stress from plane stress condition is equal to plane strain's).

Sugawara et al (1988) investigated the elasto-plastic problems in rock engineering by coupling two existing methods, the boundary element methods and the characteristics methods, into a hybrid method. The formulation of this method was presented, as well as an efficient procedure for boundary determination. It is discussed that this method is a powerful and accurate method in evaluating the extent of the plastic region around rock caverns, which is of prime importance for the construction of rock cavern. They derived the equation for coupling the methods in elastic-plastic region and gave some typical numerical examples, including underground powerhouse cavern, in order to demonstrate its applicability in rock engineering. In conclusion, they remarked that the combination of the BM-CM is an accurate method for solving the elasto-plastic problems of underground opening. Dasgupta et al (1995) presented a report pointing to the numerical modeling as a very powerful tool for analysis and design of underground excavation. Their paper deals with the stress analysis of three major powerhouse caverns in India, Sardar Sarovar, Gujarat; Srisaïlam, Andhra Pradesh and Nathpa-Jhakri, Himachal Pradesh. Main goal of their study was to investigate the behaviour of rock masses subjected to induced stress and to assess the adequacy of the current design procedures. In those studies, advanced numerical modeling played different roles, either to explain rock mechanics problem by back analysis or to predict the rock response before construction, so that the support system could be designed to ensure stability of the excavations. In the Sardar Sarovar, the effect of the shear zones on the stability of upstream wall was studied by 3D discontinuum modeling. The problem was simulated with the 3D analysis software, 3DEC which is based on the distinct element methods which can model the discontinuities. In Srisaïlam and Nathpa-

Jakri, continuum analysis was used to study the stress distribution caused by multiple excavations.

Samadhiya (1998) in his attempt to model jointed rock masses, have developed an FEM code for 3-D non-linear analysis in anisotropic rock masses (ASARM) with the capabilities to simulate in-situ stresses and geological discontinuities like shear zones, fault zones and anisotropy associated with jointed rock masses. In order to simulate the major discontinuities, he replaced the jointed rock mass with an equivalent continuum body for analysis with an appropriate associated constitutive model. A generalized formulation of the three dimensional joint/interface element has been proposed to model interface of jointed rock mass and shear zone taking into consideration the dilatancy, roughness and undulating surface of a discontinuity. He has illustrated application of ASARM code by analyzing Sardar Sarovar powerhouse cavern in three-dimensional taking into account the effect of anisotropy and shear zones.

II.3.ii) FEM Analysis for Underground Cavern

Back in the late 80's, the finite element stress analysis studies were conducted on the Thissavros powerhouse cavern in Greece, along with a complete design of the support measures on the sidewalls and roof of the cavern (Kalkani, 1988). FEM analysis for one-stage excavation is performed to identify the zone of rock in the sidewalls and the roof of the powerhouse cavern which requires support. The main emphasis is given to the consideration of material nonlinearity and to the accurate finite element modeling. Juemin et al (1988) did a study for problems of stability and supports of underground powerhouse cavern East Wind in China using non-linear FEM program. They derived the constitutive behaviour and failure modes for rock mass and incorporated in their FEM analyses. A non-linear FEM program, named NAPARM is used. It applies the increment method of change stiffness and gaussian elimination, and simulates the sequences of construction and operation in step by step. They concluded that the nonlinear FEM is proved to be valid in studying the engineering problems in complex rock formations. It can simulate the engineering process and the complex interaction between rock and support, so it is a powerful tool of rock engineering designing.

Bouvard et al (1988) presented a design method for underground cavern at Maung, Indonesia including a numerical analysis, based on the finite element method, to predict the

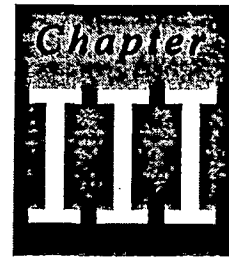
stresses and displacements around the cavity. A two dimensional finite element analysis - using isoparametric 8 noded element- has been performed taking into account the parameters such as: deformability of the rock mass and failure criterion, geometry of cavity, vicinity of neighbouring excavation, initial geostatic stress and anisotropy, main stages of excavation, effect of support. The rock mass is assumed to be homogeneous, elastic and isotropic. Failure criterion is introduced to determine the zones where stresses are excessive. Initial state of stress is defined by the overburden and ratio $k=0.5$ and 1.0 is chosen since k is unknown. Prestressed cables anchor are mobilized by applying node forces corresponding to the capacity of the cable. On the basis of the results obtained it was suggested that there is little influence of adjacent cavity, also thickness of plastic zone is slightly reduced when rock support confinement stress is applied.

Arya et al (1995) studied the stress concentration factors around D-shaped twin-cavities to observe the influence of various parameters, such as, a) ratio of horizontal stress to vertical stress, b) height to width ratio of cavity, c) distance between the two cavities, and d) distance of the boundaries of the medium. They put horizontal ground load in far field boundaries to take effect of entire medium. The medium around the cavities has been assumed to be elastic, homogeneous and isotropic to carry out the finite element analysis in 2 D plane strain approach. The findings of the study which are relevant to our present study here implied that to consider the semi infinite effect for analysis, the distance of the boundaries be kept at 4.0 times the width of cavity, also the ratio of horizontal stress to vertical stress has significant effect on the stress at the periphery of cavity and ratio 1.0 gives optimum stress concentration.

Dhawan et al (2002) studied the finite element analysis of the underground powerhouse excavated for Koyna hydroelectric project using computer code *Solvia 90* ®. 2D & 3D analysis had been conducted assuming that the rock mass obeys Drucker-Prager failure criterion. The faults and shear zones present in the rock mass are represented by an equivalent continuum material. The computed deformations and stress distribution, around those openings, have been compared with those by the recorded measurements by insitu instruments. The study reveals that the 2D elasto-plastic analysis underestimates the deformations. On the other hand, the 3D elasto-plastic analysis yield results, which compare

reasonably well with the insitu measurements. It was also noted that reduction of stresses and deformations around opening is observed due to application of the rock supports.

Thus a number of analytical studies have been carried out which investigate the behaviour (stress and displacement) of rock medium around cavern. Both 2D and 3D finite element models have been recently employed in many cases to understand the behaviour of the rock mass and to design the caverns, it has been used in this study.



NUMERICAL MODELING FOR LARGE UNDERGROUND CAVERN

III.1 GEOMECHANICAL ANALYSIS FOR MODELING UNDERGROUND OPENING

Understanding of rock mass response to underground opening is necessary to assess opening stability and its support requirements. Knowledge of rock modeling, and these involved material constitutive law (*stress-strain relationship*) and the pre-existing boundary conditions (such as *in-situ* stress) is also essential. Several approaches of varying complexity have been developed to help designer understand rock mass response. These methods do not consider all aspects of rock behavior, but are useful in quantifying rock response and providing guidance in geomechanical design & analysis. In general, geomechanical analyses for underground opening use the theory of elasticity and sometime extend to the theory of plasticity and are approached through the concepts of strain and stress (so-called '*Rational methods*'). Since it deals with response of material to an applied disturbance, most of the problems in geomechanics are focused on the problem of induced stress and displacement due to excavation of openings. The theoretical solutions assume isotropic elastic homogeneous rock. Out of many factors that affect the rock modeling, two basic factors (*stress-strain relationship* and *in-situ stress*) are discussed briefly in next section, followed by discussion on numerical methods available for rock modeling as well as Finite Element Method which has been used in the present study along with introduction of computer code ANSYS which has been employed as calculation processor.

III.1.i) Exact Solution using Elastic Stress-Strain Relationships

The elastic stress-strain relationship is the simplest and most frequently applied approach in rock mass study. The theory of elasticity idealizes rock material as a linearly elastic,

isotropic, homogeneous material. In certain circumstances the rock mass surrounding an underground opening may behave as an elastic material satisfying Hooke's law. In such situations linear elastic analysis can be used to make accurate predictions of stress and displacement. More commonly, only part of structure responds elastically, but the more critically stressed areas exhibit inelastic behaviour by yielding, fracturing, or slipping on surfaces of weakness. Even in these cases elastic analysis is useful in suggesting the influences of various parameters, and the possible extent of plastic zones. Where applicable, elastic analysis can be used to evaluate a number of factors of importance such as (*Brown (Ed), 1987*):

- a) the maximum and minimum stress on the boundary of the opening (which is the most critical area);
- b) the boundary displacement induced by excavation (which allows an assessment to be made of the interaction between supports and the surrounding rock);
- c) the extent of the zone of influence (which allows one to estimate the degree of interaction between neighbouring excavations);

For the stress and deformation analysis of opening in rock, the simplicity of the elastic solution provides insight into the significance of various parameters and can be used to understand the magnitude of the stresses and deformations induced around an opening. As an example, consider a single circular opening in massive rock, two-dimensional case in a biaxial stress field, with assumption that (1) massive elastic rock is linearly elastic, homogeneous, and isotropic with respect to its mechanical properties, and (2) the opening is in an infinite medium (this condition is satisfied if the distance from the opening to an adjacent boundary is greater than three times the dimension of the opening) (*Obert & Duvall, 1967*), the exact solution for the stresses is:

$$\sigma_r = \left(\frac{S_h + S_v}{2} \right) \left(1 - \frac{a^2}{r^2} \right) + \left(\frac{S_h - S_v}{2} \right) \left(1 - 4 \frac{a^2}{r^2} + 3 \frac{a^4}{r^4} \right) \cos(2\theta) \quad (\text{III.1})$$

$$\sigma_\theta = \left(\frac{S_h + S_v}{2} \right) \left(1 + \frac{a^2}{r^2} \right) - \left(\frac{S_h - S_v}{2} \right) \left(1 + 3 \frac{a^4}{r^4} \right) \cos(2\theta) \quad (\text{III.2})$$

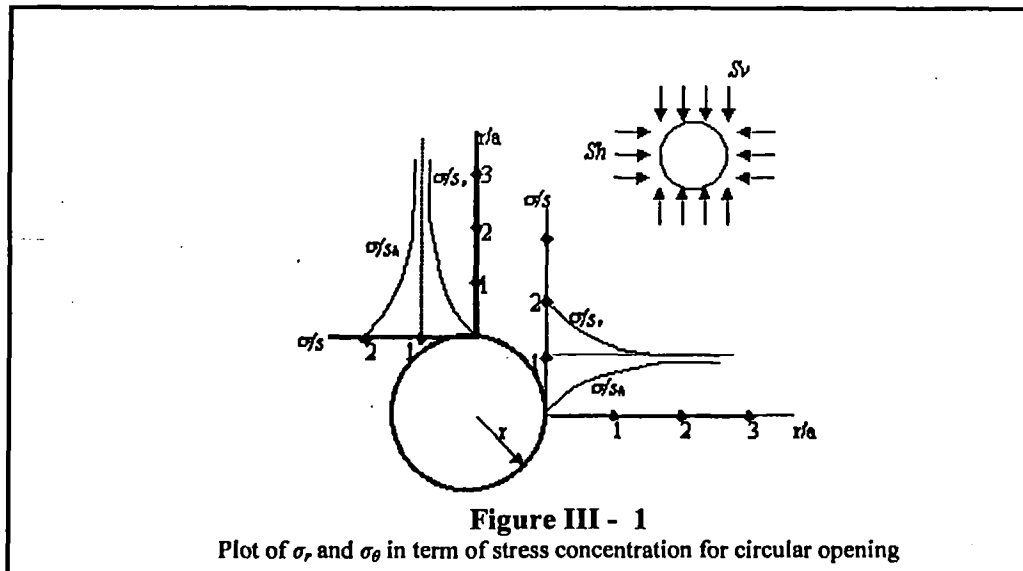
$$\tau_{\theta r} = \left(\frac{S_v - S_h}{2} \right) \left(1 + 2 \frac{a^2}{r^2} - 3 \frac{a^4}{r^4} \right) \sin(2\theta) \quad (\text{III.3})$$

where

S_h = horizontal applied stress

- S_v = vertical applied stress
 σ_r = radial stress
 σ_θ = tangential stress
 $\tau_{r\theta}$ = shear stress
 a = opening radius
 r = radial distance from center of opening
 θ = polar coordinate; horizontal axis represents $\theta=0^\circ$

The displacements for the same circular opening in an infinite media are obtained by integrating the stress displacement equations (see Appendix A for plane-stress and for plane strain condition). Plot of σ_r and σ_θ in term of stress concentration (σ_r / S_v and σ_θ / S_h) is shown in Figure III-1.

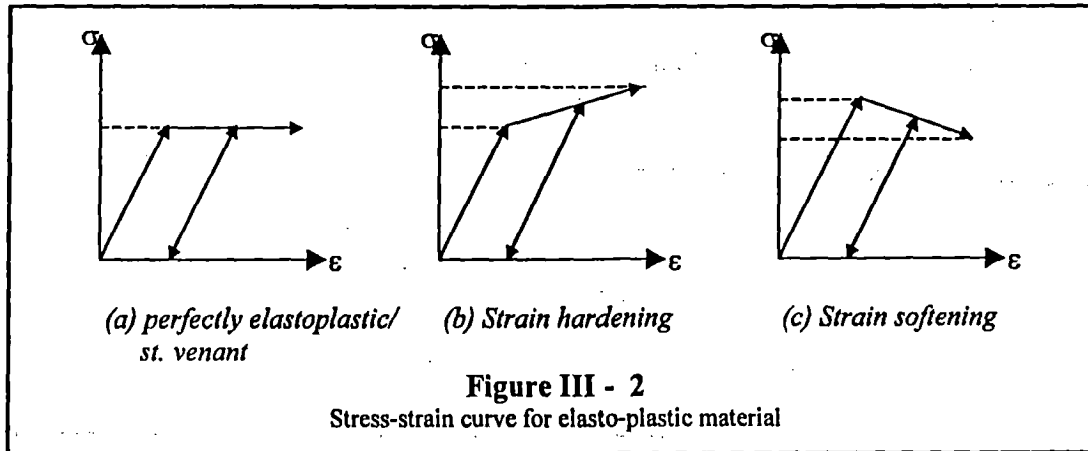


The equation (III-1) and (III-2) are used for validating the model in the present study by comparing with the numerical analysis (FEM) results.

III.1.ii) Inelastic Stress-Strain Relationships

Many rocks can be characterized as elastic without materially compromising the analysis of their performance. But when the stresses are sufficiently large then a failure zone will develop around the opening, and failure may take place in the form of fracture and disintegration (localized spalling, roof falls, slabing of side walls, etc) or excessive deformation beyond the tolerable limits (gradual closure of the opening, etc). For these conditions, nonelastic analyses are available for analyzing the stresses and strains. Nonelastic analysis is the application of theory of plasticity in geomechanics as plastic or

dissipative mechanisms of deformation may occur in rocks and rock masses. Out of the basic idealization of material model for nonelastic analysis (*perfectly viscous/Newtonian, perfectly plastic, viscoelastic/Maxwell, hyperelastic, etc*) the favourable model for application in rock mass is the *elasto-plastic* material as it can represent closely the constitutive behaviour of rock mass i.e., -in context of small strain-, rock deformation always consist of the elastic strain $\{\epsilon^e\}$ and plastic strain $\{\epsilon^p\}$. In order to describe plastic behaviour, the simple graphical representation in the stress-strain plane for elasto-plastic material is illustrated in Figure III-2.



There are three essential parts to describe plastic stress-strain relation mathematically: 1) *yield criteria*; 2) *flow rule*; 3) *hardening law*. *Yield criteria* is the criterion for specifying the maximum state of stress that can exist in a medium before yielding will occur. For plastic yielding, the state of stress when it initiates is independent of any coordinate system; therefore criteria for yielding is expressed in terms of principal stress $\sigma_1, \sigma_2, \sigma_3$ and the combination of $\sigma_1, \sigma_2, \sigma_3$ (in 3-D space) or σ_1, σ_2 (in 2-D plane) that cause yielding are described by a *yield function*

$$F(\{\sigma\}) = F(\{\sigma_1, \sigma_2, \sigma_3\}) = 0 \quad (\text{III.4})$$

The *yield function* can be represented by lines in 2D stress plane and surface in 3D stress space. Equation (III.4) mentions that if the value of the yield function is less than zero, the state assumed is elastic and no plastic flow will occur.

In contrast to elastic behaviour, the plastic strain $\{\epsilon^p\}$ is strongly dependent on the current total stress and can not be defined uniquely in terms of current state of stress. Hence to calculate the plastic strain there should be a *plastic potential function* $Q(\{\sigma\})$ such that the derivatives of the potential function define the ratio of plastic strain and the stress

increments subsequent to yielding. This function governs the relation between strain increments to the current stress and called *flow rules*. If $F = Q$, it is called *associated flow*. *Hardening law* establishes the modified yield condition during the plastic flow. In case of rock mass, the *hardening law* will depend on the type of rock, brittle strong rock will show *strain softening* behaviour but weaker rocks subjected to high stresses will tend to be ductile and show *strain hardening* behaviour.

For rock material, at present many different criteria of failure by fracture, flow, or yielding have been proposed. Out of them a few are:

- Tresca (Obert & Duvall, 1967),

$$f(\sigma) = \frac{\sigma_1 - \sigma_3}{2} = k \quad (\text{III. 5})$$

where k is constant

- Mohr-Coulomb

$$f(\sigma) = \frac{\sigma_1 - \sigma_3}{2} + \frac{\sigma_1 + \sigma_3}{2} \sin \phi - c \cos \phi \quad (\text{III. 6})$$

where c is cohesion and ϕ is the angle of internal friction

- Hoek & Brown (2002)

$$f(\sigma) = S_1 - S_3 - (m_b S_3 + s)^a \quad (\text{III. 7})$$

$$m_b = m_i \exp\left(\frac{GSI-100}{28-14D}\right), \quad S_1 = \frac{\sigma_1}{\sigma_{ci}}, \quad S_3 = \frac{\sigma_3}{\sigma_{ci}}$$

where

GSI = Geological Strength Index

σ_1 = the most compressive principal stress

σ_3 = the least compressive principal stress

σ_{ci} = the unconfined compressive strength of the rock sample

m_i, s, a = Hoek-Brown constants

$$s = \exp\left(\frac{GSI-100}{9-3D}\right), \quad a = \frac{1}{2} + \frac{1}{6} \left(e^{-GSI/15} - e^{-20/3} \right)$$

D = factor which depend upon the degree of disturbance of rock mass
= 0 for undisturbed and =1 for very disturbed rock mass.

- Drucker & Prager (1952)

$$f(\sigma) = \sqrt{\frac{1}{2} J_2} - \alpha I_1 - k \quad (\text{III. 8})$$

$$\alpha = \frac{2 \sin \varphi}{(3 - \sin \varphi) \sqrt{3}}, \quad k = \frac{6c \cos \varphi}{(3 - \sin \varphi) \sqrt{3}}$$

where

J_2 = second invariant of stress tensor

$$= \frac{1}{6} [(\sigma_x - \sigma_y)^2 + (\sigma_y - \sigma_z)^2 + (\sigma_z - \sigma_x)^2] + \tau_{xy}^2 + \tau_{yz}^2 + \tau_{zx}^2$$

I_1 = first invariant of stress tensor

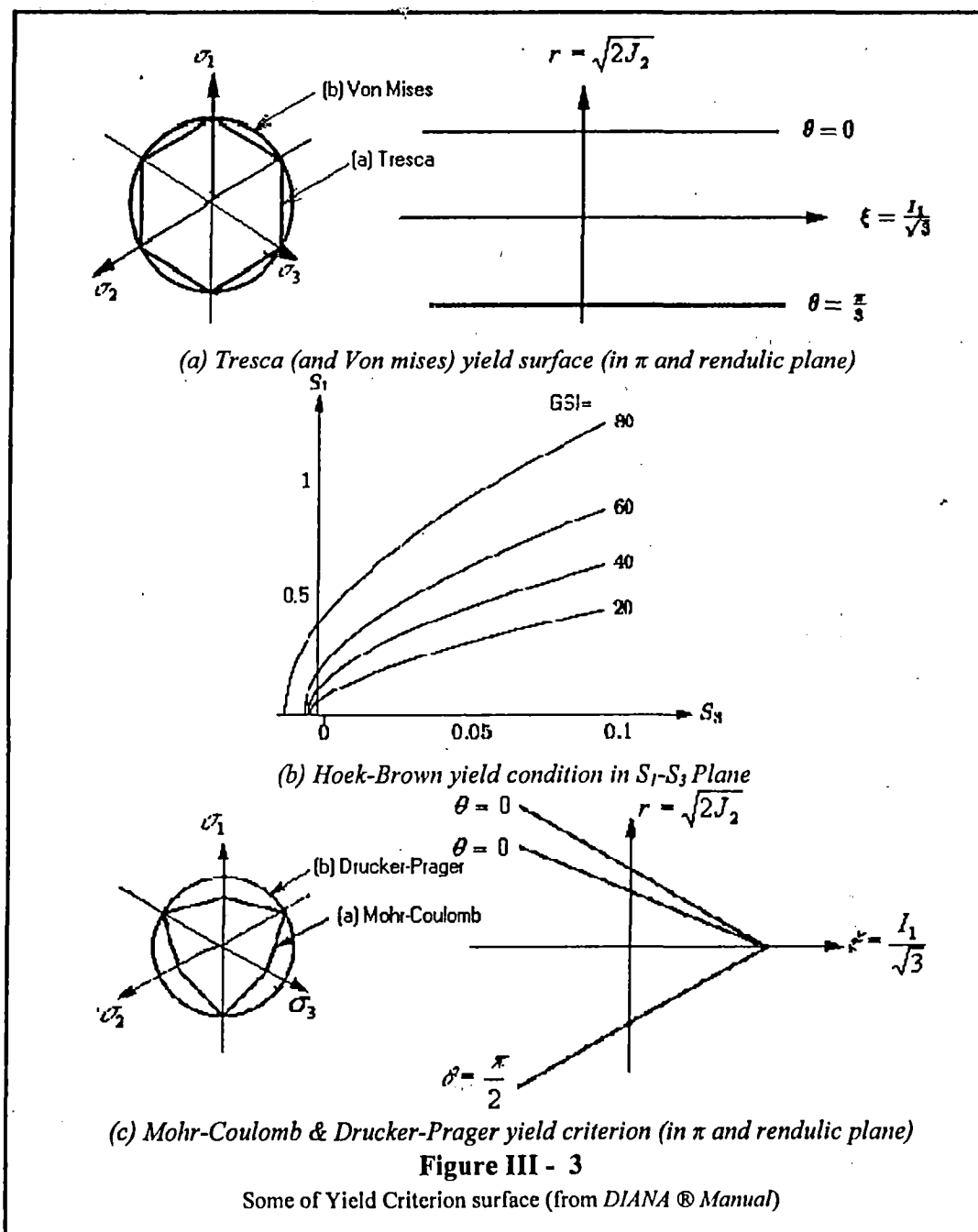
$$= \sigma_1 + \sigma_2 + \sigma_3$$

φ = angle of internal friction

c = cohesion

From some of yield criteria mentioned above, mostly using principal stresses as the stress criteria, and considering rock strength (*uniaxial compressive strength, tensile strength*) as factor affecting the modes of failure.

The graphical presentation of above yield criterion is shown in **Figure III-3**.

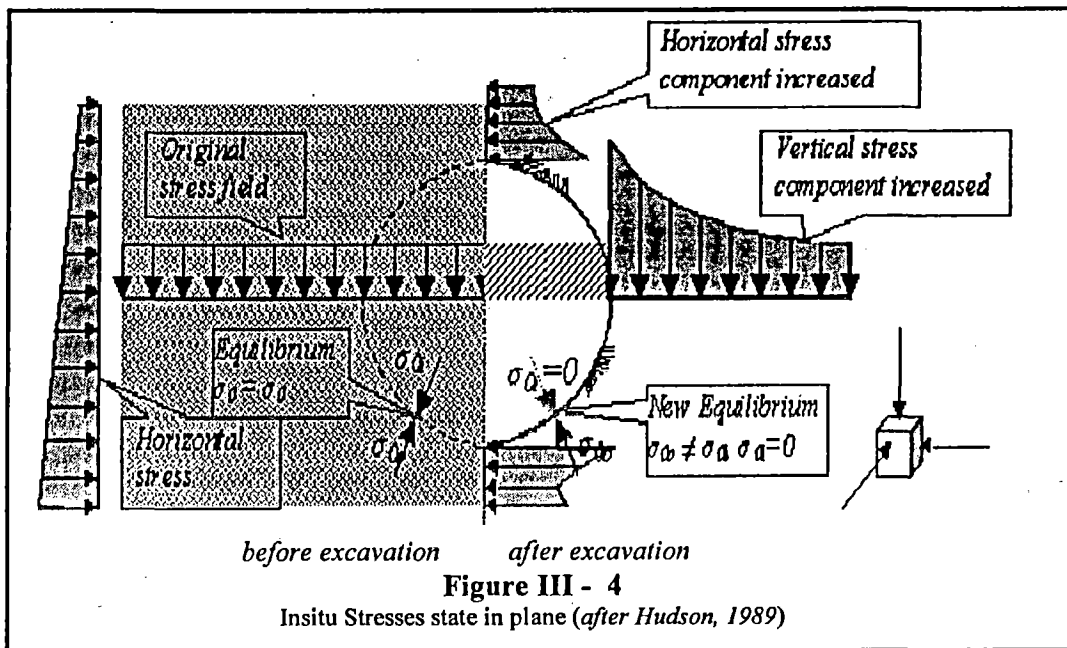


Out of the above criteria, the *Drucker-Prager* criteria is employed for the present study since it is the smooth approximation of the *Mohr-Coulomb* yield surface, and it's non-associated flow rule is more realistic to represent the stresses at yield in rock and rock masses (*Brown, 1987*).

III.1.iii) **Insitu stresses state**

Undisturbed mass of rock at depth is subjected to stresses resulting from the weight of the overlying strata and from locked-in stresses due to tectonic activities. When an opening is

excavated in this rock, the stress field is locally disrupted and a new set of stresses is induced in the rock surrounding the opening. Hence understanding the state of insitu stresses before excavation is important. They determined the boundary conditions for stress analysis as well as initial loading condition in rock mass modeling, and affect stresses and deformations that develop when an opening is created. Figure III-4 show how the vertical and horizontal stress are altered by opening excavation.



Heim (1878) was one of the first to hypothesize that vertical stress component σ_v , related and proportional to the weight of the rock overburden, and horizontal stress component σ_h is probably of magnitude similar to the vertical stress (Jaeger, 1979). The horizontal stresses acting on an element of rock at a depth z below the surface are much more difficult to estimate than the vertical stresses. Normally, the ratio of the average horizontal stress to the vertical stress is denoted by the letter k such that:

$$\sigma_h = k\sigma_v = kyz \quad (\text{III. 9})$$

Since there are three principal directions (xyz), there will be two horizontal stresses. In an undisturbed rock mass, the two horizontal stresses may be equal, but generally the effects of material anisotropy and the geologic history of the rock mass ensure that they are not. The value of k is difficult to estimate without field measurement but reasonable estimates can be made for some conditions. Terzaghi and Richart suggested that, for a gravitationally loaded rock mass in which no lateral strain was permitted during formation of the overlying strata, the value of k is independent of depth and is given by

$$k = \frac{\nu}{(1-\nu)} \quad \text{(III. 10)}$$

where ν = Poisson's ratio of the rock mass.

This relationship was widely used in the early days of rock mechanics but it proved to be inaccurate and is now seldom used (Hoek, 2000), currently it is considered as lower limiting value. The Poisson's ratio (ν) for most rocks is in between 0.2 to 0.33; hence k should lie between 0.25 and 0.5. However, most insitu measured values of k lie between 0.5 and 0.8 for hard rock and between 0.8 to 1.0 for soft or inelastic rock. In a number of instances k has been found to be greater than 1.0. In the present analysis, $k = 1.0$ as indicated by previous study (Kamemura, 1988) is taken.

III.2 NUMERICAL METHODS FOR UNDERGROUND CAVERN

Most of underground caverns are irregular in shape. In addition, because of the presence of geological features such as faults and intrusions, the rock properties are seldom uniform within the rock volume of interest. Consequently, the exact closed form solutions described in previous section (for 2-D plane analysis) are of limited value in calculating the stresses, displacements and failure of the rock mass surrounding underground cavern. In that framework, numerical methods are employed to:

- Determine stress-deformation behaviour around cavern which can be useful for
 - o Deciding shape & geometry of cavern
 - o Deciding extent of rock support (by consider tensile/plastic zone)
- Parametric studies and comparison exercises for the stability of caverns and confirmation of assumed rock mass properties as input parameters are taken to
 - o Study modes of failure
 - o Identification of stress concentration
 - o Assessment of plastic zones requiring support
- Carry out back analysis of the available measurements to define the correct geotechnical and undisturbed stress state conditions.
- Carry out other calculation which incorporated the interaction between the rock mass and the engineering structure or rock mass and support.

Hence the main task of numerical methods in underground excavation is to characterize the rock mass into a mathematical model, the so-called 'rock mass modeling', which is described in next section. In addition, to define the computer code requirement is also

important since a wide range of commercial and in-house programs are available for solving the model. Prior to performing an analysis with rock mass model using a particular computer code, the suitability of the program should be determined. Verification with example analysis of problems for which a closed form solution is available (for example by using eq. (III.1-III.3)) should be performed and the computer results checked against those solutions. The user should verify that the program is capable of modeling the rock mass and represent the various support elements correctly.

III.2.i) Rock mass modeling

The rock mass is largely discontinuous, inhomogeneous, anisotropy and nonelastic. Therefore, the mathematical characterization of rock behaviour or a theoretical rock mass model is necessary to carry out the rock mechanical calculations that encompasses the idealization with respect to the geological structure, initial rock stress conditions, as well as the material models with the associated material parameters.

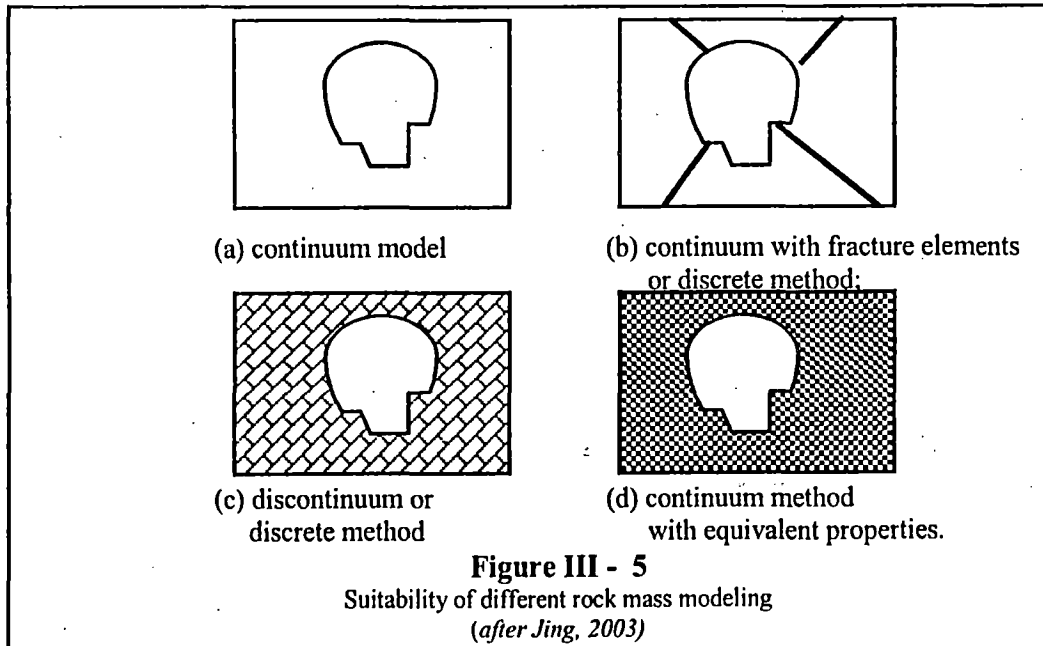
Ideally, to adequately represent the rock mass in computational models, capturing such fracturing and the complete nature of the rock mass -plus the consequences of engineering-, it is necessary to be able to include the following features during model conceptualization:

- the relevant physical processes and their mathematical representations;
- the relevant mechanisms and constitutive laws with the associated variables and parameters;
- the pre-existing state of rock stress (the rock mass being already under stress);
- the pre-existing state of temperature and water pressure (the rock mass is porous, fractured, and heated by a natural geothermal heat gradient or manmade heat sources)
- the presence of natural fractures (the rock mass is discontinuous);
- variations in properties at different locations (the rock mass is inhomogeneous);
- variations of properties in different directions (the rock mass is anisotropic);
- time/rate-dependent behaviour (the rock mass is not elastic and may undergo creep or plastic deformation);
- variations of properties at different scales (the rock mass is scale-dependent);
- the effects resulting from the engineering perturbations (the geometry is altered).

The extent to which these features can actually be incorporated into a computer model will depend on the physical processes involved and the modeling technique used. To adopt all

above features into a representative model is impracticable since not all-constitutive relations can be described by simple mathematical functions and the governing partial differential equations which are non-linear or otherwise insufficiently simple mathematically. Therefore the model is not perfect representation: but it has to be adequate for the purpose.

Traditionally, rock mass modeling is based on a completely continuous or a completely discontinuous approach. When a rock mass is modeled as a continuum, rock mass in problem domain subdivided into a finite number of sub domain (elements) whose behaviour is approximated by simpler mathematical descriptions with finite degrees of freedom. These subdomains must satisfy both the governing differential equations of the problem and the continuity condition at their interfaces with the adjacent element. This is so-called '*discretization of a continuum*'. It is an approximation of a continuous system with infinite degrees of freedom by a discrete system with finite degrees of freedom. This approach is suitable for rock masses with no fracture or with many fractures for which the behaviour being established through equivalent properties treated by a homogenization process (as shown in Figure III- 5 (a) & (d)). It can also be used if there is only no fracture in opening and no complete block detachment is possible. When a rock mass is modeled as a discontinuum, rock mass in problem domain is represented by an appropriate model using a finite number of well-defined components. The behaviour of each such component is either well known, or can be independently treated mathematically. The global behaviour of the system can be determined through well-defined inter-relations between the individual components (elements). This approach is most suitable for moderately fractured rock mass where the number of discontinuities are too large for equivalent-continuum approach, or where large-scale displacements of individual blocks are possible. (Figure III-5(c)). A simple graphical representation of continuum-discontinuum rock mass modeling is shown in Figure III-5.



In continuum and discontinuum perspectives, The most commonly applied numerical methods for rock mechanic problems are:

Continuum methods

- Finite Difference Method (FDM)
- Finite Element Method (FEM)
- Boundary Element Method (BEM)

Discontinuum methods

- Discrete Element Method (DEM)
- Discontinuous Deformation Analysis (DDA)

Hybrid continuum/discontinuum models

- Hybrid FEM/BEM,
- Hybrid DEM/BEM.
- Hybrid FEM/DEM, and
- Other hybrid models

Hybrid models are employed in order to maximize the advantages and minimize the disadvantages of each method since in most cases the continuity and discontinuity of the rock mass cannot be decoupled. The fully continuum methods cannot detect potential instabilities due to movement of individual blocks because they ignore block kinematics. On the other hand, in discontinuum methods the resolution of internal stresses inside block elements is less accurate and the possibility of intact rock failure may be overlooked (Jing,

2003). The concepts of continuum and discontinuum are therefore not absolute and problem specific. One example of the hybrid model can be seen in Figure III-6.

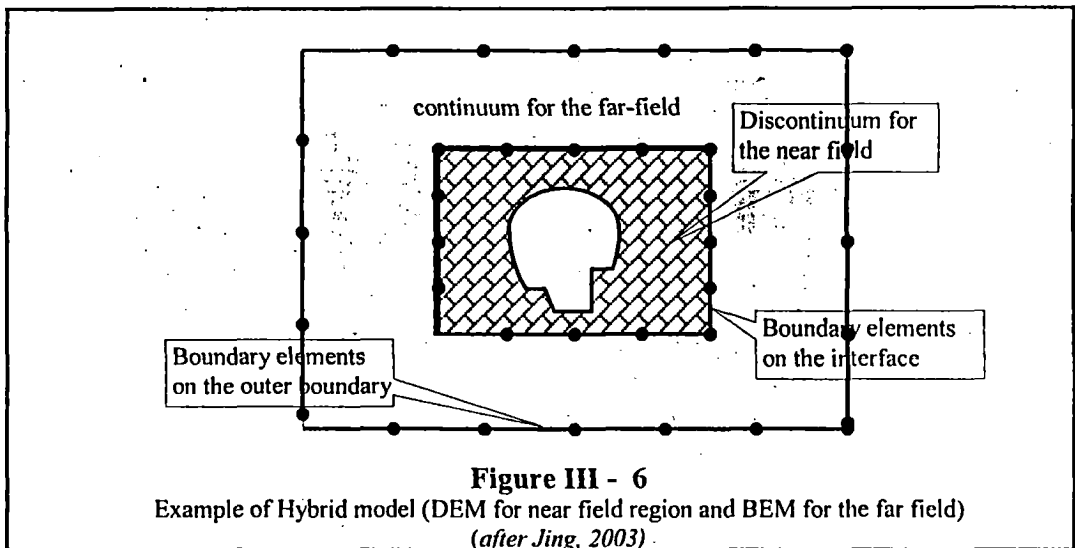
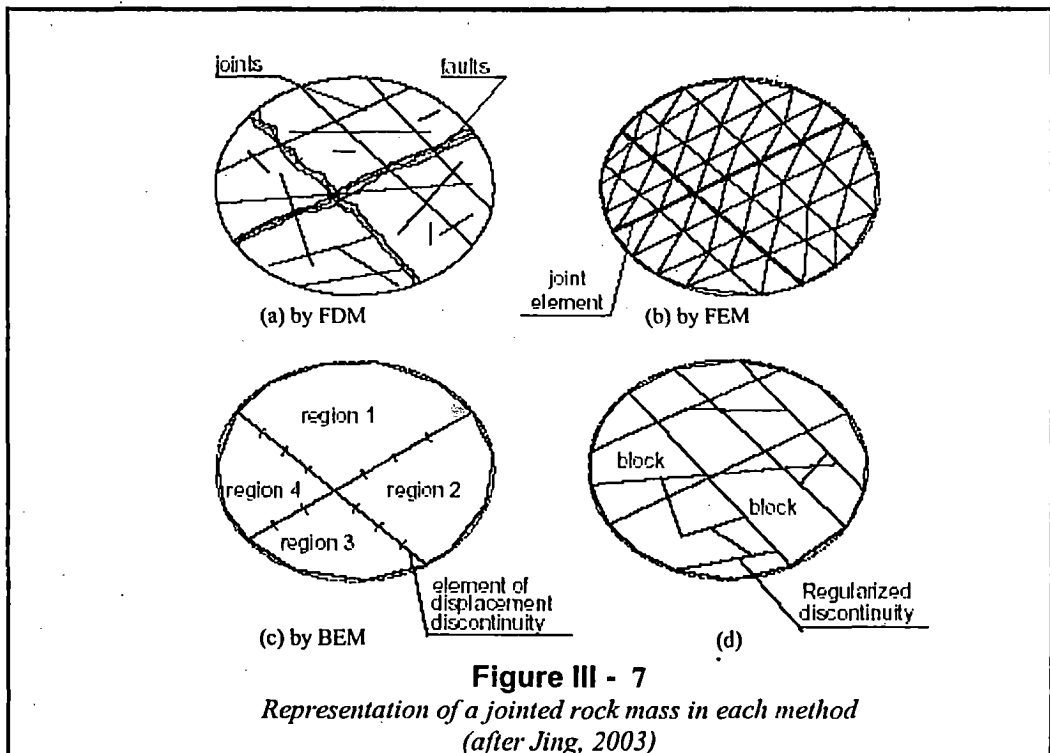


Figure III-7 illustrates the discretization concept of the FDM/FEM, BEM and DEM for discontinuous rockmass.



Out of all rock mass modeling above, only Finite Element Methods is discussed in detail in latter section since this method is chosen for modeling rock mass in the present study. Modeling of rock supports is discussed below.

III.2.ii) Modeling rock supports and construction sequences

The construction sequence of large rock cavern is complicated and involves many details. It is not practically possible to incorporate all these details in the numerical simulation. Excavation stages, blasting effects, material removal, lag-time in support installation, civil engineering structure interaction, etc. should be simplified into discrete steps. The following are a few examples of the possible simplification

III.2.ii.(1) Rock Support

Rock support for cavern typically are cast-in-place concrete arch for roof with thickness in a range of 0.5 m - 1.0 m or shotcrete of thickness in a range of 0.15 m - 0.35 m with wiremesh layers or steel fibers plus rock bolts and prestressed rock anchors. These supports can be modeled using the same type of elements as used to model the rock, but using material properties of the support material. Since the thickness is usually much less than the size of the opening, structural (beam) elements can be used to model the roof support. In modeling, these elements are preferred as they adequately capture bending behaviour of the support. Despite the fact that there is usually a time lag between the pouring of concrete (for concrete arch type) or application of shotcrete and the development of their full strength, a simple approach would be to simulate them at the stage when they develop its full strength. Example of modeling the concrete arch and shotcrete are shown in **Figure III-8**.

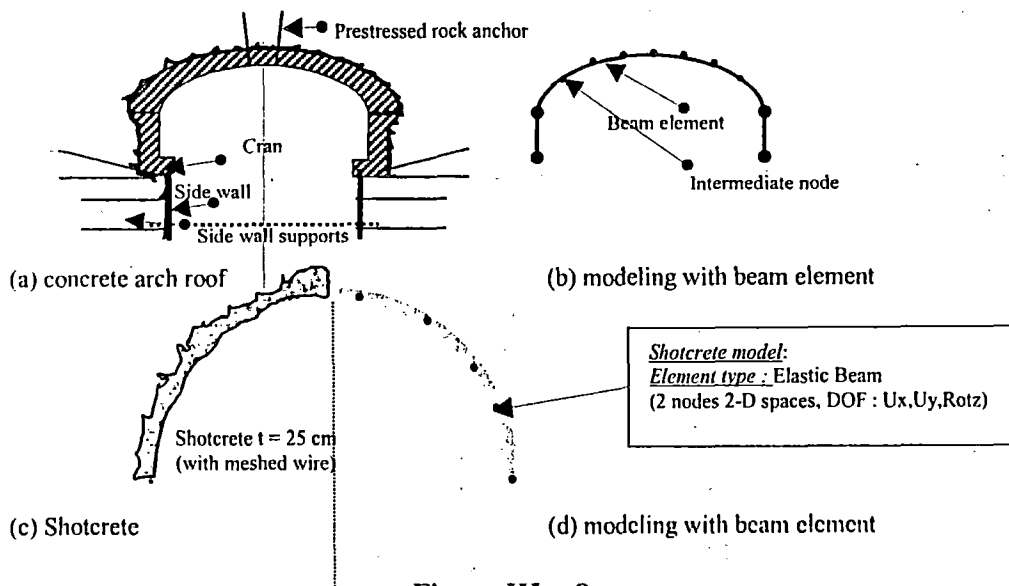


Figure III - 8
 Example of Modeling Roof support

In the present study, since it is shotcrete, it is modeled by beam element with nodes corresponding to rock mass element nodes (+ 1 intermediate node in order to make discrete closely to the arch shape and to make the deformation computation as accurate as possible).

For rock bolts (tensioned, grouted or ungrouted) or prestressing rock anchor, generally there are two options for modeling:

- By simply applying nodal forces corresponding to the capacity (design capacity or by insitu measurement with load meter) of the bolts/cables, also neglecting change in the rock mass shear strength in anchored zone.
- Using truss element (with DOF only axial force, no bending capability). It's stiffness follows the bar or cable's properties, neglecting the grout action, also neglecting the bearing plate role since it has a relatively minor role in providing support for overall system.

Particularly in prestressed rock anchor, computer code is now capable to incorporate prestressing effect into calculation so it's confining effect be more realistic to surrounding rock mass. In present study, rock bolts modeled by simply applying a pair of load at nodes near the ends of the bar position in geometry of problem domain (as per Figure III-9 (b)).

Example of modeling rock bolts is shown in Figure III - 9.

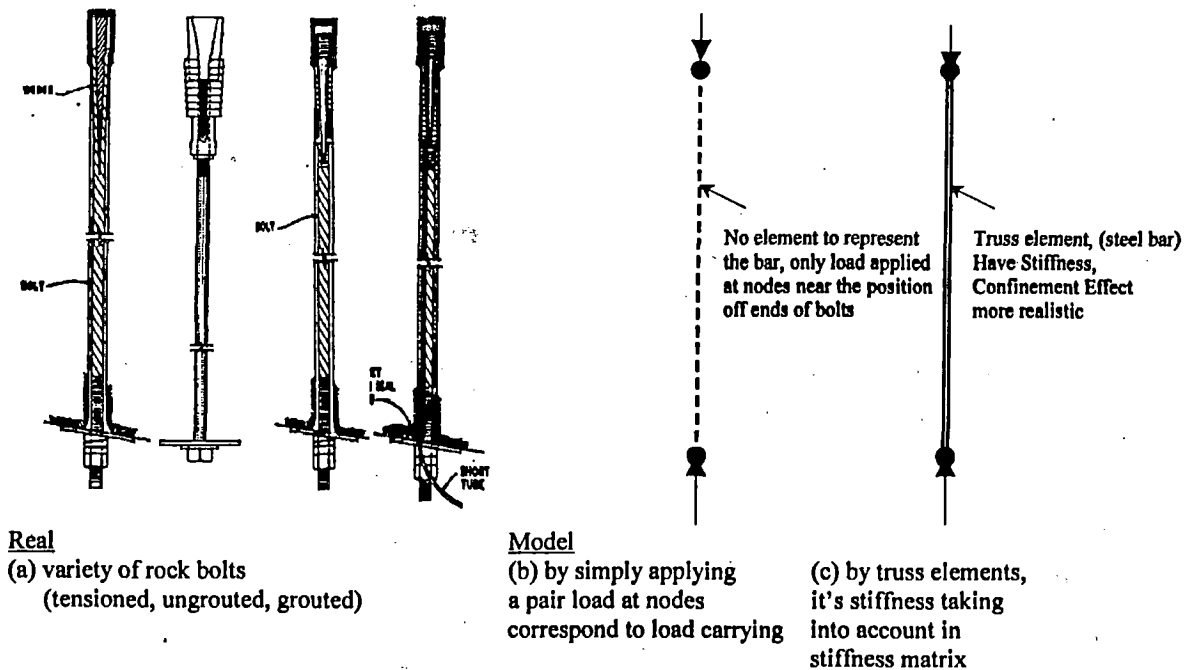
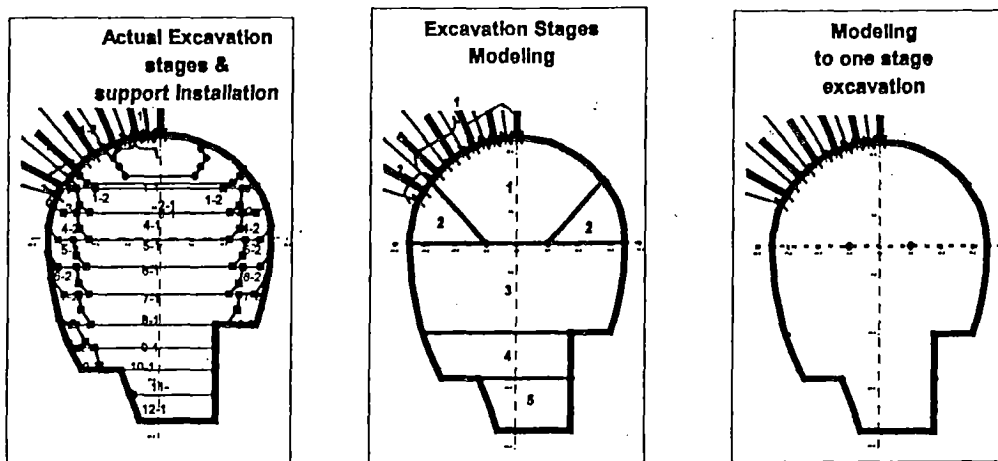


Figure III - 9
 Modeling Rock Bolts

III.2.ii.(2) Construction Sequences

Excavation sequences are usually modeled by simplifying the sequences, as long as these represent the same pattern. In 2D analysis the excavation stages can be modeled by reducing the number of stages to only one stage but it will affect the result proportionally. In 3D analysis, usually longitudinal sequences (benching) are not considered, hence each stage is assumed excavated at the same time. Example of the modeling the excavation sequences in 2D is presented in Figure III-10.



(a) actual excavation stages (b) model by reducing to less stages (c) model by reducing to one stage

Figure III - 10

Comparison between actual excavation stages and models

III.2.ii.(3) Civil Engineering Structures

Unless it is really required in design for some reason, civil engineering structure for cavern (massive foundation for draft tube, structural beam, machine floor slab, column, crane beam) are typically not taken into account for modeling, (even as external loading for cavern itself) as illustrated in Figure III - 11.

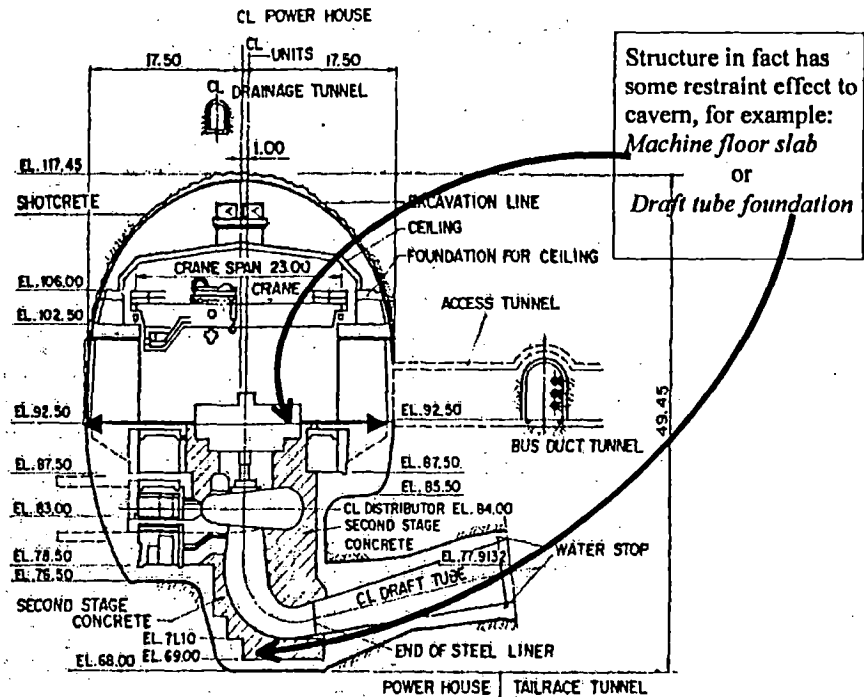


Figure III - 11

Concrete structure typically not considered in numerical analysis of Cavern

III.2.iii) Finite element analysis for rock mass

FEM has been the most popular numerical method for analysis of engineering structures, including underground structures. Its popularity is largely due to its flexibility in handling material inhomogeneity and anisotropy, complex boundary, plus many well-developed and verified commercial codes with large capacities in terms of computing power and user friendliness. Basically, three steps are required to complete a FEM analysis:

1. *domain discretization*, involves dividing the domain into a finite number of smaller sizes and standard shapes and select element type (triangle, quadrilateral, tetrahedral, etc) with fixed number of nodes at the vertices and/or on the sides;
2. *local approximation*, select a displacement trial functions, usually polynomial, and use it to approximate the behaviour of Partial Differential Equation at the element level and generate the local algebraic equations representing the behaviour of the element (*Strain/Displacement and Stress/strain relationships*); and derive Element Stiffness Matrix & Equations.

3. *assemblage and solution of the global matrix equation*, the local elemental equations are then assembled, according to the topologic relations between the nodes and elements, into a global system of algebraic equations whose solution then produces the required information in the solution domain, after imposing the properly defined initial and boundary conditions, solve the unknown degrees of freedom, solve for element stresses and strains, and interpret the results.

Typically (*note: derivation of structural matrices in the basic Finite Element Analysis can be seen in Appendix C*), a basic assumption in the FEM is that the unknown displacement function, u_i^e over each element, can be approximated through a trial function of its nodal values of the system unknowns, u_j^e in a polynomial form. The trial function must satisfy the governing Partial Differential Function (PDF) and is given by

$$u_i^e = \sum_{j=1}^M N_{ij} u_j^e \quad (\text{III. 11})$$

where

- N_{ij} = the shape functions (or interpolation functions),
 M = the order of the elements.

Using the shape functions, the original PDF of the problem is replaced by an algebraic system of equations written

$$\sum_{i=1}^N [K_{ij}^e] \{u_j^e\} = \sum_{i=1}^N (f_i^e) \text{ or } [K] u = [F] \quad (\text{III. 12})$$

where

- $[K_{ij}^e]$ = the coefficient matrix,
 $\{u_j^e\}$ = the nodal value vector of the unknown variables, and
 $\{f_i^e\}$ = comprised of contributions from body force terms and initial/
 boundary conditions.

For elasticity problems, the matrix $[K_{ij}^e]$ is called *the element stiffness matrix* given by

$$[K_{ij}^e] = \int_{\Omega} ([B_i, N_i, D]^T [D_i, B_i]) d\Omega \quad (\text{III. 13})$$

where

- $[D]$ = the elasticity matrix and
 $[B_i]$ = the geometry strain-displacement matrix

In case of linear behavior, $[K]$ is a linear factor of u , independent of the stress status and constant. The stress status is described by the stress tensor $\underline{\sigma}$, $\underline{\sigma} = \sigma(u)$. There are many available solution techniques for solving the eq. (II -13) (for elastic material), as implicit techniques which assemble systems of linear equations that are then solved using standard matrix reduction techniques –as in case elastic behaviour in the present study-.

For the case of nonlinear behavior (materially or geometrically) the $[K]$ is expressed as a function of the stress tensor: $[K]=[K(\underline{\sigma})]$, so the eq. (II – 12) is not valid. To succeed a solution for nonlinear problems, -as in the present study, the case with elastoplastic constitutive model, materially nonlinear-, vector $[F]$ is divided on i stages δF , called *increments*. The eq. (II –12) becomes then:

$$[K_{ep}] \delta u = \delta F + R_{i-0} \quad (\text{III. 14a})$$

$$\underline{\sigma}_i = \underline{\sigma}_{i-1} + \sigma(\delta u) \quad (\text{III. 14b})$$

$[K_{ep}]$ is a linear factor and it equal with $[K(\underline{\sigma})]$ depending on the $\underline{\sigma}$ (stress tensor) of the current increment, δu are the displacements induced by the increment δF . R_i is the residual (equilibrium gap) that it may effaced after j iterations :

$$[K_{ep}] \delta u = R_{i-j} \quad (\text{III. 15})$$

Eq. (III. 15) should converge after j iterations to obtain the solution, and solution techniques for solving that equation is accounted for by modifying stiffness coefficients (*secant approach*) and/or by adjusting prescribed variables (*initial stress* or *initial strain approach*). These changes are made in an iterative manner such that all constitutive and equilibrium equations are satisfied for the given load state.

For application of FEM in rock mass analysis, especially for cavern analysis, ideally the basic factors to be taken into account in the analysis are:

- The insitu stress state before excavation (should be from field measurement)
- Rock mass properties
- Rock supports pattern (+ material properties and prestressed load applied)
- Excavation sequences can be assumed in one stage
- Material properties approach could be linear elastic or elastoplastic (with yield criteria should be chosen as most representative for the rock behaviour)
- Analysis can be in 2D plane strain and only single cavity considered

- Element types can be triangular (with 6 nodes) if displacement field is in interest or tetrahedral (with 8 nodes), for accuracy in term of displacement, element have midside nodes always better.

And if advanced 'class A' FEM analysis is in demand, there should be additional factors to be considered in analysis, i.e.:

- The jointed structure of rock mass i.e. the explicit modeling of major discontinuities by joint element (the number of joints in the rock mass is many and it is not possible to obtain information about all of them; thus, it is not possible to deal with each joint individually).
- The anisotropy of the deformation and strength characteristics of rock blocks
- The nonlinearity (time-dependent of rock material)
- The viscoelastic/viscoplastic behaviour of rock material
- The constructional sequences as accurate as possible
- Analysis in 3D and considering the vicinity cavity

For a FEM analysis of rock mass, before undertaking an analysis, there should be preparatory effort resulting in:

1. developing a sense for what the final answer should be
2. obtaining insight on what parts of the problem are important and should be carefully modeled, and
3. defining the objective(s) for the more advanced finite element analysis

and the input parameters which should be considered are :

- Geometry of problem domain (opening + far-field boundary)
- Overburden
- Rock mass properties
 - o For elastic linear analysis: *density, deformation modulus, poisson ratio, natural stress ratio (k)*
 - o For elastoplastic analysis: plus parameters depend on yield criteria to be chosen, *rock mass strength (compressive & tensile)*
- Supports material properties (shotcrete, rock bolts, PS anchor, concrete).

Advantage of Finite Element method in rock mass modeling

- well-established tools with many developed general-purpose codes, make analysis and computation easier, user-friendly, and easy-to-understand, with efficient pre- and postprocessors allow the user to perform parametric analyses and assess the influence of approximated far-field boundary conditions by special '*infinite element*'.
- well suited to solving problems involving heterogeneous or non-linear material properties, since each element explicitly models the response of its contained material.
- joints can be represented explicitly using specific '*joint elements*', and joint interfaces may be modeled using quite general constitutive relations.

and its disadvantage are:

- cannot perfectly simulate the rock mass to be modeled, whether in 3D or 2D analysis, since discontinuous rock mass is randomly present.
- not well suited to modeling infinite boundaries, such as occur in underground excavation problems.
- the efficiency will decrease with too high number of DOF, which are in general proportional to the numbers of nodes.
- cannot handle large displacement caused by rigid body motion of individual elements. (as sometime presented in discontinuous rock mass).
- as other numerical methods, the reliability of the computation result will depend on how reliable the input parameter.

The Finite Element Method is employed for the present study through a computer code ANSYS Ver. 5.4 for processing the computation required.

III.3 ANSYS

ANSYS is a general-purpose finite element modeling package for numerically solving a wide variety of structural/mechanical problems. These problems include: static/dynamic structural analysis (both linear and non-linear), heat transfer and fluid problems, as well as acoustic and electro-magnetic problems. ANSYS can handle easily the static structural analysis computation, either linear or nonlinear.

Capabilities of ANSYS include all types of nonlinearities: large deformations, plasticity, creep, stress stiffening, contact (gap) elements, hyperelastic elements, etc.

Analysis Procedures in ANSYS

The procedure for a static analysis in ANSYS basically consists of three main steps:

- Building the model;
- Apply loads and obtain the solution;
- Review the results.

Detail of these three main steps is:

III.3.i) Building a Model

Building a finite element model requires more of computation time than any other part of the analysis. After specifying a title for analysis file (so-called *jobname*) then the general PREPROCESSOR (ANSYS called PREP7) can be used to define the element types, element real constants, material properties, and the model geometry. As a note, the ANSYS program does not assume a system of units for analysis. (hence units must be consistent for all input data.)

Defining Element Types: The ANSYS element library contains more than 150 different element types. The element type should be defined by name and give the element a type reference number.

Each element type has a unique number and a prefix that identifies the element category: BEAM3, PLANE2, SOLID96, etc. The element type determines, among other things: The degree-of-freedom set and whether the element lies in two-dimensional or three-dimensional space. In our present study, element type chosen is: BEAM3 elastic beam element for shotcrete modeling, and PLANE2, triangular plane strain element for rock medium modeling. It is important to note that the FEM implementation for the continuum elements such as the CST/LST are normally developed using displacement functions of a polynomial type to represent the displacements within the element, and the higher the polynomial, the greater the accuracy. The ANSYS six-node triangle as PLANE2 uses a quadratic polynomial and is capable of representing linear stress and strain variations within an element.

Defining Element Real Constants: Element real constants are properties that depend on the element type, such as cross-sectional properties of a beam element. For example, real constants for the 2-D Elastic beam element BEAM3 are area (AREA), moment of inertia

(IZZ), etc. Not all element types require real constants, and different elements of the same type may have different real constant values.

Defining Material Properties: Most element types require material properties. Depending on the application, material properties can be linear, -can be isotropic or orthotropic-, or nonlinear -such as plasticity data (stress-strain curves for different hardening laws)-. As with element types and real constants, each set of material properties has a material reference number. Our present study using two types of material model available in ANSYS library, *isotropic linear elastic* and *nonlinear elasto plastic with Drucker-Prager* criteria.

Creating the Model Geometry: Once material properties have defined, the next step in an analysis is generating a finite element model - nodes and elements - that adequately describes the model geometry. In ANSYS there are two methods to create the finite element model: solid modeling and direct generation. With *solid modeling*, the geometric shape of the model described, then as per instruction the ANSYS program automatically *mesh* the geometry with nodes and elements. The size and shape in the elements that the program creates can be easily controlled. Two-dimensional geometry as in present study is built from keypoints, lines (straight, arcs, splines), and areas. These geometric items are assigned numbers and can be listed, numbered, manipulated, and plotted. With *direct generation*, the location of each node and the connectivity of each element "manually" defined. Several convenient operations, such as copying patterns of existing nodes and elements, symmetry reflection, etc. are available. As the note; geometry for FEM analysis also can be created with solid modeling CAD or other software and imported into ANSYS. The IGES (Initial Graphics Exchange Specification) neutral file is a common format used to exchange geometry between computer programs.

III.3.ii) Apply Load and Obtain the Solution

In this step, SOLUTION processor is used to define the analysis type and analysis options, apply loads, specify load step options, and initiate the finite element solution.

Defining the Analysis Type and Analysis Options: The analysis type chosen based on the loading conditions and the response wish to calculate. The following analysis types can be performed in the ANSYS program: static (or steady-state), transient, harmonic, modal, spectrum, buckling, and substructuring. Once the analysis type and analysis options have defined, the next step is to apply loads.

Applying Loads: The word *loads* as used in ANSYS includes boundary conditions) as well as other externally and internally applied loads. Load Types in ANSYS are:

- *Displacements* : These are DOF constraints usually specified at model boundaries to define rigid support points. They can also indicate symmetry boundary conditions and points of known motion. The directions implied by the labels are in the nodal coordinate system.
- *Forces and moments:* These are concentrated loads usually specified on the model exterior. The directions implied by the labels are in the nodal coordinate system.
- *Pressures (PRES):* These are surface loads, also usually applied on the model exterior. Positive values of pressure act towards the element face (resulting in a compressive effect).

Initiating the Solution: To initiate solution calculations, the ANSYS program takes model and loading information from the database and calculates the results. Results are written to the results file and also to the database.

III.3.iii) Review the Results

Once the solution has been calculated, ANSYS postprocessors can be used to review the results. Contour displays, deformed shapes, and tabular listings can be obtained to review and interpret the results of the analysis. Many other capabilities are: error estimation, load case combinations, calculations among results data, and path operations, arithmetic calculations and complex algebra. Results from an analysis are written to the file and consist of the following data:

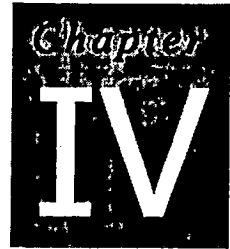
Primary data:

- Nodal displacements (UX,UY)

Derived data:

- Nodal and element stresses (SX,SY)
- Nodal and element strains
- Element forces
- Nodal reaction forces, etc.

Stepwise procedure analysis of one of model in present study is presented in **Appendix C** and explanation of capabilities of element to be chosen (BEAM3 and PLANE2) from ANSYS material library can be seen in **Appendix D**.



CASE STUDY: CAVERN HPP CIRATA INDONESIA

IV.1 SALIENT FEATURES OF CIRATA HYDROELECTRIC POWER PLANT (INDONESIA)

In the northern part of West Java province, the Citarum River Basin has been intensively studied for hydropower development. Presently, there are 3 projects in operation. Out of them, the Cirata site has the largest capacity (4x125 MW at 1st stage and 4x125 MW at 2nd stage, total 1000 MW, cavern excavation for both stages is done at the same time).

P.L.N. Inc, the Indonesian National Electricity Company, initiated consultant service from Japan (NEWJEC co. associated with local consultant companies) in 1983. The feasibility study which was first carried out followed by a detailed design completed in 1984.

Powerhouse at Cirata located at Cirata Village, Purwakarta District, about 150 km from Jakarta and 60 km west of Bandung City (Figure IV-1). The Cirata power plant complex includes the main components as mentioned in Table IV - 2. Location of the project site can be seen in Figure IV-1.

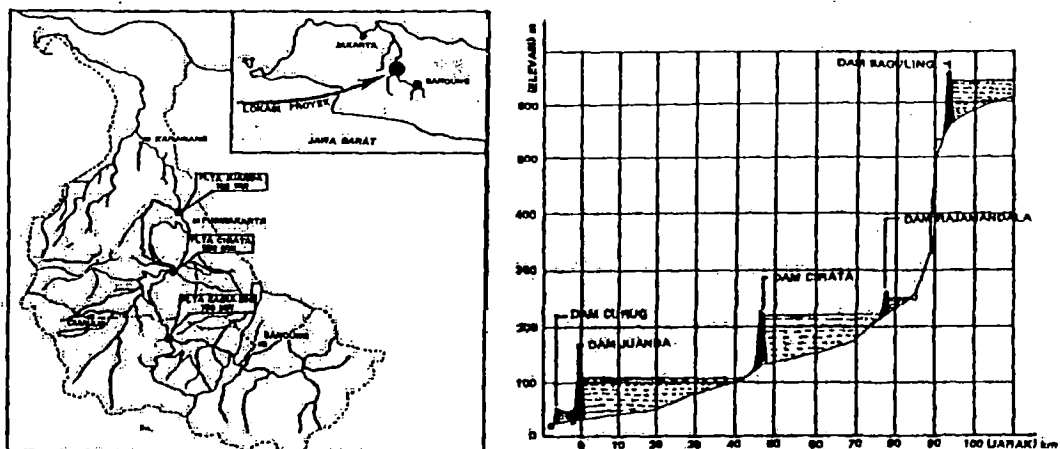


Figure IV - 1
Location of HPP Cirata in Java Island, Indonesia

From geological standpoint, the Cirata site concerns tertiary and quaternary formation (*Gamma epsilon*, 1991 for Stage II). As regional geology, the stratigraphy of the Cirata site and its surroundings consist of the following formations: (a) *Jatiluhur Formation*, consist of marl and quartz sandstone ; (b) *Cantayan Formation*, consist of *polymict Breccia*, claystone and sandstone; (c) *Hornblende Tuff*; (d) *Older alluvium*; and (e) *Older Volcanic* as laharic breccia. The breccia – rocks of the tertiary Cantayan formation exposed at the powerhouse site consist of *lapilli tuff*, *andesite*, *tuff breccia* and sheared layers. Rock grade is mostly about C1 and B (RMR value of between 55 and 72). Within sheared zones and fractured layers rock grade is RMR 18-28. Intensity of dissection of the rock mass by joints and other fractures as well as the continuity of discontinuities varies considerably. From the geological records it was obvious that the most pervasive major discontinuities would be of large continuity. All major discontinuities were steeply dipping, striking about SE or NW, that is oblique to the powerhouse axis. Sketch map of extensive discontinuities exposed at the cavern wall is presented in Figure IV-2.

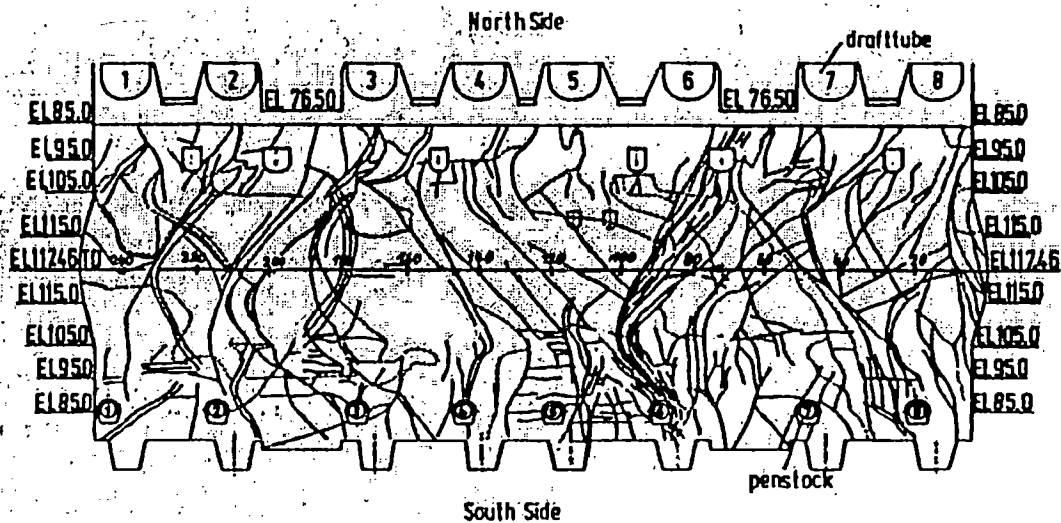


Figure IV - 2
Sketch map of extensive discontinuities exposed at the cavern wall

IV.2 POWERHOUSE TYPE AND BASIC LAYOUT

At design stage, size and basic layout of powerhouse was mainly dictated by the space demand for installation, operation and maintenance of eight turbine-generator units to be installed in a single cavern. Economics dictated a layout of the water conductor system with the axis of powerhouse oriented about parallel to the river course at the outlet area which is also about the same as the strike direction of the rock strata. Generally this would be

considered unfavorable because the bedding planes of the volcanic breccia and andesite rocks were believed to be not well developed and constitute no pronounced direction of lower shear strength, the orientation parallel to river course was considered acceptable. If the powerhouse axis oriented perpendicular to the strike, the tailrace tunnel would have been longer requiring tailrace surge tanks to avoid negative pressure, also waterway arrangement would have been much more complicated and requiring higher construction cost. Egg-shaped cross section was chosen in accordance with results of numerical modeling by finite element analysis and experience elsewhere (*Reik, 1986*). Under the given rock conditions and assumed primary stresses the egg-shaped cross section leads to a much more favourable stress distribution. Layout of cavern and adjacent tunnels is shown in **Figure IV -3**.

IV.3 SUPPORT ARRANGEMENT

Supports are combination of shotcrete, rock bolts and rock anchors for Cirata Power cavern. Length of rock bolts and rock anchors were designed by the aid of finite element analysis. The stresses calculated for each element were compared with the stresses at failure criteria. (A *Mohr-Coulomb* failure criterion was assumed to apply). Assuming that rock anchors should have their anchoring section in rock with a certain value of safety factor (*SF* of 1.5 for rock anchors and 1.2 for rock bolts). Following requirements was worked out:

Table IV - 1

| Rock support arrangement | | |
|--------------------------|-------|----------|
| | Crown | sidewall |
| Rock bolt | 7 m | 5 m |
| Rock Anchor | 15 m | 20 m |

The number of anchors, rock bolts and the thickness of shotcrete was based on experience elsewhere and not from FE analysis. Its adequacy was checked by limit equilibrium analysis of falling (roof) or sliding wedges (side-walls). The support pattern is shown in **Figure IV-4**.

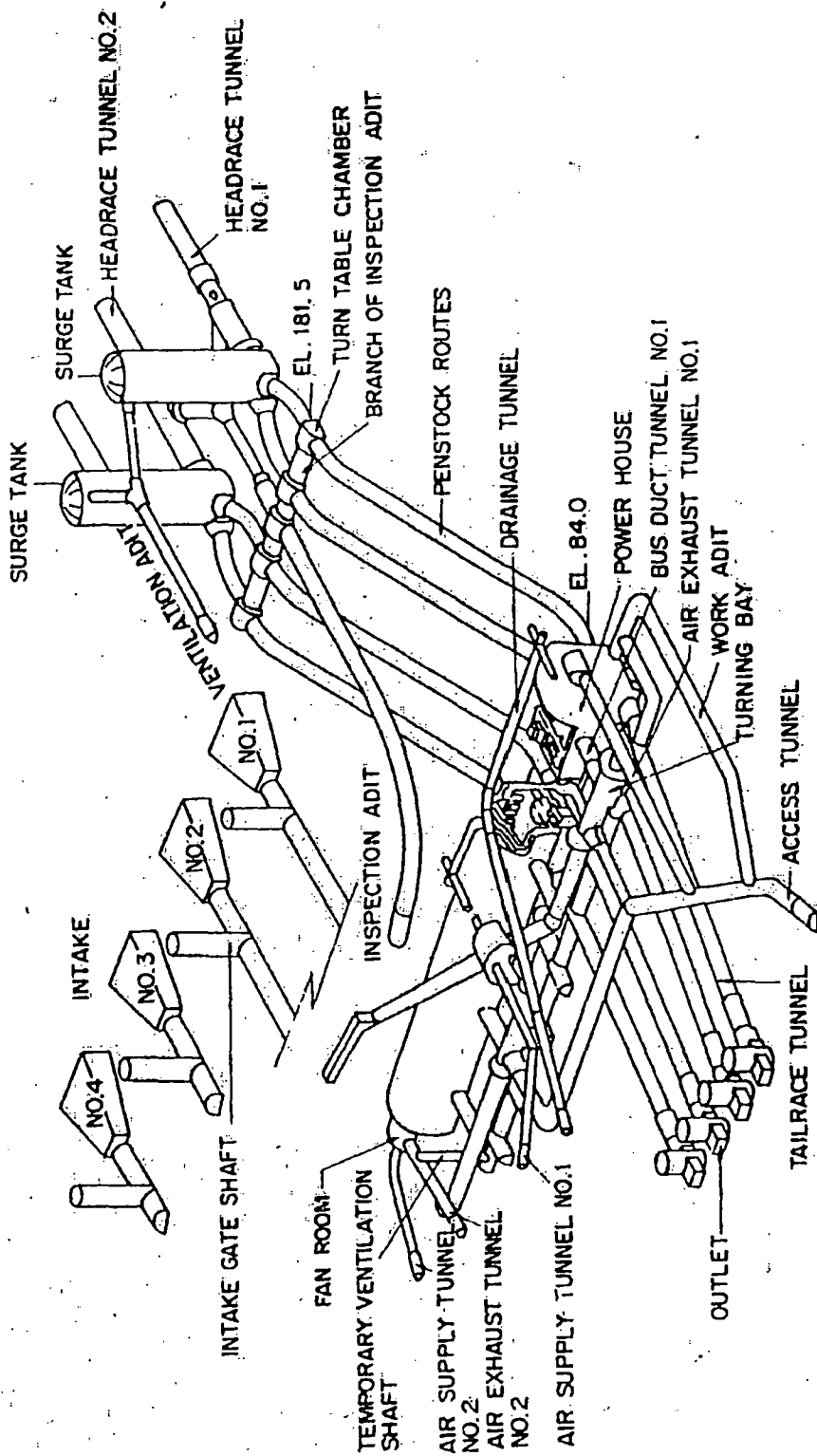


Figure IV - 3

Layout of cavern and adjacent tunnels

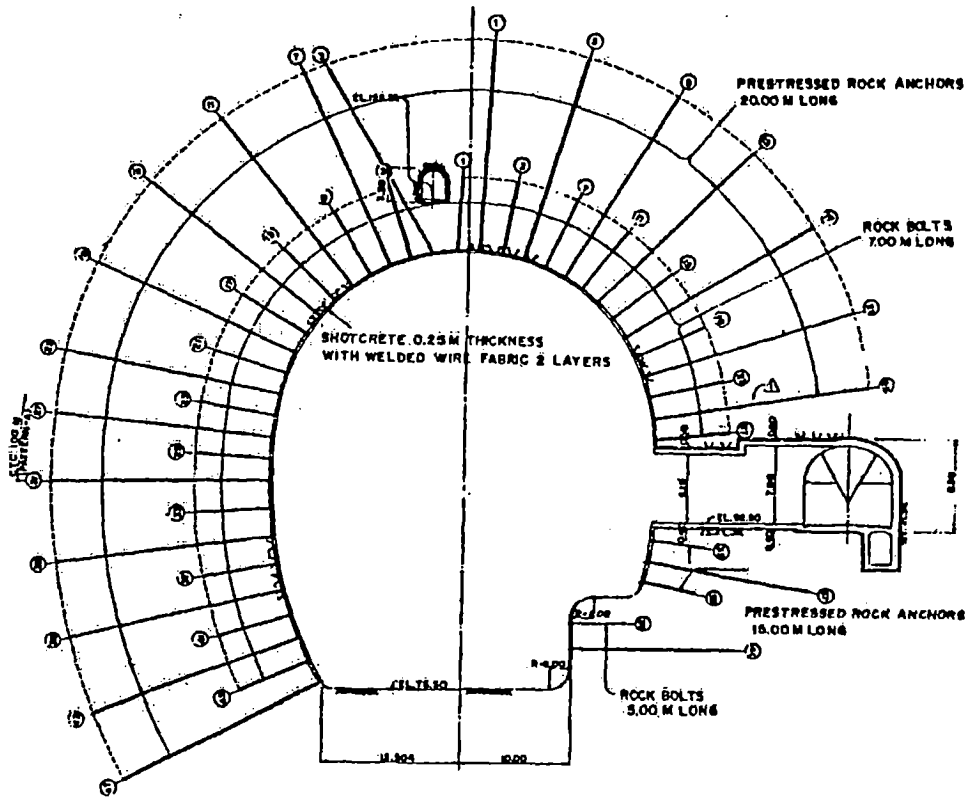


Figure IV - 4

Design Support Arrangement of rock bolts (tensioning 100 kN) and prestressed rock anchors (1000 kN)

IV.4 EXCAVATION STAGES AND MONITORING PROGRAMME

To avoid loosening of the rock mass before installation of the appropriate support, excavation of the Cirata cavern was to be carried out in 12 benches (as shown in Figure IV - 5).

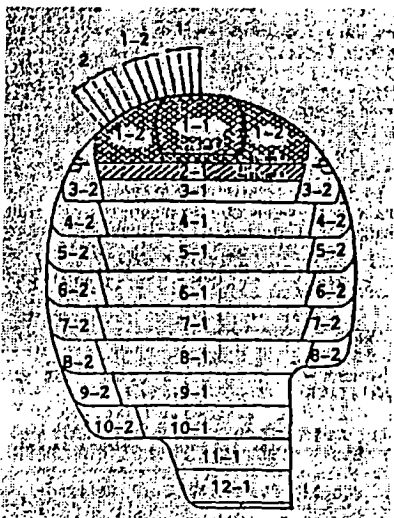


Figure IV - 5

Sequences of Excavation and support installation
(After Reik, 1986)

For each bench the central part was excavated first followed the rock close to the cavern perimeter in the second step by controlled blasting. Support was installed quickly after partial sidewall excavation of each bench.

Beside the design & construction of HPP Cirata project described above, the following information on monitoring program shown in Figure IV - 6 (a) and (b) show location of monitoring points is useful for this study.

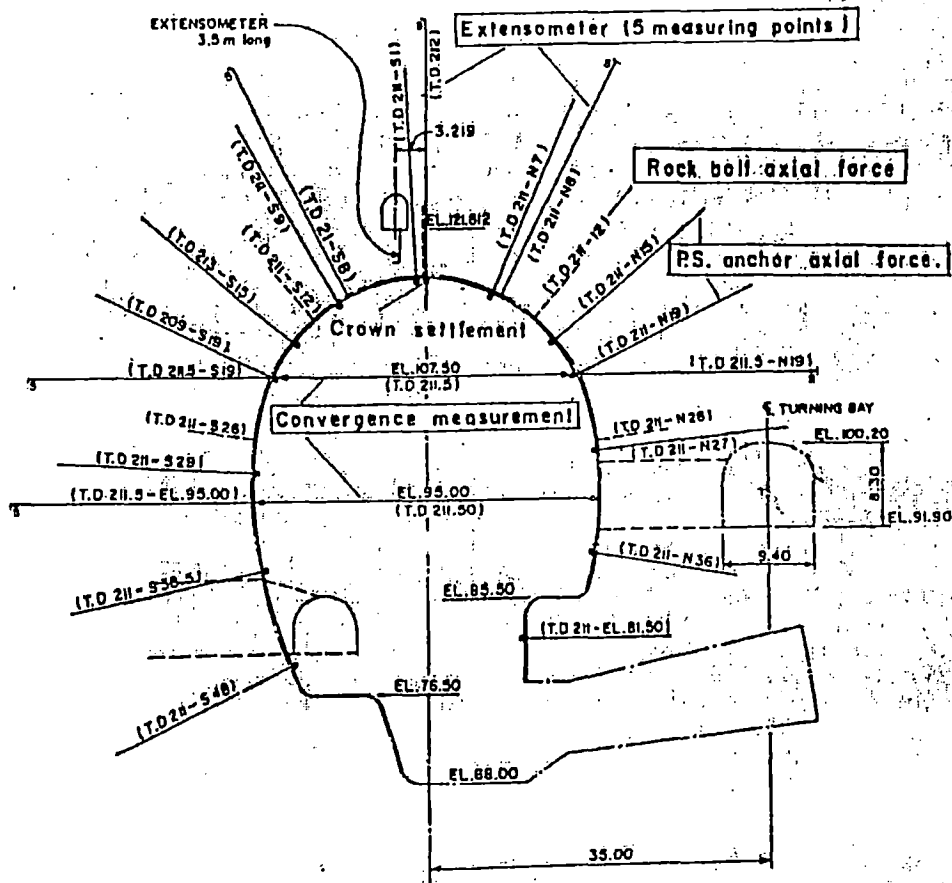


Figure IV - 6 (a)
Typical main monitoring cross-section (After Reik, 1986)

Thirteen main measuring cross sections have been installed, with additional instruments in the areas where large deformation were expected according to the geological structure. About 10 % of all PS anchors have been equipped with axial force meters for remote reading. Most measuring devices could only be installed from inside the powerhouse sometime after excavation. They could therefore not record the displacements which took place immediately upon excavation at the point of

This type of analysis is based on the evaluation of strain distribution around opening obtained by measured displacement. By back analysis the initially existing stress and material constants for 'calculation cross-section' is thus evaluated from measured displacements, and then used as input data in an ordinary finite element analysis to obtain strain distribution of present stages of excavation.

Table IV - 2

Main Features of the Cirata Hydro Power Complex

MAIN SCALE

| | | | |
|------------------------|---|-------|-------|
| Installed Capacity | : | 1000 | MW |
| Maximum Discharge | : | 540 | cumec |
| Maximum effective head | : | 112.5 | m |

OUTPUT

| | | | |
|-------------------------|---|------|-------|
| Gross Head (max) | : | 117 | m |
| Gross Head (min) | : | 102 | m |
| Minimum output | : | 872 | MW |
| Annual Generated Energy | : | 1424 | GWh |
| Firm discharge | : | 140 | cumec |
| Peak discharge | : | 540 | cumec |

STRUCTURE SCALE

DAM

| | | | |
|---------------|---|------------------------------------|---|
| Type | : | Concrete faced rockfill dam | |
| Height | : | 125 | m |
| Crest Length | : | 453 | m |
| Volume of Dam | : | 3900.000 cumec | |

SPILLWAY

| | | | |
|---------------|---|---|-----------------------------------|
| Type | : | Tunnel type spillway connected with Diversion Tunnels | |
| Max. capacity | : | 2600 | cumec (with 3 gates in operation) |
| Gate | : | Four radial gates, (8.6mx15.5m) | |
| Number | : | 2 | |
| Cross-section | : | Circular with gradual diameter of 10 m to 25 m | |

DIVERSION TUNNELS

| | | | |
|---------------|---|-----|------------------------|
| Length | : | 800 | m each approx. |
| Cross-section | : | 10 | m diameter of circular |
| Number | : | 2 | |

BOTTOM OUTLET WORKS

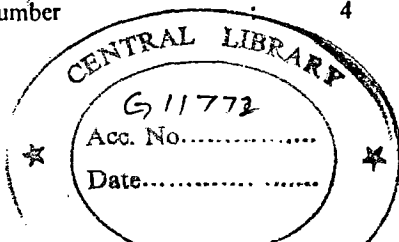
| | | | |
|----------------|---|---|---------------------|
| Location | : | Separated Tunnel | |
| Type | : | Hollow-Bunger cone valve with butterfly guard valve | |
| Number | : | 1 | |
| Max. Discharge | : | 100 | cumec approximately |
| Cross-section | : | Horse shoe shape (4.0 m x 4.5 m) | |

INTAKE

| | | | |
|----------|---|------------------------------|------------|
| Type | : | Side intake with gate shafts | |
| Capacity | : | 540 | cumec max. |
| Number | : | 4 | |

HEADRACE TUNNEL

| | | | |
|---------------|---|-----|-------------------------------|
| Length | : | 690 | m each (Approximately) |
| Cross-section | : | 8.4 | m inside diameter of circular |
| Number | : | 4 | |



SURGE TANK

| | | |
|-----------------|---|----------------------------------|
| Type | : | Circular restricted orifice type |
| Inside diameter | : | 18.6 m |
| Height | : | 80 m |
| Number | : | 4 |

PENSTOCK TUNNEL

| | | |
|-------------------------------|---|-----------------------------------|
| Length | : | 200 m approx. |
| Cross-section of steel lining | : | 5.2 m inside diameter of Circular |
| Number | : | 8 |

UNDERGROUND POWERHOUSE

| | | |
|--------|---|-------------------------|
| Type | : | Egg-shaped, underground |
| Width | : | 33 m |
| Length | : | 280 m |
| Height | : | 49.6 m |

TAILRACE

| | | |
|---------------|---|-----------------------------------|
| Length | : | 138 m Approx. |
| Cross-section | : | 6.4 m inside diameter of circular |
| Number | : | 8 |

TURBINE

| | | |
|--------|---|------------------------|
| Type | : | Vertical shaft Francis |
| Output | : | 129,600 kW |
| Speed | : | 187.5 rpm |
| Number | : | 8 |

GENERATOR

| | | |
|----------|---|------------------------|
| Type | : | AC 3-Phase synchronous |
| Capacity | : | 140,000 KVA |
| Number | : | 8 |

.....



ANALYTICAL PROGRAM

V.1 INTRODUCTION

To achieve the objectives set forth for the present study, the analytical program has been divided into the following main tasks:

- Model Preparation
 - o General
 - o Finite Element Model
- Model Calibration
- Results and Discussion in Chapter VI

V.2 MODEL PREPARATION

V.2.i) General

Two different 2-D FEM plane-strain model geometry details (named **Model I** and **Model II**) are prepared. These models use the finite element code ANSYS. Both models incorporate material behaviour as linear elastic and elastoplastic (*Drucker-Prager* yield criterion). The differences in these two models are:

1. The top far-field boundary (ground surface) of **Model I** is flat as it can accept the symmetric horizontal ground pressure from both left & right sides boundary. In **Model II**, the top far-field boundary follow the contour of the actual ground profile (*LAPI ITB, 1995 and Kamemura et. Al, 1986*).
2. Horizontal ground stress in **Model I** applied as pressure at both sides far-field boundary so it will confine entire body of rock medium, on the contrary, since the type of asymmetric domain as in **Model II** can not accept horizontal pressure at side far-field boundary (will make the domain unstable due to unbalanced pressure), horizontal pressure is applied -varies with depth-, along the cavern periphery.

Figure V - 2 & Figure V - 3 show the difference between the two models.

Loading condition, rock mass properties and support

For simulating the insitu stress field before excavation, the rock mass medium is subjected to insitu ground stress acting on biaxial directions. Vertical ground stress (σ_v) assumed equal to over burden and Horizontal ground stress (σ_h) is equal to vertical ground stress ($k=1.0$) (Kamemura, 1986). Hydrostatic groundwater pressure was not considered in the loading condition since there should be *weepholes* designed to relieve water pressure in the walls and roof of the cavern. Material properties to be incorporated in the model are based on the data from previous report (LAPI ITB, 1995 & Kamemura, 1986), and is given in Table V - 1. Support system which taken into computation are: rockbolts, length 7.0 m, prestressed rock anchor with length 20.0 m and shotcrete with thickness 25 cm. Spacing between rockbolts as well as between prestressed anchors are @ 4.0 m, and spacing of rockbolts with prestressed anchor @ 2.0 m.

V.2.ii) Finite element model

Preliminary finite element model of two of the rock medium model has been developed as for initial condition (initial condition is to obtain the insitu stress before excavation by applying gravity force and horizontal ground stress to the rock medium in problem domain). The mesh of initial condition of the two basic models are presented in Figure V - 4 & Figure V - 5. This model will serve as a benchmark for other models, particularly for deformation results. Hence the displacements due to initial condition have not been accounted for as those displacements had already taken place before excavation. Other models are then prepared to take into account the effect of opening as well as support system. Mesh pattern of other models is presented in Figure V - 6 and Figure V - 7. These figures show that the elements not distributed uniformly in entire rock mass body, since around opening usually occurs stress concentration, near stress concentrations the stress gradients vary quite sharply. To capture this variation, the number of elements near the stress concentrations must be increased proportionately. Hence from far-field boundary to periphery of cavern the so-called '*element density*' is gradual increasing. Support system model can be seen in Figure V - 8. Shotcrete is modeled with beam element having thickness 25 cm along periphery cavern, and rock bolts and prestressed rock anchor are modeled by applying a pair of external force on nodes near the position of their both ends to represent their confinement effect.

The models prepared can be grouped as follows, both for **Model I** and **Model II**: - Models for initial condition; -Models for opening without supports; -Models for opening with supports; and consists of:

- **Model I**
 - o 56 beam elements to model shotcrete (*BEAM 3*)
 - o 452 CST triangular plane strain for model rock mass (*PLANE2*),
 - o 948 nodes
- **Model II**
 - o 56 beam elements to model shotcrete (*BEAM 3*)
 - o 606 CST triangular plane strain for model rock mass (*PLANE2*),
 - o 1270 nodes

Figure V-1 show the illustration of *BEAM3* and *PLANE2*, and detail description for element *BEAM3* and *PLANE2* are presented in Appendix D.

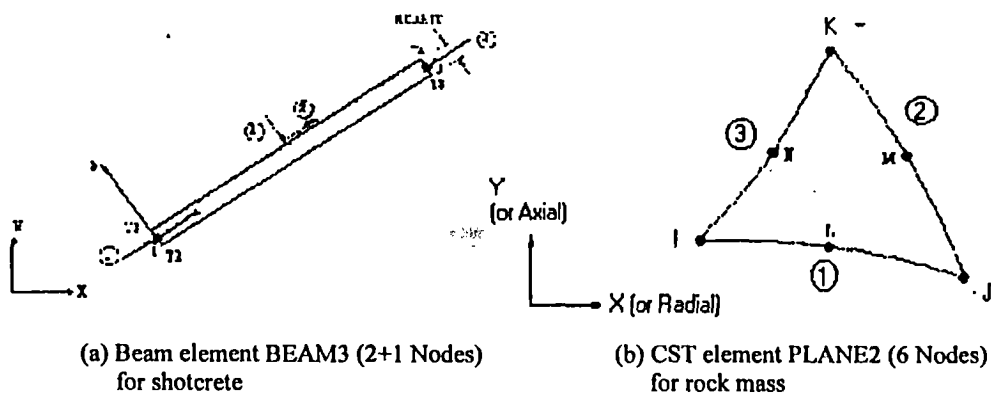


Figure V - 1

Illustration of typical elements used

V.2.iii) Model Calibration:

The model has been calibrated by preparing another model with circular opening shape (all material properties, element types, same as **Model I & II**, except the shape was full circular) and compared it's stress field results with closed form solution for circular shaped as in eqs. III-1 & III-2. The mesh pattern for additional model is presented in **Figure V - 9**. Since the domain is symmetric, only half section has been analyzed. The result, in term of

sidewall stress concentration is shown in Table V - 2. From the comparison, it may be noted that the difference in magnitude of σ_y/σ_v between FEM result and exact solution may be due to two main reasons: Firstly, the difference in assumption of σ_v , in exact solution σ_v is equal at every point of depth (assumption of exact solution is opening in infinite depth), but in FEM model σ_v varies with the depth from ground surface (for radius 17.5 m it is enough to make differences in results). Secondly, in exact solution stress field is independent of elastic constant and dimension of opening, but in FE analysis material properties and dimension will affect its stiffness matrix as well as the results. From Table V-2 it can be seen that for 10 % difference between FEM results and exact solution, we can consider the stress field only up to 4 times radii of cavern.

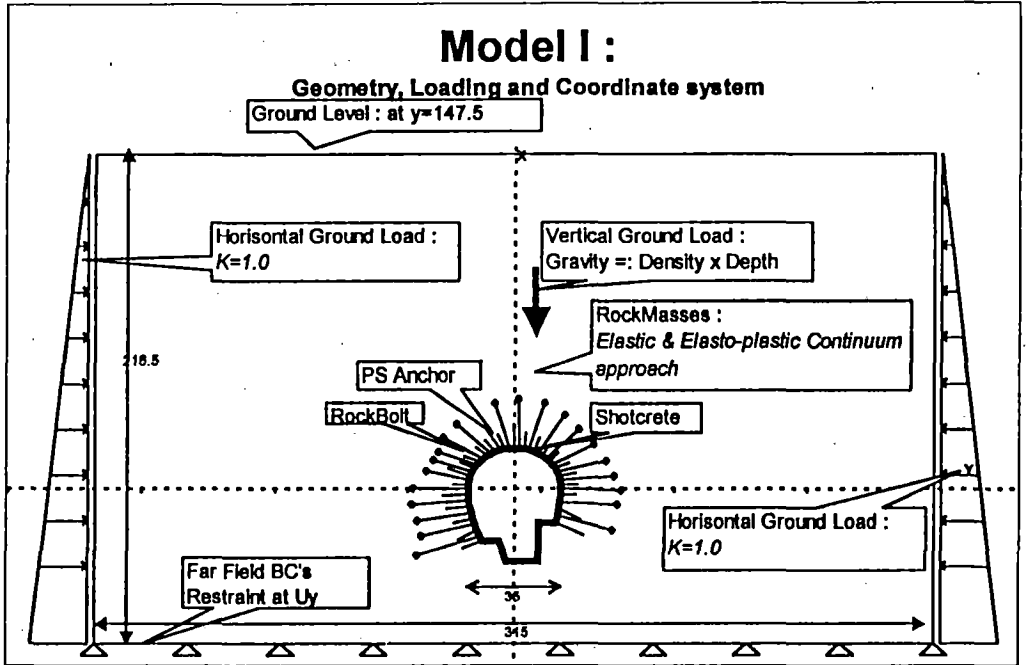


Figure V - 2
 Model I: Geometry, Loading condition, and coordinate system

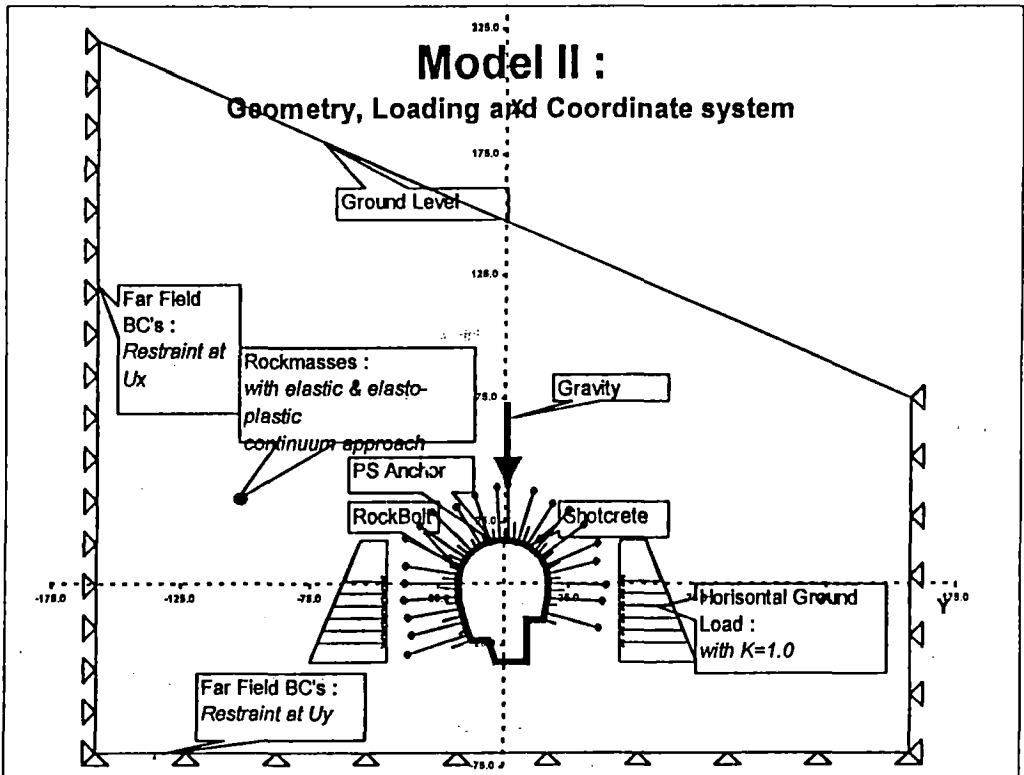


Figure V - 3
 Model II: Geometry, Loading condition, and coordinate system

Table V - 1 Data Model

| Model | Analysis | Rock Properties | | | | | Prestressed Load (kN) | | Note |
|-------|----------|------------------------------|-------------|-----------|-----------|--------------|-----------------------|--------------------|-------------------------|
| | | γ (T/m ³) | E_m (kPa) | ν | c (kpa) | ϕ (deg) | Rock Bolts | Prestressed anchor | |
| I | E00 | Elastic | 2.6 | 4,400,000 | 0.3 | | | | Initial condition |
| | E01 | Elastic | 2.6 | 4,400,000 | 0.3 | | | | Opening without support |
| | E02 | Elastic | 2.6 | 4,400,000 | 0.3 | | | | Opening with support |
| | EP00 | Elastoplastic | 2.6 | 4,400,000 | 0.3 | 2,000 | | 98.0980.0 (design) | Initial condition |
| | EP01 | Elastoplastic | 2.6 | 4,400,000 | 0.3 | 2,000 | | | Opening without support |
| | EP02 | Elastoplastic | 2.6 | 4,400,000 | 0.3 | 2,000 | | 98.0980.0 (design) | Opening with support |
| II | CRT-E00 | Elastic | 2.6 | 4,400,000 | 0.3 | | | | Initial condition |
| | CRT-E01 | Elastic | 2.6 | 4,400,000 | 0.3 | | | | Opening without support |
| | CRT-E02 | Elastic | 2.6 | 4,400,000 | 0.3 | | | 98.0980.0 (design) | Opening with support |
| | CRT-EP00 | Elastoplastic | 2.6 | 4,400,000 | 0.3 | 2,000 | | | Initial condition |
| | CRT-EP01 | Elastoplastic | 2.6 | 4,400,000 | 0.3 | 2,000 | | | Opening without support |
| | CRT-EP02 | Elastoplastic | 2.6 | 4,400,000 | 0.3 | 2,000 | | 98.0980.0 (design) | Opening with support |

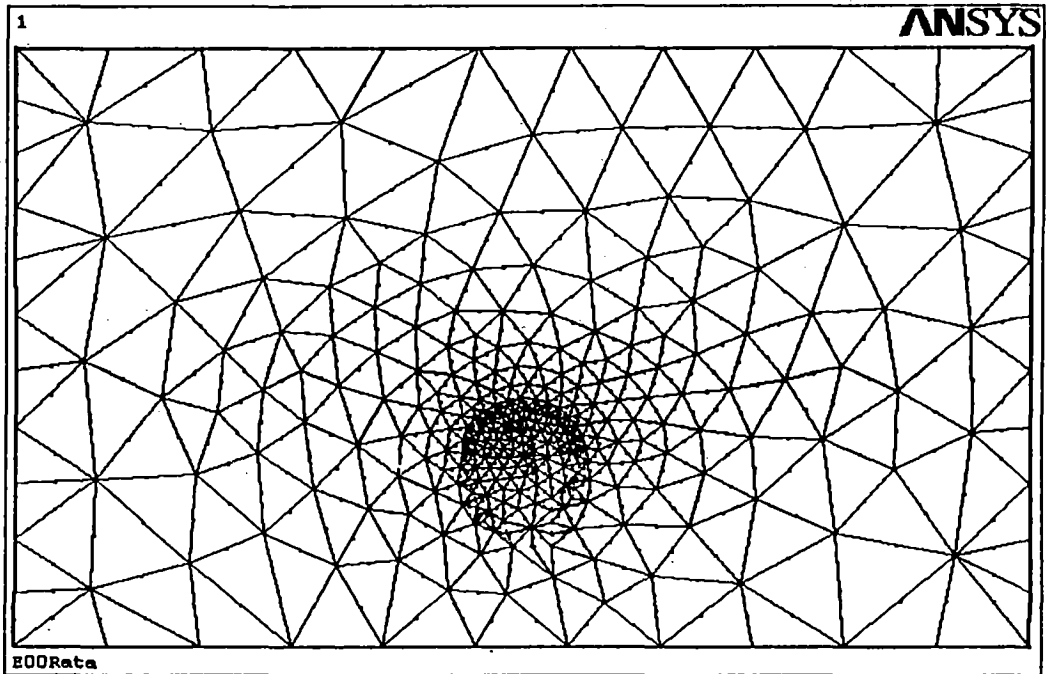


Figure V - 4
Meshing Pattern of Preliminary Model I

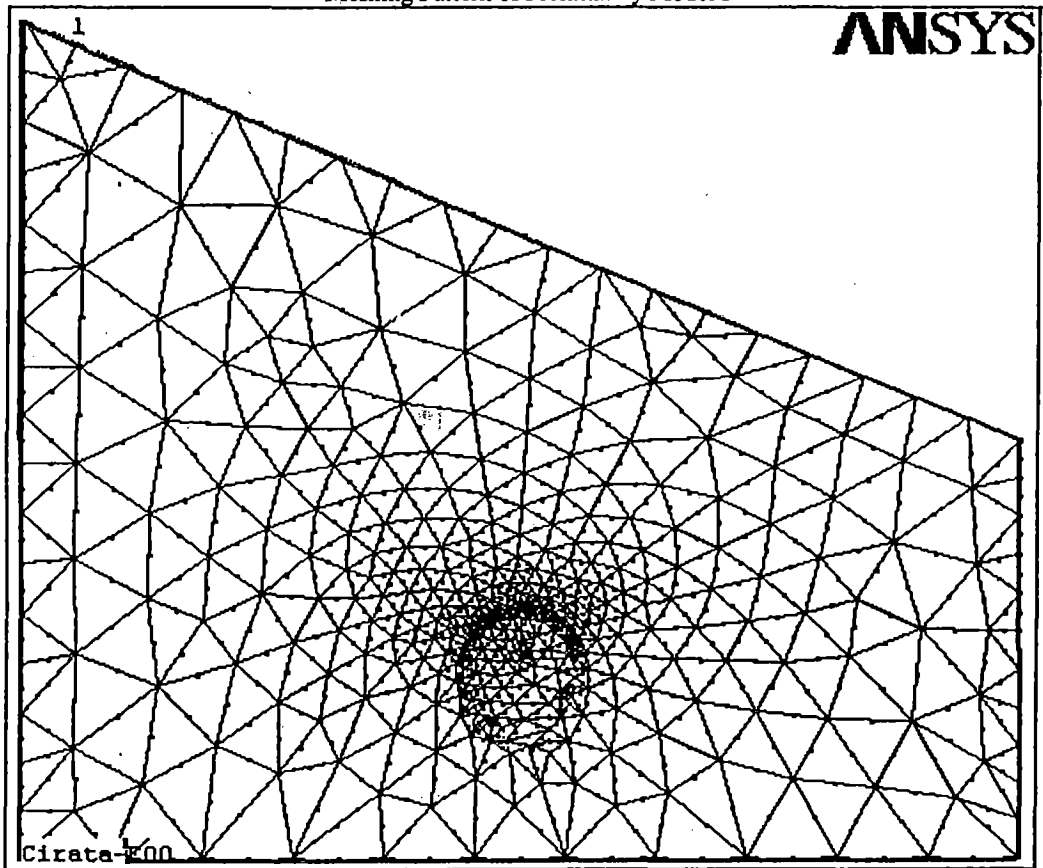


Figure V - 5
Meshing Pattern of Preliminary Model II

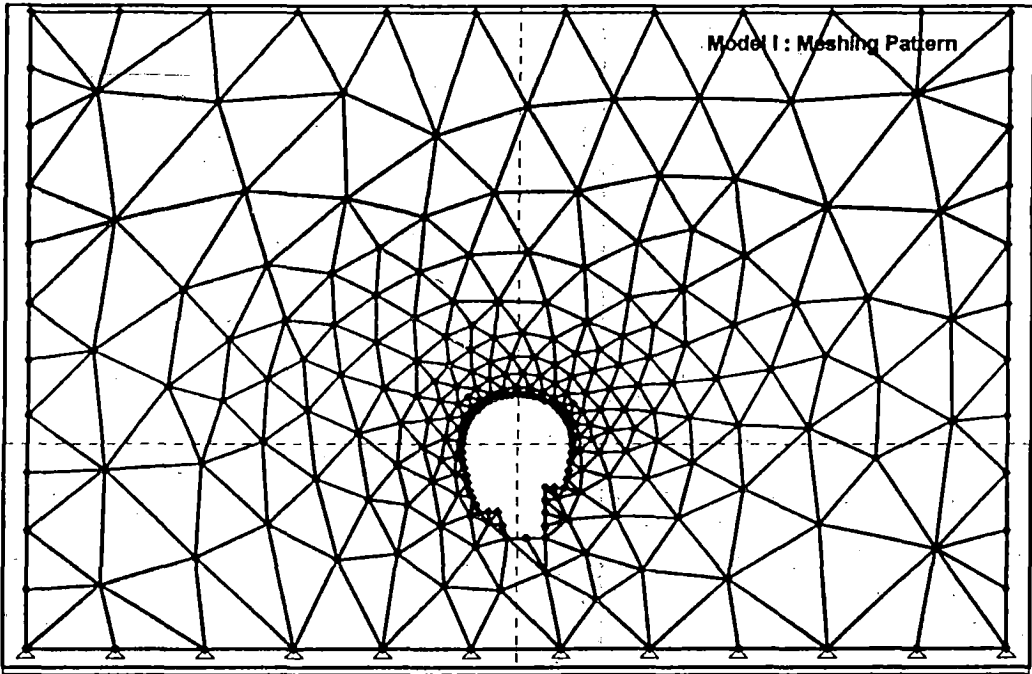


Figure V - 6
Meshing Pattern for Model I with opening

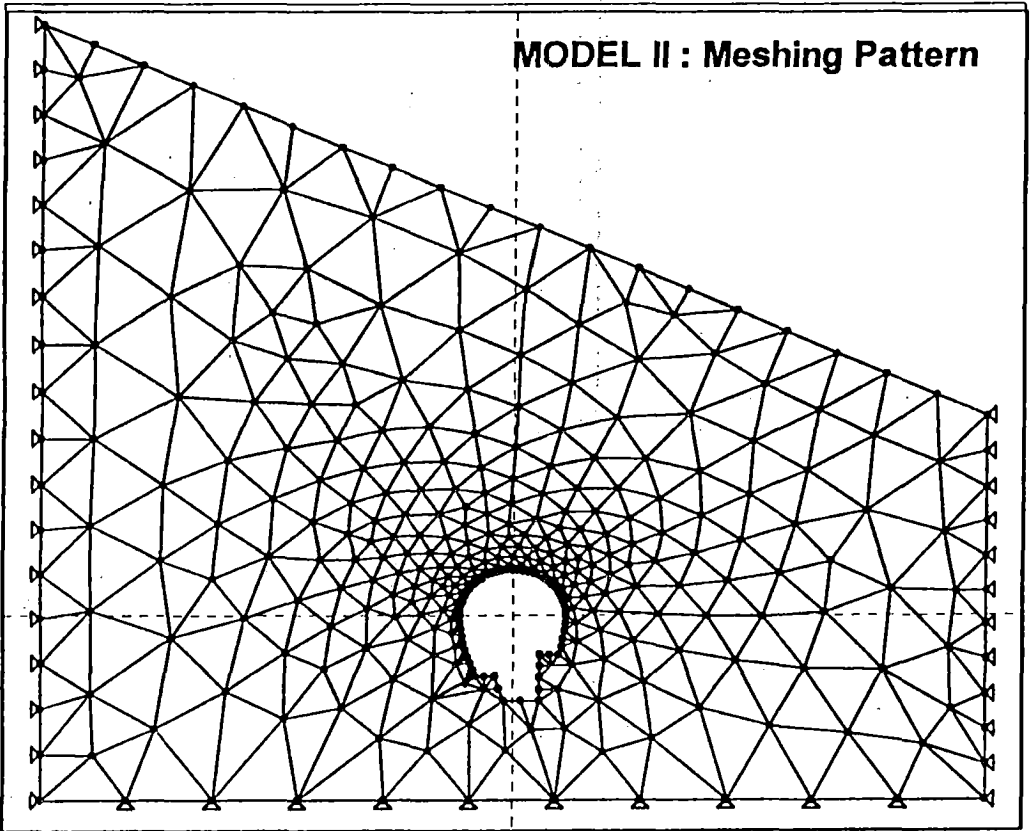


Figure V - 7
Meshing Pattern for Model II with opening

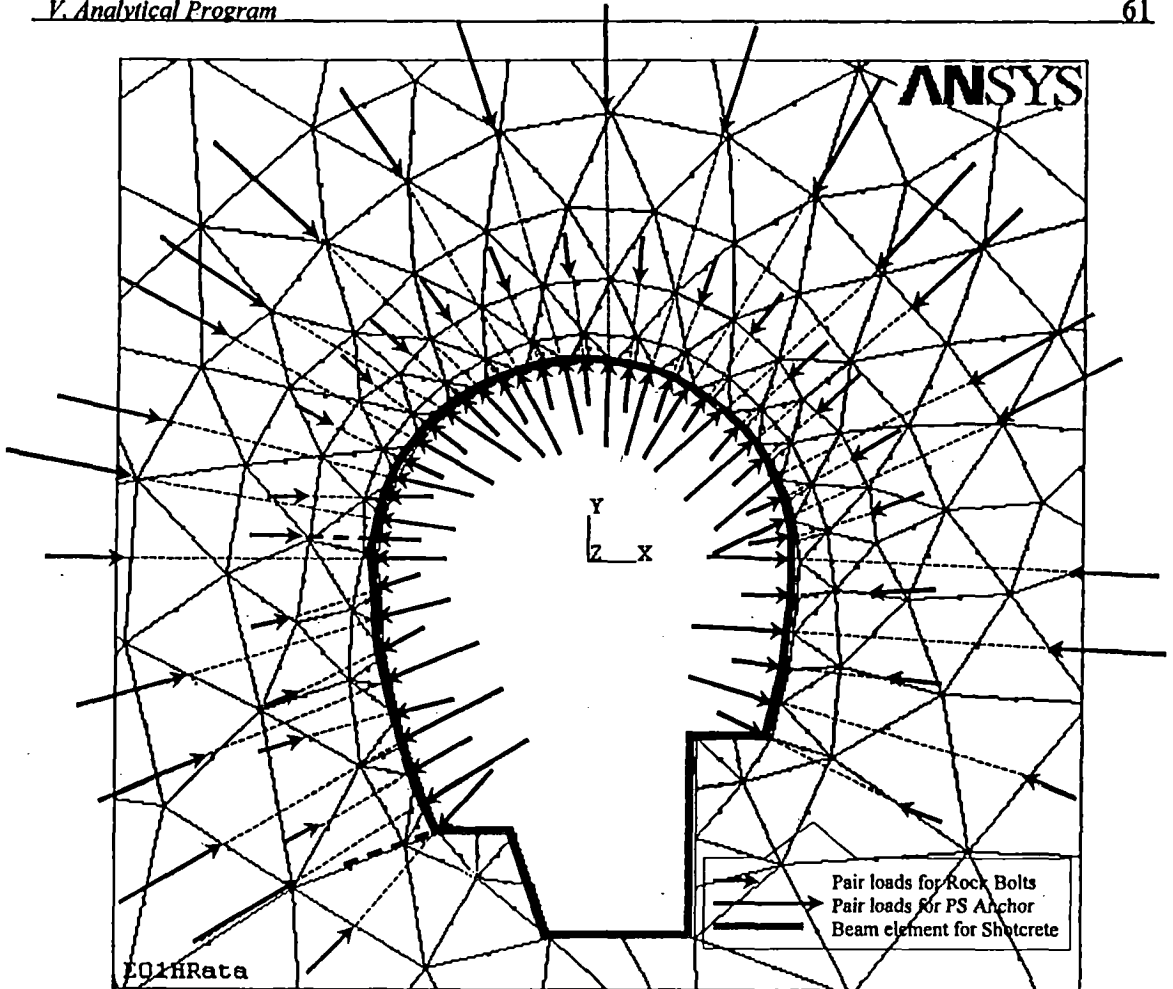
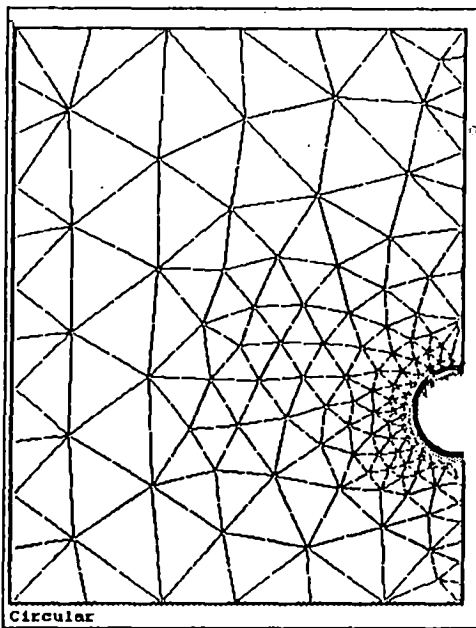


Figure V - 8
Support Modeling



ANSYS 5.4
APR 23 2004
08:13:30
A-E-L-R-N
PowerGraphics
EFACET=1

Figure V - 9
Meshing pattern for additional model
(circular shaped)

Table V - 2
Stress Concentration sidewall for model calibration

PRINT ALONG PATH DEFINED BY LPATH COMMAND. DSYS= 0
 ***** PATH VARIABLE SUMMARY *****

| Distance (m) | oh (kPa) ov (kPa) | | r/a | FEM Result | | EXACT Sol | | Difference (%) | |
|--------------|-------------------|---------------|-----|---------------------|---------------------|---------------------|---------------------|---------------------|---------------------|
| | σ_{XR} | σ_{YR} | | σ_x/σ_h | σ_y/σ_v | σ_x/σ_h | σ_y/σ_v | σ_x/σ_h | σ_y/σ_v |
| 0 | -12.142 | -6323.7 | 1.0 | 0.003 | 1.908 | 0.000 | 1.893 | 0.00% | -0.80% |
| 7 | -1756.1 | -5044.4 | 1.4 | 0.478 | 1.522 | 0.453 | 1.496 | -5.50% | -1.74% |
| 14 | -2515.6 | -4482.9 | 1.8 | 0.685 | 1.352 | 0.660 | 1.310 | -3.77% | -3.24% |
| 21 | -2986.5 | -4137.4 | 2.2 | 0.813 | 1.248 | 0.770 | 1.211 | -5.71% | -3.08% |
| 28 | -3203.6 | -3995.6 | 2.6 | 0.873 | 1.205 | 0.834 | 1.152 | -4.67% | -4.60% |
| 35 | -3357.1 | -3908.6 | 3.0 | 0.914 | 1.179 | 0.875 | 1.115 | -4.56% | -5.74% |
| 42 | -3468.7 | -3853.7 | 3.4 | 0.945 | 1.163 | 0.902 | 1.090 | -4.75% | -6.66% |
| 49 | -3544.8 | -3833.6 | 3.8 | 0.966 | 1.156 | 0.921 | 1.072 | -4.80% | -7.86% |
| 56 | -3608.1 | -3829.7 | 4.2 | 0.983 | 1.155 | 0.936 | 1.059 | -5.05% | -9.07% |
| 63 | -3652.5 | -3838.4 | 4.6 | 0.995 | 1.158 | 0.946 | 1.049 | -5.15% | -10.33% |
| 70 | -3684.6 | -3871.3 | 5.0 | 1.004 | 1.168 | 0.954 | 1.042 | -5.16% | -12.09% |
| 77 | -3713.2 | -3906.1 | 5.4 | 1.011 | 1.178 | 0.961 | 1.036 | -5.26% | -13.74% |
| 84 | -3726.5 | -3950.7 | 5.8 | 1.015 | 1.192 | 0.966 | 1.031 | -5.07% | -15.57% |
| 91 | -3744.5 | -3999.1 | 6.2 | 1.020 | 1.206 | 0.970 | 1.027 | -5.12% | -17.43% |
| 98 | -3752.7 | -4082.7 | 6.6 | 1.022 | 1.232 | 0.974 | 1.024 | -4.97% | -20.26% |
| 105 | -3759.2 | -4172.2 | 7.0 | 1.024 | 1.259 | 0.977 | 1.021 | -4.84% | -23.22% |
| 112 | -3764.6 | -4255.9 | 7.4 | 1.025 | 1.284 | 0.979 | 1.019 | -4.73% | -25.97% |
| 119 | -3765.4 | -4314.5 | 7.8 | 1.026 | 1.302 | 0.981 | 1.017 | -4.53% | -27.94% |
| 126 | -3764.2 | -4383.2 | 8.2 | 1.025 | 1.322 | 0.983 | 1.016 | -4.31% | -30.19% |
| 133 | -3762.4 | -4471.4 | 8.6 | 1.025 | 1.349 | 0.985 | 1.014 | -4.09% | -32.99% |
| 140 | -3760.4 | -4573 | 9.0 | 1.024 | 1.379 | 0.986 | 1.013 | -3.90% | -36.18% |

Note:

For Model Circular (circular shaped d=17.5 m, same elastic material properties)
 (for Elastic rock medium with opening without supports)

Exact Solution (for circular shaped):

Radial Stress = $0.5(\sigma_v + \sigma_h)(1 - a^2/r^2) + 0.5(\sigma_v - \sigma_h)(1 + 3a^4/r^4 - 4a^2/r^2)\cos^2\theta$

Tangential stress = $0.5(\sigma_v + \sigma_h)(1 + a^2/r^2) - 0.5(\sigma_v - \sigma_h)(1 + 3a^4/r^4)\cos^2\theta$

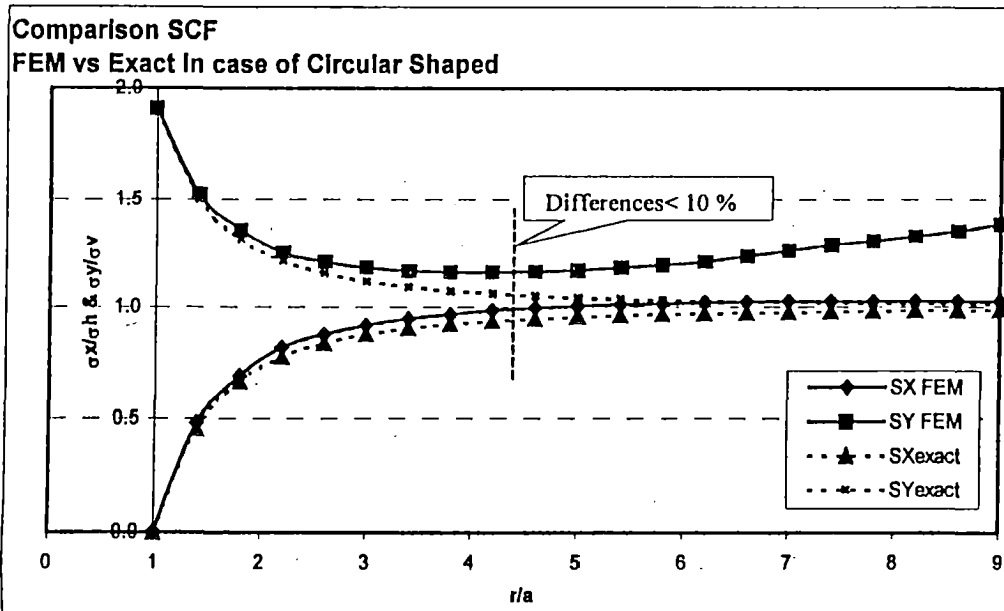
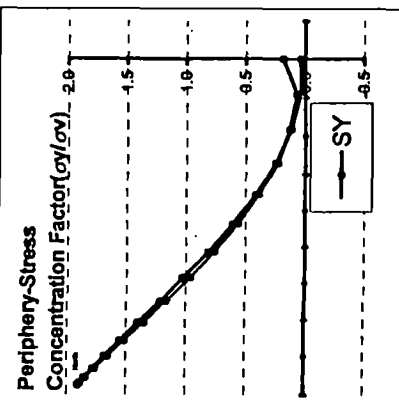
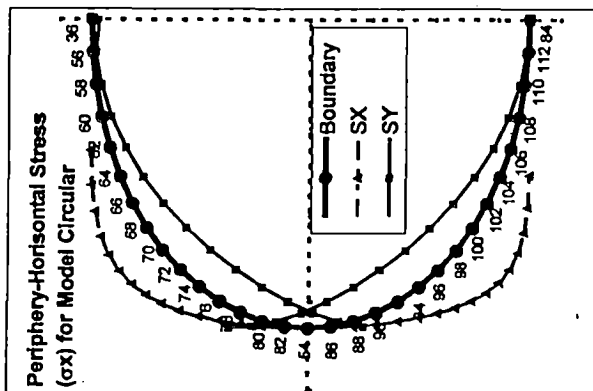
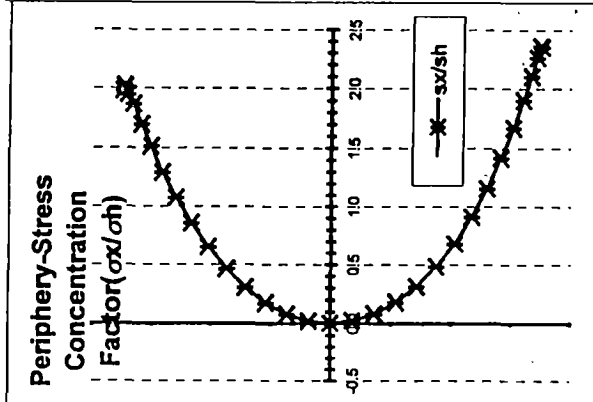


Table V-2 (cont.)

PRINT ALONG PATH DEFINED BY LPATH COMMAND. DSYS= 0

***** PATH VARIABLE SUMMARY *****

| Node | X | Y | σ_{XR} | σ_{YR} | $\sigma_{X/oh}$ | σ_y/σ_v | Coord X | Coord Y |
|------|---------|---------|---------------|---------------|-----------------|---------------------|---------|---------|
| 36 | 0 | 17.5 | -7262.7 | -622.34 | 1.98 | 0.19 | -7.26 | 16.88 |
| 56 | -1.829 | 17.404 | -7411.7 | -234.81 | 2.02 | 0.07 | -9.24 | 17.17 |
| 58 | -3.639 | 17.118 | -7154.7 | -428.37 | 1.95 | 0.13 | -10.79 | 16.69 |
| 60 | -5.408 | 16.643 | -6850.4 | -764.83 | 1.87 | 0.23 | -12.26 | 15.88 |
| 62 | -7.118 | 15.987 | -6216 | -1288.4 | 1.69 | 0.39 | -13.33 | 14.70 |
| 64 | -8.75 | 15.155 | -5551 | -1859.5 | 1.51 | 0.56 | -14.30 | 13.30 |
| 66 | -10.286 | 14.158 | -4745.1 | -2522.9 | 1.29 | 0.76 | -15.03 | 11.64 |
| 68 | -11.71 | 13.005 | -3949.1 | -3193.2 | 1.08 | 0.96 | -15.66 | 9.81 |
| 70 | -13.005 | 11.71 | -3139.1 | -3852.3 | 0.86 | 1.16 | -16.14 | 7.86 |
| 72 | -14.158 | 10.286 | -2385 | -4473.7 | 0.65 | 1.35 | -16.54 | 5.81 |
| 74 | -15.155 | 8.75 | -1696.1 | -5016.9 | 0.46 | 1.51 | -16.85 | 3.73 |
| 76 | -15.987 | 7.118 | -1109.3 | -5485.4 | 0.30 | 1.65 | -17.10 | 1.63 |
| 78 | -16.643 | 5.408 | -633.88 | -5845.9 | 0.17 | 1.76 | -17.28 | -0.44 |
| 80 | -17.118 | 3.639 | -288.93 | -6111.7 | 0.08 | 1.84 | -17.41 | -2.47 |
| 82 | -17.404 | 1.829 | -80.122 | -6262.7 | 0.02 | 1.89 | -17.48 | -4.43 |
| 54 | -17.5 | 0 | -12.142 | -6323.7 | 0.00 | 1.91 | -17.51 | 6.32 |
| 86 | -17.404 | -1.829 | -84.921 | -6279.8 | 0.02 | 1.89 | -17.49 | 4.45 |
| 88 | -17.118 | -3.639 | -295.03 | -6143.9 | 0.08 | 1.85 | -17.41 | 2.50 |
| 90 | -16.643 | -5.408 | -651.75 | -5901.9 | 0.18 | 1.78 | -17.29 | 0.49 |
| 92 | -15.987 | -7.118 | -1132.2 | -5579.7 | 0.31 | 1.68 | -17.12 | -1.54 |
| 94 | -15.155 | -8.75 | -1764.9 | -5140.1 | 0.48 | 1.55 | -16.92 | -3.61 |
| 96 | -14.158 | -10.286 | -2487.4 | -4646.4 | 0.68 | 1.40 | -16.65 | -5.64 |
| 98 | -13.005 | -11.71 | -3345.3 | -4031.1 | 0.91 | 1.22 | -16.35 | -7.68 |
| 100 | -11.71 | -13.005 | -4242.8 | -3400.6 | 1.16 | 1.03 | -15.95 | -9.60 |
| 102 | -10.286 | -14.158 | -5202.3 | -2694.5 | 1.42 | 0.81 | -15.49 | -11.46 |
| 104 | -8.75 | -15.155 | -6131.7 | -2030.5 | 1.67 | 0.61 | -14.88 | -13.12 |
| 106 | -7.118 | -15.987 | -6984.1 | -1365.7 | 1.90 | 0.41 | -14.10 | -14.62 |
| 108 | -5.408 | -16.643 | -7711.9 | -824.77 | 2.10 | 0.25 | -13.12 | -15.82 |
| 110 | -3.639 | -17.118 | -8290.2 | -388.98 | 2.26 | 0.12 | -11.93 | -16.73 |
| 112 | -1.829 | -17.404 | -8654.2 | -117.22 | 2.36 | 0.04 | -10.48 | -17.29 |
| 84 | 0 | -17.5 | -8623.8 | -138.14 | 2.35 | 0.04 | -8.62 | -17.36 |



- **Figure VI- 3** for vertical stress concentration around periphery for Model II (a) & (b) ((a) for model without horizontal ground pressure applied and (b) with horizontal ground pressure)
- **Figure VI- 4** for horizontal stress concentration around periphery for Model II (a) & (b)
- **Table VI- 2** for magnitude of stresses around periphery for Model II

As may be noted that all the data is reproduced in worksheet MSEXcel and not directly from ANSYS output format so for better presentation of results.

- **Figure VI- 5** for near-field contour plot in ANSYS output format -in term of stress in horizontal direction (SX) and vertical direction (SY)- (a) for elastic behaviour & (b) for elasto-plastic behaviour from **Model I**; and
- **Figure VI- 6 (a) & (b)** for near-field contour plot ANSYS output SX & SY in elastic and elasto-plastic behaviour respectively from **Model II**
- **Figure VI- 7 (a) & (b)** show vector of principal stresses surrounding cavern without support as well as with support for both of model correspondingly in ANSYS output format.

Stress contours with continuity across element indicating that the number of element used (so-called '*element density*') is adequate to calculate the stress value near opening. It is important to note that these contour plot are generated from *Nodal Solution option* in ANSYS, meaning that the stress values are averaged before plotting, and any contour discontinuities (and thus errors) are hidden selecting. In *nodal solution stresses* smooth contours would always be generated. Another option in ANSYS is *Element Solution* in order to look for stress contour discontinuities.

Safety Factor for rock mass and shotcrete are not shown since no data was available for compressive strength of rock mass and shotcrete. Also normal stress and bending moment in shotcrete cannot be shown since there is no option in ANSYS to separately show result from particular element.

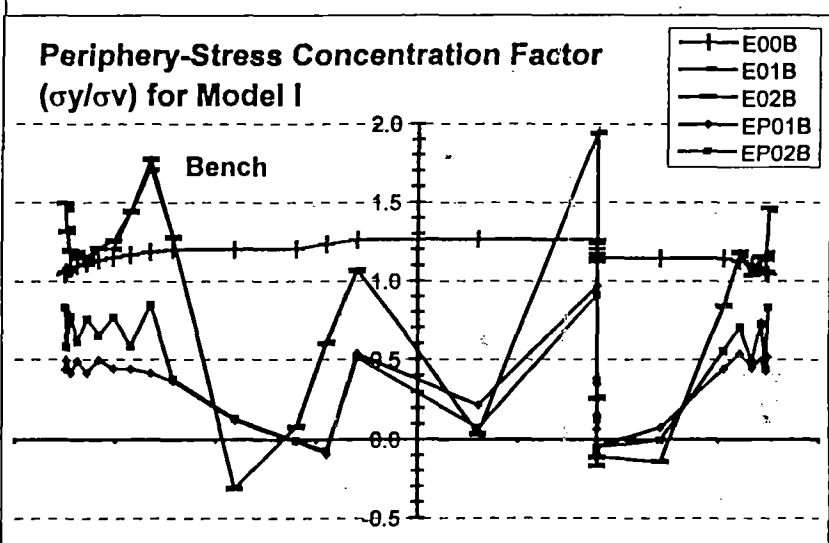
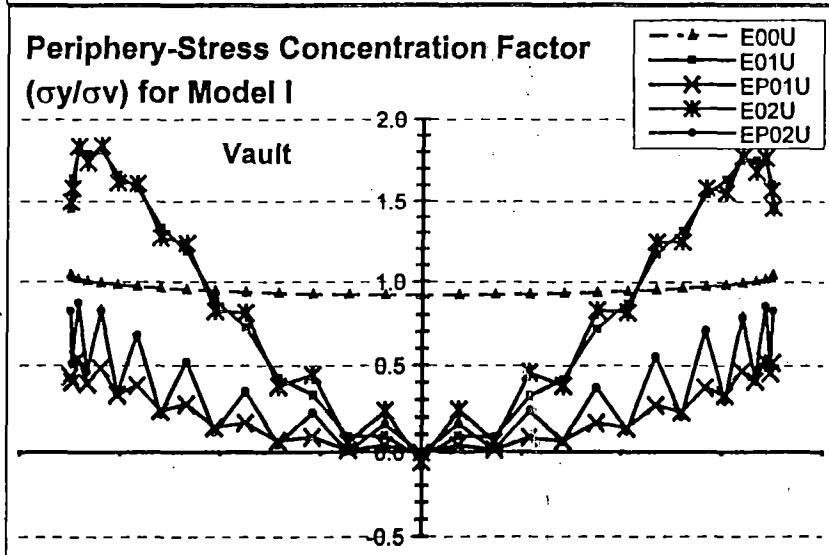
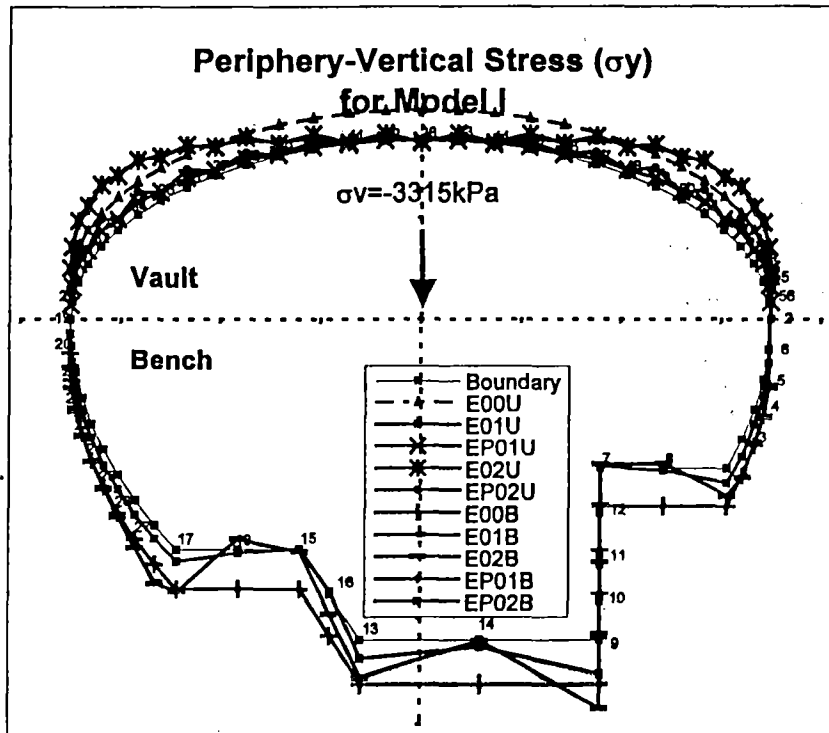


Figure VI-2 Horizontal Stress Concentration around periphery - Model I

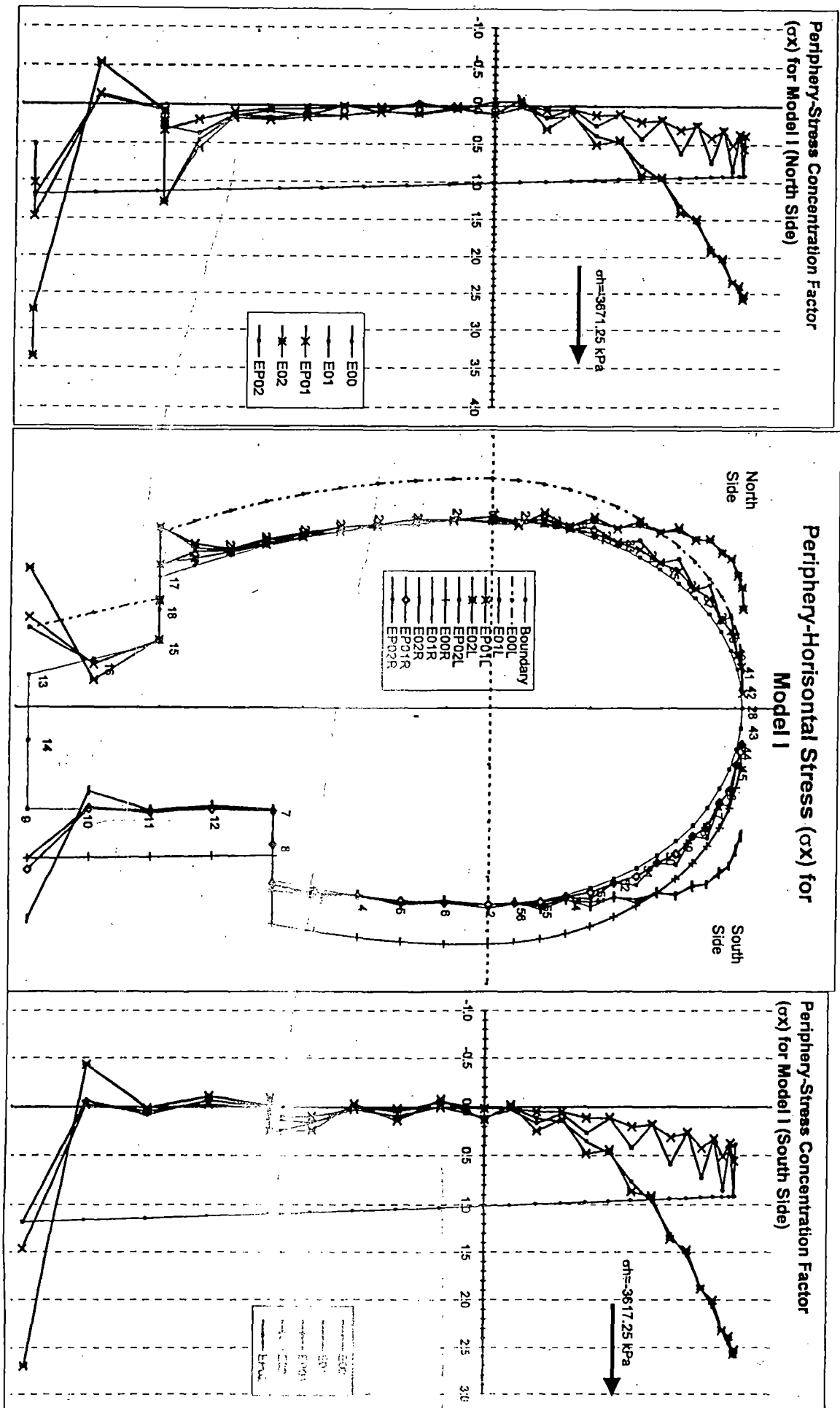
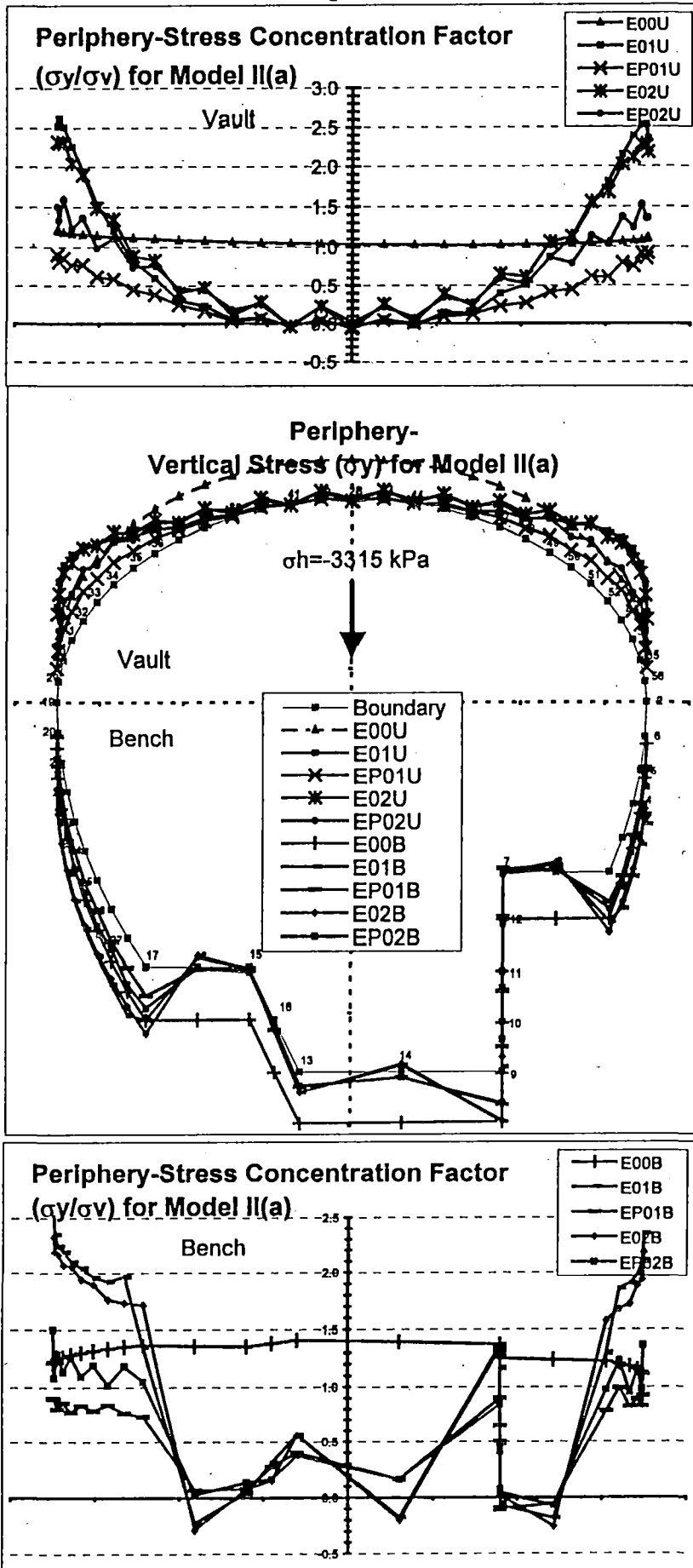


Table VI-1 Magnitude of stress around periphery - Model I

| Stresses on Periphery LIST ALL PICKED NODE | | | Stresses at y-direction | | | | | | Stresses at x-direction | | | | | |
|---|--------|--------|-------------------------|----------|----------|----------------|----------|----------|-------------------------|----------|----------|----------------|----------|----------|
| | | | Elastic | | | Elasto-Plastic | | | Elastic | | | Elasto-Plastic | | |
| Model I | | | E00 | E01 | E02H | EP00 | EP01 | EP02 | E00 | E01 | E02H | EP00 | EP01 | EP02 |
| Node | X | Y | SY(kPa) | SY(kPa) | SY(kPa) | SY(kPa) | SY(kPa) | SY(kPa) | SX(kPa) | SX(kPa) | SX(kPa) | SX(kPa) | SX(kPa) | SX(kPa) |
| 1 | 15.31 | -15.00 | -3787.90 | -2791.80 | -2773.80 | -3787.90 | -1467.10 | -1832.60 | -4023.50 | -950.79 | -902.23 | -4023.50 | -348.86 | -449.87 |
| 3 | 16.10 | -12.06 | -3729.10 | -3846.50 | -3912.90 | -3729.10 | -1772.40 | -2315.60 | -3976.00 | -604.96 | -873.94 | -3976.00 | -332.57 | -570.28 |
| 4 | 16.71 | -9.08 | -3661.00 | -3542.80 | -3435.90 | -3661.00 | -1479.30 | -1610.60 | -3913.30 | 44.79 | 107.29 | -3913.30 | -81.77 | -90.66 |
| 5 | 17.15 | -6.07 | -3592.10 | -3792.50 | -3823.60 | -3592.10 | -1639.30 | -2392.50 | -3853.20 | -165.67 | -499.42 | -3853.20 | -63.03 | -325.26 |
| 6 | 17.41 | -3.04 | -3521.50 | -3897.40 | -3765.80 | -3521.50 | -1422.00 | -1456.20 | -3790.70 | 192.63 | 289.76 | -3790.70 | -0.97 | 12.07 |
| 2 | 17.50 | 0.00 | -3456.10 | -4786.40 | -4840.90 | -3456.10 | -1710.30 | -2740.30 | -3729.30 | -64.39 | -469.35 | -3729.30 | -59.00 | -398.13 |
| 56 | 17.40 | 1.83 | -3410.40 | -5332.20 | -5200.00 | -3410.40 | -1509.90 | -1655.70 | -3689.40 | 18.25 | 79.51 | -3689.40 | -37.30 | -100.15 |
| 55 | 17.12 | 3.64 | -3369.30 | -5797.50 | -5856.60 | -3369.30 | -1758.40 | -2832.20 | -3651.40 | -415.10 | -902.32 | -3651.40 | -170.42 | -606.49 |
| 54 | 16.64 | 5.41 | -3328.80 | -5812.70 | -5581.80 | -3328.80 | -1357.10 | -1374.90 | -3613.60 | -535.79 | -455.79 | -3613.60 | -166.24 | -232.35 |
| 53 | 15.99 | 7.12 | -3289.10 | -5839.40 | -5886.30 | -3289.10 | -1550.90 | -2606.20 | -3576.30 | -1305.50 | -1760.30 | -3576.30 | -404.86 | -985.11 |
| 52 | 15.16 | 8.75 | -3251.40 | -5431.50 | -5154.70 | -3251.40 | -1088.40 | -982.71 | -3541.50 | -1756.00 | -1625.60 | -3541.50 | -400.70 | -429.12 |
| 51 | 14.16 | 10.29 | -3215.20 | -5118.90 | -5253.60 | -3215.20 | -1224.40 | -2348.60 | -3507.40 | -2822.80 | -3178.10 | -3507.40 | -738.89 | -1552.10 |
| 50 | 13.01 | 11.71 | -3182.20 | -4361.10 | -4126.50 | -3182.20 | -763.26 | -681.98 | -3476.70 | -3548.60 | -3346.20 | -3476.70 | -665.29 | -654.80 |
| 49 | 11.71 | 13.01 | -3151.50 | -3862.30 | -4124.60 | -3151.50 | -894.39 | -1830.20 | -3447.40 | -4804.40 | -5011.50 | -3447.40 | -1161.60 | -2178.30 |
| 48 | 10.29 | 14.16 | -3124.50 | -2880.30 | -2707.70 | -3124.50 | -460.96 | -409.64 | -3422.40 | -5651.60 | -5415.90 | -3422.40 | -953.31 | -939.48 |
| 47 | 8.75 | 15.16 | -3100.60 | -2377.20 | -2747.80 | -3100.60 | -554.25 | -1227.80 | -3400.20 | -6849.00 | -6925.30 | -3400.20 | -1566.70 | -2683.70 |
| 46 | 7.12 | 15.99 | -3081.20 | -1383.80 | -1263.10 | -3081.20 | -207.44 | -202.85 | -3382.20 | -7632.20 | -7356.90 | -3382.20 | -1201.10 | -1229.70 |
| 45 | 5.41 | 16.64 | -3065.30 | -1069.60 | -1524.70 | -3065.30 | -276.77 | -792.43 | -3367.50 | -8542.10 | -8523.30 | -3367.50 | -1871.10 | -3134.10 |
| 44 | 3.64 | 17.12 | -3054.40 | -279.22 | -193.85 | -3054.40 | -39.43 | -34.47 | -3357.30 | -9042.80 | -8734.90 | -3357.30 | -1364.30 | -1411.60 |
| 43 | 1.83 | 17.40 | -3047.10 | -312.87 | -803.08 | -3047.10 | -127.10 | -541.32 | -3350.50 | -9508.80 | -9458.90 | -3350.50 | -2046.60 | -3356.40 |
| 28 | 0.00 | 17.50 | -3045.10 | 127.34 | 211.69 | -3045.10 | 22.28 | 39.71 | -3348.70 | -9559.00 | -9261.20 | -3348.70 | -1400.00 | -1430.90 |
| 42 | -1.83 | 17.40 | -3047.10 | -313.74 | -783.56 | -3047.10 | -129.12 | -533.40 | -3350.50 | -9515.80 | -9494.90 | -3350.50 | -2035.40 | -3367.60 |
| 41 | -3.64 | 17.12 | -3054.40 | -290.64 | -180.25 | -3054.40 | -38.78 | -2.50 | -3357.20 | -9048.90 | -8779.30 | -3357.20 | -1330.90 | -1312.60 |
| 40 | -5.41 | 16.64 | -3065.40 | -1089.80 | -1481.50 | -3065.40 | -290.37 | -753.51 | -3367.30 | -8564.90 | -8635.90 | -3367.30 | -1864.60 | -3127.00 |
| 39 | -7.12 | 15.99 | -3081.30 | -1419.30 | -1261.90 | -3081.30 | -214.85 | -153.31 | -3382.10 | -7641.60 | -7404.80 | -3382.10 | -1164.50 | -1094.20 |
| 38 | -8.75 | 15.16 | -3100.80 | -2400.00 | -2692.40 | -3100.80 | -559.74 | -1155.50 | -3400.30 | -6872.80 | -7085.30 | -3400.30 | -1517.80 | -2744.60 |
| 37 | -10.29 | 14.16 | -3124.50 | -2931.00 | -2728.40 | -3124.50 | -474.32 | -389.53 | -3422.50 | -5666.60 | -5480.50 | -3422.50 | -922.98 | -850.57 |
| 36 | -11.71 | 13.01 | -3151.60 | -3923.00 | -4091.90 | -3151.60 | -912.44 | -1726.50 | -3447.70 | -4829.30 | -5175.10 | -3447.70 | -1123.50 | -2264.70 |
| 35 | -13.01 | 11.71 | -3182.20 | -4431.10 | -4210.50 | -3182.20 | -798.54 | -728.37 | -3476.20 | -3559.40 | -3437.80 | -3476.20 | -654.58 | -609.82 |

Table VI-1 Magnitude of stress around periphery - Model I

| Stresses on Periphery LIST ALL PICKED NODE | | | Stresses at y-direction | | | | | | Stresses at x-direction | | | | | |
|---|---------|---------|-------------------------|----------|----------|----------------|----------|----------|-------------------------|-----------|-----------|----------------|----------|----------|
| | | | Elastic | | | Elasto-Plastic | | | Elastic | | | Elasto-Plastic | | |
| Model I | E00 | E01 | E02H | EP00 | EP01 | EP02 | E00 | E01 | E02H | EP00 | EP01 | EP02 | | |
| Node | SY(kPa) | SY(kPa) | SY(kPa) | SY(kPa) | SY(kPa) | SY(kPa) | SX(kPa) | SX(kPa) | SX(kPa) | SX(kPa) | SX(kPa) | SX(kPa) | | |
| 34 | -14.16 | 10.29 | -3215.40 | -5223.40 | -5339.20 | -3215.40 | -1272.40 | -2251.30 | -3507.30 | -2879.80 | -3320.80 | -3507.30 | -729.14 | -1566.40 |
| 33 | -15.16 | 8.75 | -3251.30 | -5512.90 | -5358.30 | -3251.30 | -1096.70 | -1120.90 | -3541.20 | -1734.20 | -1640.80 | -3541.20 | -377.40 | -385.61 |
| 32 | -15.99 | 7.12 | -3289.30 | -5991.70 | -6100.80 | -3289.30 | -1605.20 | -2733.00 | -3576.40 | -1408.80 | -1847.10 | -3576.40 | -410.35 | -935.24 |
| 31 | -16.64 | 5.41 | -3328.60 | -5931.40 | -5769.00 | -3328.60 | -1309.10 | -1541.10 | -3613.40 | -452.77 | -349.61 | -3613.40 | -139.20 | -124.02 |
| 30 | -17.12 | 3.64 | -3370.00 | -6012.80 | -6082.40 | -3370.00 | -1786.30 | -2891.00 | -3651.70 | -576.53 | -1085.60 | -3651.70 | -172.75 | -524.34 |
| 29 | -17.40 | 1.83 | -3410.10 | -5453.00 | -5239.70 | -3410.10 | -1340.00 | -1703.20 | -3688.70 | 222.29 | 328.69 | -3688.70 | 10.23 | -57.92 |
| 19 | -17.50 | 0.00 | -3455.40 | -4814.50 | -4953.40 | -3455.40 | -1444.00 | -2735.60 | -3728.90 | 213.09 | -380.46 | -3728.90 | 0.13 | -410.88 |
| 20 | -17.43 | -2.66 | -3512.70 | -4431.70 | -4342.60 | -3512.70 | -1632.90 | -1920.10 | -3783.50 | -189.75 | -109.95 | -3783.50 | -42.77 | -138.86 |
| 21 | -17.23 | -5.31 | -3574.70 | -3809.20 | -3950.00 | -3574.70 | -1382.30 | -2557.80 | -3838.50 | 172.65 | -328.53 | -3838.50 | -5.74 | -413.44 |
| 22 | -16.90 | -7.94 | -3634.20 | -3923.20 | -3890.70 | -3634.20 | -1620.00 | -2021.30 | -3891.30 | -277.27 | -304.45 | -3891.30 | -79.15 | -246.66 |
| 23 | -16.43 | -10.56 | -3694.80 | -3664.10 | -3820.50 | -3694.80 | -1379.90 | -2497.90 | -3943.30 | 7.16 | -461.43 | -3943.30 | -50.54 | -482.34 |
| 24 | -15.83 | -13.15 | -3753.50 | -4007.60 | -3999.90 | -3753.50 | -1636.80 | -2155.20 | -3993.90 | -462.38 | -548.29 | -3993.90 | -149.22 | -388.62 |
| 25 | -15.10 | -15.70 | -3812.20 | -3991.00 | -4163.40 | -3812.20 | -1465.30 | -2531.90 | -4042.00 | -264.97 | -698.75 | -4042.00 | -162.72 | -588.72 |
| 26 | -14.24 | -18.22 | -3870.10 | -4766.40 | -4779.10 | -3870.10 | -1461.10 | -1935.80 | -4090.80 | -497.67 | -598.76 | -4090.80 | -299.57 | -445.23 |
| 27 | -13.25 | -20.69 | -3926.90 | -5649.10 | -5867.80 | -3926.90 | -1373.20 | -2804.70 | -4134.50 | -1686.00 | -2089.80 | -4134.50 | -709.12 | -1357.30 |
| 17 | -12.15 | -23.10 | -3976.40 | -4233.70 | -4231.50 | -3976.40 | -1213.40 | -1249.50 | -4174.90 | -4763.30 | -4698.80 | -4174.90 | -1208.80 | -1054.90 |
| 18 | -9.07 | -23.10 | -3981.30 | 1044.50 | 1041.20 | -3981.30 | -401.30 | -438.92 | -4177.70 | -1005.70 | -958.61 | -4177.70 | -779.41 | -859.29 |
| 15 | -6.00 | -23.10 | -3988.30 | -276.76 | -262.61 | -3988.30 | 29.81 | 22.99 | -4179.90 | -313.54 | -293.60 | -4179.90 | -275.71 | -268.65 |
| 16 | -4.50 | -27.60 | -4085.90 | -2013.50 | -1983.20 | -4085.90 | 318.75 | 230.88 | -4256.80 | 1967.60 | 1965.60 | -4256.80 | 500.81 | 441.50 |
| 13 | -3.00 | -32.10 | -4177.10 | -3554.60 | -3533.40 | -4177.10 | -1774.80 | -1691.70 | -4331.80 | -10052.00 | -10041.00 | -4331.80 | -5394.20 | -4407.00 |
| 14 | 3.00 | -32.10 | -4189.40 | -121.34 | -121.98 | -4189.40 | -719.25 | -243.22 | -4334.10 | -12325.00 | -12313.00 | -4334.10 | -3780.80 | -1927.10 |
| 9 | 9.00 | -32.10 | -4178.00 | -6442.50 | -6423.00 | -4178.00 | -3195.30 | -3010.50 | -4330.50 | -9929.30 | -9923.60 | -4330.50 | -5372.40 | -4364.30 |
| 10 | 9.00 | -27.83 | -4093.50 | -3758.10 | -3724.50 | -4093.50 | -509.49 | -426.00 | -4262.50 | 1579.20 | 1581.60 | -4262.50 | 89.30 | 230.64 |
| 11 | 9.00 | -23.55 | -3991.00 | -878.83 | -848.83 | -3991.00 | -1149.20 | -1212.20 | -4185.80 | -42.61 | -45.04 | -4185.80 | -137.17 | -273.67 |
| 12 | 9.00 | -19.28 | -3889.90 | 551.68 | 569.23 | -3889.90 | -217.98 | 289.15 | -4108.10 | 402.19 | 401.34 | -4108.10 | 103.14 | 253.38 |
| 7 | 9.00 | -15.00 | -3800.70 | 374.46 | 383.16 | -3800.70 | 146.16 | 169.39 | -4029.20 | 90.40 | 101.31 | -4029.20 | -66.48 | 25.11 |
| 8 | 12.16 | -15.00 | -3793.80 | 475.23 | 473.35 | -3793.80 | -248.53 | 16.28 | -4027.90 | 316.70 | 344.29 | -4027.90 | 100.16 | 143.75 |
| 1 | 15.31 | -15.00 | -3787.90 | -2791.80 | -2773.80 | -3787.90 | -1467.10 | -1832.60 | -4023.50 | -950.79 | -902.23 | -4023.50 | -348.86 | -449.87 |



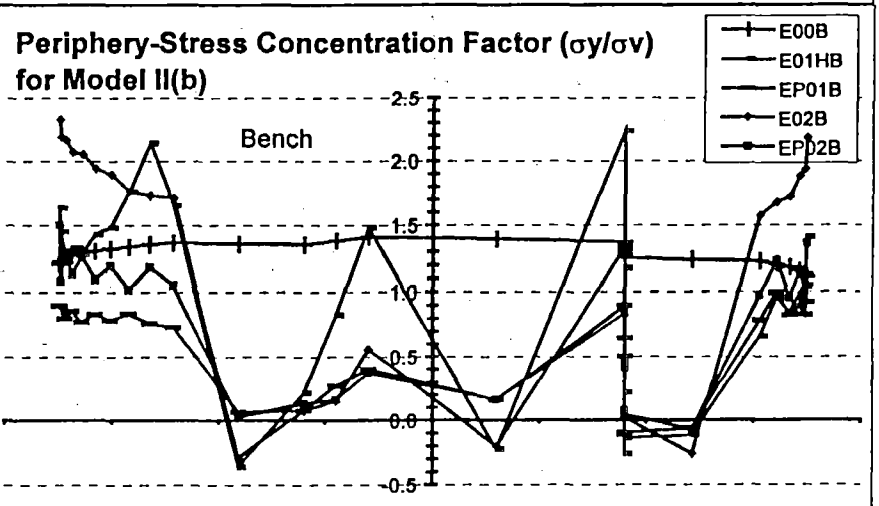
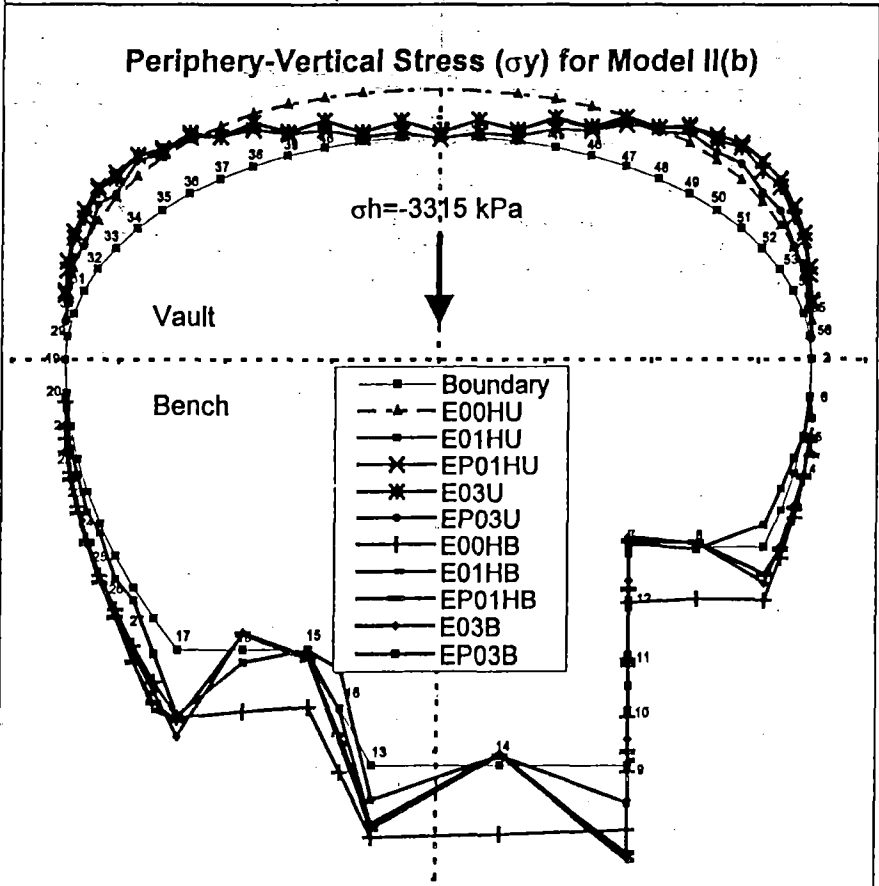
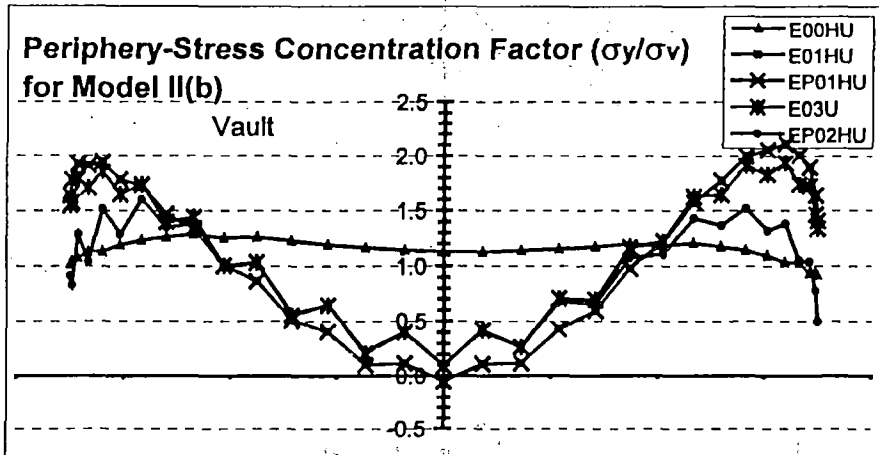


Figure VI - 4 Horizontal Stress Concentration around periphery - Model II(a)

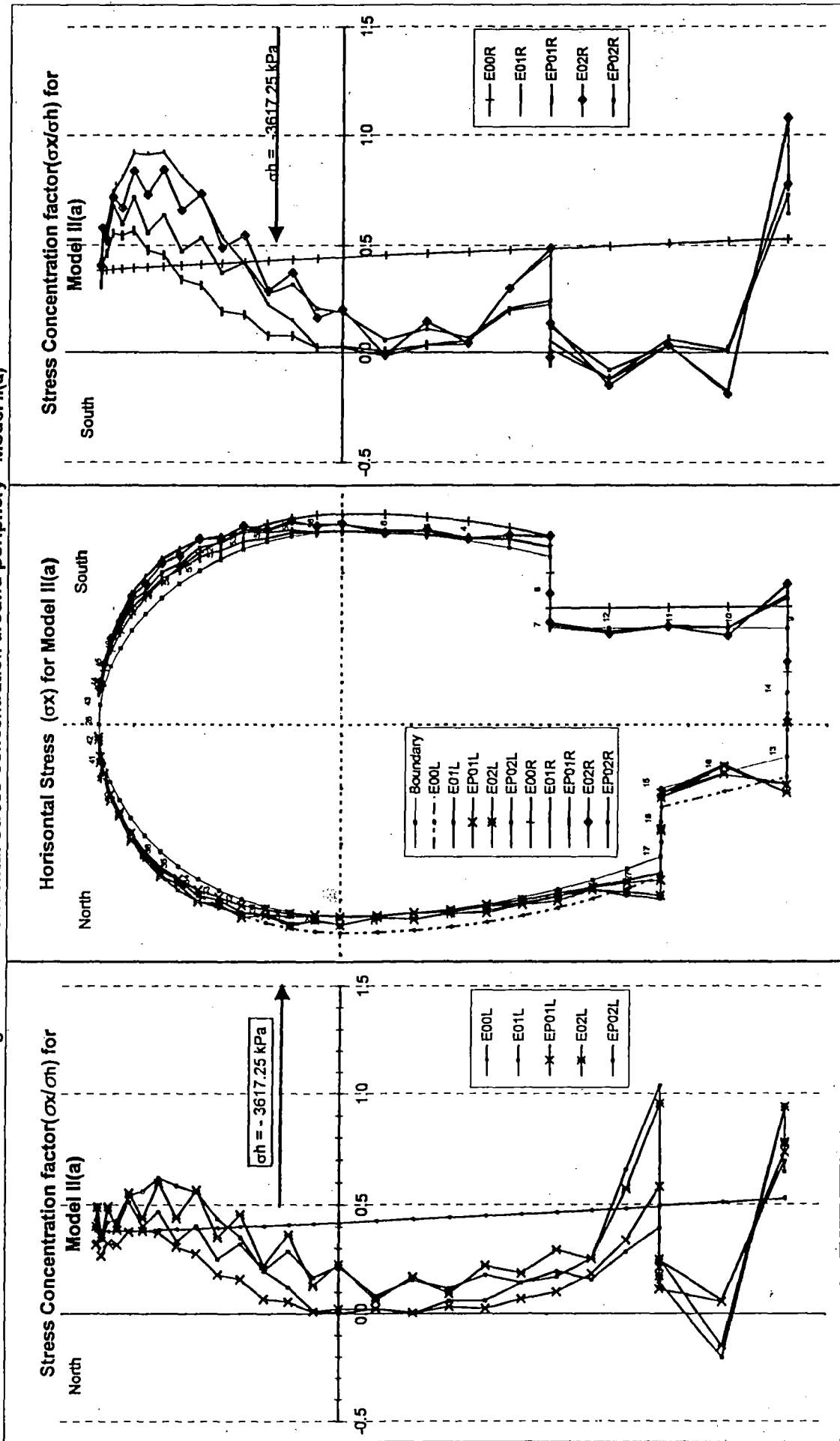


Figure VI - 4 Horizontal Stress Concentration around periphery - Model II(b)

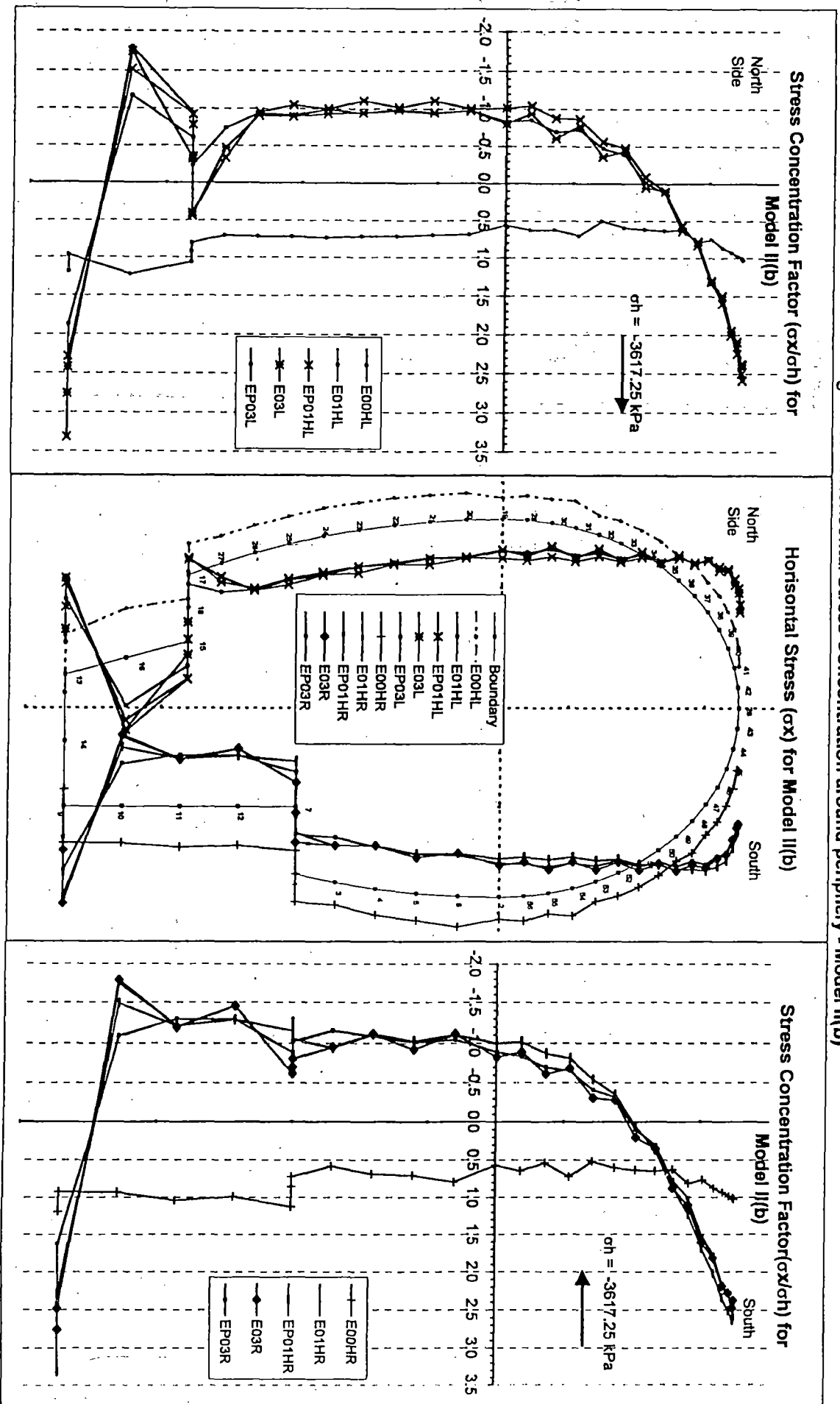


Table VI-2 Magnitude of Stress in X-direction around periphery -Model II(a)

| Stresses at x-direction L,ST ALL PICKED NODES | | Model II(a) : Without Horizontal Ground Load | | | | | | | | | | Model II(b) : With Horizontal Ground Load | | | | | | | | | |
|--|-------|--|-------------------|-------------------|--------------------|--------------------|--------------------|--------------------|--------------------|-------------------|---------------------|---|--------------------|--------------------|--------------------|-------------------|---------------------|---------------------|--------------------|--|--|
| | | Elastic | | | | | Elasto-Plastic | | | | | Elastic | | | | | Elasto-Plastic | | | | |
| | | CRTE00 SX(kPa) | CRTE01 SX(kPa) | CRTE02 SX(kPa) | CRTEP00 SX(kPa) | CRTEP01 SX(kPa) | crtep02 SX(kPa) | CRTE00H SX(kPa) | CRTE01H SX(kPa) | CRTE03 SX(kPa) | CRTEP00H SX(kPa) | CRTEP01H SX(kPa) | CRTEP03 SX(kPa) | CRTE00H SX(kPa) | CRTE01H SX(kPa) | CRTE03 SX(kPa) | CRTEP00H SX(kPa) | CRTEP01H SX(kPa) | CRTEP03 SX(kPa) | | |
| 14 | 3.00 | -32.10 | -1936.80 | -3476.00 | -2861.10 | -1936.80 | -2832.30 | -2376.30 | -1936.80 | -2832.30 | -2376.30 | -4374.60 | -12205.00 | -10123.00 | -4374.60 | -12179.00 | -8995.40 | | | | |
| 9 | 9.00 | -32.10 | -1942.90 | -3869.40 | -3942.10 | -1942.90 | -2966.00 | -2691.30 | -1942.90 | -2966.00 | -2691.30 | -3383.10 | -9068.60 | -9131.90 | -3383.10 | -8423.40 | -5964.40 | | | | |
| 10 | 9.00 | -27.83 | -1908.10 | 653.04 | 703.37 | -1908.10 | -54.63 | -18.30 | -1908.10 | -54.63 | -18.30 | -3423.70 | 6396.10 | 6551.40 | -3423.70 | 5467.40 | 3990.60 | | | | |
| 11 | 9.00 | -23.55 | -1863.30 | -109.27 | -127.35 | -1863.30 | -228.59 | -119.61 | -1863.30 | -228.59 | -119.61 | -3819.70 | 4465.00 | 4387.20 | -3819.70 | 4431.50 | 4751.60 | | | | |
| 12 | 9.00 | -19.28 | -1815.90 | 461.21 | 554.84 | -1815.90 | 441.53 | 292.59 | -1815.90 | 441.53 | 292.59 | -3640.40 | 4723.10 | 5357.60 | -3640.40 | 4725.50 | 4745.60 | | | | |
| 7 | 9.00 | -15.00 | -1776.00 | -197.28 | -494.28 | -1776.00 | -50.41 | -425.53 | -1776.00 | -50.41 | -425.53 | -4127.30 | 4226.20 | 2282.00 | -4127.30 | 4226.50 | 3260.60 | | | | |
| 8 | 12.16 | -15.00 | -1778.20 | -66.02 | 85.61 | -1778.20 | 177.44 | 20.78 | -1778.20 | 177.44 | 20.78 | -3146.40 | 4608.40 | 2580.10 | -3146.40 | 4611.60 | 2238.00 | | | | |
| 1 | 15.31 | -15.00 | -1779.30 | -1688.20 | -1782.60 | -1779.30 | -815.77 | -882.42 | -1779.30 | -815.77 | -882.42 | -2652.90 | 3861.50 | 2977.00 | -2652.90 | 3870.80 | 3754.10 | | | | |
| 3 | 16.10 | -12.06 | -1756.80 | -1100.90 | -1088.10 | -1756.80 | -709.92 | -751.90 | -1756.80 | -709.92 | -751.90 | -2146.70 | 3460.80 | 3495.20 | -2146.70 | 3464.60 | 4230.80 | | | | |
| 4 | 16.71 | -9.08 | -1724.80 | -147.84 | -161.52 | -1724.80 | -206.59 | -253.88 | -1724.80 | -206.59 | -253.88 | -2524.20 | 4070.90 | 4080.30 | -2524.20 | 4071.30 | 3989.30 | | | | |
| 5 | 17.15 | -6.07 | -1694.20 | -128.16 | -524.36 | -1694.20 | -132.22 | -400.22 | -1694.20 | -132.22 | -400.22 | -2586.60 | 3766.00 | 3400.60 | -2586.60 | 3766.10 | 3734.50 | | | | |
| 6 | 17.41 | -3.04 | -1662.70 | 68.02 | 47.23 | -1662.70 | -23.14 | -213.10 | -1662.70 | -23.14 | -213.10 | -2923.10 | 4051.50 | 4078.10 | -2923.10 | 4051.40 | 3830.20 | | | | |
| 2 | 17.50 | 0.00 | -1627.40 | -89.31 | -736.57 | -1627.40 | -112.04 | -675.29 | -1627.40 | -112.04 | -675.29 | -2100.90 | 3668.00 | 3045.10 | -2100.90 | 3668.10 | 3281.00 | | | | |
| 56 | 17.40 | 1.83 | -1607.00 | -98.86 | -587.13 | -1607.00 | -81.77 | -751.88 | -1607.00 | -81.77 | -751.88 | -2369.20 | 3723.20 | 3265.70 | -2369.20 | 3723.20 | 3052.20 | | | | |
| 55 | 17.12 | 3.64 | -1585.00 | -536.63 | -1353.60 | -1585.00 | -282.25 | -1151.90 | -1585.00 | -282.25 | -1151.90 | -1977.80 | 3206.40 | 2261.70 | -1977.80 | 3206.60 | 2577.10 | | | | |
| 54 | 16.64 | 5.41 | -1566.50 | -810.41 | -1055.20 | -1566.50 | -289.78 | -996.82 | -1566.50 | -289.78 | -996.82 | -2651.50 | 2982.60 | 2513.60 | -2651.50 | 2982.70 | 2400.20 | | | | |
| 53 | 15.99 | 7.12 | -1543.30 | -1512.20 | -1997.90 | -1543.30 | -641.20 | -1531.20 | -1543.30 | -641.20 | -1531.20 | -1907.90 | 1999.10 | 1129.10 | -1907.90 | 1999.30 | 1510.70 | | | | |
| 52 | 15.16 | 8.75 | -1524.20 | -1969.80 | -1792.20 | -1524.20 | -705.92 | -1361.60 | -1524.20 | -705.92 | -1361.60 | -2225.10 | 1295.10 | 1012.70 | -2225.10 | 1295.10 | 1164.30 | | | | |
| 51 | 14.16 | 10.29 | -1504.60 | -2665.60 | -2700.30 | -1504.60 | -1142.40 | -1957.60 | -1504.60 | -1142.40 | -1957.60 | -2326.30 | -192.61 | -739.80 | -2326.30 | -192.60 | -366.93 | | | | |
| 50 | 13.01 | 11.71 | -1486.50 | -2983.40 | -2426.50 | -1486.50 | -1246.50 | -1733.70 | -1486.50 | -1246.50 | -1733.70 | -2381.40 | -1362.20 | -1283.60 | -2381.40 | -1362.40 | -1102.20 | | | | |
| 49 | 11.71 | 13.01 | -1467.20 | -3387.10 | -3103.90 | -1467.20 | -1663.50 | -2340.90 | -1467.20 | -1663.50 | -2340.90 | -2305.40 | -3137.10 | -3224.40 | -2305.40 | -3137.50 | -2804.40 | | | | |
| 48 | 10.29 | 14.16 | -1454.50 | -3361.40 | -2692.20 | -1454.50 | -1745.60 | -2043.80 | -1454.50 | -1745.60 | -2043.80 | -2985.70 | -4522.10 | -4068.80 | -2985.70 | -4522.80 | -3716.00 | | | | |
| 47 | 8.75 | 15.16 | -1436.70 | -3373.20 | -3078.90 | -1436.70 | -2070.40 | -2643.20 | -1436.70 | -2070.40 | -2643.20 | -2828.50 | -6212.90 | -5901.40 | -2828.50 | -6213.90 | -5596.10 | | | | |
| 46 | 7.12 | 15.99 | -1425.80 | -2975.50 | -2463.80 | -1425.80 | -1997.40 | -2192.20 | -1425.80 | -1997.40 | -2192.20 | -3227.70 | -7408.60 | -6667.30 | -3227.70 | -7410.00 | -6472.50 | | | | |
| 45 | 5.41 | 16.64 | -1414.70 | -2732.00 | -2649.20 | -1414.70 | -2031.60 | -2505.50 | -1414.70 | -2031.60 | -2505.50 | -3447.90 | -8603.10 | -8045.00 | -3447.90 | -8604.70 | -7920.30 | | | | |
| 44 | 3.64 | 17.12 | -1405.70 | -2151.10 | -1941.00 | -1405.70 | -1688.70 | -1874.80 | -1405.70 | -1688.70 | -1874.80 | -3629.90 | -9221.90 | -8374.80 | -3629.90 | -9223.70 | -8363.60 | | | | |
| 43 | 1.83 | 17.40 | -1398.40 | -1926.00 | -2119.10 | -1398.40 | -1541.50 | -2097.30 | -1398.40 | -1541.50 | -2097.30 | -3711.80 | -9661.60 | -9078.50 | -3711.80 | -9663.60 | -9125.80 | | | | |
| 28 | 0.00 | 17.50 | -1393.00 | -1432.60 | -1477.50 | -1393.00 | -1161.80 | -1587.50 | -1393.00 | -1161.80 | -1587.50 | -3780.00 | -9481.40 | -8734.50 | -3780.00 | -9483.60 | -8868.50 | | | | |
| 42 | -1.83 | 17.40 | -1393.00 | -1432.60 | -1477.50 | -1393.00 | -1161.80 | -1587.50 | -1393.00 | -1161.80 | -1587.50 | -3780.00 | -9481.40 | -8734.50 | -3780.00 | -9483.60 | -8868.50 | | | | |
| 41 | -3.64 | 17.12 | -1391.30 | -1460.40 | -1796.20 | -1391.30 | -1178.00 | -1825.90 | -1391.30 | -1178.00 | -1825.90 | -3697.10 | -9160.60 | -8731.10 | -3697.10 | -9162.70 | -8886.40 | | | | |

Table VI-2 Magnitude of Stress in X-direction around periphery -Model II(a)

| Stresses at x-direction LIST ALL PICKED NODES | | | Model II(a) : Without Horizontal Ground Load | | | | | | Model II(b) : With Horizontal Ground Load | | | | | |
|--|--------|--------|--|-------------------|-------------------|--------------------|--------------------|--------------------|---|--------------------|-------------------|---------------------|---------------------|--------------------|
| Model II (CRT) | | | Elastic | | | Elasto-Plastic | | | Elastic | | | Elasto-Plastic | | |
| Node | X | Y | CRTE00 SX(kPa) | CRTE01 SX(kPa) | CRTE02 SX(kPa) | CRTEP00 SX(kPa) | CRTEP01 SX(kPa) | crtep02 SX(kPa) | CRTE00H SX(kPa) | CRTE01H SX(kPa) | CRTE03 SX(kPa) | CRTEP00H SX(kPa) | CRTEP01H SX(kPa) | CRTEP03 SX(kPa) |
| 40 | -5.41 | 16.64 | -1389.30 | -1240.10 | -1295.50 | -1389.30 | -974.99 | -1324.20 | -3605.60 | -8213.50 | -7655.70 | -3605.60 | -8215.60 | -7853.10 |
| 39 | -7.12 | 15.99 | -1393.50 | -1581.30 | -1414.40 | -1393.50 | -1160.30 | -1467.60 | -3184.40 | -5860.10 | -5499.80 | -3184.40 | -5861.90 | -5671.80 |
| 38 | -8.75 | 15.16 | -1401.00 | -1981.90 | -2025.30 | -1401.00 | -1379.80 | -1883.00 | -2770.70 | -4777.00 | -4819.70 | -2770.70 | -4778.60 | -4939.00 |
| 37 | -10.29 | 14.16 | -1401.40 | -2055.80 | -1614.80 | -1401.40 | -1396.60 | -1473.60 | -2925.20 | -3056.80 | -2867.80 | -2925.20 | -3058.10 | -2954.40 |
| 36 | -11.71 | 13.01 | -1416.20 | -2274.50 | -2191.60 | -1416.20 | -1363.90 | -1718.90 | -2242.20 | -2057.80 | -2341.00 | -2242.20 | -2058.90 | -2193.40 |
| 35 | -13.01 | 11.71 | -1423.40 | -2145.80 | -1612.40 | -1423.40 | -1123.00 | -1215.80 | -2321.90 | -385.85 | -361.14 | -2321.90 | -386.63 | -496.18 |
| 34 | -14.16 | 10.29 | -1435.40 | -2041.40 | -2074.20 | -1435.40 | -1011.90 | -1481.90 | -2257.00 | 328.67 | -195.31 | -2257.00 | 328.12 | 50.23 |
| 33 | -15.16 | 8.75 | -1448.10 | -1606.90 | -1287.30 | -1448.10 | -651.97 | -918.54 | -2163.50 | 1755.90 | 1596.60 | -2163.50 | 1755.60 | 1404.80 |
| 32 | -15.99 | 7.12 | -1466.30 | -1291.90 | -1670.60 | -1466.30 | -575.47 | -1171.90 | -1842.30 | 2064.90 | 1330.00 | -1842.30 | 2064.70 | 1742.60 |
| 31 | -16.64 | 5.41 | -1477.60 | -714.93 | -803.74 | -1477.60 | -249.63 | -717.38 | -2574.60 | 3173.40 | 2843.80 | -2574.60 | 3173.30 | 2622.20 |
| 30 | -17.12 | 3.64 | -1496.50 | -443.16 | -1325.50 | -1496.50 | -199.81 | -1048.10 | -2284.70 | 3217.00 | 2225.30 | -2284.70 | 3217.00 | 2542.30 |
| 29 | -17.40 | 1.83 | -1513.80 | -60.34 | -465.84 | -1513.80 | -31.16 | -606.56 | -2305.80 | 3831.20 | 3447.30 | -2305.80 | 3831.20 | 3116.90 |
| 19 | -17.50 | 0.00 | -1534.20 | -7.16 | -824.89 | -1534.20 | -81.35 | -787.09 | -2044.30 | 3729.00 | 2945.70 | -2044.30 | 3729.00 | 3044.60 |
| 20 | -17.43 | -2.66 | -1561.30 | -86.27 | -225.89 | -1561.30 | -88.18 | -300.37 | -2513.10 | 3680.50 | 3561.20 | -2513.10 | 3680.50 | 3592.00 |
| 21 | -17.23 | -5.31 | -1588.80 | -7.56 | -610.29 | -1588.80 | -15.43 | -556.89 | -2548.00 | 4062.60 | 3487.40 | -2548.00 | 4062.50 | 3423.70 |
| 22 | -16.90 | -7.94 | -1617.90 | -219.27 | -336.94 | -1617.90 | -121.87 | -426.84 | -2627.40 | 3735.30 | 3619.10 | -2627.40 | 3735.30 | 3555.50 |
| 23 | -16.43 | -10.56 | -1646.20 | -223.89 | -805.99 | -1646.20 | -88.87 | -648.36 | -2633.00 | 4063.00 | 3462.10 | -2633.00 | 4063.00 | 3438.50 |
| 24 | -15.83 | -13.15 | -1675.90 | -514.99 | -677.30 | -1675.90 | -248.14 | -522.83 | -2698.60 | 3668.00 | 3417.80 | -2698.60 | 3668.20 | 3647.30 |
| 25 | -15.10 | -15.70 | -1704.30 | -617.93 | -1066.30 | -1704.30 | -365.40 | -709.66 | -2641.50 | 3850.40 | 3272.00 | -2641.50 | 3850.80 | 3345.70 |
| 26 | -14.24 | -18.22 | -1734.30 | -925.64 | -921.22 | -1734.30 | -666.63 | -570.57 | -2635.20 | 3506.00 | 3319.30 | -2635.20 | 3505.00 | 3445.20 |
| 27 | -13.25 | -20.69 | -1763.10 | -2410.60 | -2086.90 | -1763.10 | -1238.90 | -1038.00 | -2585.90 | 1227.90 | 1742.20 | -2585.90 | 1244.20 | 2705.50 |
| 17 | -12.15 | -23.10 | -1795.20 | -3807.10 | -3505.20 | -1795.20 | -2124.40 | -1447.60 | -2949.10 | -1502.70 | -1613.50 | -2949.10 | -1463.50 | 863.81 |
| 18 | -9.07 | -23.10 | -1801.90 | -852.08 | -636.35 | -1801.90 | -778.14 | -591.75 | -3376.80 | 2900.20 | 1307.50 | -3376.80 | 2868.60 | 1418.50 |
| 15 | -6.00 | -23.10 | -1810.50 | -533.31 | -915.50 | -1810.50 | -415.69 | -892.78 | -3908.60 | 3456.70 | 1180.60 | -3908.60 | 3380.70 | 2212.10 |
| 16 | -4.50 | -27.60 | -1863.90 | 752.82 | 549.74 | -1863.90 | -201.69 | -225.70 | -4503.20 | 6618.70 | 6431.50 | -4503.20 | 5593.70 | 4306.50 |
| 13 | -3.00 | -32.10 | -1922.50 | -3436.50 | -3448.00 | -1922.50 | -2693.90 | -2552.30 | -3576.60 | -9005.30 | -8883.50 | -3576.60 | -8379.00 | -6882.90 |
| 14 | 3.00 | -32.10 | -1936.80 | -3476.00 | -2861.10 | -1936.80 | -2832.30 | -2376.30 | -4374.60 | -12205.00 | -10123.00 | -4374.60 | -12179.00 | -8895.40 |

Table VI-2 Magnitude of Stress in Y-Direction around periphery - Model II

| Stresses at y-direction LIST ALL PICKED NODES Model II (CRT) | | | Model II(a) : Without Horizontal Ground Load | | | | | | Model II(b) : With Horizontal Ground Load | | | | | | |
|--|--------|--------|--|-------------------|-------------------|--------------------|--------------------|--------------------|---|--------------------|-------------------|---------------------|---------------------|--------------------|----------|
| | | | Elastic | | | Elasto-Plastic | | | Elastic | | | Elasto-Plastic | | | |
| | | | CRTE00 SY(kPa) | CRTE01 SY(kPa) | CRTE02 SY(kPa) | CRTEP00 SY(kPa) | CRTEP01 SY(kPa) | crtep02 SY(kPa) | CRTE00H SY(kPa) | CRTE01H SY(kPa) | CRTE03 SY(kPa) | CRTEP00H SY(kPa) | CRTEP01H SY(kPa) | CRTEP03 SY(kPa) | |
| 1 | 15.31 | -15.00 | -4059.70 | -4299.90 | -5217.30 | -3223.90 | -4059.70 | -2594.00 | -3223.90 | -4284.30 | -2183.60 | -2883.80 | -4284.30 | -2172.40 | 1763.30 |
| 3 | 16.10 | -12.06 | -3989.80 | -6147.40 | -5553.10 | -4069.10 | -3989.80 | -3286.30 | -4069.10 | -3853.80 | -3143.50 | -2876.30 | -3853.80 | -3130.30 | 1763.00 |
| 4 | 16.71 | -9.08 | -3912.40 | -6302.00 | -5693.70 | -3150.90 | -3912.40 | -2723.20 | -3150.90 | -3612.60 | -2808.70 | -2524.90 | -3612.60 | -2799.10 | 1247.80 |
| 5 | 17.15 | -6.07 | -3833.50 | -6583.50 | -6230.90 | -3817.90 | -3833.50 | -2950.70 | -3817.90 | -3440.00 | -3240.50 | -3174.40 | -3440.00 | -3233.70 | 2.80 |
| 6 | 17.41 | -3.04 | -3754.60 | -6942.70 | -6409.00 | -3257.80 | -3754.60 | -2736.70 | -3257.80 | -3434.90 | -3448.20 | -3212.10 | -3434.90 | -3443.30 | 60.66 |
| 2 | 17.50 | 0.00 | -3681.70 | -7794.30 | -7221.60 | -4509.20 | -3681.70 | -3055.60 | -4509.20 | -3041.30 | -4659.40 | -4425.90 | -3041.30 | -4655.40 | -1640.20 |
| 56 | 17.40 | 1.83 | -3632.50 | -8392.50 | -7482.10 | -4492.80 | -3632.50 | -2819.90 | -4492.80 | -3108.20 | -5427.00 | -4844.30 | -3108.20 | -5423.90 | -2556.40 |
| 55 | 17.12 | 3.64 | -3591.50 | -8361.70 | -7579.40 | -5044.40 | -3591.50 | -3048.30 | -5044.40 | -3078.70 | -6280.40 | -5698.00 | -3078.70 | -6278.00 | -3436.50 |
| 54 | 16.64 | 5.41 | -3551.20 | -7891.40 | -6986.80 | -4111.10 | -3551.20 | -2491.50 | -4111.10 | -3396.30 | -6638.70 | -5757.70 | -3396.30 | -6637.10 | -3485.20 |
| 53 | 15.99 | 7.12 | -3516.60 | -7119.50 | -6706.90 | -4538.30 | -3516.60 | -2629.70 | -4538.30 | -3414.70 | -6991.80 | -6410.40 | -3414.70 | -6990.80 | -4570.90 |
| 52 | 15.16 | 8.75 | -3483.90 | -5988.80 | -5568.70 | -3415.90 | -3483.90 | -2007.60 | -3415.90 | -3622.50 | -6820.10 | -6065.10 | -3622.50 | -6819.70 | -4365.90 |
| 51 | 14.16 | 10.29 | -3455.30 | -4999.80 | -5153.20 | -3770.40 | -3455.30 | -2030.90 | -3770.40 | -3776.70 | -6620.80 | -6323.10 | -3776.70 | -6620.80 | -5034.30 |
| 50 | 13.01 | 11.71 | -3431.90 | -3663.40 | -3723.70 | -2601.20 | -3431.90 | -1473.50 | -2601.20 | -3886.20 | -5870.40 | -5439.00 | -3886.20 | -5870.70 | -4522.40 |
| 49 | 11.71 | 13.01 | -3411.70 | -2877.90 | -3511.70 | -2842.70 | -3411.70 | -1375.90 | -2842.70 | -3989.00 | -5219.80 | -5386.00 | -3989.00 | -5220.20 | -4740.40 |
| 48 | 10.29 | 14.16 | -3399.20 | -1680.90 | -2034.70 | -1733.70 | -3399.20 | -901.48 | -1733.70 | -3916.00 | -4043.00 | -4040.80 | -3916.00 | -4043.40 | -3658.00 |
| 47 | 8.75 | 15.16 | -3387.60 | -1314.90 | -2156.40 | -1951.80 | -3387.60 | -762.22 | -1951.80 | -3972.70 | -3243.30 | -3859.60 | -3972.70 | -3243.60 | -3568.20 |
| 46 | 7.12 | 15.99 | -3384.60 | -444.99 | -790.01 | -917.97 | -3384.60 | -406.02 | -917.97 | -3883.70 | -1969.10 | -2302.00 | -3883.70 | -1969.40 | -2182.80 |
| 45 | 5.41 | 16.64 | -3385.30 | -489.20 | -1287.00 | -1136.80 | -3385.30 | -308.59 | -1136.80 | -3811.70 | -1410.70 | -2334.40 | -3811.70 | -1410.90 | -2229.30 |
| 44 | 3.64 | 17.12 | -3391.50 | 84.55 | -79.31 | -266.53 | -3391.50 | -23.82 | -266.53 | -3764.80 | -388.31 | -885.10 | -3764.80 | -388.41 | -878.73 |
| 43 | 1.83 | 17.40 | -3402.20 | -201.84 | -859.72 | -733.72 | -3402.20 | -163.78 | -733.72 | -3724.40 | -358.20 | -1385.80 | -3724.40 | -358.22 | -1357.20 |
| 28 | 0.00 | 17.50 | -3416.90 | 195.66 | 190.38 | -67.85 | -3416.90 | 159.24 | -67.85 | -3741.10 | 186.50 | -294.76 | -3741.10 | 186.49 | -326.23 |
| 42 | -1.83 | 17.40 | -3439.70 | -164.77 | -756.47 | -754.47 | -3439.70 | -139.70 | -754.47 | -3771.30 | -377.63 | -1330.10 | -3771.30 | -377.66 | -1332.40 |
| 41 | -3.64 | 17.12 | -3462.50 | 125.91 | 113.35 | 106.33 | -3462.50 | 107.17 | 106.33 | -3857.90 | -340.82 | -687.85 | -3857.90 | -340.92 | -733.17 |
| 40 | -5.41 | 16.64 | -3491.50 | -286.09 | -955.58 | -851.07 | -3491.50 | -229.72 | -851.07 | -3942.30 | -1347.50 | -2124.40 | -3942.30 | -1347.70 | -2139.30 |
| 39 | -7.12 | 15.99 | -3523.60 | -175.34 | -349.23 | -617.30 | -3523.60 | -117.60 | -617.30 | -4060.80 | -1676.20 | -1846.60 | -4060.80 | -1676.60 | -1887.00 |
| 38 | -8.75 | 15.16 | -3566.00 | -777.48 | -1573.30 | -1448.50 | -3566.00 | -552.15 | -1448.50 | -4181.30 | -2862.60 | -3423.60 | -4181.30 | -2863.20 | -3414.20 |
| 37 | -10.29 | 14.16 | -3592.20 | -1021.50 | -1342.30 | -1517.40 | -3592.20 | -814.31 | -1517.40 | -4144.50 | -3335.10 | -3320.80 | -4144.50 | -3335.90 | -3297.20 |
| 36 | -11.71 | 13.01 | -3646.20 | -1979.00 | -2753.50 | -2516.90 | -3646.20 | -1257.80 | -2516.90 | -4252.70 | -4447.60 | -4764.20 | -4252.70 | -4448.40 | -4582.60 |
| 35 | -13.01 | 11.71 | -3683.30 | -2692.40 | -2941.90 | -2432.90 | -3683.30 | -1480.30 | -2432.90 | -4173.60 | -4855.30 | -4642.10 | -4173.60 | -4856.30 | -4467.60 |

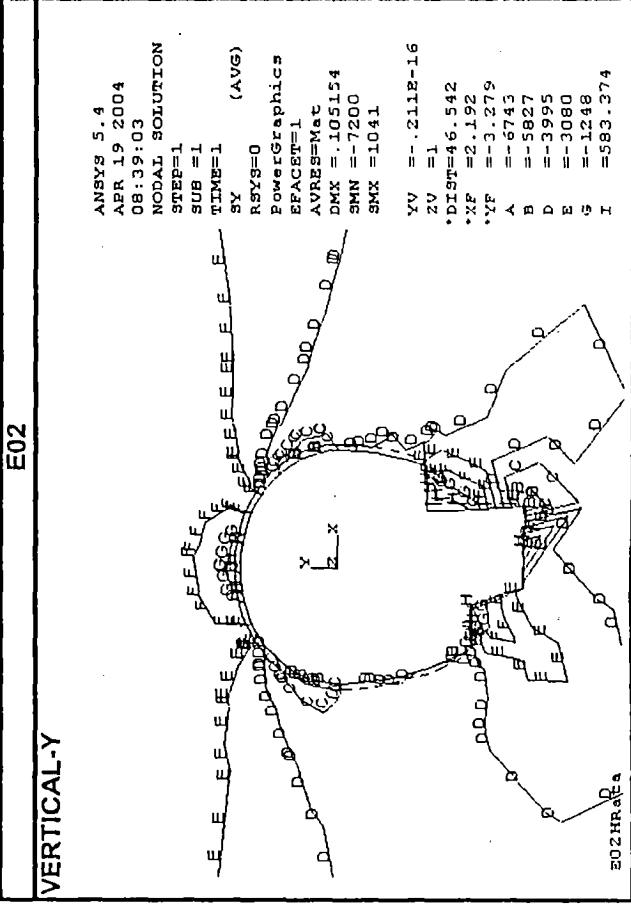
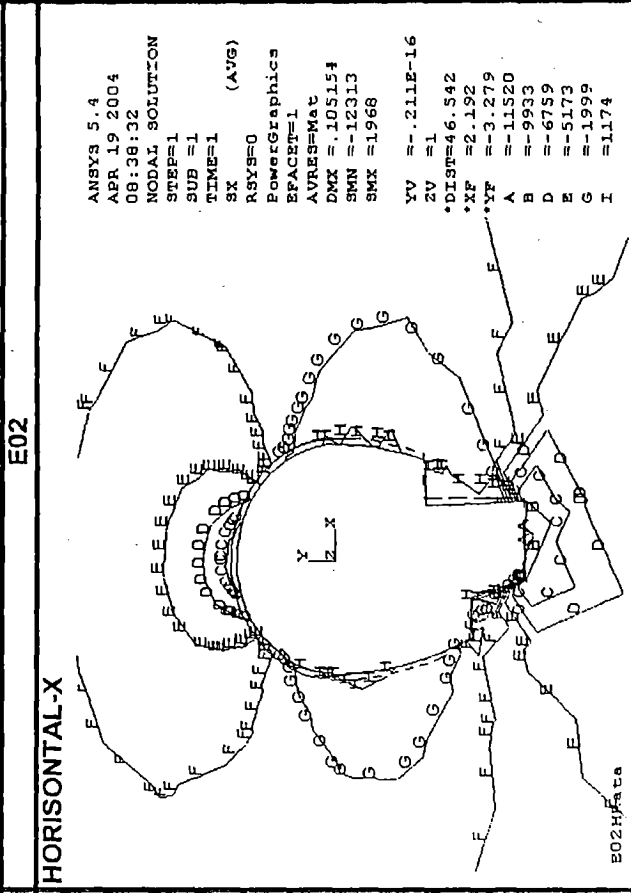
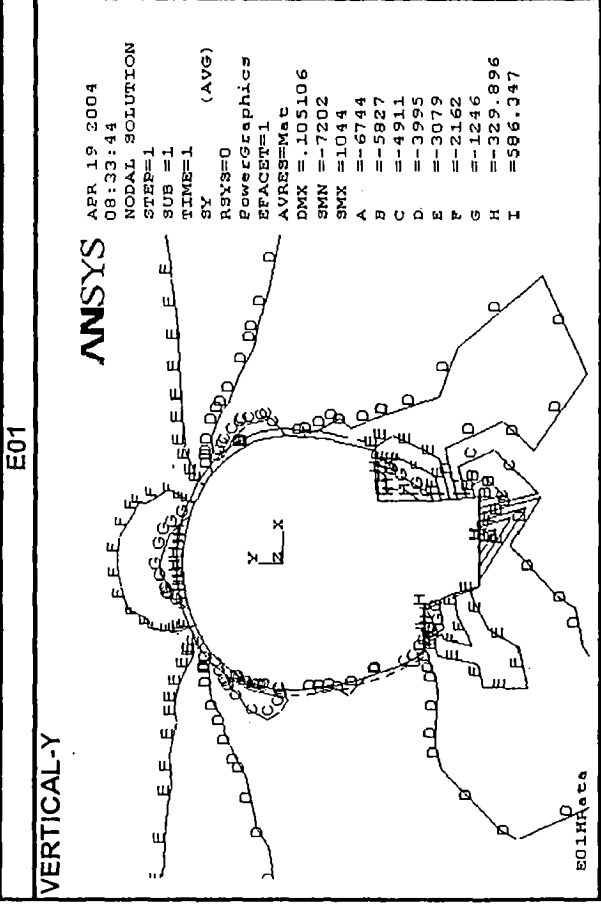
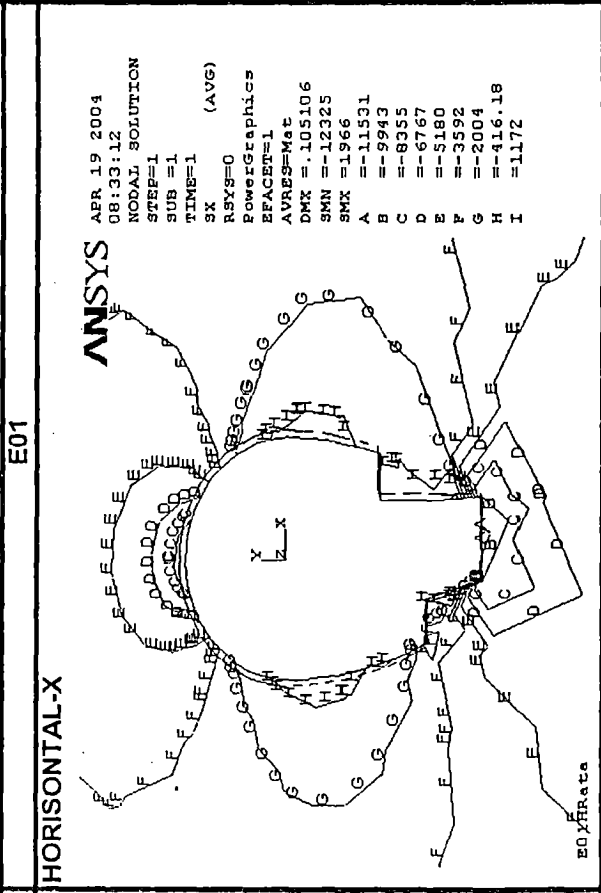
Table VI-2 Magnitude of Stress in Y-Direction around periphery - Model II

| Stresses at y-direction LIST ALL PICKED NODES Model II (CRT) | | | Model II(a) : Without Horizontal Ground Load | | | | | | Model II(b) : With Horizontal Ground Load | | | | | |
|--|--------|--------|--|-------------------|-------------------|--------------------|--------------------|--------------------|---|--------------------|-------------------|---------------------|---------------------|--------------------|
| Node | X | Y | Elastic | | | Elasto-Plastic | | | Elastic | | | Elasto-Plastic | | |
| | | | CRTE00 SY(kPa) | CRTE01 SY(kPa) | CRTE02 SY(kPa) | CRTEP00 SY(kPa) | CRTEP01 SY(kPa) | crtep02 SY(kPa) | CRTE00H SY(kPa) | CRTE01H SY(kPa) | CRTE03 SY(kPa) | CRTEP00H SY(kPa) | CRTEP01H SY(kPa) | CRTEP03 SY(kPa) |
| 34 | -14.16 | 10.29 | -3728.80 | -4000.50 | -4453.30 | -3728.80 | -1947.20 | -3662.30 | -4078.00 | -5712.30 | -5744.70 | -4078.00 | -5713.30 | -5304.30 |
| 33 | -15.16 | 8.75 | -3774.90 | -5072.60 | -4927.90 | -3774.90 | -2050.30 | -3263.90 | -3947.00 | -5905.10 | -5458.00 | -3947.00 | -5906.10 | -4267.90 |
| 32 | -15.99 | 7.12 | -3827.30 | -6438.60 | -6282.50 | -3827.30 | -2564.20 | -4517.70 | -3748.30 | -6431.50 | -6141.20 | -3748.30 | -6432.30 | -5008.60 |
| 31 | -16.64 | 5.41 | -3866.20 | -7475.20 | -6762.80 | -3866.20 | -2521.50 | -4075.10 | -3742.30 | -6325.60 | -5654.20 | -3742.30 | -6326.30 | -3454.50 |
| 30 | -17.12 | 3.64 | -3918.00 | -8312.00 | -7622.60 | -3918.00 | -2841.30 | -5269.40 | -3551.30 | -6377.60 | -5916.70 | -3551.30 | -6378.00 | -4260.70 |
| 29 | -17.40 | 1.83 | -3963.70 | -8671.10 | -7637.70 | -3963.70 | -2681.20 | -4424.40 | -3465.10 | -5899.10 | -5214.50 | -3465.10 | -5899.10 | -2749.50 |
| 19 | -17.50 | 0.00 | -4012.80 | -8352.80 | -7706.00 | -4012.80 | -2982.90 | -4971.70 | -3377.60 | -5412.90 | -5133.30 | -3377.60 | -5412.60 | -3024.50 |
| 20 | -17.43 | -2.66 | -4074.20 | -7791.60 | -7247.90 | -4074.20 | -2968.40 | -3595.20 | -3644.20 | -4797.20 | -4566.30 | -3644.20 | -4796.40 | -1154.90 |
| 21 | -17.23 | -5.31 | -4137.20 | -7427.10 | -7173.10 | -4137.20 | -2648.50 | -4285.60 | -3719.80 | -4270.90 | -4306.80 | -3719.80 | -4269.70 | -1801.60 |
| 22 | -16.90 | -7.94 | -4199.40 | -7257.10 | -6860.50 | -4199.40 | -2840.00 | -3763.50 | -3835.90 | -4394.70 | -4257.80 | -3835.90 | -4392.80 | -1252.90 |
| 23 | -16.43 | -10.56 | -4259.50 | -6957.30 | -6804.90 | -4259.50 | -2563.10 | -4188.50 | -3938.30 | -4242.60 | -4313.10 | -3938.30 | -4240.10 | -1690.00 |
| 24 | -15.83 | -13.15 | -4318.00 | -6770.00 | -6425.80 | -4318.00 | -2752.80 | -3632.40 | -4112.30 | -4723.10 | -4517.20 | -4112.30 | -4719.30 | -787.21 |
| 25 | -15.10 | -15.70 | -4374.50 | -6488.50 | -6276.90 | -4374.50 | -2602.90 | -3947.90 | -4270.00 | -4905.30 | -4734.90 | -4270.00 | -4899.90 | -1829.20 |
| 26 | -14.24 | -18.22 | -4429.10 | -6371.40 | -5844.30 | -4429.10 | -2770.00 | -3370.40 | -4574.60 | -5828.00 | -5082.20 | -4574.60 | -5819.20 | -1044.30 |
| 27 | -13.25 | -20.69 | -4481.40 | -6513.30 | -5741.80 | -4481.40 | -2522.90 | -3923.50 | -4888.10 | -7081.20 | -5634.50 | -4888.10 | -6503.52 | -2732.10 |
| 17 | -12.15 | -23.10 | -4529.20 | -4484.90 | -5679.70 | -4529.20 | -2427.20 | -3484.70 | -5228.80 | -5479.50 | -6740.20 | -5228.80 | -5465.30 | -5121.10 |
| 18 | -9.07 | -23.10 | -4504.90 | 754.13 | 954.75 | -4504.90 | -222.36 | -87.14 | -4804.80 | 1196.00 | 1284.00 | -4804.80 | 1192.90 | -982.85 |
| 15 | -6.00 | -23.10 | -4486.10 | -135.26 | -254.29 | -4486.10 | -260.62 | -453.15 | -4446.90 | -714.61 | -566.44 | -4446.90 | -748.67 | -45.67 |
| 16 | -4.50 | -27.60 | -4577.60 | -1019.90 | -501.97 | -4577.60 | -901.28 | -539.55 | -5003.70 | -2740.60 | -224.94 | -5003.70 | -2050.50 | 2994.10 |
| 13 | -3.00 | -32.10 | -4665.80 | -1857.20 | -1848.00 | -4665.80 | -1325.80 | -1224.90 | -5544.80 | -4899.30 | -4466.60 | -5544.80 | -4461.90 | -2646.10 |
| 14 | 3.00 | -32.10 | -4616.70 | 586.23 | 675.31 | -4616.70 | -528.47 | -530.57 | -5326.90 | 745.83 | 936.15 | -5326.90 | 741.80 | 750.30 |
| 9 | 9.00 | -32.10 | -4544.10 | -4528.00 | -4425.40 | -4544.10 | -2969.80 | -2778.40 | -4960.40 | -7400.20 | -7105.90 | -4960.40 | -6796.50 | -2896.20 |
| 10 | 9.00 | -27.83 | -4456.20 | -3865.70 | -2995.90 | -4456.20 | -2135.20 | -1475.60 | -4764.30 | -3894.00 | -2238.80 | -4764.30 | -3219.60 | 1909.30 |
| 11 | 9.00 | -23.55 | -4348.00 | -1575.30 | -1604.40 | -4348.00 | -1655.70 | -1358.70 | -4753.20 | -717.73 | -530.34 | -4753.20 | -739.01 | 3685.50 |
| 12 | 9.00 | -19.28 | -4239.70 | 154.03 | -56.92 | -4239.70 | 367.19 | -240.07 | -4568.50 | 867.57 | 1587.00 | -4568.50 | 868.07 | 3718.40 |
| 7 | 9.00 | -15.00 | -4149.90 | 237.60 | -59.05 | -4149.90 | 322.77 | -143.75 | -4476.10 | 461.50 | 809.55 | -4476.10 | 460.20 | 245.36 |
| 8 | 12.16 | -15.00 | -4104.60 | 613.26 | 857.84 | -4104.60 | 194.46 | 228.03 | -4176.20 | 378.98 | 309.72 | -4176.20 | 378.05 | -183.62 |
| 1 | 15.31 | -15.00 | -4059.70 | -4299.90 | -5217.30 | -4059.70 | -2594.00 | -3223.90 | -4284.30 | -2183.60 | -2883.80 | -4284.30 | -2172.40 | 1763.30 |

MODEL I-Elastic

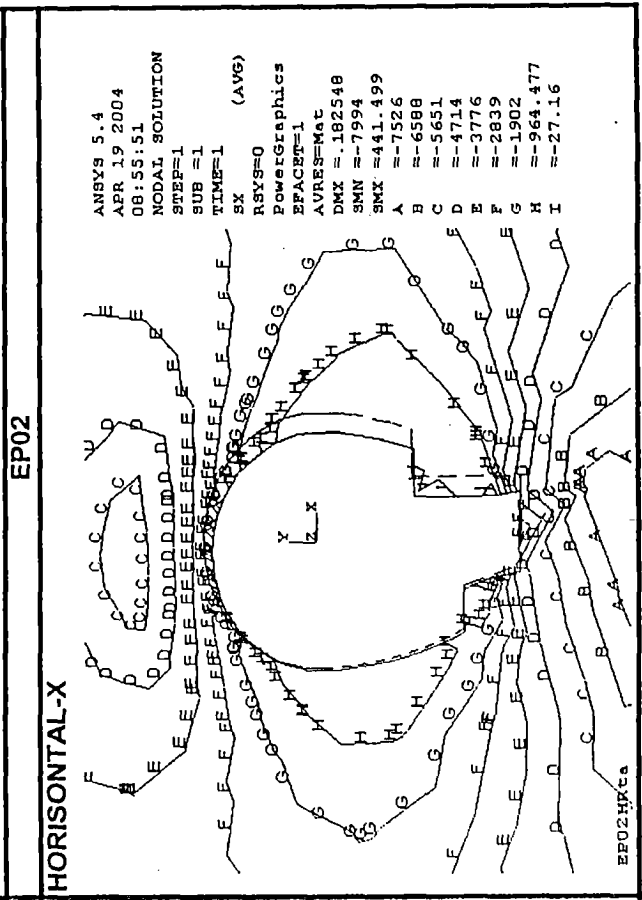
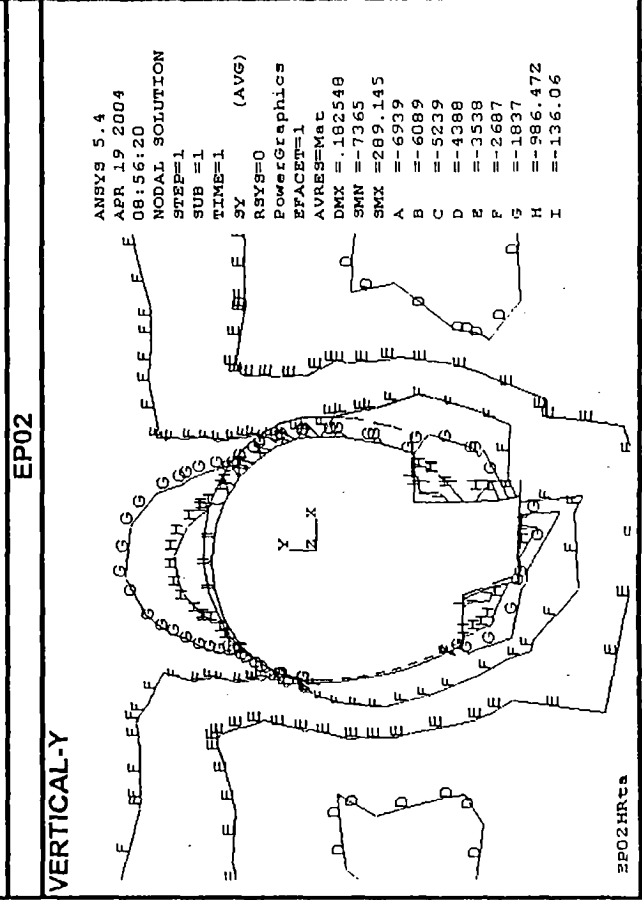
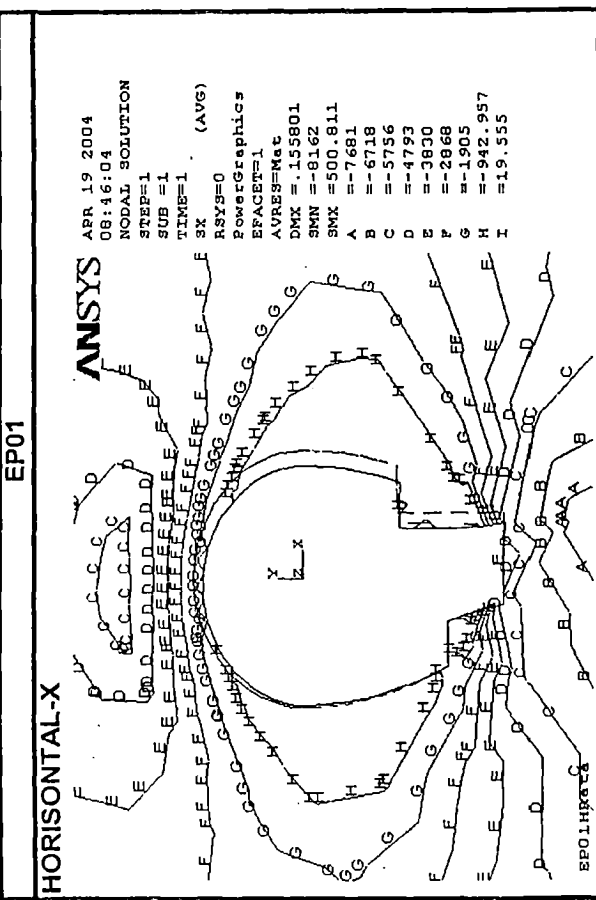
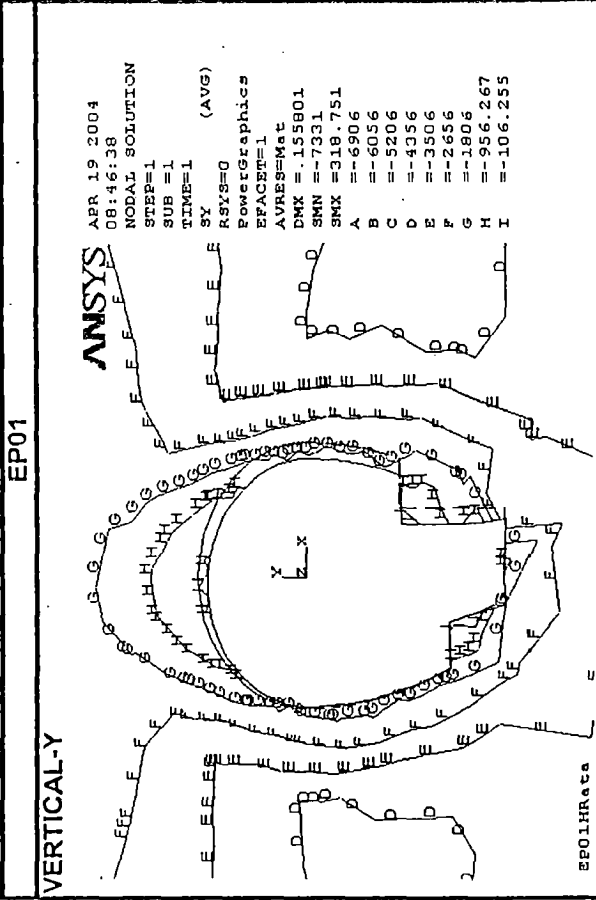
Figure VI-5(a) SX/SY for Model I - Elastic behaviour

ANSYS RESULTS - Contour Plot
SX & SY - STRESS



ANSYS RESULTS - Contour Plot SX & SY - STRESS

MODEL I-Elastoplastic



ANSYS RESULTS - Contour Plot
SX & SY - STRESS

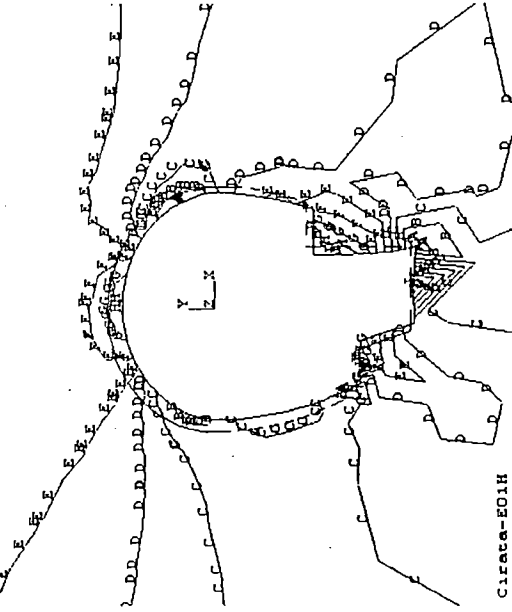
Figure VI-6 (a) SX/SY Model II - Elastic

67

MODEL II-Elastic

CRT-E01H

VERTICAL-Y

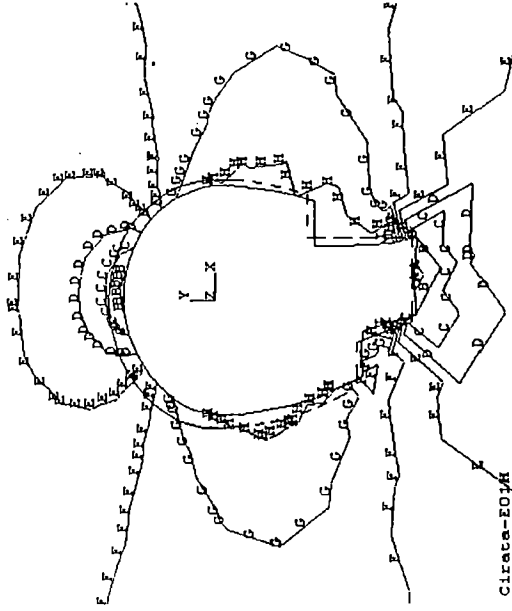


Cirata-E01H

ANSYS 5.4
APR 18 2004
22:04:21
YV =-.211E-16
ZV =1
*DIST=41.982
*XF =.385548
*YF =-6.775
A =-6923
B =-5969
C =-5012
D =-4057
E =-3102
F =-2147
G =-1192
H =-236.68
I =-718.46

CRT-E01H

HORIZONTAL-X

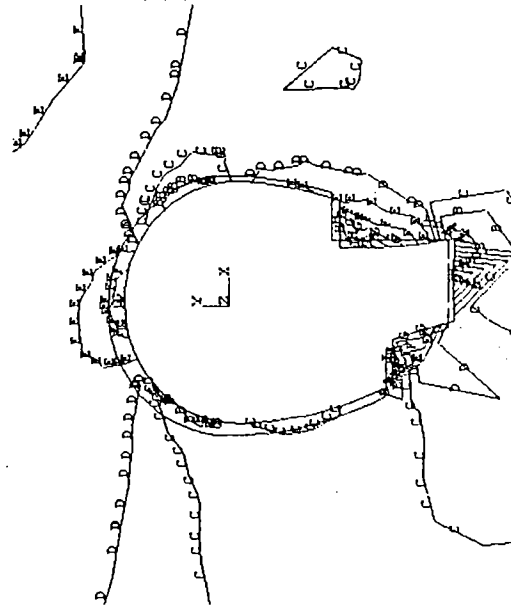


Cirata-E01H

ANSYS 5.4
APR 19 2004
22:03:41
YV =-.211E-16
ZV =1
*DIST=41.982
*XF =.385548
*YF =-6.775
A =-11159
B =-9067
C =-6976
D =-4884
E =-2793
F =-701.466
G =1390
H =-3481
I =-5573

CRT-E03

VERTICAL-Y

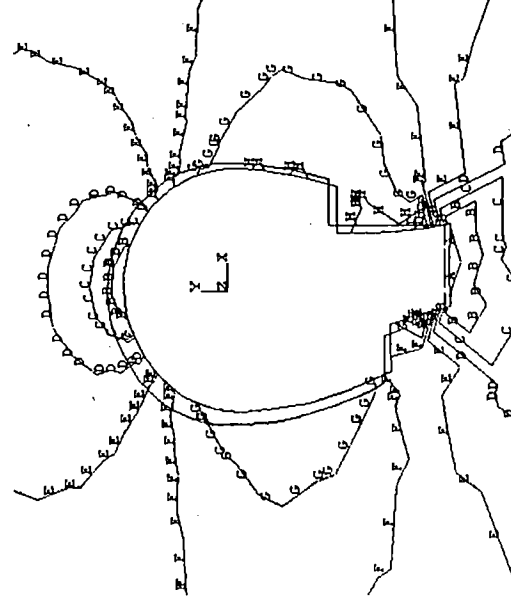


Cirata-E03

ANSYS 5.4
APR 19 2004
00:06:17
YV =-.211E-16
ZV =1
*DIST=39.56
*XF =.048631
*YF =-8.185
A =-6623
B =-5657
C =-4691
D =-3725
E =-2759
F =-1794
G =-827.69
H =138.181
I =1104

CRT-E03

HORIZONTAL-X

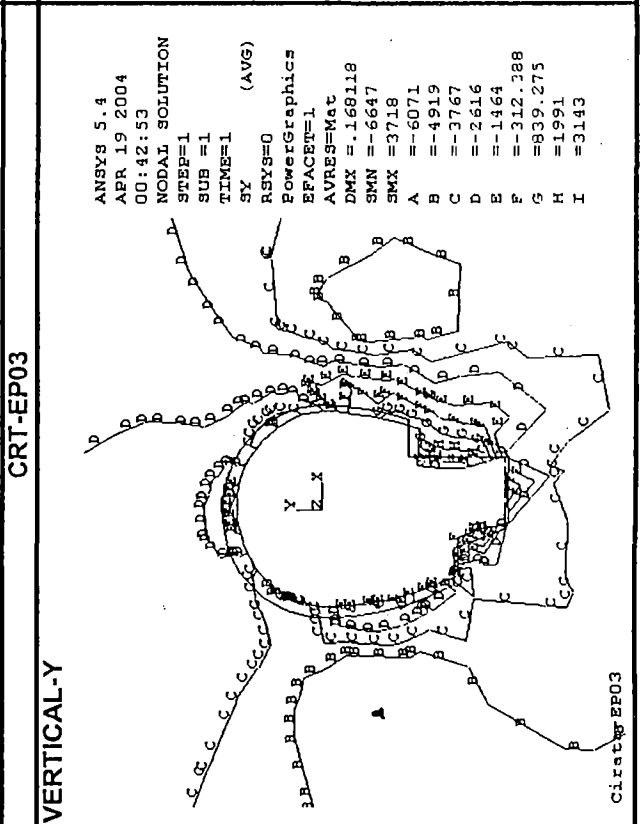
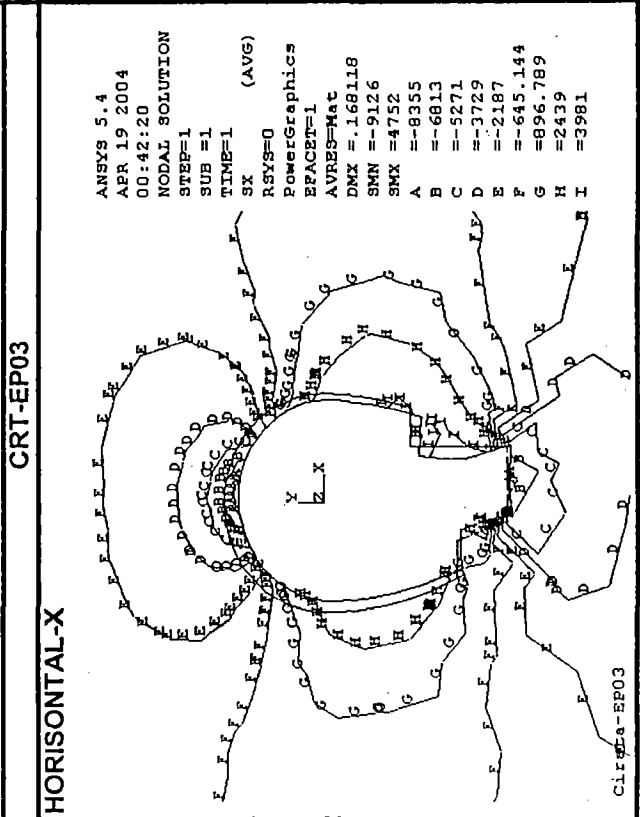
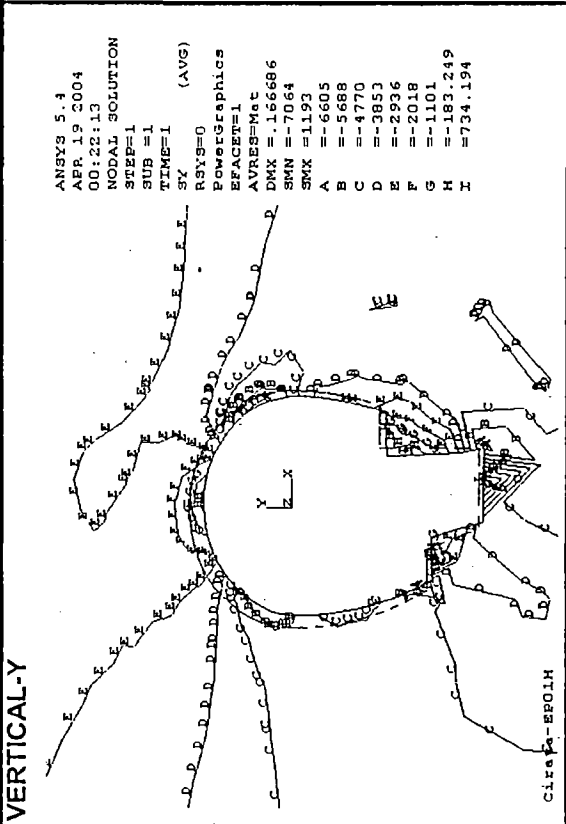
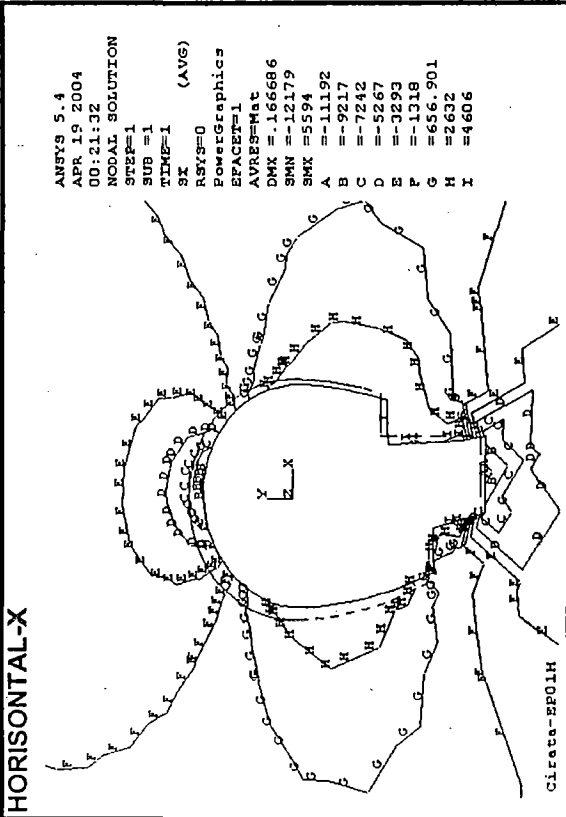


Cirata-E03

ANSYS 5.4
APR 19 2004
00:05:51
YV =-.211E-16
ZV =1
*DIST=39.56
*XF =.048631
*YF =-8.185
A =-9196
B =-7344
C =-5491
D =-3638
E =-1786
F =67.001
G =1920
H =3772
I =5625

ANSYS RESULTS - Contour Plot
SX & SY - STRESS

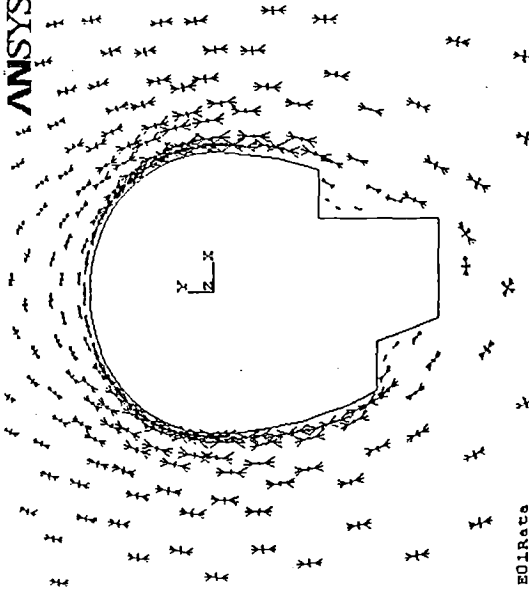
68 MODEL II-Elastoplastic CRT-EP01H



ANSYS RESULTS - Contour Plot
Principal Stress Vector

E01

ANSYS
APR 19 2004
09:30:29
VECTOR
STEP=1
SUB =1
TIME=1
9
PRIN1
PRIN2
PRIN3



E01Reta

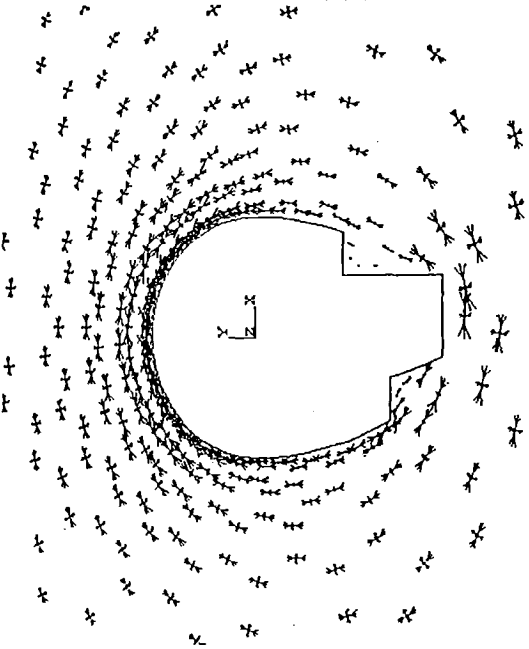
Figure VI - 7 (a)

69

MODEL I

E02H

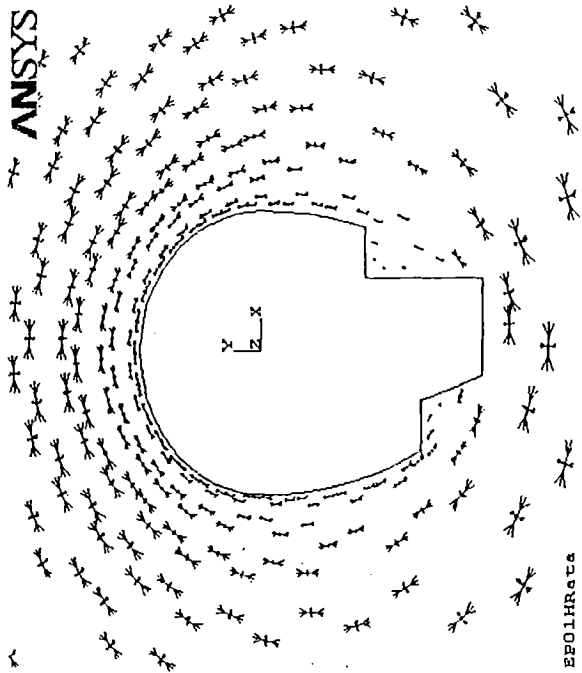
ANSYS 5.4
APR 19 2004
08:40:53
VECTOR
STEP=1
SUB =1
TIME=1
9
PRIN1
PRIN2
PRIN3
YV =-.211E-16
ZV =1
*DISTW=46.542
*XF =2.192
*YF =-3.279
EDGE



E02HReta

EP01

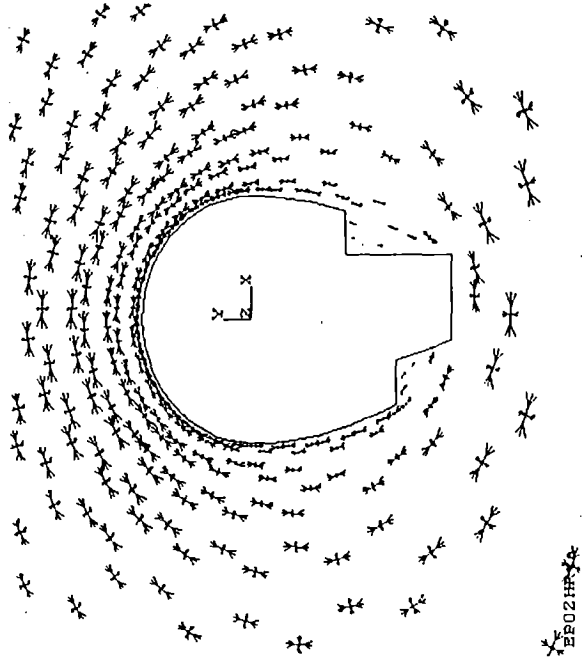
ANSYS
APR 19 2004
08:51:19
VECTOR
STEP=1
SUB =1
TIME=1
9
PRIN1
PRIN2
PRIN3



EP01Reta

EP02H

ANSYS 5.4
APR 19 2004
09:00:03
VECTOR
STEP=1
SUB =1
TIME=1
9
PRIN1
PRIN2
PRIN3



EP02HReta

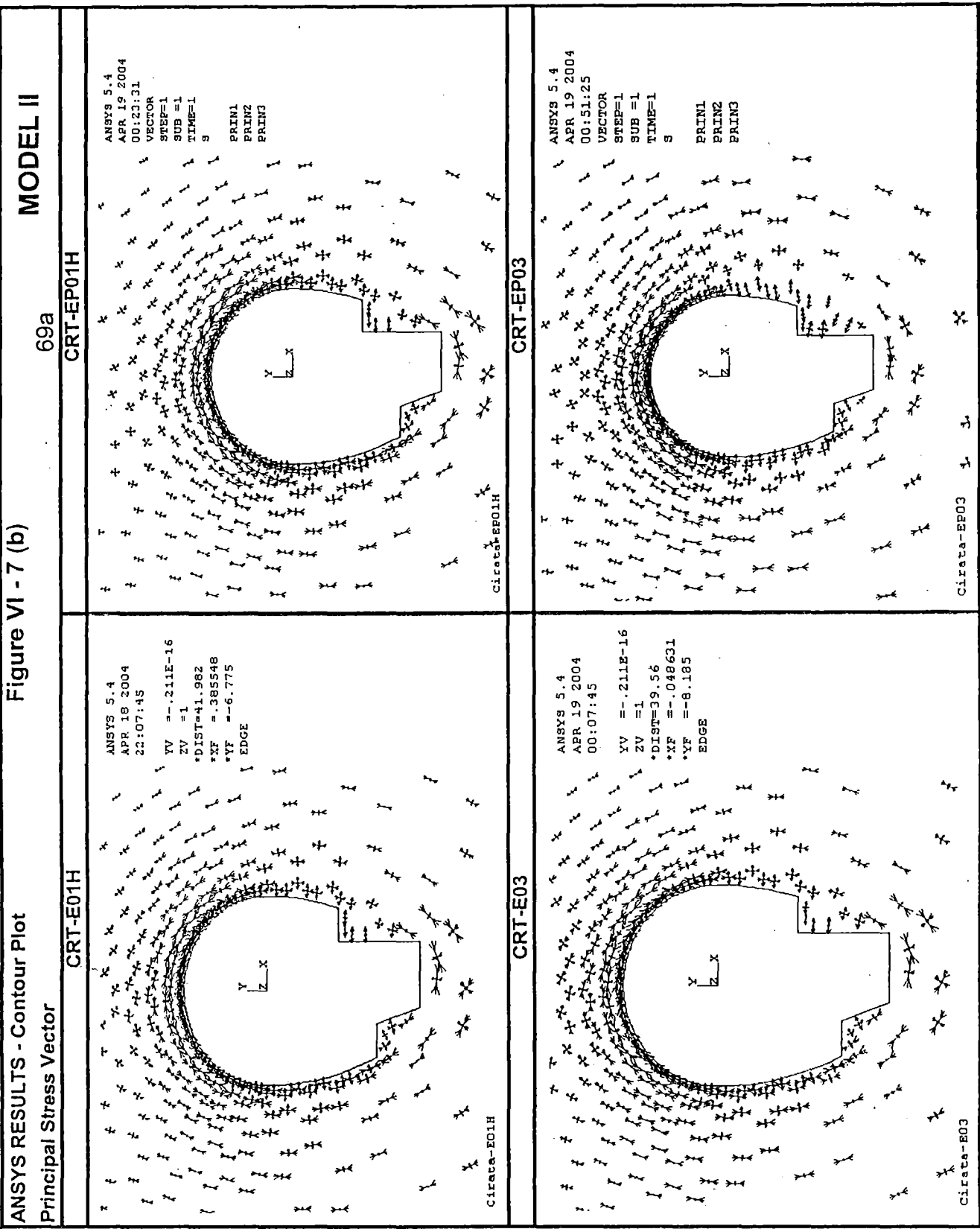


Figure VI - 7 (b)

From result in Figure VI-1 to Figure VI-7 and Table VI – 1 & Table VI – 2 some inferences are made (convention sign: (+) for compressive stress, and (–) for tensile stress):

VI.2.i.(1) General

Elasto-plastic model always give magnitude of SX lesser than elastic model, in both model without support and with support. In Model II, elasto-plastic and elastic parameters give qualitatively equals for max SX and min SX. But in Model I, the difference is significant, max SX elasto-plastic only 43,8 % (+5394 kPa) of elastic's (+12,325 kPa) and min SX elasto-plastic 25,5 % (-500 kPa) of elastic's (+1967,4 kPa).

In term of SY, Elasto-plastic model does not always give magnitude lesser than elastic model. In Model II the difference between elasto-plastic and elastic is small for max SY less than 5 %, but in min SY elasto-plastic model give a value of 234 % times of elastic, at same location (+3,718 kPa for elasto-plastic compared to +1,587 kPa for elastic, at node 12). In Model I, the difference is significant, max SY elasto-plastic only 43,8 % (+5394 kPa) of elastic's (+12,325 kPa) and min SY elasto-plastic 25,5 % (-500 kPa) of elastic's (+1967,4 kPa).

The model in elasto-plastic behaviour for both models always give max SY maximum greater than elastic and min SX lesser than elastic.

All the minimum and maximum magnitude of SX & SY always occur on lower part of cavern (bench), due to two main reason, firstly in modeling no support is provided in bench, hence no confinement effect take place in that part, secondly, structurally lower part always have greater insitu stress (gravity & horizontal pressure) which will be redistributed after opening is made.

It is also seen that in vault portion of the cavern (i.e. roof part) the stresses both in X & Y direction in all models remains in compression except in Model II(b) (with horizontal ground load) where SX in tensile. Because of the supports in this portion compression generally seen increasing but the tensile stresses (SX) are seen to be slightly decreasing. The results do not confirm the utility of supports in respect of significant stress reduction.

VI.2.i.(2) Stresses in X-direction

The maximum stresses in the X-direction (max SX) is +12,325 kPa from Model I elastic without support (E01H), and in term of stress concentration factor it is equal to 3.36 and

occurs at toe of cavern (node 14). For *model with support (E02H)* the **SX** reduces to +12,313 kPa or 3.35 (practically the same, it may be due to no support is provided at the bench, so no effect of confinement). The **max SX** for Model II is +12,205 kPa (nearly same as Model I) or 3.32 from *model elastic without support (CRT-E01H)*, also occurs at node 14, whereas for *model elastic with support (CRT- E03)* it becomes +10,123 kPa or 2.75.


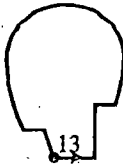
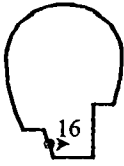
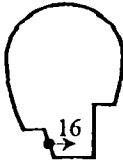
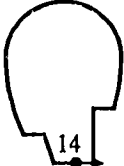

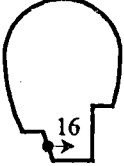
Out of all models, the minimum stresses in the X-direction (**min SX**) is about -6,618 kPa (tensile stress) from *Model II elastic without support (CRT-E01H)* and in term of stress concentration factor it is equal to -1.8 and occurs at south wall of bench (node 16), and in same Model with support the **SX** little reduce to -6,431 kPa or -2.41 (also practically no difference with model with support by same reason that no support provided at bench in modeling). In Model I, the **min SX** is -1,967 kPa (tensile stress) or -0.54 by *Model elastic without support (E01H)* and in model with support no difference -1,965 kPa or -0.54 due to same reason, confinement effect from support in upper part does not influence the bench part. The magnitude of tensile stress in X-direction is very high.

In middle of cavern (node 2 in south side & node 19 in north side) the stress concentration factor of **SX** is nearly zero and at nearby crown (node 42 & 43) the stress concentration is max (about 2.5 times). It confirms the closed-form solution for opening circular shaped for σ_r (see eq. II-1 for $\theta = 0^\circ$ and $\theta = 90^\circ$), whatever is the differences, it may be due to effect of the irregular shape of cavern at bench part.

From the results of **SX**, it is recognized that **Max SX** for upper part of cavern in model without support for Model I elastic is +6012,8 kPa and occurs at node 30, and for model with support the **Max SX** increase to +6100,8 kPa. Model I elasto-plastic gives **Max SX** for upper part as +1786.3 kPa in model without support, occurs at node 30, whereas in model with support it also increase to +2891 kPa and occurs at same node, 30. The increasing in **SX** for model with support due to the fact that applying a pair of external load is creating additional compressive stress to rock mass surrounding cavern. The pattern is also indicated in the results of **SY**.

Resume results of **SX** is shown in Table VI- 3 below

Table VI – 3
Resume results of SX

| Model | Max SX (kPa) | | Min SX (kPa) | |
|-------|---|---|--|---|
| | Elastic | Elasto-plastic | Elastic | Elasto-plastic |
| I | E01  +12,325 | EP01  +5,394 | E01  -1,967 | EP01  -501 |
| | II | E01  +12,205 | EP01  +12,179 | E01  -6,618 |

VI.2.i.(3) Stresses in Y-direction

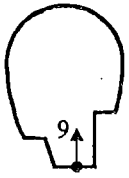
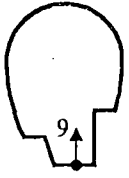
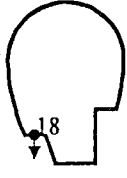
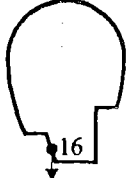
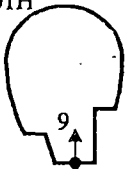
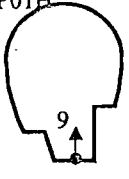
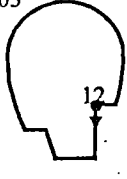
Out of all models, the maximum stress in the Y-direction (SY) is about +7400 kPa (compressive stress) from model II elastic without support (CRT-E01) and in term of stress concentration factor it is equal to 2.23 and occurs at node 9 at toe of bench. For model with support (CRT-E02H) the SY reduce to +7106 kPa or 2.14 (almost the same, probably caused by no support provided at bench in model so no confinement effect takes place). The max SY for Model I is +6,442 kPa (lesser than Model II) or 1.94 from model elastic without support (CRT-E01H), also occurs at same node 9, when model elastic with support (CRT-E03) become +6,423 kPa or 1.94.

Out of all models, the minimum stresses in the Y-direction (min SY) is about -1,587 kPa (tensile stress) from Model II elasto-plastic with support (CRT-EP03) and in term of stress concentration factor it is equal to -1.12 and occurs at node 12, and in same Model without support the SY only -868 kPa or -0.26. In Model I, the min SY is -1,044 kPa (tensile stress) or -0.32 by Model elastic without support (E01H) and in model with support no difference -1,041 kPa or -0.32 due to same reason, confinement effect from support in upper part does not influence the bench part. The magnitude of tensile stress in Y-direction is high.

In middle of cavern (node 2 in south side & node 19 in north side) the stress concentration factor of SY is reached the maximum and at nearby crown (node 42 & 43) the stress concentration factor is nearly zero, it confirms the closed-form solution for circular shaped for σ_r (see eq. II-1 for $\theta = 0^\circ$ and $\theta = 90^\circ$), small differences may be due to the effect of the irregular shape of cavern at bench part.

Resume result of SY is shown in Table VI - 4 below

Table VI- 4
Resume results of SY

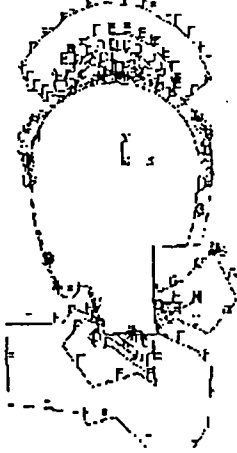
| Model | Max SY (kPa) | | Min SY (kPa) | |
|-------|--|--|---|---|
| | Elastic | Elasto-plastic | Elastic | Elasto-plastic |
| I | E01  +6,442 | EP01  +3,195 | E01  -1,044 | EP01  -318 |
| | II | CRT-E01H  +7,400 | CRT-EP01H  +6,796 | CRT-E03  -1,587 |

VI.2.i.(4) Plastic Zone

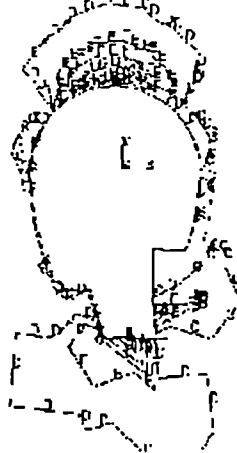
From ANSYS plot of contours for *plastic strain* (EPPL) in X & Y direction and its *equivalent plastic stress* (SEPL) for model with *elasto-plastic* behaviour (Figure VI- 8 (a)), it may be seen that plastic zones developed surrounding cavern in a depth of about 0.8 radii of cavern (17.5 m) or equal to 12 meter (Figure VI- 8 (b)). These zones indicate a potential for rock spalling and rock falls if located near the excavated surface. Larger yielded zones indicate a general weakening of the rock and the need to provide supports. The extent of these zones may be helpful in the design of length of rock bolts/anchors etc. The rock bolts should be anchored beyond the plastic zone.

(1) Plastic Zone Model I

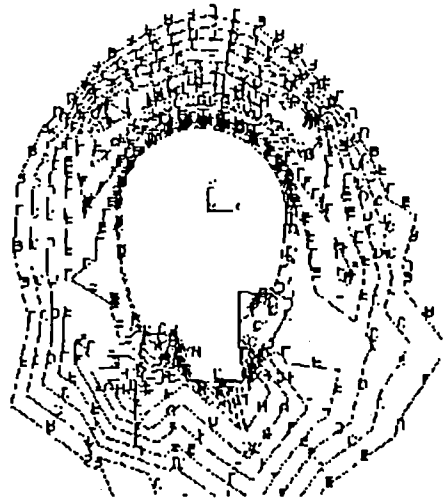
EP02HRta



EPPLX (AVG)



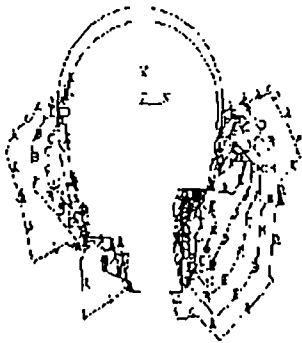
EPPLY (AVG)



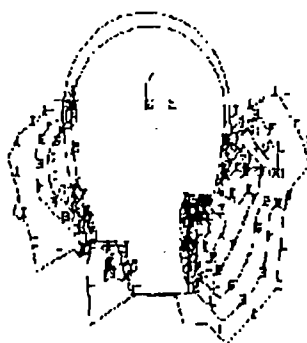
SEPL (AVG)

(2) Plastic Zone Model II

Cirata-EP03



EPPLX (AVG)



EPPLY (AVG)



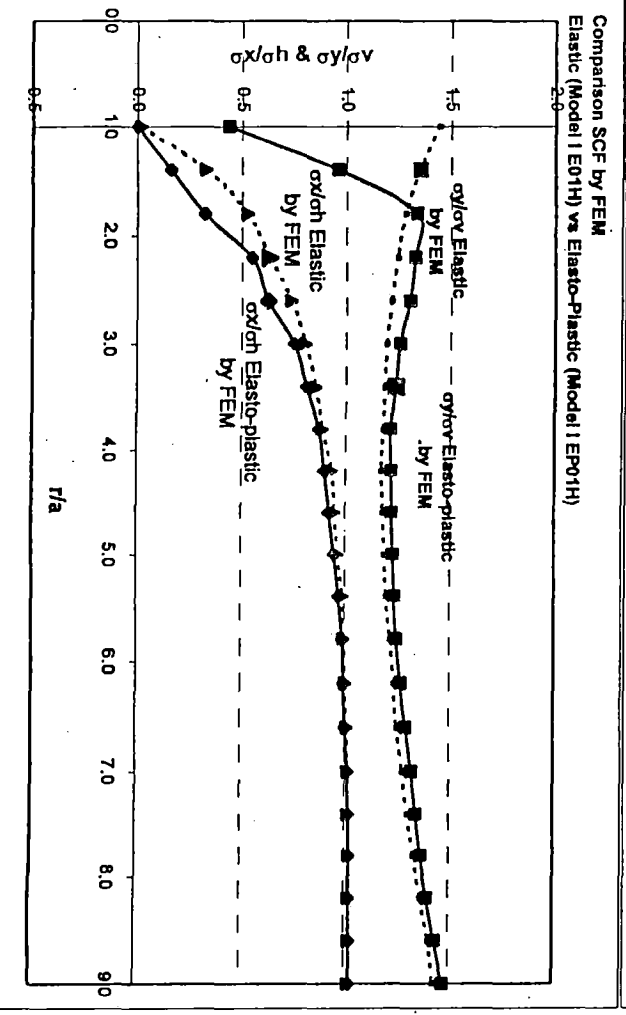
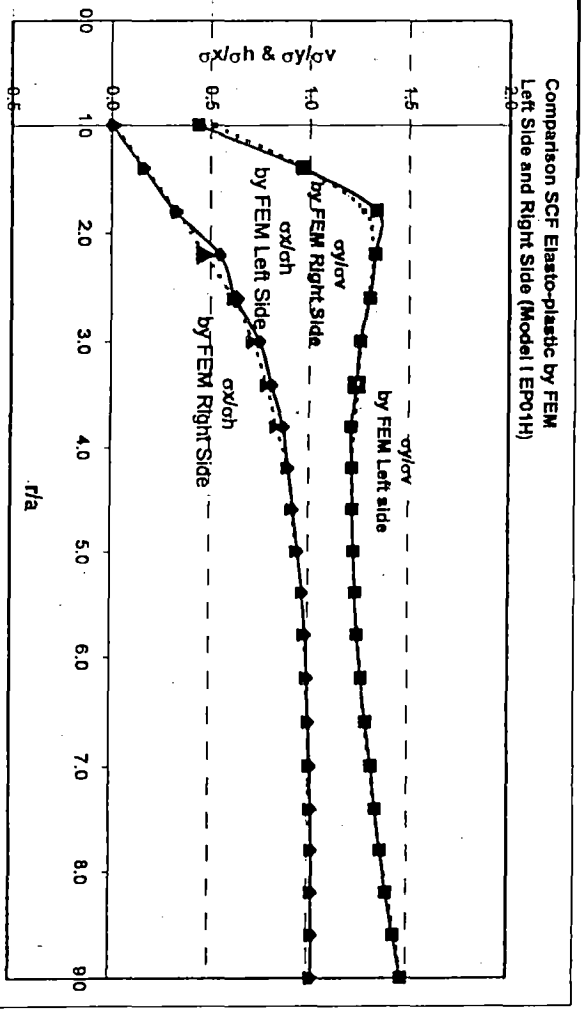
SEPL (AVG)

Figure VI - 8 (a)

Plastic Zone in Model I & Model II

FIGURE VI-8(B) ELASTO-PLASTIC STRESS PATH AT SIDEWALL (NODE 2 & 19)

| Distanc ce (m) | FEM Result | | r/a | σ _{x/oh} | σ _{y/ov} |
|----------------------|-----------------|-----------------|-----|-------------------|-------------------|
| | σ _{yr} | σ _{yr} | | | |
| 0 | 0.13 | -1444.00 | 1.0 | 0.000 | 0.436 |
| 7 | -589.82 | -3177.20 | 1.4 | 0.161 | 0.958 |
| 14 | -1178.70 | -4423.40 | 1.8 | 0.321 | 1.334 |
| 21 | -2009.60 | -4405.40 | 2.2 | 0.547 | 1.329 |
| 28 | -2295.50 | -4316.80 | 2.6 | 0.625 | 1.302 |
| 35 | -2751.10 | -4167.20 | 3.0 | 0.749 | 1.257 |
| 42 | -2971.00 | -4101.20 | 3.4 | 0.809 | 1.237 |
| 49 | -3199.10 | -4021.00 | 3.8 | 0.871 | 1.213 |
| 56 | -3291.80 | -4034.80 | 4.2 | 0.897 | 1.217 |
| 63 | -3384.40 | -4048.70 | 4.6 | 0.922 | 1.221 |
| 70 | -3475.20 | -4071.10 | 5.0 | 0.947 | 1.228 |
| 77 | -3558.10 | -4096.30 | 5.4 | 0.969 | 1.236 |
| 84 | -3625.40 | -4127.80 | 5.8 | 0.988 | 1.245 |
| 91 | -3654.60 | -4198.40 | 6.2 | 0.995 | 1.266 |
| 98 | -3687.60 | -4284.50 | 6.6 | 1.004 | 1.292 |
| 105 | -3720.60 | -4370.60 | 7.0 | 1.013 | 1.318 |
| 112 | -3742.70 | -4447.60 | 7.4 | 1.019 | 1.342 |
| 119 | -3747.90 | -4526.90 | 7.8 | 1.021 | 1.366 |
| 126 | -3752.10 | -4628.10 | 8.2 | 1.022 | 1.396 |
| 133 | -3757.30 | -4755.20 | 8.6 | 1.023 | 1.434 |
| 140 | -3762.80 | -4886.50 | 9.0 | 1.025 | 1.474 |
| Dist. SXR | -59.00 | -1710.30 | 1.0 | 0.016 | 0.516 |
| | -603.93 | -3206.40 | 1.4 | 0.165 | 0.967 |
| | -1212.20 | -4212.70 | 1.8 | 0.330 | 1.271 |
| | -1733.60 | -4366.20 | 2.2 | 0.472 | 1.317 |
| | -2264.00 | -4292.30 | 2.6 | 0.617 | 1.295 |
| | -2629.50 | -4187.30 | 3.0 | 0.716 | 1.263 |
| | -2885.10 | -4125.30 | 3.4 | 0.786 | 1.244 |
| | -3071.50 | -4086.00 | 3.8 | 0.837 | 1.233 |
| | -3285.30 | -4031.90 | 4.2 | 0.895 | 1.216 |
| | -3370.60 | -4049.80 | 4.6 | 0.918 | 1.222 |
| | -3455.90 | -4067.70 | 5.0 | 0.941 | 1.227 |
| | -3563.40 | -4083.50 | 5.4 | 0.971 | 1.232 |
| | -3602.90 | -4152.30 | 5.8 | 0.981 | 1.253 |
| | -3645.70 | -4221.30 | 6.2 | 0.993 | 1.270 |
| | -3692.30 | -4259.30 | 6.6 | 1.006 | 1.285 |
| | -3705.00 | -4348.00 | 7.0 | 1.009 | 1.312 |
| | -3724.60 | -4437.50 | 7.4 | 1.015 | 1.339 |
| | -3747.90 | -4527.00 | 7.8 | 1.021 | 1.366 |
| | -3755.40 | -4659.40 | 8.2 | 1.023 | 1.406 |
| | -3757.30 | -4789.80 | 8.6 | 1.023 | 1.445 |
| | -3761.70 | -4888.60 | 9.0 | 1.025 | 1.475 |



VI.2 ii) Deformation Field Study

FEM results in term of rock deformation are presented as follows:

- **Figure VI - 1** for deformed shape of Model I
- **Figure VI - 2 (a)** for deformation horizontal around periphery of Model I and (b) for deformation vertical around periphery of Model I
- **Figure VI - 3** for deformed shape of Model II
- **Figure VI - 4** for deformation horizontal around periphery of Model II
- **Figure VI - 5** for deformation vertical around periphery of Model II
- **Table VI - 1** for vertical deformation at some critical points around periphery of cavern.

As may be note that all the data is reproduced in worksheet MSEXcel for better presentation of results.

- **Figure VI - 6** for near-field contour plot in ANSYS output format -in term of deformation in horizontal direction (UX) and vertical direction (UY) (a) for elastic behaviour & (b) for elasto-plastic behaviour (Model I)
- **Figure VI- 7** for plastic zone of Model I
- **Figure VI- 8** for displacement vector surrounding cavern of Model I
- **Figure VI- 9** for near-field contour plot in ANSYS output format -in term of deformation in horizontal direction (UX) and vertical direction (UY) (a) for elastic behaviour & (b) for elasto-plastic behaviour (Model II)
- **Figure VI- 10** for plastic zone of Model I
- **Figure VI- 11** for displacement vector surrounding cavern of Model I

It may be note that deformation considered here is the sum of the model to initial model's results hence the values shown is a deformation relative to initial model.

Table VI-5 Displacement vertical at Critical point

| Model | Calculated vertical deformation at critical points (in mm) | | | | | | | Location |
|------------------------|--|--------|--------|---------|--------|--------|--------|----------|
| | 7 | 1 | 2 | 28 | 19 | 17 | 15 | |
| I | | | | | | | | |
| E00 | -28.11 | -28.15 | -34.26 | -40.40 | -34.26 | -24.56 | -24.54 | |
| E01 | -19.73 | -20.08 | -32.66 | -51.45 | -31.81 | -10.76 | -8.61 | |
| E02 | -19.61 | -20.05 | -32.48 | -50.65 | -31.67 | -10.81 | -8.57 | |
| Disp. Relative (01-00) | 8.38 | 8.07 | 1.60 | -11.05 | 2.45 | 13.81 | 15.93 | |
| Disp. Relative (02-00) | 8.50 | 8.10 | 1.78 | -10.26 | 2.59 | 13.76 | 15.97 | |
| Diff. (%) | -1.42 | -0.35 | -11.05 | 7.16 | -5.70 | 0.36 | -0.25 | |
| EP00 | -28.11 | -28.15 | -34.26 | -40.40 | -34.26 | -24.56 | -24.54 | |
| EP01 | -17.83 | -19.87 | -35.09 | -73.79 | -34.56 | -8.49 | 2.28 | |
| EP02 | -15.97 | -20.28 | -34.67 | -69.51 | -32.89 | -9.71 | 7.03 | |
| Disp. Relative (01-00) | 10.29 | 8.28 | -0.83 | -33.39 | -0.30 | 16.07 | 26.82 | |
| Disp. Relative (02-00) | 12.14 | 7.88 | -0.41 | -29.11 | 1.37 | 14.85 | 31.56 | |
| Diff. (%) | -18.04 | 4.88 | 51.08 | 12.82 | 563 | 7.62 | -17.70 | |
| CRT-E00H | -44.63 | -44.01 | -51.13 | -60.90 | -56.26 | -42.31 | -42.25 | |
| CRT-E01 | -26.65 | -33.26 | -55.14 | -91.87 | -64.68 | -26.88 | -18.50 | |
| CRT-E03 | -37.93 | -38.43 | -53.11 | -79.01 | -60.90 | -31.69 | -26.36 | |
| Disp. Relative (01-00) | 17.98 | 10.75 | -4.01 | -30.97 | -8.42 | 15.43 | 23.75 | |
| Disp. Relative (02-00) | 6.70 | 5.58 | -1.98 | -18.11 | -4.64 | 10.62 | 15.89 | |
| Diff. (%) | 62.72 | 48.05 | 50.70 | 41.53 | 44.91 | 31.18 | 33.12 | |
| II | | | | | | | | |
| CRT-EP00H | -44.63 | -44.01 | -51.13 | -60.90 | -56.26 | -42.31 | -42.25 | |
| CRT-EP01 | -24.60 | -30.61 | -59.40 | -100.97 | -72.21 | -20.85 | -13.94 | |
| CRT-EP03 | -50.34 | -61.67 | -68.83 | -86.31 | -68.64 | -30.66 | -25.50 | |
| Disp. Relative (01-00) | 20.03 | 13.40 | -8.27 | -40.07 | -15.95 | 21.46 | 28.31 | |
| Disp. Relative (02-00) | -5.71 | -17.66 | -17.70 | -25.41 | -12.38 | 11.65 | 16.75 | |
| Diff. (%) | 128.5 | 231.7 | -114.1 | 36.59 | 22.40 | 45.71 | 40.82 | |

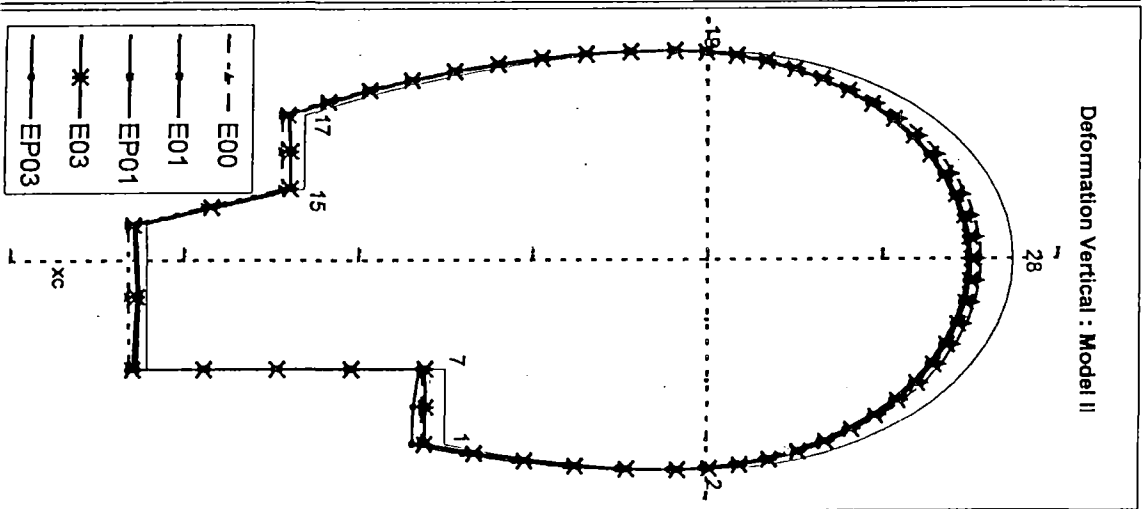
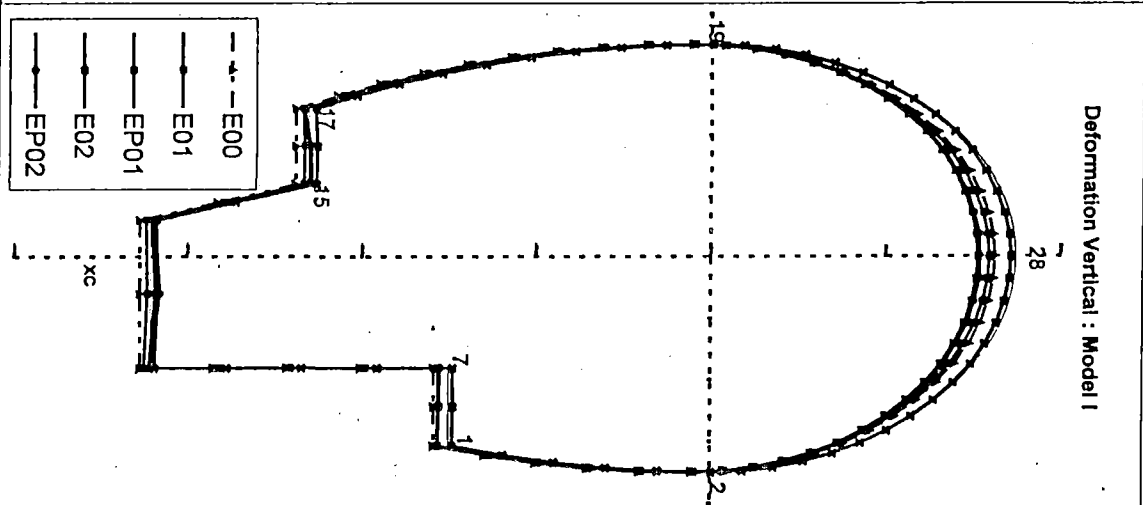


Figure VI-9
Deformed shape for Model I

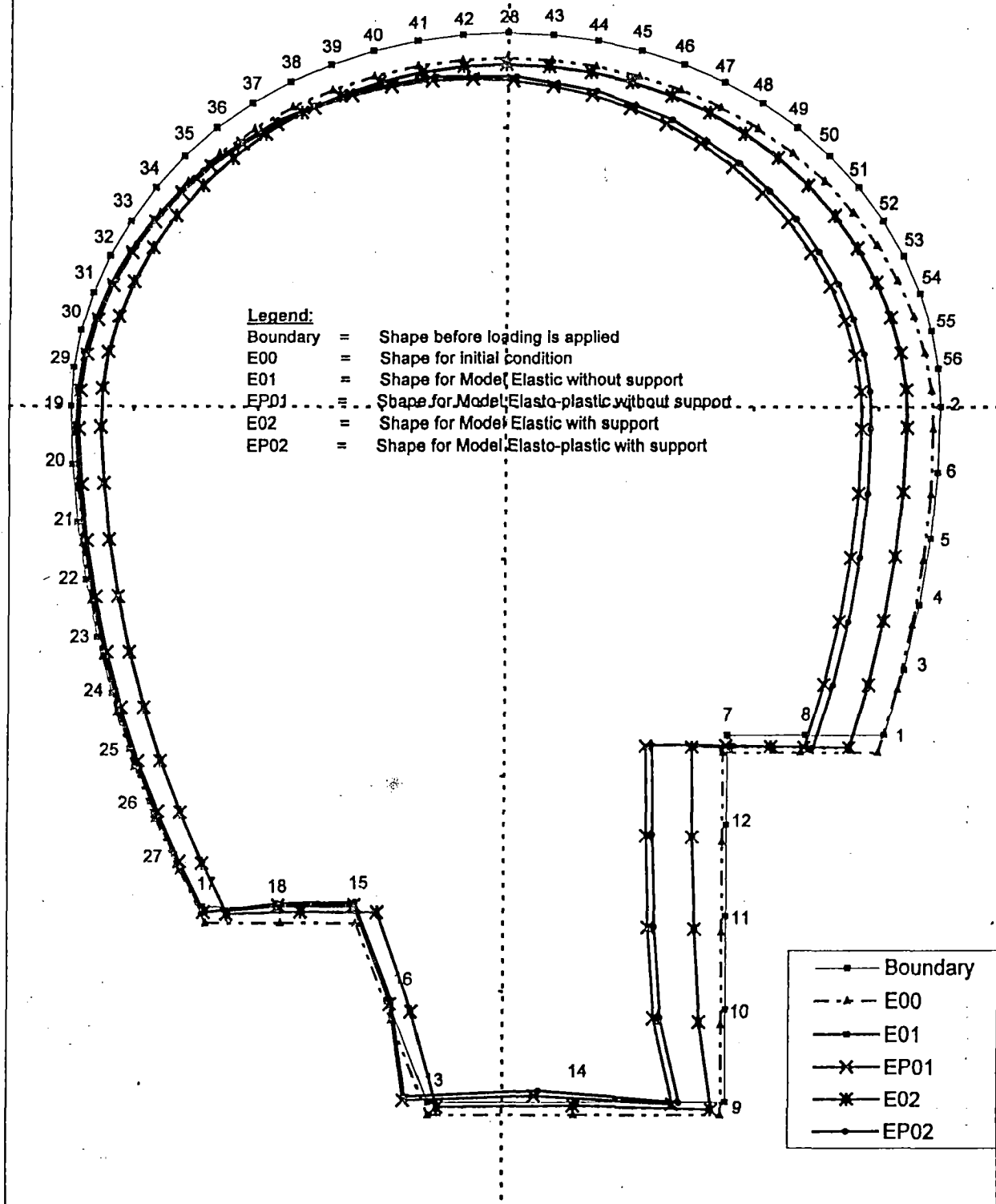


Table VI-10 (a)
Periphery-Deformation Horizontal for Model I

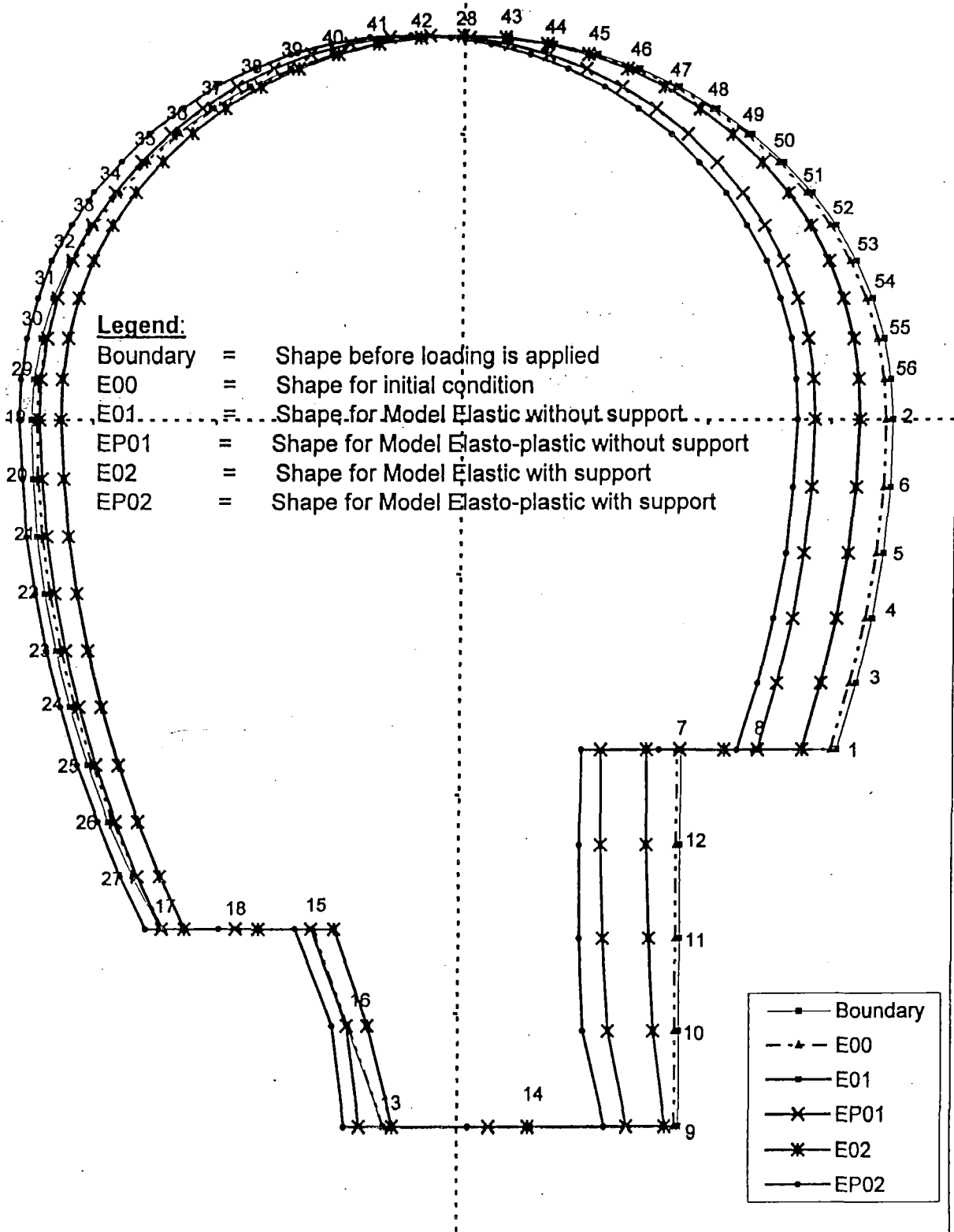


Figure VI -10 (b)
Periphery-Deformation Vertical for Model I

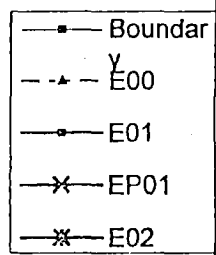
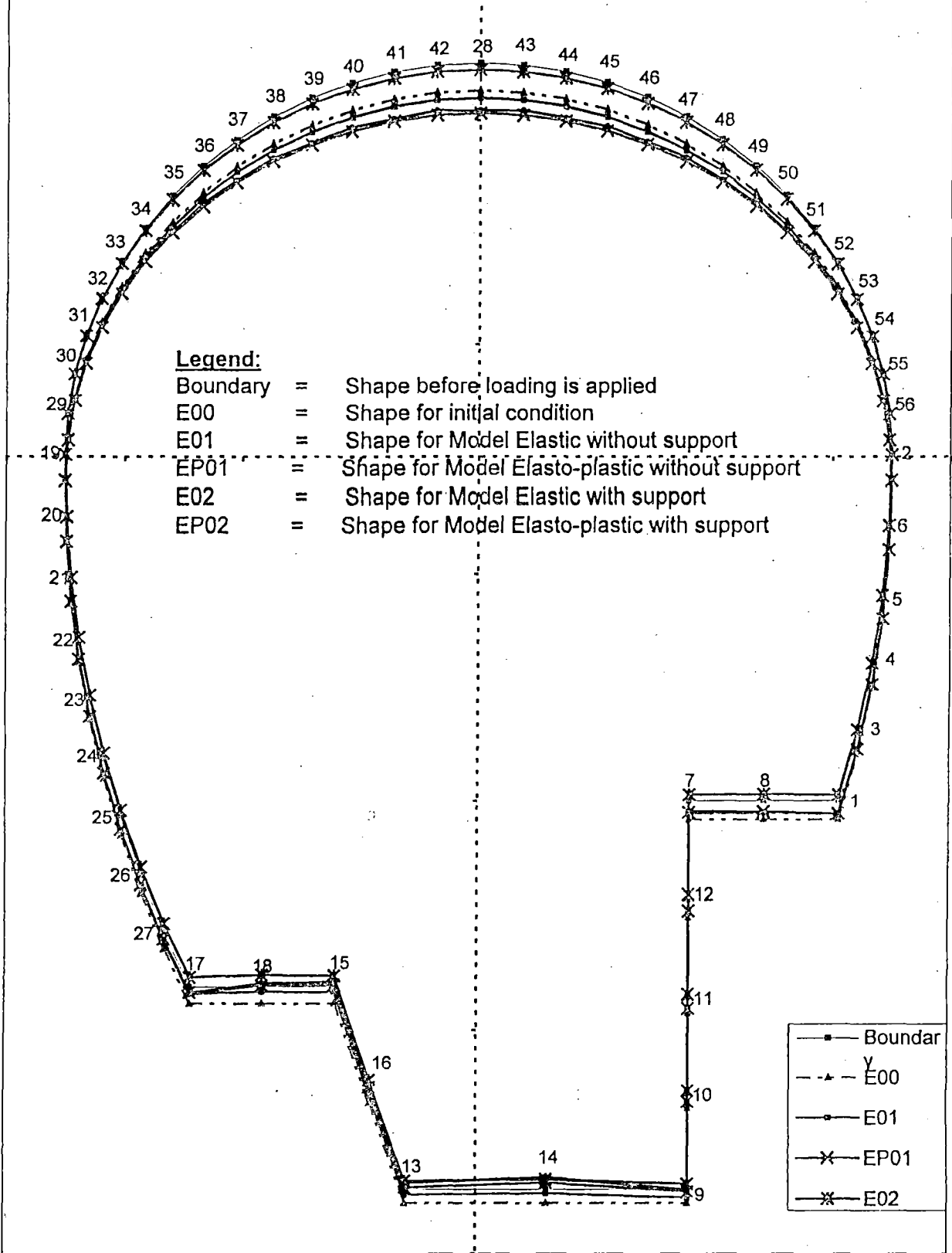
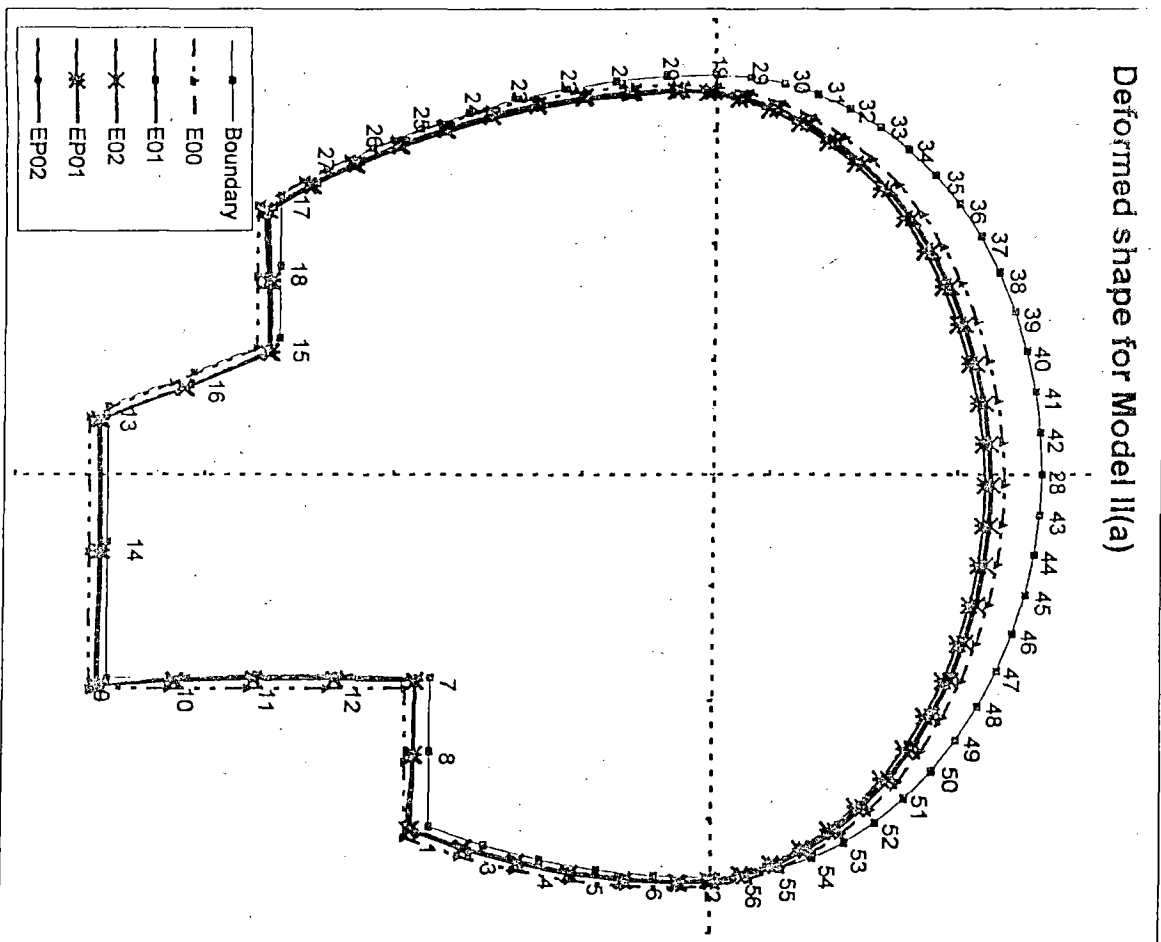


Figure VI-12 Deformed Shape Model II

Deformed shape for Model II(a)



Deformed shape for Model II(b)

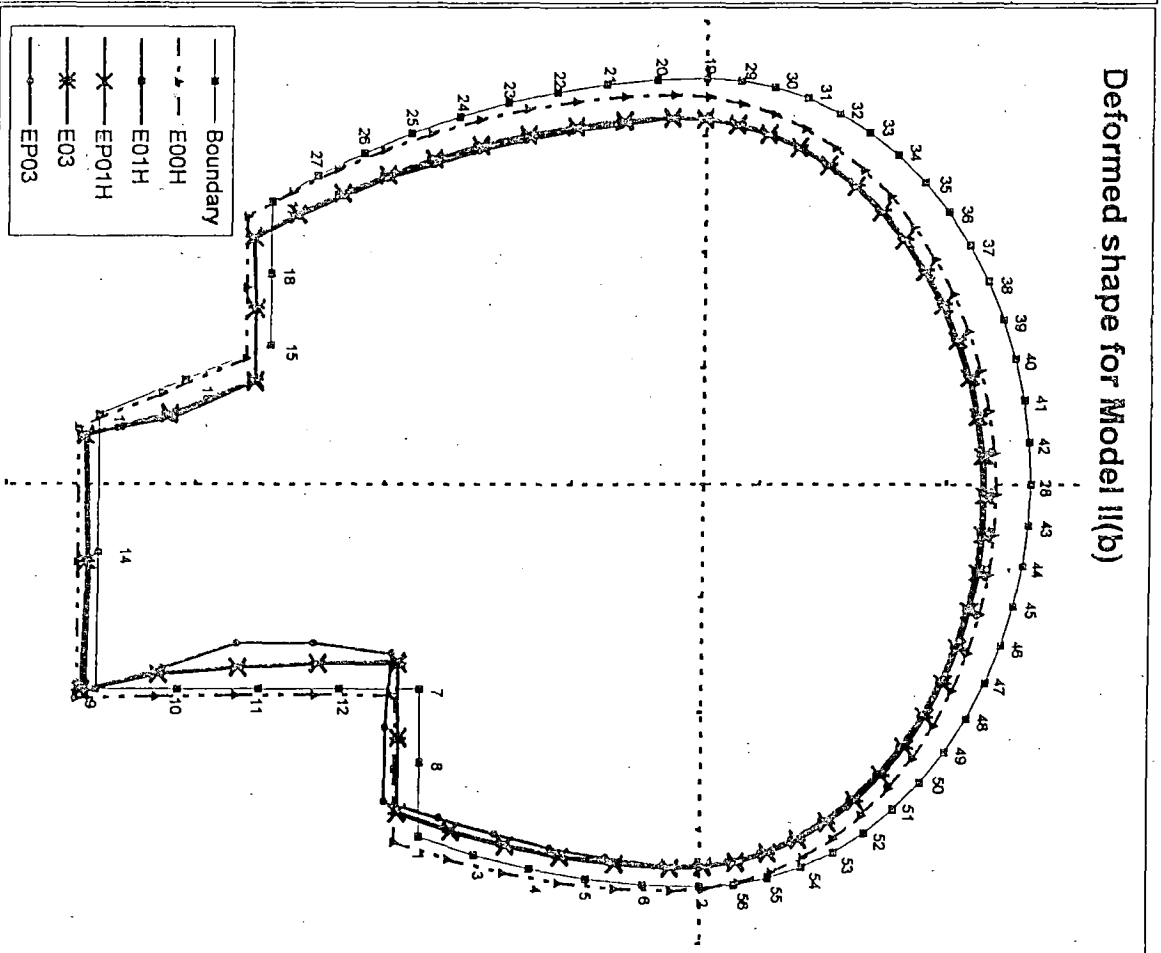


Table VI-9 Magnitude of Vertical Deformation around periphery - Model I

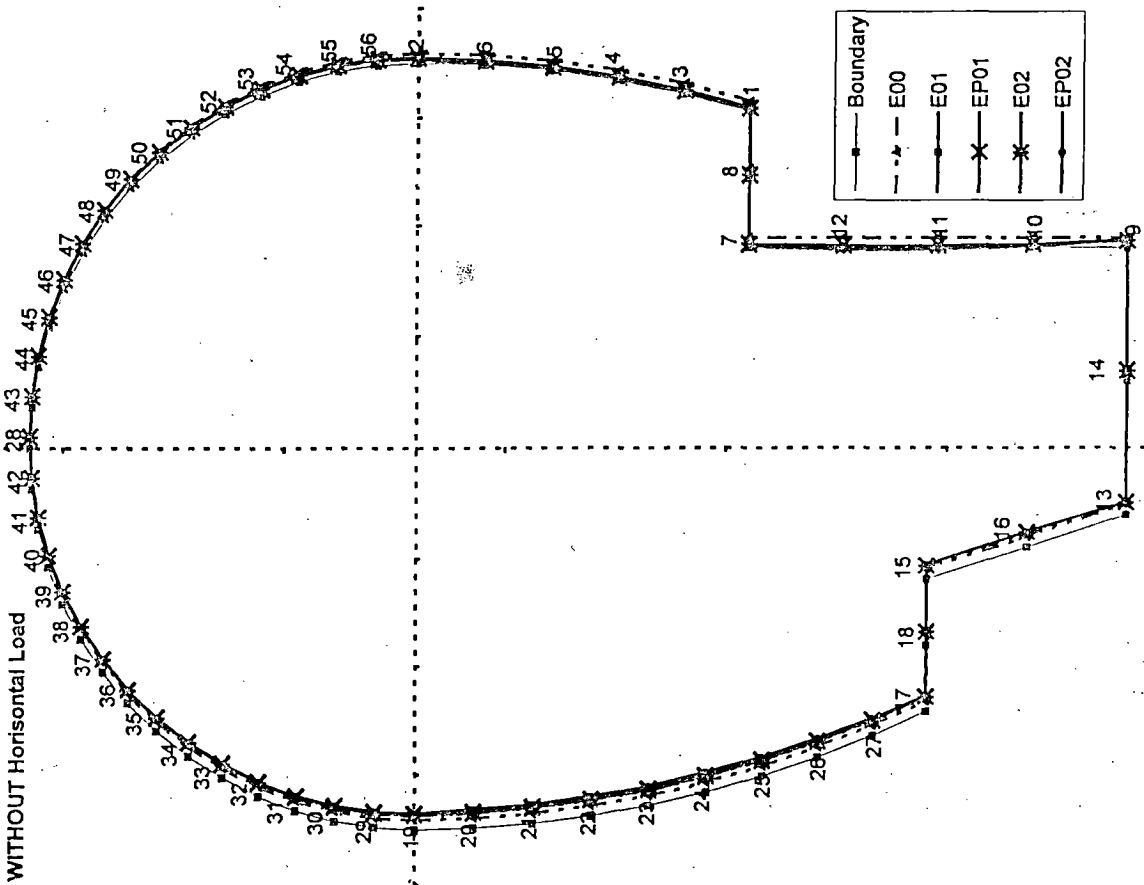
| H & V Deformation | | | Y-Direction | | | | | | | | | | | |
|-----------------------|--------|--------|--------------|--------------|--------------|----------------|---------------|---------------|----------------|---------------|--------------|----------------|----------------|---------------|
| LIST ALL PICKED NODES | | | Elastic | | | | | | Elasto-Plastic | | | | | |
| Model II (CRT) | | | Elastic | | | Elasto-Plastic | | | Elastic | | | Elasto-Plastic | | |
| Node | X | Y | E00 UX(m) | E01 UX(m) | E02 UX(m) | EP00 UX(m) | EP01 UX(m) | EP02 UX(m) | E00H UY(m) | E01H UY(m) | E03 UY(m) | E00H UY(m) | EP01H UY(m) | EP03 UY(m) |
| 1 | 15.31 | -15.00 | -0.00879 | -0.04714 | -0.04690 | -0.01177 | -0.10715 | -0.13479 | -0.02815 | -0.02008 | -0.02005 | -0.02815 | -0.01987 | -0.02028 |
| 3 | 16.10 | -12.06 | -0.00909 | -0.04815 | -0.04762 | -0.01206 | -0.10715 | -0.13274 | -0.02941 | -0.02263 | -0.02266 | -0.02941 | -0.02222 | -0.02320 |
| 4 | 16.71 | -9.08 | -0.00929 | -0.04844 | -0.04804 | -0.01226 | -0.10726 | -0.13300 | -0.03065 | -0.02507 | -0.02504 | -0.03065 | -0.02559 | -0.02666 |
| 5 | 17.15 | -6.07 | -0.00939 | -0.04799 | -0.04736 | -0.01237 | -0.10704 | -0.13099 | -0.03188 | -0.02744 | -0.02737 | -0.03188 | -0.02895 | -0.02924 |
| 6 | 17.41 | -3.04 | -0.00940 | -0.04683 | -0.04637 | -0.01238 | -0.10642 | -0.13152 | -0.03308 | -0.02996 | -0.02984 | -0.03308 | -0.03202 | -0.03235 |
| 2 | 17.50 | 0.00 | -0.00932 | -0.04493 | -0.04419 | -0.01230 | -0.10519 | -0.12837 | -0.03426 | -0.03266 | -0.03248 | -0.03426 | -0.03509 | -0.03467 |
| 56 | 17.40 | 1.83 | -0.00921 | -0.04338 | -0.04277 | -0.01218 | -0.10391 | -0.12773 | -0.03496 | -0.03454 | -0.03435 | -0.03496 | -0.03757 | -0.03682 |
| 55 | 17.12 | 3.64 | -0.00900 | -0.04161 | -0.04081 | -0.01198 | -0.10240 | -0.12506 | -0.03563 | -0.03645 | -0.03619 | -0.03563 | -0.03993 | -0.03822 |
| 54 | 16.64 | 5.41 | -0.00872 | -0.03960 | -0.03898 | -0.01169 | -0.10084 | -0.12460 | -0.03628 | -0.03840 | -0.03813 | -0.03628 | -0.04294 | -0.04150 |
| 53 | 15.99 | 7.12 | -0.00835 | -0.03736 | -0.03659 | -0.01133 | -0.09895 | -0.12143 | -0.03690 | -0.04025 | -0.03985 | -0.03690 | -0.04580 | -0.04264 |
| 52 | 15.16 | 8.75 | -0.00792 | -0.03489 | -0.03433 | -0.01090 | -0.09661 | -0.12069 | -0.03748 | -0.04206 | -0.04167 | -0.03748 | -0.04928 | -0.04755 |
| 51 | 14.16 | 10.29 | -0.00742 | -0.03223 | -0.03155 | -0.01040 | -0.09395 | -0.11639 | -0.03801 | -0.04373 | -0.04316 | -0.03801 | -0.05269 | -0.04825 |
| 50 | 13.01 | 11.71 | -0.00687 | -0.02937 | -0.02891 | -0.00984 | -0.09056 | -0.11489 | -0.03850 | -0.04530 | -0.04477 | -0.03850 | -0.05628 | -0.05368 |
| 49 | 11.71 | 13.01 | -0.00626 | -0.02633 | -0.02578 | -0.00924 | -0.08681 | -0.10938 | -0.03894 | -0.04668 | -0.04595 | -0.03894 | -0.05970 | -0.05416 |
| 48 | 10.29 | 14.16 | -0.00562 | -0.02316 | -0.02280 | -0.00859 | -0.08237 | -0.10696 | -0.03932 | -0.04795 | -0.04731 | -0.03932 | -0.06303 | -0.05948 |
| 47 | 8.75 | 15.16 | -0.00493 | -0.01983 | -0.01945 | -0.00791 | -0.07752 | -0.10129 | -0.03965 | -0.04899 | -0.04812 | -0.03965 | -0.06600 | -0.05963 |
| 46 | 7.12 | 15.99 | -0.00422 | -0.01642 | -0.01620 | -0.00719 | -0.07214 | -0.09711 | -0.03991 | -0.04990 | -0.04917 | -0.03991 | -0.06869 | -0.06444 |
| 45 | 5.41 | 16.64 | -0.00348 | -0.01291 | -0.01271 | -0.00646 | -0.06644 | -0.09126 | -0.04013 | -0.05056 | -0.04960 | -0.04013 | -0.07079 | -0.06384 |
| 44 | 3.64 | 17.12 | -0.00272 | -0.00933 | -0.00926 | -0.00570 | -0.06027 | -0.08579 | -0.04028 | -0.05108 | -0.05030 | -0.04028 | -0.07247 | -0.06789 |
| 43 | 1.83 | 17.40 | -0.00196 | -0.00572 | -0.00573 | -0.00493 | -0.05400 | -0.08009 | -0.04037 | -0.05133 | -0.05034 | -0.04037 | -0.07341 | -0.06624 |
| 28 | 0.00 | 17.50 | -0.00118 | -0.00207 | -0.00215 | -0.00416 | -0.04744 | -0.07337 | -0.04040 | -0.05145 | -0.05065 | -0.04040 | -0.07379 | -0.06951 |
| 42 | -1.83 | 17.40 | -0.00041 | 0.00155 | 0.00134 | -0.00339 | -0.04106 | -0.06830 | -0.04037 | -0.05129 | -0.05033 | -0.04037 | -0.07341 | -0.06651 |
| 41 | -3.64 | 17.12 | 0.00036 | 0.00519 | 0.00496 | -0.00262 | -0.03461 | -0.06072 | -0.04028 | -0.05098 | -0.05024 | -0.04028 | -0.07242 | -0.06861 |
| 40 | -5.41 | 16.64 | 0.00111 | 0.00874 | 0.00835 | -0.00186 | -0.02860 | -0.05673 | -0.04013 | -0.05042 | -0.04955 | -0.04013 | -0.07076 | -0.06448 |
| 39 | -7.12 | 15.99 | 0.00185 | 0.01227 | 0.01192 | -0.00112 | -0.02268 | -0.04830 | -0.03991 | -0.04970 | -0.04904 | -0.03991 | -0.06857 | -0.06538 |
| 38 | -8.75 | 15.16 | 0.00257 | 0.01567 | 0.01513 | -0.00041 | -0.01727 | -0.04571 | -0.03965 | -0.04875 | -0.04801 | -0.03965 | -0.06594 | -0.06048 |
| 37 | -10.29 | 14.16 | 0.00325 | 0.01900 | 0.01856 | 0.00027 | -0.01237 | -0.03780 | -0.03932 | -0.04765 | -0.04710 | -0.03932 | -0.06281 | -0.05966 |
| 36 | -11.71 | 13.01 | 0.00390 | 0.02216 | 0.02151 | 0.00092 | -0.00789 | -0.03620 | -0.03894 | -0.04633 | -0.04574 | -0.03894 | -0.05951 | -0.05421 |
| 35 | -13.01 | 11.71 | 0.00450 | 0.02521 | 0.02470 | 0.00153 | -0.00412 | -0.03026 | -0.03850 | -0.04489 | -0.04446 | -0.03850 | -0.05597 | -0.05254 |

Table VI-9 Magnitude of Vertical Deformation around periphery - Model I

| H & V Deformation LIST ALL PICKED NODES Model II (CRT) | | X-Direction | | | | | | Y-Direction | | | | | | |
|--|--------|-------------|--------------|--------------|--------------|----------------|---------------|---------------|---------------|---------------|--------------|----------------|----------------|---------------|
| Node | X | Y | Elastic | | | Elasto-Plastic | | | Elastic | | | Elasto-Plastic | | |
| | | | E00 UX(m) | E01 UX(m) | E02 UX(m) | EP00 UX(m) | EP01 UX(m) | EP02 UX(m) | E00H UY(m) | E01H UY(m) | E03 UY(m) | E00H UY(m) | EP01H UY(m) | EP03 UY(m) |
| 34 | -14.16 | 10.29 | 0.00506 | 0.02803 | 0.02732 | 0.00208 | -0.00070 | -0.02926 | -0.03801 | -0.04325 | -0.04279 | -0.03801 | -0.05236 | -0.04773 |
| 33 | -15.16 | 8.75 | 0.00555 | 0.03072 | 0.03018 | 0.00258 | 0.00200 | -0.02476 | -0.03748 | -0.04153 | -0.04118 | -0.03748 | -0.04896 | -0.04561 |
| 32 | -15.99 | 7.12 | 0.00599 | 0.03313 | 0.03240 | 0.00301 | 0.00427 | -0.02424 | -0.03690 | -0.03966 | -0.03928 | -0.03690 | -0.04557 | -0.04188 |
| 31 | -16.64 | 5.41 | 0.00635 | 0.03539 | 0.03482 | 0.00337 | 0.00634 | -0.02052 | -0.03628 | -0.03772 | -0.03744 | -0.03628 | -0.04252 | -0.03948 |
| 30 | -17.12 | 3.64 | 0.00664 | 0.03734 | 0.03659 | 0.00366 | 0.00802 | -0.01996 | -0.03563 | -0.03573 | -0.03547 | -0.03563 | -0.03961 | -0.03682 |
| 29 | -17.40 | 1.83 | 0.00684 | 0.03911 | 0.03850 | 0.00387 | 0.00955 | -0.01757 | -0.03496 | -0.03372 | -0.03353 | -0.03496 | -0.03692 | -0.03474 |
| 19 | -17.50 | 0.00 | 0.00696 | 0.04058 | 0.03985 | 0.00398 | 0.01077 | -0.01689 | -0.03426 | -0.03181 | -0.03167 | -0.03426 | -0.03456 | -0.03289 |
| 20 | -17.43 | -2.66 | 0.00703 | 0.04229 | 0.04177 | 0.00406 | 0.01235 | -0.01405 | -0.03323 | -0.02923 | -0.02915 | -0.03323 | -0.03138 | -0.03036 |
| 21 | -17.23 | -5.31 | 0.00704 | 0.04335 | 0.04264 | 0.00406 | 0.01312 | -0.01426 | -0.03218 | -0.02696 | -0.02693 | -0.03218 | -0.02861 | -0.02753 |
| 22 | -16.90 | -7.94 | 0.00697 | 0.04386 | 0.04334 | 0.00400 | 0.01351 | -0.01251 | -0.03112 | -0.02471 | -0.02471 | -0.03112 | -0.02595 | -0.02557 |
| 23 | -16.43 | -10.56 | 0.00684 | 0.04384 | 0.04314 | 0.00386 | 0.01322 | -0.01334 | -0.03004 | -0.02258 | -0.02263 | -0.03004 | -0.02348 | -0.02319 |
| 24 | -15.83 | -13.15 | 0.00662 | 0.04322 | 0.04272 | 0.00365 | 0.01253 | -0.01270 | -0.02895 | -0.02046 | -0.02052 | -0.02895 | -0.02115 | -0.02126 |
| 25 | -15.10 | -15.70 | 0.00634 | 0.04202 | 0.04137 | 0.00336 | 0.01115 | -0.01409 | -0.02785 | -0.01836 | -0.01850 | -0.02785 | -0.01827 | -0.01927 |
| 26 | -14.24 | -18.22 | 0.00598 | 0.04026 | 0.03980 | 0.00300 | 0.00974 | -0.01412 | -0.02675 | -0.01628 | -0.01637 | -0.02675 | -0.01472 | -0.01599 |
| 27 | -13.25 | -20.69 | 0.00554 | 0.03733 | 0.03682 | 0.00256 | 0.00621 | -0.01699 | -0.02566 | -0.01390 | -0.01405 | -0.02566 | -0.01141 | -0.01370 |
| 17 | -12.15 | -23.10 | 0.00503 | 0.03324 | 0.03296 | 0.00205 | 0.00211 | -0.01958 | -0.02456 | -0.01076 | -0.01081 | -0.02456 | -0.00849 | -0.00971 |
| 18 | -9.07 | -23.10 | 0.00346 | 0.03091 | 0.03069 | 0.00048 | -0.00022 | -0.02267 | -0.02455 | -0.00763 | -0.00764 | -0.02455 | 0.00165 | 0.00486 |
| 15 | -6.00 | -23.10 | 0.00189 | 0.03139 | 0.03117 | -0.00109 | -0.00013 | -0.02217 | -0.02454 | -0.00861 | -0.00857 | -0.02454 | 0.00228 | 0.00703 |
| 16 | -4.50 | -27.60 | 0.00115 | 0.02747 | 0.02734 | -0.00182 | -0.00093 | -0.02075 | -0.02247 | -0.01027 | -0.01022 | -0.02247 | 0.00158 | 0.00704 |
| 13 | -3.00 | -32.10 | 0.00039 | 0.01194 | 0.01190 | -0.00258 | -0.03309 | -0.05369 | -0.02033 | -0.00814 | -0.00811 | -0.02033 | 0.00291 | 0.00939 |
| 14 | 3.00 | -32.10 | -0.00276 | -0.00379 | -0.00381 | -0.00573 | -0.05696 | -0.08507 | -0.02032 | -0.00609 | -0.00607 | -0.02032 | 0.00952 | 0.01787 |
| 9 | 9.00 | -32.10 | -0.00591 | -0.01852 | -0.01853 | -0.00888 | -0.07053 | -0.10038 | -0.02034 | -0.01256 | -0.01253 | -0.02034 | 0.00337 | 0.00075 |
| 10 | 9.00 | -27.83 | -0.00585 | -0.03504 | -0.03503 | -0.00883 | -0.09651 | -0.13056 | -0.02237 | -0.01913 | -0.01907 | -0.02237 | -0.01307 | -0.01249 |
| 11 | 9.00 | -23.55 | -0.00579 | -0.04199 | -0.04194 | -0.00877 | -0.10472 | -0.13648 | -0.02435 | -0.02040 | -0.02031 | -0.02435 | -0.01730 | -0.01629 |
| 12 | 9.00 | -19.28 | -0.00572 | -0.04585 | -0.04572 | -0.00870 | -0.10766 | -0.13663 | -0.02626 | -0.02013 | -0.02002 | -0.02626 | -0.01745 | -0.01622 |
| 7 | 9.00 | -15.00 | -0.00565 | -0.04729 | -0.04708 | -0.00863 | -0.10915 | -0.13510 | -0.02811 | -0.01973 | -0.01961 | -0.02811 | -0.01783 | -0.01597 |
| 8 | 12.16 | -15.00 | -0.00722 | -0.04705 | -0.04684 | -0.01020 | -0.10687 | -0.13493 | -0.02813 | -0.01884 | -0.01877 | -0.02813 | -0.01650 | -0.01712 |
| 1 | 15.31 | -15.00 | -0.00879 | -0.04714 | -0.04690 | -0.01177 | -0.10715 | -0.13479 | -0.02815 | -0.02008 | -0.02005 | -0.02815 | -0.01987 | -0.02028 |

Figure VI-13 (a) Deformation Horizontal around periphery - Model II

Periphery-Deformation Horizontal for Model II(a)



Periphery-Deformation Horizontal for Model II(b)

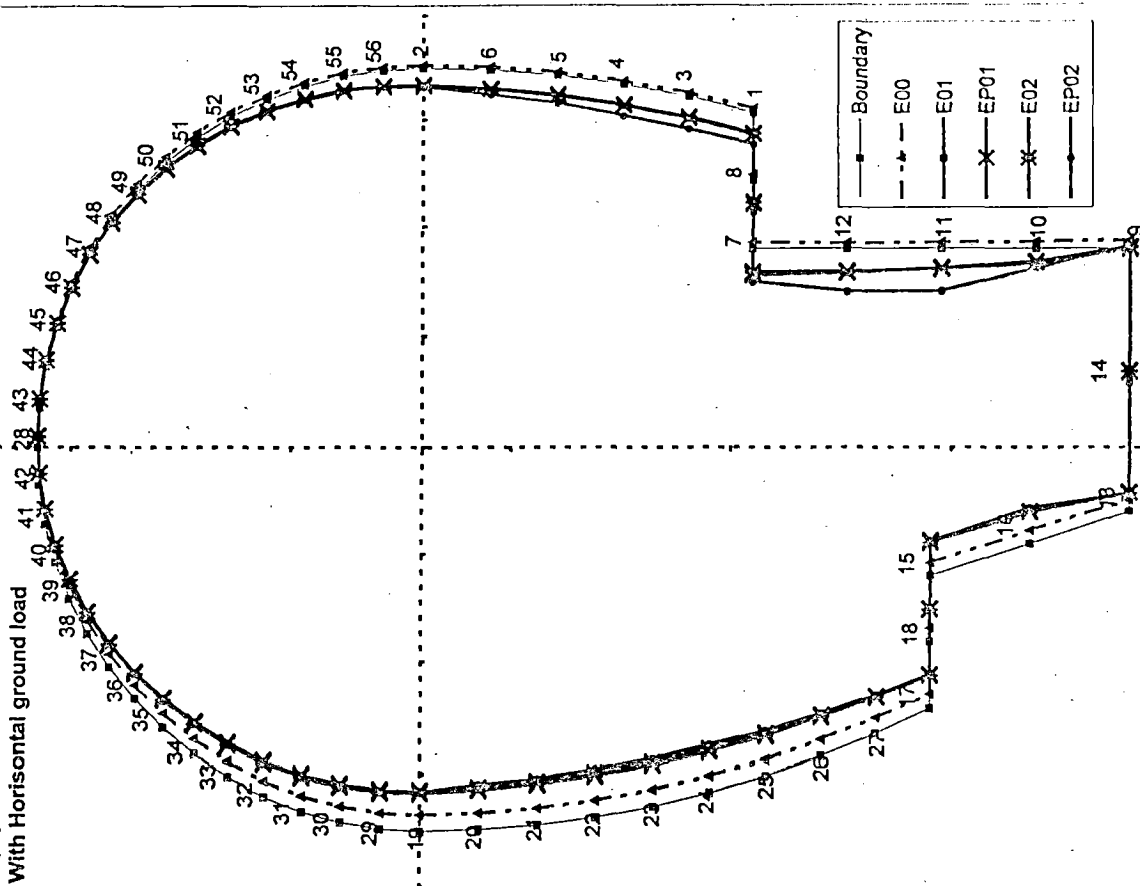


Figure VI -13 (b) Deformation Vertical around periphery - Model II

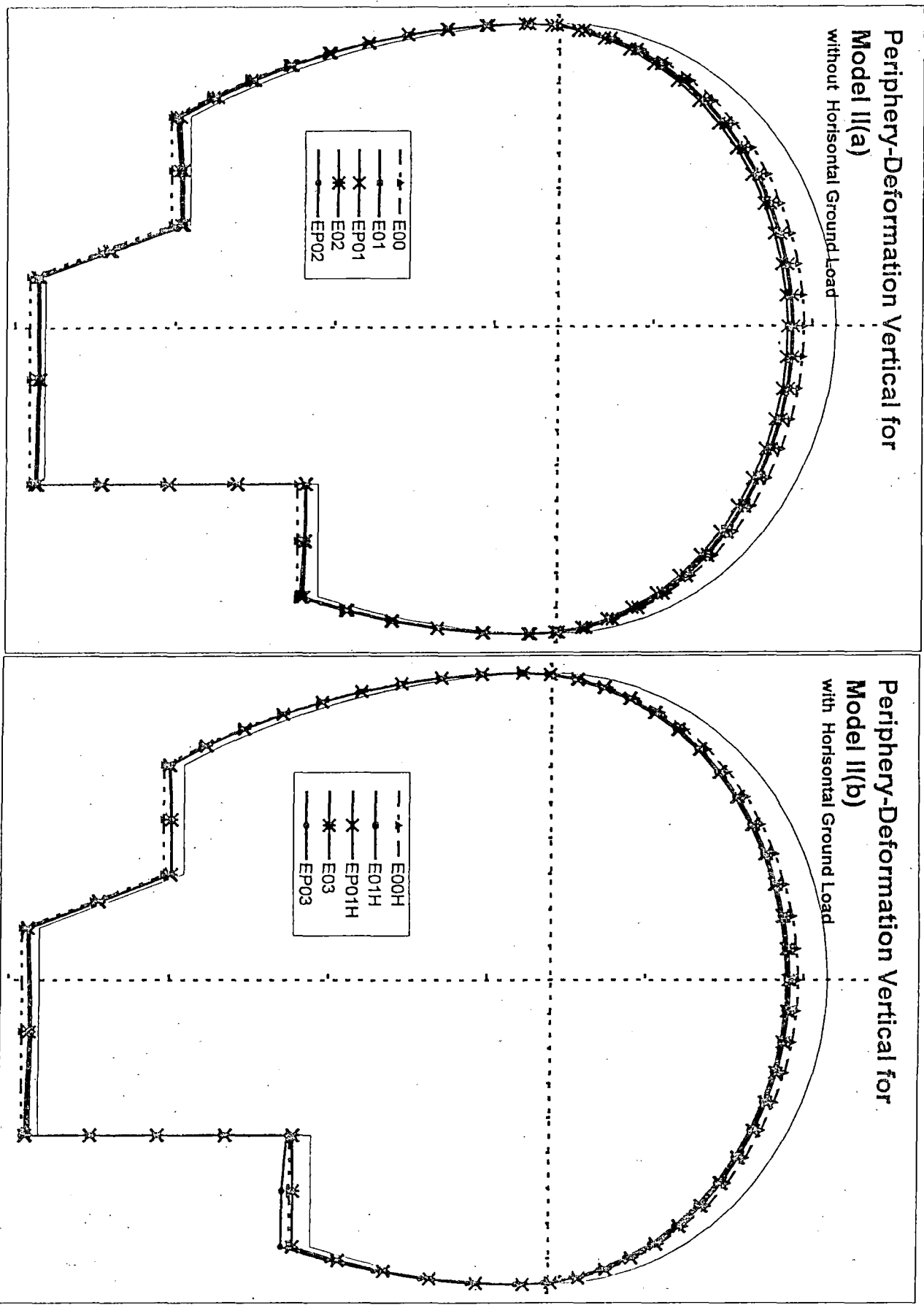


Table VI - 10 (a) Magnitude of Horizontal deformation around periphery - Model II

| Horizontal Deformation | | | Without Horizontal Ground Load | | | | | | Without Horizontal Ground Load | | | | | |
|------------------------|--------|--------|--------------------------------|---------|---------|----------------|---------|---------|--------------------------------|----------|----------|----------------|----------|---------|
| LIST ALL PICKED NODES | | | Elastic | | | Elasto-Plastic | | | Elastic | | | Elasto-Plastic | | |
| Model II (CRT) | | | CRTE00 | CRTE01 | CRTE02 | CRTEP00 | CRTEP01 | CRTEP02 | CRTE00H | CRTE01H | CRTE03 | CRTE00HC | CRTEP01F | CRTEP03 |
| Node | X | Y | UX(m) | UX(m) | UX(m) | UX(m) | UX(m) | UX(m) | UX(m) | UX(m) | UX(m) | UX(m) | UX(m) | |
| 1 | 15.31 | -15.00 | 0.01539 | 0.00382 | 0.00464 | 0.01539 | 0.00382 | 0.00089 | 0.00720 | -0.03488 | -0.03316 | 0.00720 | -0.03492 | |
| 3 | 16.10 | -12.06 | 0.01534 | 0.00403 | 0.00492 | 0.01534 | 0.00403 | 0.00147 | 0.00597 | -0.03537 | -0.03346 | 0.00597 | -0.03541 | |
| 4 | 16.71 | -9.08 | 0.01529 | 0.00410 | 0.00504 | 0.01529 | 0.00410 | 0.00075 | 0.00558 | -0.03518 | -0.03324 | 0.00558 | -0.03521 | |
| 5 | 17.15 | -6.07 | 0.01523 | 0.00460 | 0.00587 | 0.01523 | 0.00460 | 0.00216 | 0.00544 | -0.03420 | -0.03192 | 0.00544 | -0.03422 | |
| 6 | 17.41 | -3.04 | 0.01518 | 0.00531 | 0.00651 | 0.01518 | 0.00531 | 0.00287 | 0.00548 | -0.03241 | -0.03018 | 0.00548 | -0.03243 | |
| 2 | 17.50 | 0.00 | 0.01512 | 0.00635 | 0.00798 | 0.01512 | 0.00635 | 0.00605 | 0.00566 | -0.02974 | -0.02703 | 0.00566 | -0.02976 | |
| 56 | 17.40 | 1.83 | 0.01508 | 0.00705 | 0.00865 | 0.01508 | 0.00705 | 0.00706 | 0.00586 | -0.02772 | -0.02497 | 0.00586 | -0.02773 | |
| 55 | 17.12 | 3.64 | 0.01504 | 0.00780 | 0.00956 | 0.01504 | 0.00780 | 0.00860 | 0.00613 | -0.02552 | -0.02251 | 0.00613 | -0.02554 | |
| 54 | 16.64 | 5.41 | 0.01500 | 0.00851 | 0.00998 | 0.01500 | 0.00851 | 0.00876 | 0.00649 | -0.02309 | -0.02024 | 0.00649 | -0.02311 | |
| 53 | 15.99 | 7.12 | 0.01497 | 0.00926 | 0.01072 | 0.01497 | 0.00926 | 0.00986 | 0.00690 | -0.02052 | -0.01754 | 0.00690 | -0.02053 | |
| 52 | 15.16 | 8.75 | 0.01493 | 0.00997 | 0.01106 | 0.01493 | 0.00997 | 0.01002 | 0.00740 | -0.01769 | -0.01499 | 0.00740 | -0.01770 | |
| 51 | 14.16 | 10.29 | 0.01489 | 0.01073 | 0.01170 | 0.01489 | 0.01073 | 0.01108 | 0.00794 | -0.01476 | -0.01207 | 0.00794 | -0.01477 | |
| 50 | 13.01 | 11.71 | 0.01485 | 0.01144 | 0.01201 | 0.01485 | 0.01144 | 0.01136 | 0.00856 | -0.01160 | -0.00929 | 0.00856 | -0.01161 | |
| 49 | 11.71 | 13.01 | 0.01482 | 0.01219 | 0.01260 | 0.01482 | 0.01219 | 0.01232 | 0.00920 | -0.00837 | -0.00621 | 0.00920 | -0.00838 | |
| 48 | 10.29 | 14.16 | 0.01478 | 0.01289 | 0.01297 | 0.01478 | 0.01289 | 0.01272 | 0.00990 | -0.00496 | -0.00322 | 0.00990 | -0.00496 | |
| 47 | 8.75 | 15.16 | 0.01475 | 0.01361 | 0.01356 | 0.01475 | 0.01361 | 0.01351 | 0.01063 | -0.00150 | -0.00002 | 0.01063 | -0.00151 | |
| 46 | 7.12 | 15.99 | 0.01471 | 0.01428 | 0.01401 | 0.01471 | 0.01428 | 0.01397 | 0.01140 | 0.00207 | 0.00310 | 0.01140 | 0.00206 | |
| 45 | 5.41 | 16.64 | 0.01468 | 0.01495 | 0.01462 | 0.01468 | 0.01495 | 0.01462 | 0.01218 | 0.00565 | 0.00636 | 0.01218 | 0.00565 | |
| 44 | 3.64 | 17.12 | 0.01465 | 0.01559 | 0.01516 | 0.01465 | 0.01559 | 0.01517 | 0.01298 | 0.00931 | 0.00958 | 0.01298 | 0.00930 | |
| 43 | 1.83 | 17.40 | 0.01462 | 0.01620 | 0.01577 | 0.01462 | 0.01620 | 0.01579 | 0.01380 | 0.01294 | 0.01286 | 0.01380 | 0.01293 | |
| 28 | 0.00 | 17.50 | 0.01459 | 0.01680 | 0.01637 | 0.01459 | 0.01680 | 0.01641 | 0.01462 | 0.01658 | 0.01613 | 0.01462 | 0.01658 | |
| 42 | -1.83 | 17.40 | 0.01457 | 0.01735 | 0.01694 | 0.01457 | 0.01735 | 0.01700 | 0.01545 | 0.02017 | 0.01937 | 0.01545 | 0.02016 | |
| 41 | -3.64 | 17.12 | 0.01454 | 0.01789 | 0.01755 | 0.01454 | 0.01789 | 0.01763 | 0.01627 | 0.02373 | 0.02264 | 0.01627 | 0.02373 | |
| 40 | -5.41 | 16.64 | 0.01452 | 0.01838 | 0.01803 | 0.01452 | 0.01838 | 0.01812 | 0.01708 | 0.02719 | 0.02576 | 0.01708 | 0.02719 | |
| 39 | -7.12 | 15.99 | 0.01450 | 0.01887 | 0.01858 | 0.01450 | 0.01887 | 0.01870 | 0.01787 | 0.03060 | 0.02897 | 0.01787 | 0.03060 | |
| 38 | -8.75 | 15.16 | 0.01449 | 0.01931 | 0.01891 | 0.01449 | 0.01931 | 0.01904 | 0.01864 | 0.03386 | 0.03191 | 0.01864 | 0.03386 | |
| 37 | -10.29 | 14.16 | 0.01448 | 0.01975 | 0.01936 | 0.01448 | 0.01975 | 0.01954 | 0.01939 | 0.03705 | 0.03497 | 0.01939 | 0.03705 | |
| 36 | -11.71 | 13.01 | 0.01447 | 0.02015 | 0.01953 | 0.01447 | 0.02015 | 0.01972 | 0.02010 | 0.04005 | 0.03766 | 0.02010 | 0.04005 | |
| 35 | -13.01 | 11.71 | 0.01447 | 0.02054 | 0.01988 | 0.01447 | 0.02054 | 0.02022 | 0.02078 | 0.04205 | 0.04054 | 0.02078 | 0.04205 | |

Table VI - 10 (a) Magnitude of Horizontal deformation around periphery - Model II

| Horizontal Deformation LIST ALL PICKED NODES Model II (CRT) | | | Without Horizontal Ground Load | | | | | | Without Horizontal Ground Load | | | | | |
|---|--------|--------|--------------------------------|-----------------|-----------------|------------------|------------------|------------------|--------------------------------|------------------|-----------------|------------------|-------------------|------------------|
| | | | Elastic | | | Elasto-Plastic | | | Elastic | | | Elasto-Plastic | | |
| Node | X | Y | CRTE00 UX(m) | CRTE01 UX(m) | CRTE02 UX(m) | CRTEP00 UX(m) | CRTEP01 UX(m) | CRTEP02 UX(m) | CRTE00H UX(m) | CRTE01H UX(m) | CRTE03 UX(m) | CRTE00H UX(m) | CRTEP01H UX(m) | CRTEP03 UX(m) |
| 34 | -14.16 | 10.29 | 0.01448 | 0.02092 | 0.01992 | 0.01448 | 0.02092 | 0.02033 | 0.02140 | 0.04564 | 0.04290 | 0.02140 | 0.04564 | 0.04266 |
| 33 | -15.16 | 8.75 | 0.01449 | 0.02129 | 0.02023 | 0.01449 | 0.02129 | 0.02114 | 0.02199 | 0.04821 | 0.04549 | 0.02199 | 0.04822 | 0.04542 |
| 32 | -15.99 | 7.12 | 0.01450 | 0.02165 | 0.02022 | 0.01450 | 0.02165 | 0.02093 | 0.02251 | 0.05054 | 0.04757 | 0.02251 | 0.05055 | 0.04745 |
| 31 | -16.64 | 5.41 | 0.01452 | 0.02203 | 0.02057 | 0.01452 | 0.02203 | 0.02179 | 0.02298 | 0.05275 | 0.04987 | 0.02298 | 0.05276 | 0.05014 |
| 30 | -17.12 | 3.64 | 0.01455 | 0.02241 | 0.02063 | 0.01455 | 0.02241 | 0.02159 | 0.02337 | 0.05473 | 0.05164 | 0.02337 | 0.05474 | 0.05174 |
| 29 | -17.40 | 1.83 | 0.01458 | 0.02284 | 0.02119 | 0.01458 | 0.02284 | 0.02303 | 0.02370 | 0.05657 | 0.05372 | 0.02370 | 0.05658 | 0.05477 |
| 19 | -17.50 | 0.00 | 0.01461 | 0.02328 | 0.02152 | 0.01461 | 0.02328 | 0.02372 | 0.02396 | 0.05822 | 0.05532 | 0.02396 | 0.05823 | 0.05728 |
| 20 | -17.43 | -2.66 | 0.01467 | 0.02383 | 0.02244 | 0.01467 | 0.02383 | 0.02770 | 0.02423 | 0.06013 | 0.05766 | 0.02423 | 0.06014 | 0.06514 |
| 21 | -17.23 | -5.31 | 0.01473 | 0.02424 | 0.02271 | 0.01473 | 0.02424 | 0.02763 | 0.02438 | 0.06140 | 0.05882 | 0.02438 | 0.06141 | 0.06659 |
| 22 | -16.90 | -7.94 | 0.01479 | 0.02447 | 0.02321 | 0.01479 | 0.02447 | 0.02907 | 0.02443 | 0.06208 | 0.05977 | 0.02443 | 0.06210 | 0.06927 |
| 23 | -16.43 | -10.56 | 0.01485 | 0.02460 | 0.02321 | 0.01485 | 0.02460 | 0.02842 | 0.02437 | 0.06216 | 0.05972 | 0.02437 | 0.06217 | 0.06834 |
| 24 | -15.83 | -13.15 | 0.01492 | 0.02455 | 0.02345 | 0.01492 | 0.02455 | 0.02930 | 0.02422 | 0.06167 | 0.05948 | 0.02422 | 0.06169 | 0.06931 |
| 25 | -15.10 | -15.70 | 0.01498 | 0.02435 | 0.02323 | 0.01498 | 0.02435 | 0.02799 | 0.02392 | 0.06040 | 0.05819 | 0.02392 | 0.06043 | 0.06485 |
| 26 | -14.24 | -18.22 | 0.01504 | 0.02395 | 0.02317 | 0.01504 | 0.02395 | 0.02775 | 0.02354 | 0.05861 | 0.05671 | 0.02354 | 0.05865 | 0.06288 |
| 27 | -13.25 | -20.69 | 0.01511 | 0.02317 | 0.02251 | 0.01511 | 0.02317 | 0.02571 | 0.02274 | 0.05529 | 0.05356 | 0.02274 | 0.05533 | 0.05775 |
| 17 | -12.15 | -23.10 | 0.01517 | 0.02193 | 0.02153 | 0.01517 | 0.02193 | 0.02374 | 0.02145 | 0.05092 | 0.04954 | 0.02145 | 0.05098 | 0.05183 |
| 18 | -9.07 | -23.10 | 0.01526 | 0.02025 | 0.02025 | 0.01526 | 0.02025 | 0.02270 | 0.02052 | 0.05075 | 0.04897 | 0.02052 | 0.05082 | 0.05171 |
| 15 | -6.00 | -23.10 | 0.01533 | 0.02043 | 0.02020 | 0.01533 | 0.02043 | 0.02259 | 0.01977 | 0.05396 | 0.05050 | 0.01977 | 0.05397 | 0.05250 |
| 16 | -4.50 | -27.60 | 0.01541 | 0.02246 | 0.02214 | 0.01541 | 0.02246 | 0.02318 | 0.01999 | 0.04949 | 0.04765 | 0.01999 | 0.04974 | 0.05547 |
| 13 | -3.00 | -32.10 | 0.01548 | 0.01912 | 0.01864 | 0.01548 | 0.01912 | 0.01792 | 0.01761 | 0.02989 | 0.02780 | 0.01761 | 0.02986 | 0.02694 |
| 14 | 3.00 | -32.10 | 0.01556 | 0.01448 | 0.01463 | 0.01556 | 0.01448 | 0.01440 | 0.01503 | 0.01427 | 0.01449 | 0.01503 | 0.01427 | 0.01509 |
| 9 | 9.00 | -32.10 | 0.01558 | 0.00987 | 0.01082 | 0.01558 | 0.00987 | 0.01124 | 0.01241 | -0.00119 | 0.00168 | 0.01241 | -0.00116 | 0.00407 |
| 10 | 9.00 | -27.83 | 0.01555 | 0.00418 | 0.00461 | 0.01555 | 0.00418 | 0.00158 | 0.00998 | -0.02258 | -0.02100 | 0.00998 | -0.02282 | -0.03095 |
| 11 | 9.00 | -23.55 | 0.01551 | 0.00224 | 0.00263 | 0.01551 | 0.00224 | -0.00377 | 0.00892 | -0.03213 | -0.03062 | 0.00892 | -0.03214 | -0.06587 |
| 12 | 9.00 | -19.28 | 0.01546 | 0.00204 | 0.00246 | 0.01546 | 0.00204 | -0.00362 | 0.00829 | -0.03770 | -0.03607 | 0.00829 | -0.03772 | -0.06657 |
| 7 | 9.00 | -15.00 | 0.01541 | 0.00425 | 0.00500 | 0.01541 | 0.00425 | 0.00092 | 0.00897 | -0.04068 | -0.03636 | 0.00897 | -0.04072 | -0.05122 |
| 8 | 12.16 | -15.00 | 0.01541 | 0.00445 | 0.00510 | 0.01541 | 0.00445 | 0.00103 | 0.00814 | -0.03776 | -0.03469 | 0.00814 | -0.03780 | -0.05068 |
| 1 | 15.31 | -15.00 | 0.01539 | 0.00382 | 0.00464 | 0.01539 | 0.00382 | 0.00089 | 0.00720 | -0.03488 | -0.03316 | 0.00720 | -0.03492 | -0.05043 |

Table VI-10 (b) Magnitude of Vertical Deformation around periphery - Model II

| Vertical Deformation | | | Without Horizontal Ground Load | | | | | | | | | | | | | | | |
|-----------------------|--------|--------|--------------------------------|----------|----------|----------|----------------|----------|----------|----------|----------|----------|----------|----------|----------------|----------|----------|--|
| LIST ALL PICKED NODES | | | Elastic | | | | Elasto-Plastic | | | | Elastic | | | | Elasto-Plastic | | | |
| Model II (CRT) | | | CRTE00 | CRTE01 | CRTE02 | CRTEP00 | CRTEP01 | CRTEP02 | CRTE00H | CRTE01H | CRTE03 | CRTE00H | CRTE01H | CRTE03 | CRTE00H | CRTE01H | CRTEP03 | |
| Node | X | Y | UY(m) | UY(m) | UY(m) | UY(m) | UY(m) | UY(m) | UY(m) | UY(m) | UY(m) | UY(m) | UY(m) | UY(m) | UY(m) | UY(m) | UY(m) | |
| 1 | 15.31 | -15.00 | -0.04310 | -0.03326 | -0.03529 | -0.04310 | -0.03061 | -0.03900 | -0.04401 | -0.03710 | -0.03843 | -0.04401 | -0.03710 | -0.03843 | -0.04401 | -0.03714 | -0.06167 | |
| 3 | 16.10 | -12.06 | -0.04499 | -0.03773 | -0.03901 | -0.04499 | -0.03501 | -0.04225 | -0.04555 | -0.04010 | -0.04105 | -0.04555 | -0.04010 | -0.04105 | -0.04555 | -0.04014 | -0.06209 | |
| 4 | 16.71 | -9.08 | -0.04688 | -0.04201 | -0.04275 | -0.04688 | -0.04076 | -0.04580 | -0.04701 | -0.04306 | -0.04371 | -0.04701 | -0.04306 | -0.04371 | -0.04701 | -0.04308 | -0.06296 | |
| 5 | 17.15 | -6.07 | -0.04878 | -0.04622 | -0.04665 | -0.04878 | -0.04697 | -0.05019 | -0.04841 | -0.04609 | -0.04663 | -0.04841 | -0.04609 | -0.04663 | -0.04841 | -0.04612 | -0.06478 | |
| 6 | 17.41 | -3.04 | -0.05067 | -0.05055 | -0.05064 | -0.05067 | -0.05320 | -0.05482 | -0.04978 | -0.04933 | -0.04972 | -0.04978 | -0.04933 | -0.04972 | -0.04978 | -0.04935 | -0.06648 | |
| 2 | 17.50 | 0.00 | -0.05255 | -0.05514 | -0.05487 | -0.05255 | -0.05940 | -0.05957 | -0.05113 | -0.05288 | -0.05311 | -0.05113 | -0.05288 | -0.05311 | -0.05113 | -0.05289 | -0.06883 | |
| 56 | 17.40 | 1.83 | -0.05368 | -0.05826 | -0.05760 | -0.05368 | -0.06427 | -0.06241 | -0.05192 | -0.05533 | -0.05532 | -0.05192 | -0.05533 | -0.05532 | -0.05192 | -0.05534 | -0.07031 | |
| 55 | 17.12 | 3.64 | -0.05482 | -0.06146 | -0.06035 | -0.05482 | -0.06883 | -0.06503 | -0.05269 | -0.05782 | -0.05750 | -0.05269 | -0.05782 | -0.05750 | -0.05269 | -0.05784 | -0.07166 | |
| 54 | 16.64 | 5.41 | -0.05596 | -0.06475 | -0.06321 | -0.05596 | -0.07373 | -0.06800 | -0.05346 | -0.06042 | -0.05975 | -0.05346 | -0.06042 | -0.05975 | -0.05346 | -0.06043 | -0.07321 | |
| 53 | 15.99 | 7.12 | -0.05709 | -0.06797 | -0.06593 | -0.05709 | -0.07808 | -0.07051 | -0.05422 | -0.06296 | -0.06184 | -0.05422 | -0.06296 | -0.06184 | -0.05422 | -0.06297 | -0.07448 | |
| 52 | 15.16 | 8.75 | -0.05819 | -0.07115 | -0.06880 | -0.05819 | -0.08211 | -0.07355 | -0.05497 | -0.06550 | -0.06404 | -0.05497 | -0.06550 | -0.06404 | -0.05497 | -0.06551 | -0.07600 | |
| 51 | 14.16 | 10.29 | -0.05927 | -0.07418 | -0.07142 | -0.05927 | -0.08565 | -0.07586 | -0.05571 | -0.06793 | -0.06599 | -0.05571 | -0.06793 | -0.06599 | -0.05571 | -0.06794 | -0.07720 | |
| 50 | 13.01 | 11.71 | -0.06030 | -0.07711 | -0.07419 | -0.06030 | -0.08861 | -0.07877 | -0.05643 | -0.07030 | -0.06805 | -0.05643 | -0.07030 | -0.06805 | -0.05643 | -0.07031 | -0.07863 | |
| 49 | 11.71 | 13.01 | -0.06128 | -0.07981 | -0.07658 | -0.06128 | -0.09115 | -0.08080 | -0.05713 | -0.07251 | -0.06979 | -0.05713 | -0.07251 | -0.06979 | -0.05713 | -0.07252 | -0.07975 | |
| 48 | 10.29 | 14.16 | -0.06221 | -0.08236 | -0.07914 | -0.06221 | -0.09319 | -0.08341 | -0.05780 | -0.07460 | -0.07167 | -0.05780 | -0.07460 | -0.07167 | -0.05780 | -0.07461 | -0.08109 | |
| 47 | 8.75 | 15.16 | -0.06307 | -0.08463 | -0.08120 | -0.06307 | -0.09493 | -0.08515 | -0.05844 | -0.07650 | -0.07316 | -0.05844 | -0.07650 | -0.07316 | -0.05844 | -0.07651 | -0.08210 | |
| 46 | 7.12 | 15.99 | -0.06386 | -0.08669 | -0.08339 | -0.06386 | -0.09649 | -0.08732 | -0.05903 | -0.07823 | -0.07480 | -0.05903 | -0.07823 | -0.07480 | -0.05903 | -0.07824 | -0.08331 | |
| 45 | 5.41 | 16.64 | -0.06456 | -0.08843 | -0.08499 | -0.06456 | -0.09786 | -0.08874 | -0.05959 | -0.07973 | -0.07597 | -0.05959 | -0.07973 | -0.07597 | -0.05959 | -0.07973 | -0.08411 | |
| 44 | 3.64 | 17.12 | -0.06517 | -0.08992 | -0.08665 | -0.06517 | -0.09916 | -0.09038 | -0.06008 | -0.08101 | -0.07730 | -0.06008 | -0.08101 | -0.07730 | -0.06008 | -0.08102 | -0.08511 | |
| 43 | 1.83 | 17.40 | -0.06569 | -0.09105 | -0.08765 | -0.06569 | -0.10019 | -0.09131 | -0.06052 | -0.08203 | -0.07808 | -0.06052 | -0.08203 | -0.07808 | -0.06052 | -0.08203 | -0.08562 | |
| 28 | 0.00 | 17.50 | -0.06609 | -0.09187 | -0.08865 | -0.06609 | -0.10097 | -0.09231 | -0.06090 | -0.08281 | -0.07901 | -0.06090 | -0.08281 | -0.07901 | -0.06090 | -0.08281 | -0.08631 | |
| 42 | -1.83 | 17.40 | -0.06638 | -0.09233 | -0.08895 | -0.06638 | -0.10147 | -0.09261 | -0.06120 | -0.08327 | -0.07934 | -0.06120 | -0.08327 | -0.07934 | -0.06120 | -0.08328 | -0.08645 | |
| 41 | -3.64 | 17.12 | -0.06655 | -0.09243 | -0.08920 | -0.06655 | -0.10166 | -0.09290 | -0.06144 | -0.08349 | -0.07979 | -0.06144 | -0.08349 | -0.07979 | -0.06144 | -0.08350 | -0.08676 | |
| 40 | -5.41 | 16.64 | -0.06660 | -0.09220 | -0.08877 | -0.06660 | -0.10158 | -0.09252 | -0.06158 | -0.08337 | -0.07961 | -0.06158 | -0.08337 | -0.07961 | -0.06158 | -0.08337 | -0.08648 | |
| 39 | -7.12 | 15.99 | -0.06652 | -0.09155 | -0.08825 | -0.06652 | -0.10117 | -0.09209 | -0.06164 | -0.08298 | -0.07952 | -0.06164 | -0.08298 | -0.07952 | -0.06164 | -0.08299 | -0.08633 | |
| 38 | -8.75 | 15.16 | -0.06631 | -0.09059 | -0.08710 | -0.06631 | -0.10051 | -0.09105 | -0.06160 | -0.08226 | -0.07880 | -0.06160 | -0.08226 | -0.07880 | -0.06160 | -0.08226 | -0.08560 | |
| 37 | -10.29 | 14.16 | -0.06597 | -0.08920 | -0.08585 | -0.06597 | -0.09956 | -0.08996 | -0.06148 | -0.08126 | -0.07813 | -0.06148 | -0.08126 | -0.07813 | -0.06148 | -0.08126 | -0.08497 | |
| 36 | -11.71 | 13.01 | -0.06550 | -0.08753 | -0.08405 | -0.06550 | -0.09848 | -0.08831 | -0.06125 | -0.07993 | -0.07689 | -0.06125 | -0.07993 | -0.07689 | -0.06125 | -0.07994 | -0.08380 | |
| 35 | -13.01 | 11.71 | -0.06490 | -0.08546 | -0.08219 | -0.06490 | -0.09705 | -0.08671 | -0.06094 | -0.07835 | -0.07566 | -0.06094 | -0.07835 | -0.07566 | -0.06094 | -0.07836 | -0.08271 | |

Table VI-10 (b) Magnitude of Vertical Deformation around periphery - Model II

| Vertical Deformation | | | Without Horizontal Ground Load | | | | | | Without Horizontal Ground Load | | | | | |
|-----------------------|--------|--------|--------------------------------|----------|----------|----------------|----------|----------|--------------------------------|----------|----------|----------------|----------|----------|
| LIST ALL PICKED NODES | | | Elastic | | | Elasto-Plastic | | | Elastic | | | Elasto-Plastic | | |
| Model II (CRT) | | | CRTE00 | CRTE01 | CRTE02 | CRTEP00 | CRTEP01 | CRTEP02 | CRTE00H | CRTE01H | CRTE03 | CRTE00H | CRTEP01H | CRTEP03 |
| Node | X | Y | UY(m) | UY(m) | UY(m) | UY(m) | UY(m) | UY(m) | UY(m) | UY(m) | UY(m) | UY(m) | UY(m) | |
| 34 | -14.16 | 10.29 | -0.06418 | -0.08314 | -0.07987 | -0.06418 | -0.09542 | -0.08447 | -0.06052 | -0.07648 | -0.07394 | -0.06052 | -0.07649 | -0.08117 |
| 33 | -15.16 | 8.75 | -0.06335 | -0.08048 | -0.07754 | -0.06335 | -0.09297 | -0.08243 | -0.06002 | -0.07438 | -0.07223 | -0.06002 | -0.07439 | -0.07968 |
| 32 | -15.99 | 7.12 | -0.06241 | -0.07762 | -0.07487 | -0.06241 | -0.09026 | -0.07972 | -0.05942 | -0.07206 | -0.07012 | -0.05942 | -0.07206 | -0.07776 |
| 31 | -16.64 | 5.41 | -0.06138 | -0.07451 | -0.07221 | -0.06138 | -0.08633 | -0.07718 | -0.05875 | -0.06956 | -0.06802 | -0.05875 | -0.06956 | -0.07587 |
| 30 | -17.12 | 3.64 | -0.06026 | -0.07128 | -0.06935 | -0.06026 | -0.08207 | -0.07426 | -0.05799 | -0.06692 | -0.06567 | -0.05799 | -0.06692 | -0.07361 |
| 29 | -17.40 | 1.83 | -0.05907 | -0.06796 | -0.06654 | -0.05907 | -0.07725 | -0.07145 | -0.05716 | -0.06421 | -0.06333 | -0.05716 | -0.06422 | -0.07134 |
| 19 | -17.50 | 0.00 | -0.05782 | -0.06468 | -0.06369 | -0.05782 | -0.07221 | -0.06835 | -0.05626 | -0.06152 | -0.06090 | -0.05626 | -0.06152 | -0.06864 |
| 20 | -17.43 | -2.66 | -0.05595 | -0.06029 | -0.05968 | -0.05595 | -0.06503 | -0.06337 | -0.05485 | -0.05789 | -0.05746 | -0.05485 | -0.05789 | -0.06389 |
| 21 | -17.23 | -5.31 | -0.05404 | -0.05606 | -0.05580 | -0.05404 | -0.05874 | -0.05877 | -0.05339 | -0.05442 | -0.05417 | -0.05339 | -0.05442 | -0.05984 |
| 22 | -16.90 | -7.94 | -0.05210 | -0.05190 | -0.05188 | -0.05210 | -0.05255 | -0.05372 | -0.05190 | -0.05105 | -0.05087 | -0.05190 | -0.05105 | -0.05510 |
| 23 | -16.43 | -10.56 | -0.05013 | -0.04777 | -0.04807 | -0.05013 | -0.04642 | -0.04929 | -0.05037 | -0.04768 | -0.04768 | -0.05037 | -0.04769 | -0.05113 |
| 24 | -15.83 | -13.15 | -0.04815 | -0.04371 | -0.04421 | -0.04815 | -0.04047 | -0.04436 | -0.04883 | -0.04439 | -0.04443 | -0.04883 | -0.04440 | -0.04603 |
| 25 | -15.10 | -15.70 | -0.04615 | -0.03967 | -0.04050 | -0.04615 | -0.03501 | -0.04043 | -0.04726 | -0.04106 | -0.04131 | -0.04726 | -0.04107 | -0.04255 |
| 26 | -14.24 | -18.22 | -0.04415 | -0.03565 | -0.03671 | -0.04415 | -0.02986 | -0.03598 | -0.04566 | -0.03765 | -0.03806 | -0.04566 | -0.03766 | -0.03749 |
| 27 | -13.25 | -20.69 | -0.04216 | -0.03146 | -0.03308 | -0.04216 | -0.02442 | -0.03270 | -0.04400 | -0.03383 | -0.03494 | -0.04400 | -0.03384 | -0.03339 |
| 17 | -12.15 | -23.10 | -0.04018 | -0.02688 | -0.02946 | -0.04018 | -0.02085 | -0.02999 | -0.04231 | -0.02912 | -0.03169 | -0.04231 | -0.02915 | -0.03066 |
| 18 | -9.07 | -23.10 | -0.03988 | -0.02091 | -0.02212 | -0.03988 | -0.01532 | -0.01725 | -0.04253 | -0.02533 | -0.02599 | -0.04253 | -0.02541 | -0.02663 |
| 15 | -6.00 | -23.10 | -0.03958 | -0.01850 | -0.01932 | -0.03958 | -0.01394 | -0.01551 | -0.04225 | -0.02722 | -0.02636 | -0.04225 | -0.02733 | -0.02550 |
| 16 | -4.50 | -27.60 | -0.03596 | -0.01790 | -0.01839 | -0.03596 | -0.01363 | -0.01487 | -0.03927 | -0.02761 | -0.02630 | -0.03927 | -0.02765 | -0.02203 |
| 13 | -3.00 | -32.10 | -0.03228 | -0.01560 | -0.01689 | -0.03228 | -0.01192 | -0.01399 | -0.03589 | -0.02330 | -0.02508 | -0.03589 | -0.02324 | -0.02034 |
| 14 | 3.00 | -32.10 | -0.03180 | -0.01331 | -0.01416 | -0.03180 | -0.00980 | -0.01140 | -0.03542 | -0.01848 | -0.01933 | -0.03542 | -0.01844 | -0.01439 |
| 9 | 9.00 | -32.10 | -0.03131 | -0.01924 | -0.02076 | -0.03131 | -0.01496 | -0.01711 | -0.03348 | -0.02583 | -0.02775 | -0.03348 | -0.02574 | -0.01896 |
| 10 | 9.00 | -27.83 | -0.03457 | -0.02447 | -0.02468 | -0.03457 | -0.02145 | -0.02154 | -0.03645 | -0.03474 | -0.03417 | -0.03645 | -0.03474 | -0.02817 |
| 11 | 9.00 | -23.55 | -0.03774 | -0.02657 | -0.02660 | -0.03774 | -0.02492 | -0.02450 | -0.03931 | -0.03756 | -0.03668 | -0.03931 | -0.03764 | -0.03929 |
| 12 | 9.00 | -19.28 | -0.04084 | -0.02696 | -0.02721 | -0.04084 | -0.02498 | -0.02540 | -0.04208 | -0.03843 | -0.03750 | -0.04208 | -0.03851 | -0.04641 |
| 7 | 9.00 | -15.00 | -0.04387 | -0.02665 | -0.02712 | -0.04387 | -0.02460 | -0.02531 | -0.04463 | -0.03960 | -0.03793 | -0.04463 | -0.03968 | -0.05034 |
| 8 | 12.16 | -15.00 | -0.04348 | -0.02855 | -0.02928 | -0.04348 | -0.02600 | -0.02887 | -0.04480 | -0.03743 | -0.03742 | -0.04480 | -0.03750 | -0.06082 |
| 1 | 15.31 | -15.00 | -0.04310 | -0.03326 | -0.03529 | -0.04310 | -0.03061 | -0.03900 | -0.04401 | -0.03710 | -0.03843 | -0.04401 | -0.03714 | -0.06167 |

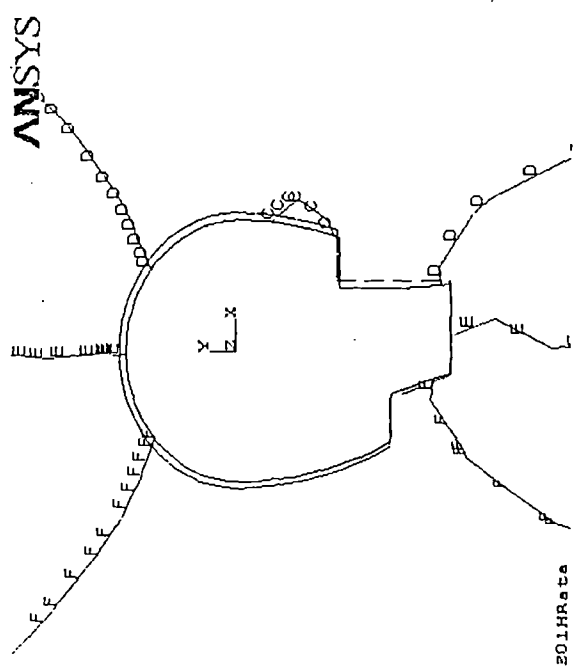
ANSYS RESULTS - Contour Plot
UX - Deformation Horizontal

Figure VI - 14 (a)

MODEL I

90

E01

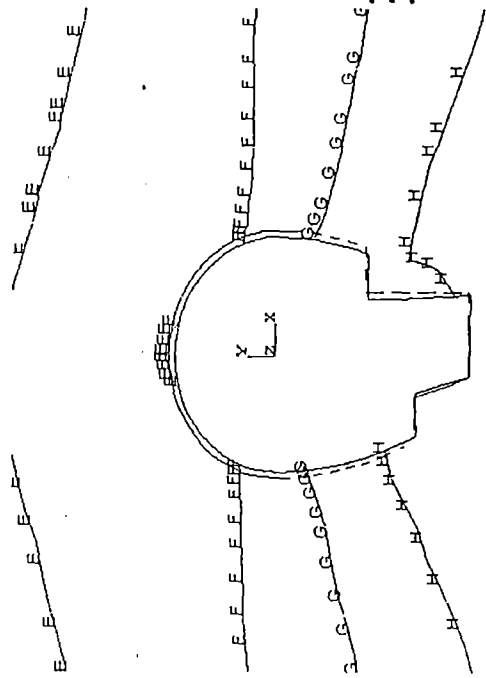


201HRata

ANSYS
APR 19 2004
08:31:46
NODAL SOLUTION
STEP=1
SUB =1
TIME=1
UX (AVG)

PowerGraphics
EPACET=1
AVRES=Mat
DMX =.105106
SMN =-.105106
SMX =.102387
A =-.093579
B =-.070524
C =-.047469
D =-.024414
E =-.001359
F =.021695
G =.044475
H =.067805
I =.09086

E02

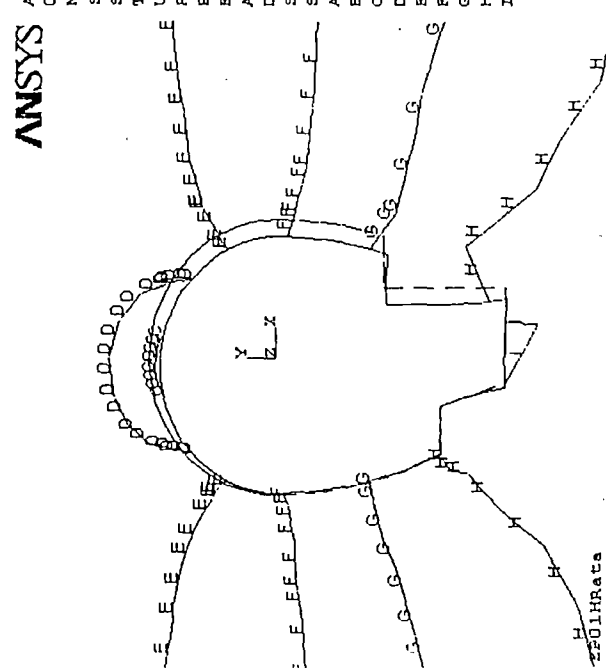


E02HRata

ANSYS 5.4
APR 19 2004
08:37:58
NODAL SOLUTION
STEP=1
SUB =1
TIME=1
UX (AVG)

PowerGraphics
EPACET=1
AVRES=Mat
DMX =.105154
SMN =-.099448
SMX =.111E-16
YV =-.211E-16
ZV =1
DIST=46.542
*XF =2.192
*YF =-3.279
A =-.093923
B =-.082873
C =-.071823
E =-.049724
F =-.038674
G =-.027624
I =-.005525

EP01

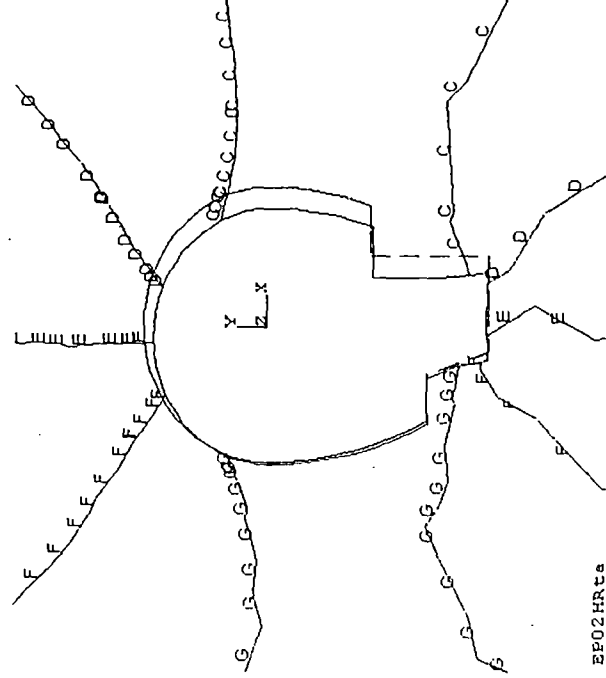


2201HRata

ANSYS
APR 19 2004
08:45:22
NODAL SOLUTION
STEP=1
SUB =1
TIME=1
UX (AVG)

PowerGraphics
EPACET=1
AVRES=Mat
DMX =.155801
SMN =-.103107
SMX =.009521
A =-.09685
B =-.084336
C =-.071822
D =-.059307
E =-.046793
F =-.034279
G =-.021764
H =-.00925
I =.003264

EP02



EP02HRata

ANSYS 5.4
APR 19 2004
08:54:46
NODAL SOLUTION
STEP=1
SUB =1
TIME=1
UX (AVG)

PowerGraphics
EPACET=1
AVRES=Mat
DMX =.182548
SMN =-.182548
SMX =.038612
A =-.170261
B =-.145688
C =-.121115
D =-.096541
E =-.071968
F =-.047395
G =-.022821
H =-.001752
I =-.026325

ANSYS RESULTS - Contour Plot
UY - DEFORMATION VERTICAL

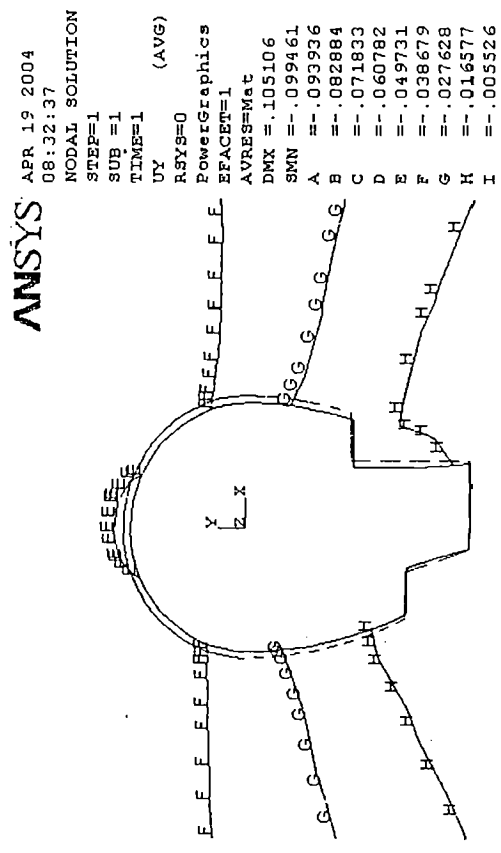
Figure VI - 14 (b)

MODEL I

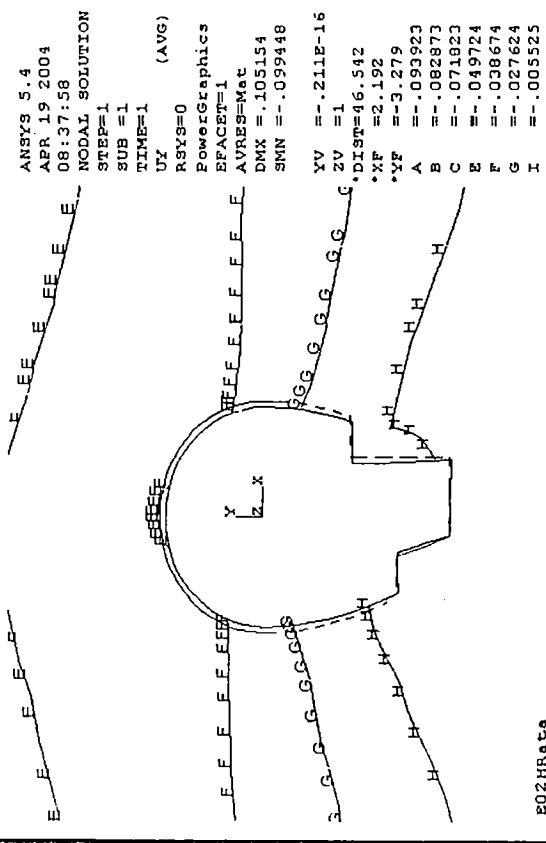
91

E01

E02



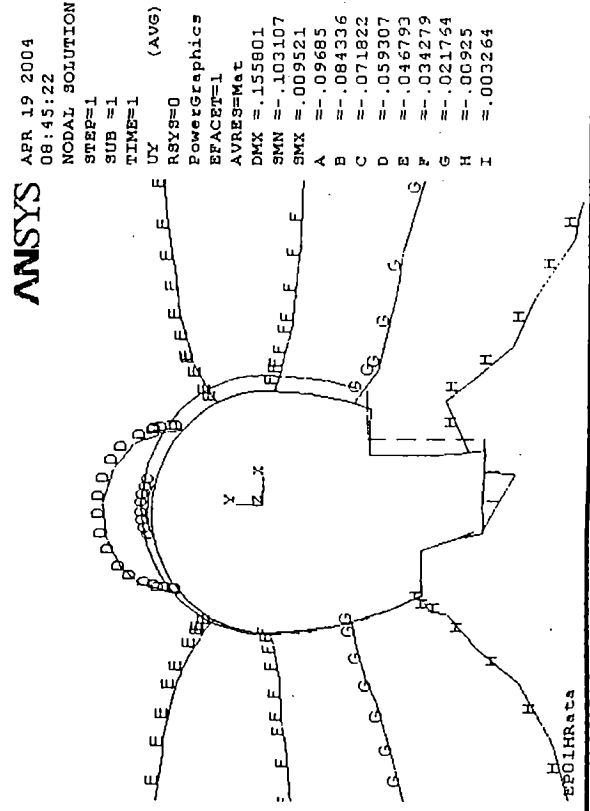
E01HRata



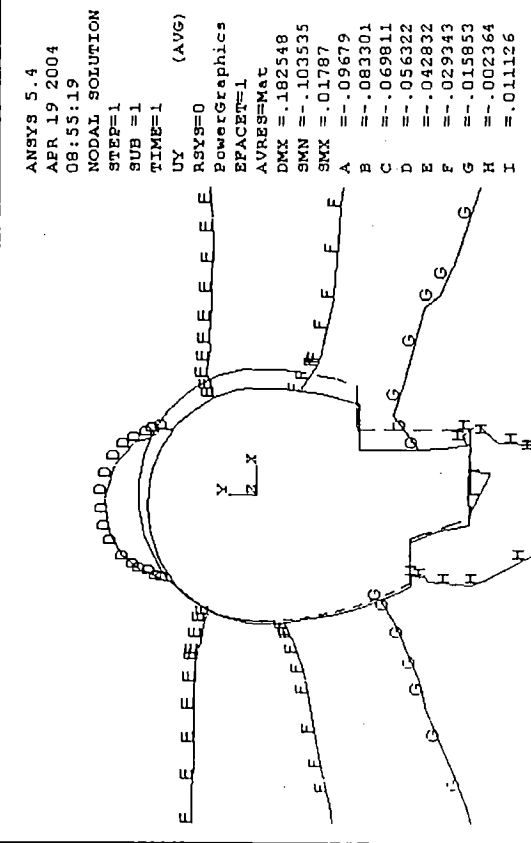
E02HRata

EP01

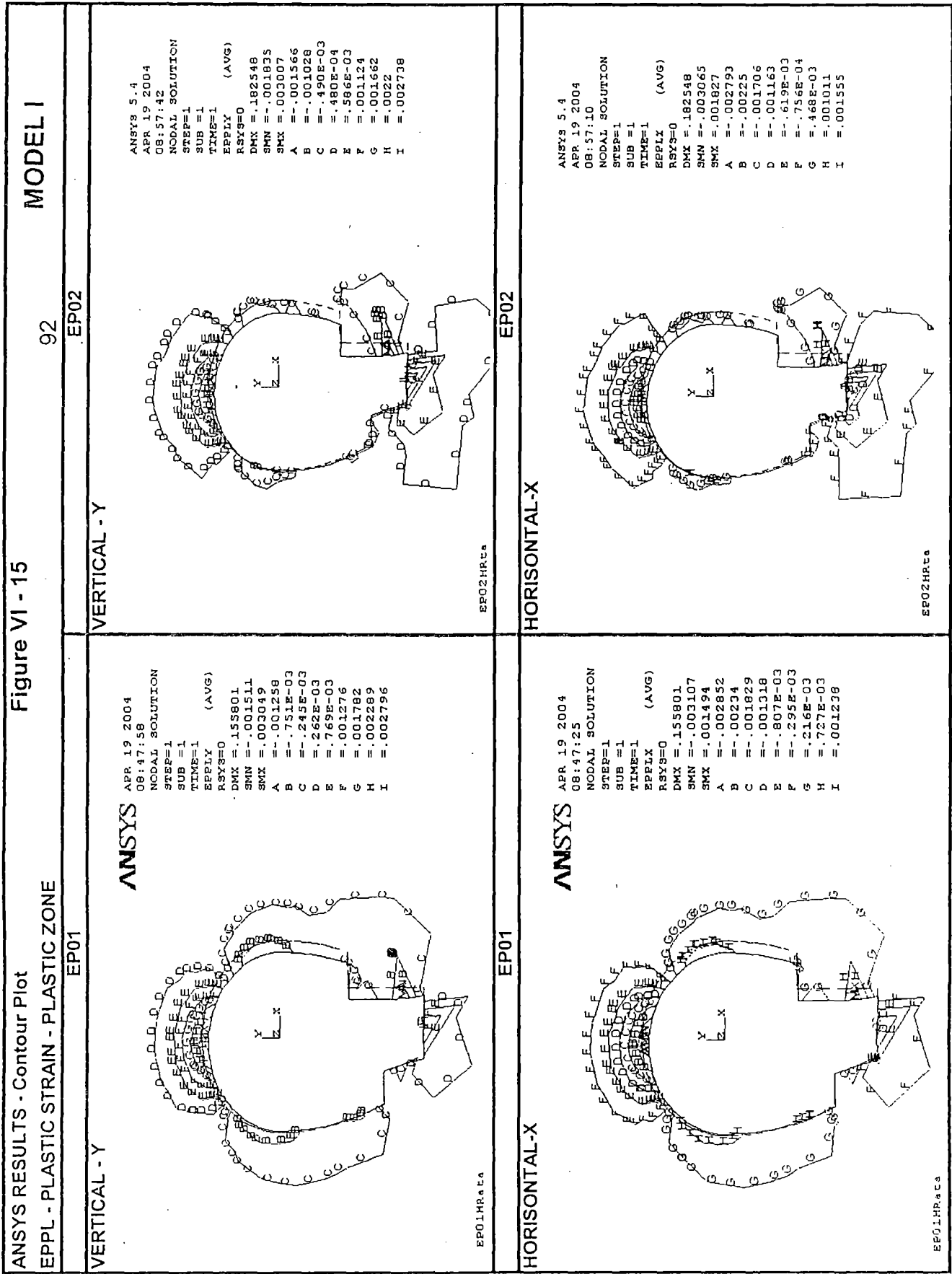
EP02



EP01HRata



EP02HRata

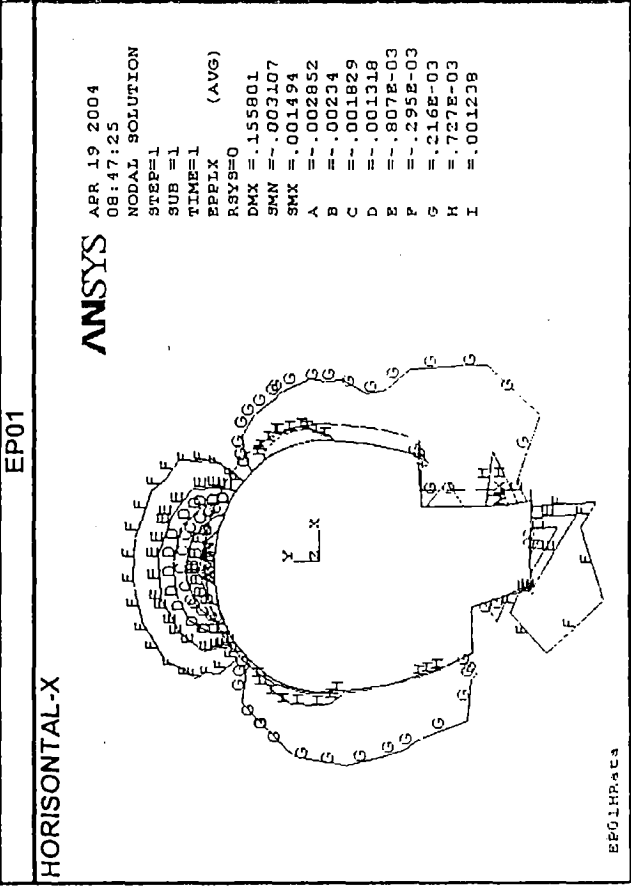
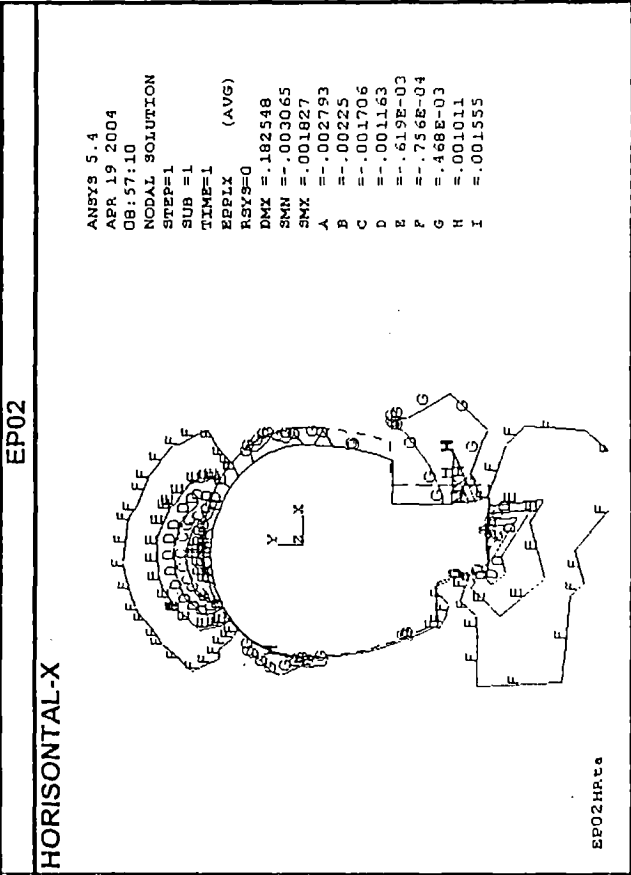
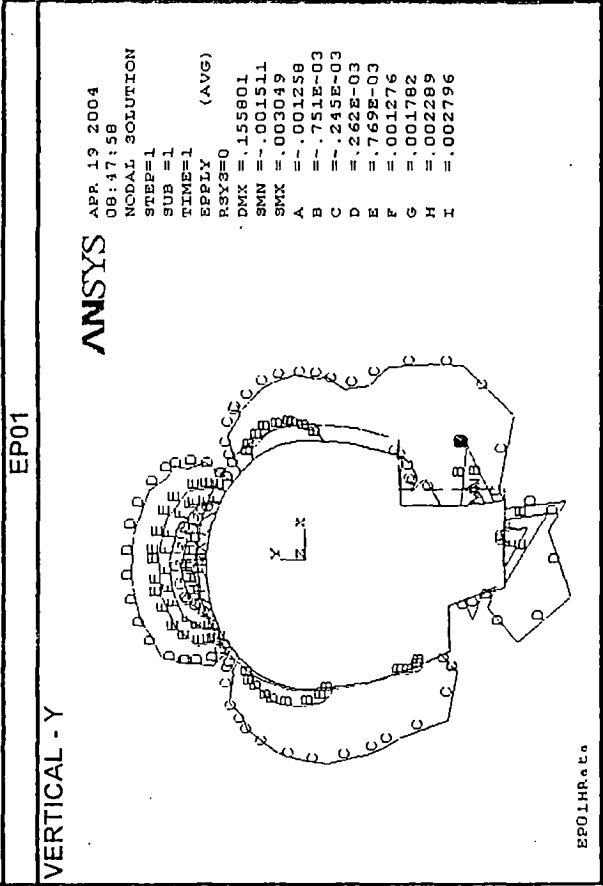
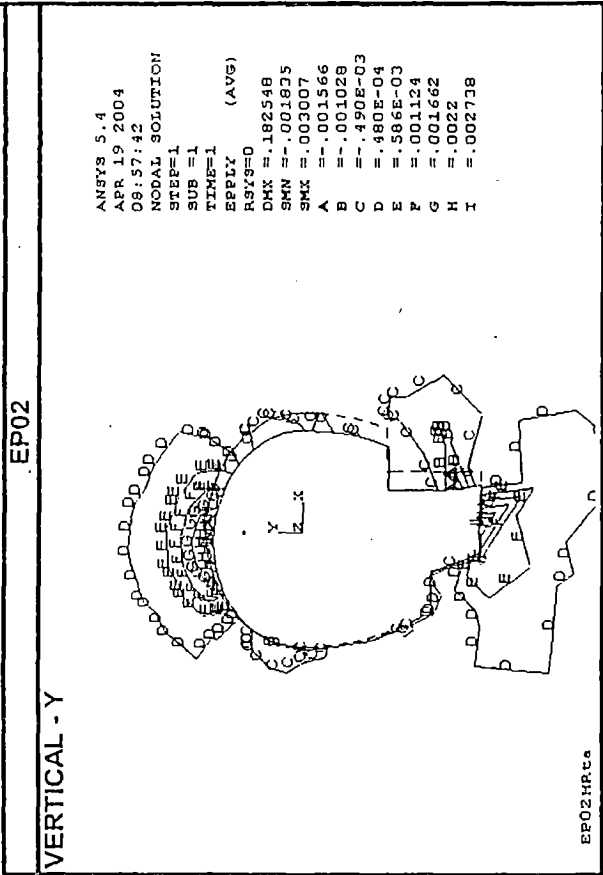


MODEL I

Figure VI - 15

ANSYS RESULTS - Contour Plot
EPPL - PLASTIC STRAIN - PLASTIC ZONE

92



ANSYS RESULTS - Contour Plot
Displacement Vector

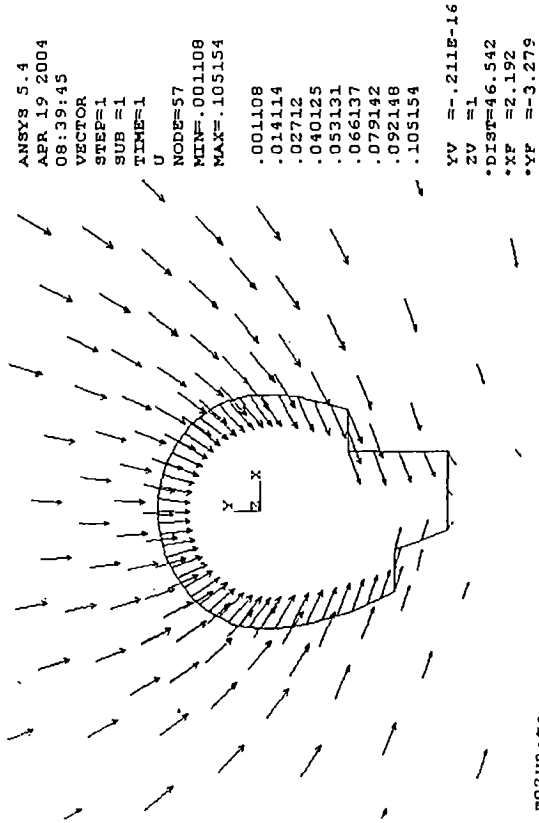
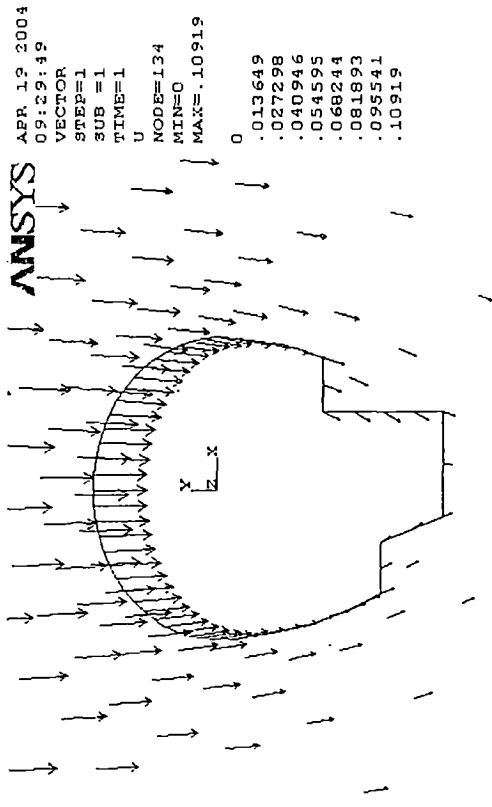
Figure VI - 16

MODEL I

93

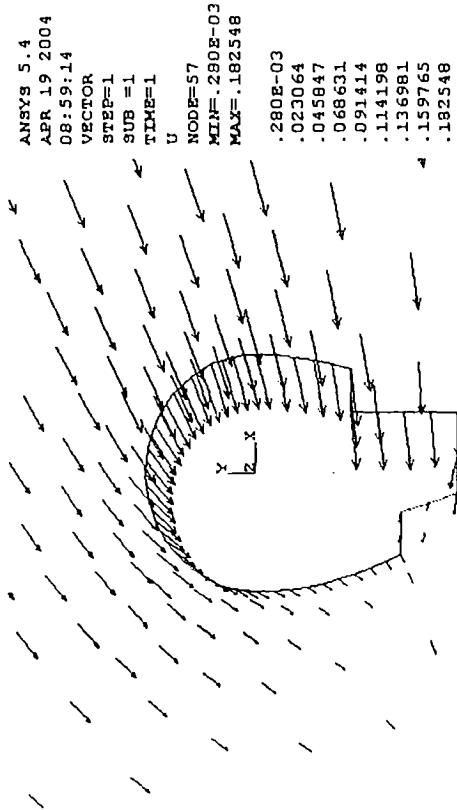
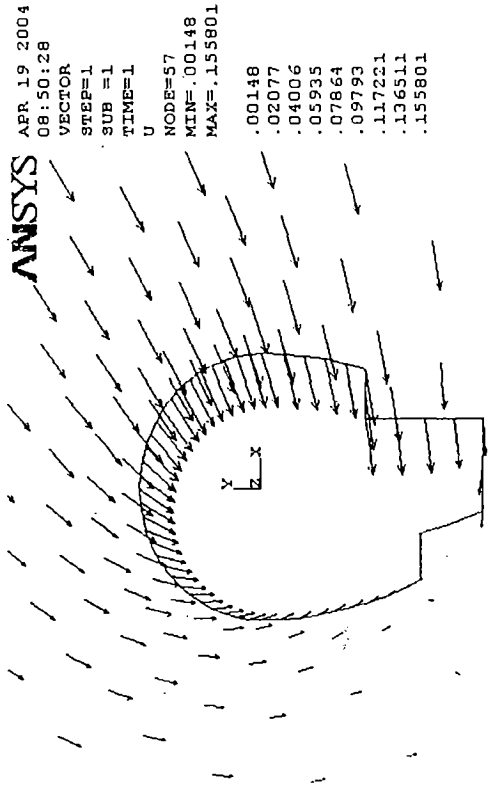
E01

E02H



EP01

EP02H



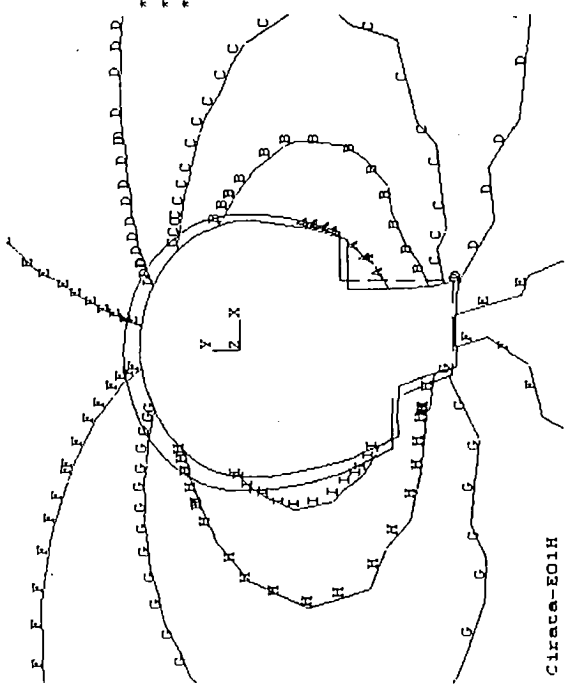
MODEL II

94

Figure VI - 17 (a)

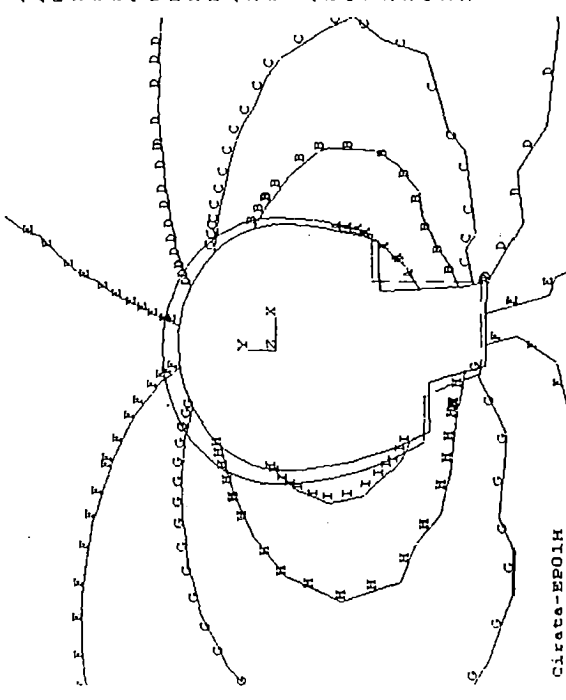
ANSYS RESULTS - Contour Plot
UX- Deformation Horizontal

CRT-E01H



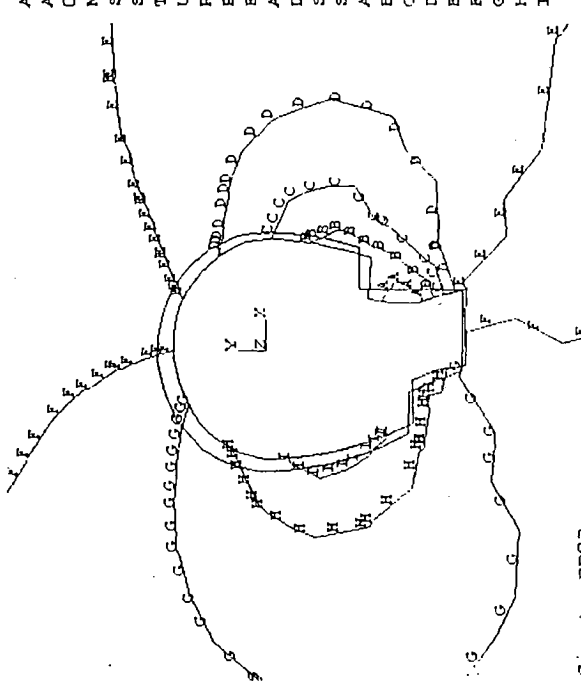
Cirata-E01H

CRT-EP01H



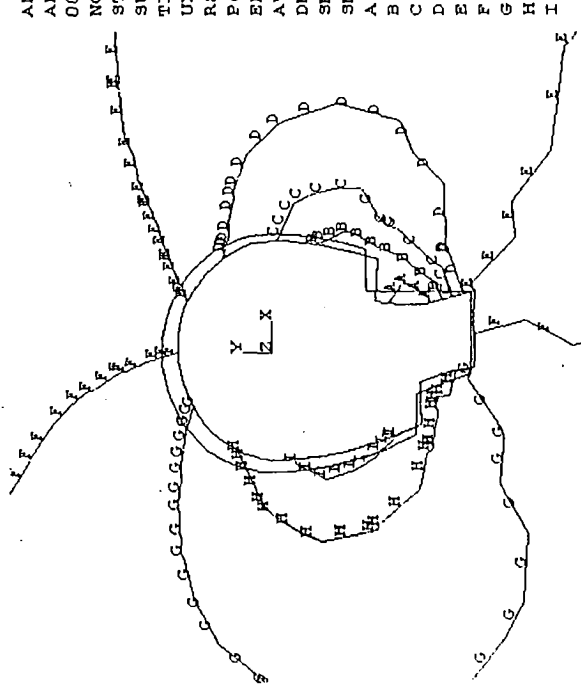
Cirata-EP01H

CRT-E03



Cirata-E03

CRT-EP03



Cirata-EP03

Figure VI - 18

MODEL II

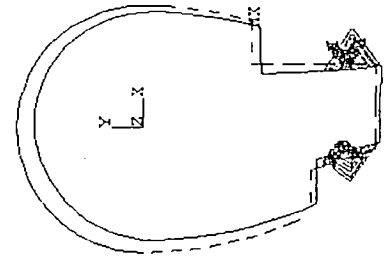
96

ANSYS RESULTS - Contour Plot
EPPL - STRAIN PLASTIC - PLASTIC ZONE

CRT-EP01H

VERTICAL - Y

HORIZONTAL - X

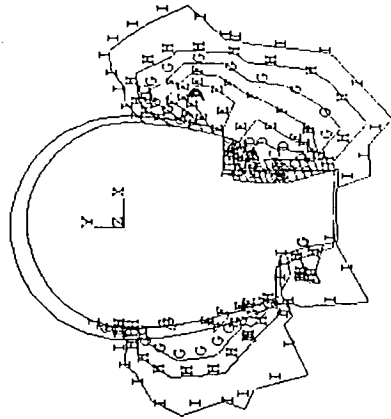


ANSYS 5.4
 APR 19 2004
 01:34:01
 NODAL SOLUTION
 STEP=1
 SUB =1
 TIME=1
 EPPLX (AVG)
 RSYS=0
 DMX =.166686
 SMN =-.103E-03
 A =-.973E-04
 B =-.859E-04
 C =-.744E-04
 D =-.630E-04
 E =-.515E-04
 F =-.401E-04
 G =-.286E-04
 H =-.172E-04
 I =-.573E-05

Cirata-EP01H

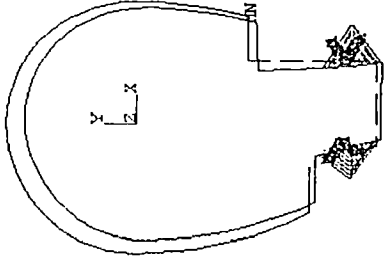
CRT-EP03

VERTICAL - Y



ANSYS 5.4
 APR 19 2004
 00:49:57
 NODAL SOLUTION
 STEP=1
 SUB =1
 TIME=1
 EPPLX (AVG)
 RSYS=0
 DMX =.168118
 SMN =-.003601
 A =-.003401
 B =-.003001
 C =-.0026
 D =-.0022
 E =-.0018
 F =-.0014
 G =-.001
 H =-.600E-03
 I =-.200E-03

Cirata-EP03

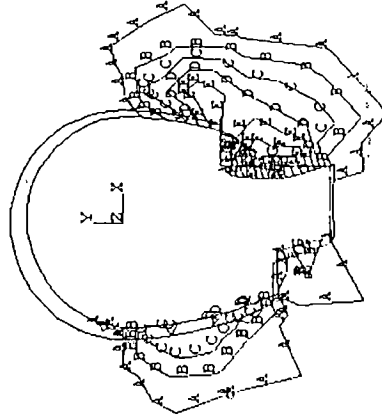


ANSYS 5.4
 APR 19 2004
 01:33:15
 NODAL SOLUTION
 STEP=1
 SUB =1
 TIME=1
 EPPLX (AVG)
 RSYS=0
 DMX =.166686
 SMX =.907E-04
 A =.504E-05
 B =.151E-04
 C =.252E-04
 D =.353E-04
 E =.453E-04
 F =.554E-04
 G =.655E-04
 H =.755E-04
 I =.856E-04

Cirata-EP01H

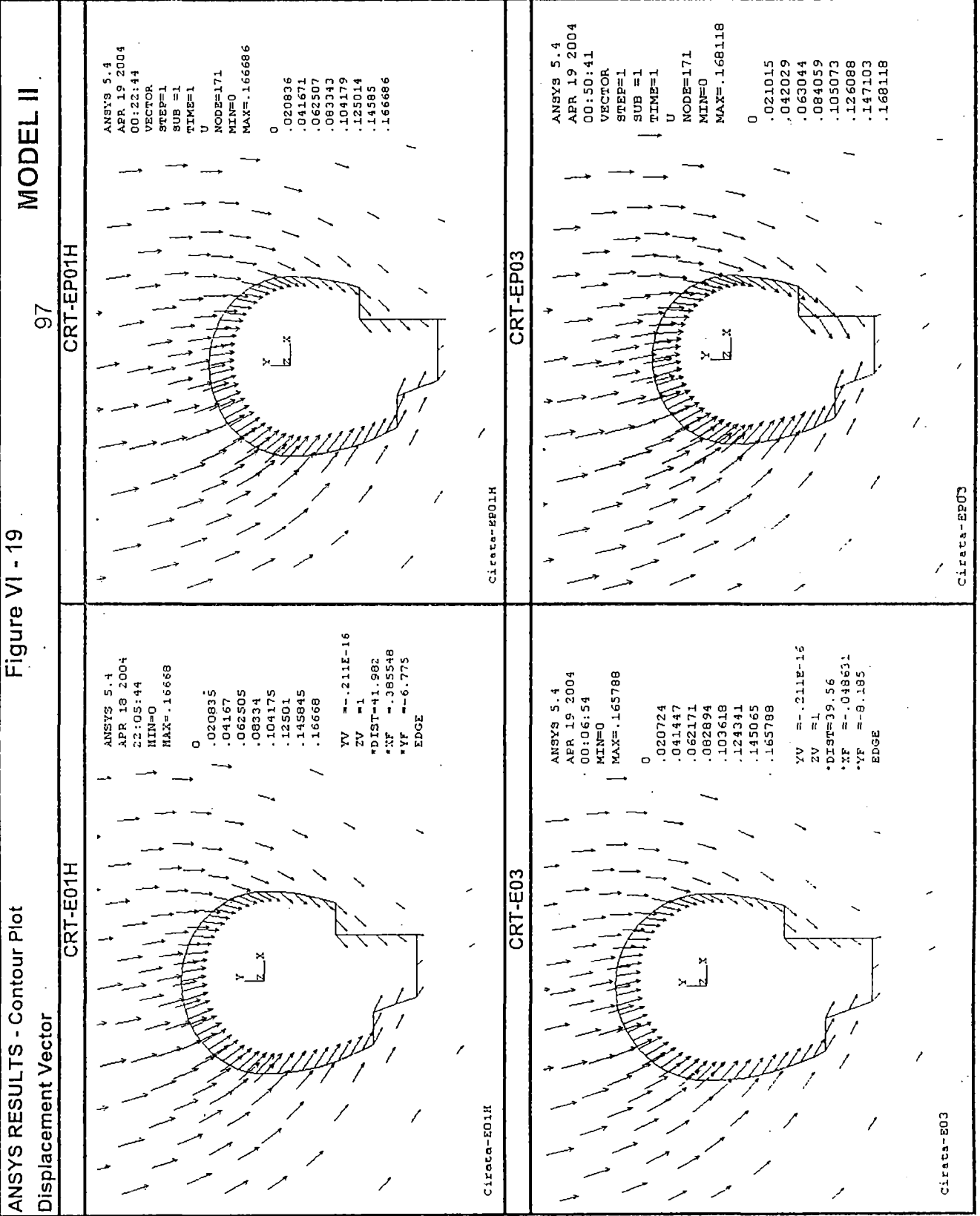
CRT-EP03

HORIZONTAL - X



ANSYS 5.4
 APR 19 2004
 00:43:37
 NODAL SOLUTION
 STEP=1
 SUB =1
 TIME=1
 EPPLX (AVG)
 RSYS=0
 DMX =.168118
 SMX =.003974
 A =.221E-03
 B =.662E-03
 C =.001104
 D =.001546
 E =.001987
 F =.002429
 G =.00287
 H =.003312
 I =.003753

Cirata-EP03



From results presented in Figure VI – 9 to Figure VI – 14 and Table VI – 5 some conclusions can be made:

The maximum deformation in the X-direction (max UX) is about 0.1279 m from *model I elasto-plastic with support* and occurs as predicted at wall of bench (node 12), whereas for model I elastic max UX is 0.04164 m from *model elastic without support* and occurs at node 7. Model II gives the max UX as 0.07486 m from *model elasto-plastic with support* at node 12 i.e at wall of bench, and max UX for *model II elastic* is 0.04965 m at node 7.

The maximum deformation in the Y-direction (max UY) is about 0,03819 m from *model I elasto-plastic with support* and occurs at floor of bench (node 14), whereas for model I elastic max UY is 0,001694 m come from *model elastic without support* at node 18. Model II gives the max UY as 0.04007 m from *model elasto-plastic without support* and and takes place at node 28 at the crown of cavern, and max UY for *model II elastic* is 0.03113 m at node 42 near the crown.

Result in term of UX & UY can be seen in Table VI- 6. The deformations are in mm.

Table VI – 6 (a)
Resume results of max UX & max UY

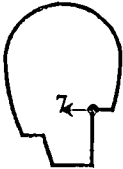
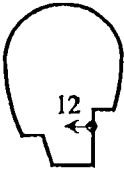
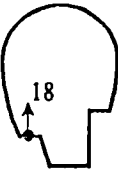
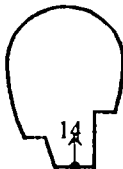

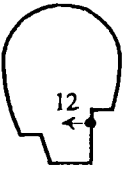

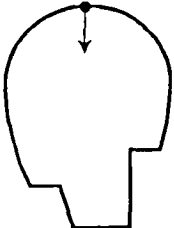
| Model | Max UX (mm) | | Max UY (mm) | |
|-------|---|---|--|--|
| | Elastic | Elasto-plastic | Elastic | Elasto-plastic |
| I | E01  41.64 | EP02  127.93 | E01  16.92 | EP02  38.19 |
| | II | E01H  49.65 | EP01  74.86 | E01  31.13 |

Table VI – 6 (b)
Resume results of UY at crown

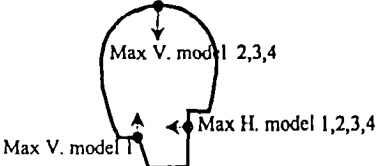
| Model | | | Disp. On crown | Location |
|-------|-----------|------|----------------|--|
| No | ID | E/EP | | |
| 1. | E01H | E | 11.05 |  |
| 2. | E02 | E | 10.26 | |
| 3. | EP01H | E-P | 33.39 | |
| 4. | EP02 | E-P | 29.11 | |
| 5. | CRT-E01H | E | 30.97 | |
| 6. | CRT-E03 | E | 18.11 | |
| 7. | CRT-EP01H | E-P | 40.07 | |
| 8. | CRT-EP03 | E-P | 25.41 | |

VI.2.ii.(1) Comparison with previous studies and field measurement record (data available for June 1994).

Reik et. al (1986) as owner hired-expert did the finite element analyses of the same cavern but their analysis mentioned qualitatively, same as Kamemura et. al (1986) as joint field team presented, their analysis also qualitatively. Only LAPI ITB (1995) presented a complete report on stability analysis of same cavern using finite element (code not mentioned) and UDEC, computer code based on distinct element method (DEM), in two-dimensional analysis. Their problem domain is adopted to Model II in the present study. Also excavation stages assume as one stage same as that of present study. The results of their analysis which relevant to the present study, in term of calculated displacement, are presented in Table VI- 7 below.

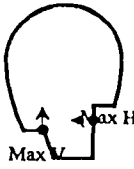
Table VI – 7

(a) Calculated maximum displacement on Periphery Cavern
Finite Element Results (LAPI ITB, 1995)

| Model | | Max. Disp (mm) | | Location |
|-------|-----|----------------|----------|--|
| No | E | Horizontal | Vertical | |
| 1. | 0.3 | 6.01 | 19.18 |  |
| 2. | 0.3 | 9.55 | 29.91 | |
| 3. | 0.4 | 6.90 | 17.11 | |
| 4. | 0.4 | 11.42 | 29.23 | |


(b) Calculated maximum displacement on Periphery Cavern

UDEC Distinct Element Results (LAPI ITB, 1995)

| Model | | Max. Disp (mm) | | Location |
|-------|-----|----------------|----------|---|
| No | E | Horizontal | Vertical | |
| 1. | 0.3 | 12.19 | 28.06 |  |
| 2. | 0.3 | 53.24 | 47.00 | |
| 3. | 0.4 | 20.04 | 25.72 | |
| 4. | 0.4 | 49.00 | 45.89 | |

(c) Calculated maximum displacement on crown

UDEC Distinct Element Results (LAPI ITB, 1995)

| Model | | Disp. On crown | Location |
|-------|-----|----------------|--|
| No | E | | |
| 1. | 0.3 | 12.01 |  |
| 2. | 0.3 | 13.46 | |
| 3. | 0.4 | 23.17 | |
| 4. | 0.4 | 23.85 | |

The results of the present study in term of rock displacement/deformation have been compared to previous study (finite element and UDEC) and also with field monitoring result (as recorded in June 1994, when the plant already functioning) and can be seen on Table VI- 8 below.

As explained in previous section, displacement measurement with multipoint extensometer placed on points along the periphery of cavern. Each point having 5/6 devices in certain distances from periphery; 0 m, 2 m, 5 m, 10 m, 15 m, and 25 m.

From comparison between present study with previous study and monitoring results, as presented in Table VI- 8, some conclusions can be drawn:

1. Generally there is similar evolution of deformation on nodal2 investigated with slightly anomalies.
2. Present study on model with elasto-plastic behaviour shows the results comparing well with the record measurement: vertical deformation UY about 25 – 35 mm on model I.

3. **Model I** in present study gives the deformation closer to previous study and monitoring result compared to **Model II**.
4. The deformation in Y-direction U_Y , the maximum value not always occur on roof, such as in **Model I**, but occurs on the bottom part (node 18 for elastic and node 14 for elasto-plastic). The same pattern is also indicated in previous study.
5. **Max U_X** in present study has best agreement with previous study in term of location, always occur at the wall of bench.
6. Overall, from deformation results **Model I** gives the result closer to the previous study and instrumented data.

Table VI - 8
Comparison between present study's results with previous study in term of Rock deformation

| Location | Depth | Record (as per June 1994) | Displacement/Deformation | | | | | | | | | | | | | | | | | |
|--------------------------|-------|------------------------------------|-----------------------------------|-------|-------|---------|-------|-------|---------|-------|-------|---------------|-------|-------|---------|---------|---------|--------------------|---------|--------------------|
| | | | Previous study | | | | | | | | | Present study | | | | | | | | |
| | | | Finite Element Results v = 0.3 | | | v = 0.4 | | | v = 0.3 | | | v = 0.4 | | | Model I | | | Model II | | |
| | | | E | E-P | E | E | E-P | E | E | E-P | E | E | E-P | E | Elastic | Elastic | Elastic | Elasto- plastic | Elastic | Elasto- plastic |
| Line 2 N-211-8 | 0 | 29.00 | 16.29 | 27.94 | 16.11 | 27.52 | 12.07 | 21.11 | 12.42 | 20.11 | 9.99 | 9.25 | 28.77 | 24.52 | 19.20 | 15.77 | 24.28 | 19.21 | | |
| | 2 | 2.00 | | | | | | | | | | | | | | | | | | |
| | 5 | 0.90 | | | | | | | | | | | | | | | | | | |
| | 10 | 0.60 | | | | | | | | | | | | | | | | | | |
| | 15 | 1.50 | | | | | | | | | | | | | | | | | | |
| | 25 | 0.00 | | | | | | | | | | | | | | | | | | |
| Line 2 C-212-0 | 0 | 32.00 | 17.59 | 30.11 | 17.25 | 29.34 | 13.46 | 23.85 | 12.40 | 20.55 | 11.05 | 10.26 | 33.39 | 29.11 | 30.97 | 18.11 | 40.07 | 25.41 | | |
| | 2 | 2.50 | | | | | | | | | | | | | | | | | | |
| | 10 | 0.25 | | | | | | | | | | | | | | | | | | |
| | 15 | 1.00 | | | | | | | | | | | | | | | | | | |
| | 25 | 0.00 | | | | | | | | | | | | | | | | | | |
| | 25 | 0.00 | | | | | | | | | | | | | | | | | | |
| Line 2 S-211-8 | 0 | 27.5 | 15.14 | 25.91 | 14.95 | 25.5 | 12.10 | 21.31 | 12.68 | 20.59 | 9.79 | 9.13 | 28.65 | 25.46 | 21.34 | 17.87 | 24.68 | 21.96 | | |
| | 2 | 1.00 | | | | | | | | | | | | | | | | | | |
| | 5 | 3.00 | | | | | | | | | | | | | | | | | | |
| | 10 | 6.00 | | | | | | | | | | | | | | | | | | |
| | 15 | 1.00 | | | | | | | | | | | | | | | | | | |
| | 25 | 0.00 | | | | | | | | | | | | | | | | | | |
| Line 2 S-211- 18.5 | 0 | 20.00 | 10.33 | 18.05 | 10.68 | 18.49 | 7.95 | 13.91 | 12.56 | 19.44 | 6.39 | 5.96 | 17.47 | 14.04 | 17.41 | 14.72 | 21.77 | 18.04 | | |
| | 2 | 9.50 | | | | | | | | | | | | | | | | | | |
| | 5 | 7.50 | | | | | | | | | | | | | | | | | | |
| | 15 | 6.50 | | | | | | | | | | | | | | | | | | |
| | 25 | 0.00 | | | | | | | | | | | | | | | | | | |
| | 25 | 0.00 | | | | | | | | | | | | | | | | | | |

Note : E = Elastic
EP = Elasto-plastic
w/o = without support
w/ = with support



CONCLUSIONS

The conclusions are presented in three parts: firstly, summary of present study, and then specific conclusions related to the present study; and finally, the overview of the scope of prospective area of interest for extending the present study.

VII.1 SUMMARY OF PRESENT STUDY

The 2D finite-element analysis of a large powerhouse cavern is presented in this dissertation. The strength and deformation properties used in the analysis are based on information taken from previous study. One stage excavation is assumed in homogeneous rock mass, which is subjected to a uniform original stress field in the region of the cavern. The finite-element analysis defines the distribution of the stress and deformation due to cavern excavation in entire rock mass domain. The results, in term of the stress and deformation along periphery of cavern, have been studied and evaluated. The maximum and minimum magnitude as well as its location are identified, also the differences between elastic model results and elastoplastic model's are discussed. The deformation predicted by the finite element analysis are compared with the previous study and the actual in-situ measurement by extensometer. The study reveals that the deformations obtained by elastic model analysis are less as compared to the borehole extensometer whereas elastoplastic results yield a better matching. Such a study is found to be very helpful for evaluating stress and deformation behaviour of the rock surrounding underground cavern in elastic model as well as elastoplastic model.

VII.2 CONCLUSIONS

Based on the results and discussion of the present study, the following conclusions can be drawn:

Stress and Deformation Study

Due to unsymmetrical shape of the cavern, rock deformation at sidewalls are different for both models. Deformed shape of Model I tend to be displaced to the left-direction for model without support and to right-direction for model with support. The situation is dissimilar for Model II, which tends to displace to the right-direction for both model with and without support. This may be due to the fact that the supports (rock bolts/PS anchors) provided only at arch parts of cavern and it makes the unbalanced confinement effect to rock surrounding cavern.

Both max SX & SY occur at the lower part of cavern since confinement effect from support in upper part does not influence the lower part.

The Max UY, vertical deformation, not always occur at crown of vault part of cavern as in Model I both the elastic and elasto-plastic model, those came from lower part of cavern

Reduction of deformation around cavern are observed due to the application of support. It confirmed that modeling support by applying a pair of external load at nodes suitably represents the confinement effect of support to rock mass.

While comparing the results from 2D analysis with instrumentation data, it is important to note that the cross section for measurement should be carefully selected to match the geometry of opening in modeling. As in the present study, the opening geometry of model is simply represented by the actual cross section Line 2, but the difference at bench part will affected the results as illustrated in Figure VII-1 below.

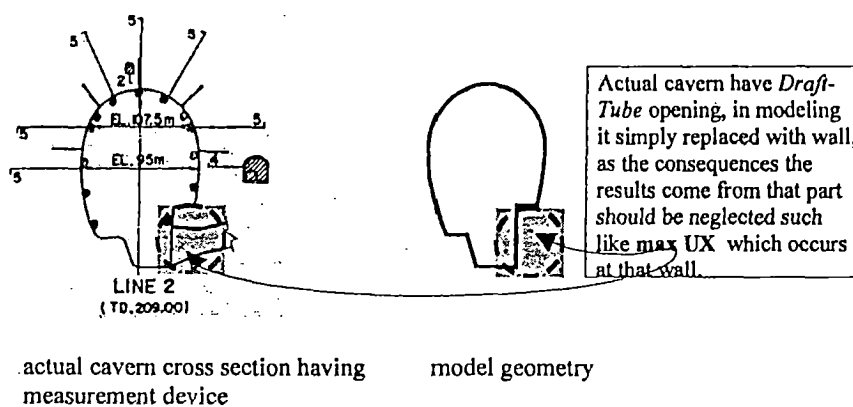


Figure VII-1

Comparison of actual cross section and its model geometry

Comparison between Model I and Model II

The Model II gives the SX at nodes along the periphery very high which seem to be unreasonable, hence Model II in term of applying Horizontal ground pressure directly along the periphery is not recommended to simulate the insitu horizontal stress state.

From deformation consideration Model I is close to the site condition, as the results are close to the measured values.

Comparison between Elastic behaviour and Elastoplastic behaviour

Elastoplastic behaviour always shows maximum deformation greater than elastic model whereas in term of stresses elastoplastic tends to give lesser magnitude compared to the elastic results.

In term of deformation, elastoplastic behaviour results are closer to the previous study and measurement record compared to the elastic result.

ANSYS capability for Analysis of Underground Structure

ANSYS (ver. 5.4), as commercial general purpose FEM package, generally not so 'geotechnical user friendly', due to some limitation such as:

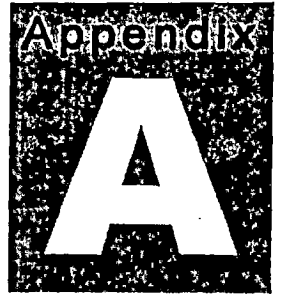
- to simulate the insitu horizontal ground stress user should apply the pressure as external load at both sides far-field boundary with the magnitude as desired. The external pressure will affect the entire problem domain in horizontal compressive stress. The option of horizontal components (x & z direction) of gravity loading in ANSYS can not be used for this purpose since that option only give one way direction of load vector.
- to simulate the contour profile of ground surface (top far-field boundary) for making unsymmetrical effect of problem domain, the difficulty arise when user want to apply external pressure as horizontal ground stress at both sides far-field because it will make model unstable due to unbalanced horizontal pressure;
- to modeling insitu stress state and the excavation stages it would be better if using *death & birth element option* since it will make continuity in the calculation sequences and only using one model. Using option as in the present study which separately calculated models with different step (*initial condition* for model the insitu stress state, model with opening, model with opening and supports) require another step to calculate the relative

displacement result and it makes the geometry of cavern not as per plan since the geometry is deformed at the initial condition.

VII.3 SCOPE OF FURTHER STUDY

In the view of limitation of the present study, which author describe fairly as ‘ a *basic application of finite element analysis in underground structures*’, the present study can be extended to the following with advanced version of ANSYS (ver. 7.0):

- Parametric study of parameters affecting stability of underground opening in rock;
- Advanced analysis of Underground cavern with one or more of the following:
 - Consider the three dimensionality of problem geometry
 - Consider the anisotropy of rock in 3D analysis
 - Consider the presence of inhomogenities and discontinuous features in the rock mass with the help of ‘*joint element*’ in equivalent continuum approach as ANSYS capable for it.
 - Effect of multiple cavities
 - Taking into account the excavation stages
 - Consider the restraint effect of civil engineering structure inside cavern;
 - Modeling rock bolts/PS anchor with truss element and include the shear resistance between bolts and rock medium with aid of ‘*contact element*’;
 - Modeling the rock material with different model behaviour like Mohr-Coulomb, or with more complex model as visco-elastic or consider time-dependent behaviour as creep as long as it represent the material;
 - Exploit so-called ‘*infinite element*’ to simulate far-field boundary as it will reduce limitation of finite element analysis for unbound problem domain such as in underground structures problems.

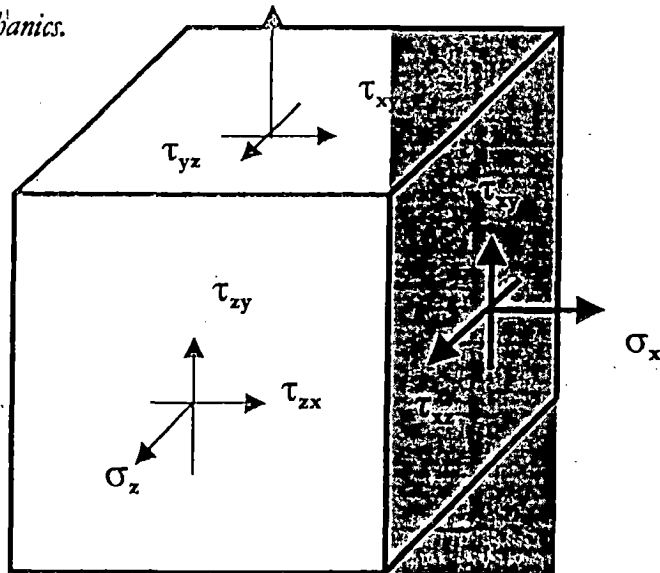


ELASTIC EQUATIONS IN UNDERGROUND OPENING

- Stress-strain relations
- Basic Differential Equations in Elastic Theory
- Plane Stress Equation
- Plane Strain Equation
- Stress – Displacement for circular opening in plane-strain condition

Elastic stress-strain relations

Continuum mechanics.



In three dimensional loaded body, there are six independent components of stresses at a point. For an isotropic homogeneous elastic material subject to normal stress σ_x in the x direction, the strains in the x, y, and z directions are :

$$\epsilon_x = \frac{\sigma_x}{E}, \epsilon_y = \epsilon_z = -\nu \frac{\sigma_x}{E} \quad (A. 1)$$

Where:

σ_x = applied stress in x-direction

ν = Poisson's ratio

E = modulus Elasticity

Since the principle of superposition applies, the stress/strain relationships in three dimensions are:

$$\epsilon_x = (\sigma_x - \nu(\sigma_y + \sigma_z))/E, \epsilon_y = (\sigma_y - \nu(\sigma_x + \sigma_z))/E, \epsilon_z = (\sigma_z - \nu(\sigma_x + \sigma_y))/E \quad (A. 2)$$

and the relationship between the components of shear stress and shear strain are

$$\gamma_{xy} = \frac{\tau_{xy}}{G}, \gamma_{yz} = \frac{\tau_{yz}}{G}, \gamma_{zx} = \frac{\tau_{zx}}{G} \quad (A. 3)$$

Where:

γ = Shear strain

τ = Shear stress

$$G = \text{modulus of rigidity} = \frac{E}{2(1+\nu)}$$

The *static* modulus of elasticity of rock, E , and the associated Poisson's ratio, ν , are measured from rock samples during uniaxial unconfined compression tests. (*E.T. Brown, 1979*). But establishing values for these 'laboratory test' elastic parameters that apply in the field takes judgment and should be made on a case-by-case basis. A

reduction or magnification in the value of E & ν from the laboratory values of an order of magnitude may be in order to take into account the sample disturbance or scale effect of rock mass. For most rocks, Poisson's ratio lies between 0.20 and 0.30 (Jaeger, 1979)

Basic Differential Equations in Elastic Theory

The problem in the theory of elasticity is to determine in every direction at every point within an elastic body the six stress components ($\sigma_x, \sigma_y, \sigma_z, \sigma_{xy}, \sigma_{yz}, \sigma_{zx}$), the six strain components ($\epsilon_x, \epsilon_y, \epsilon_z, \epsilon_{xy}, \epsilon_{yz}, \epsilon_{zx}$), and the three components of displacements ($u_x, u_y, u_z, u_{xy}, u_{yz}, u_{zx}$), given the elastic constants of the body, the size and shape of the body, and the boundary conditions. The necessary and sufficient conditions which the components of stress, strain, and displacement must satisfy in order to obtain a solution of an elasticity problem are the following:

1. the stress-strain relations (from eq. (A.1), (A.2), (A.3))

$$\{\sigma\} = [D]\{\epsilon\}$$

$$\begin{bmatrix} \sigma_x \\ \sigma_y \\ \sigma_z \\ \tau_{xy} \\ \tau_{yz} \\ \tau_{zx} \end{bmatrix} = \frac{E}{(1+\nu)(1-2\nu)} \begin{bmatrix} 1-\nu & \nu & \nu & 0 & 0 & 0 \\ \nu & 1-\nu & \nu & 0 & 0 & 0 \\ \nu & \nu & 1-\nu & 0 & 0 & 0 \\ 0 & 0 & 0 & \frac{(1-2\nu)}{2} & 0 & 0 \\ 0 & 0 & 0 & 0 & \frac{(1-2\nu)}{2} & 0 \\ 0 & 0 & 0 & 0 & 0 & \frac{(1-2\nu)}{2} \end{bmatrix} \begin{bmatrix} \epsilon_x \\ \epsilon_y \\ \epsilon_z \\ \gamma_{xy} \\ \gamma_{yz} \\ \gamma_{zx} \end{bmatrix}$$

(A. 4)

2. the strain-displacement relations

$$\begin{aligned} \epsilon_x &= \frac{\partial u}{\partial x} \quad \gamma_{xy} = \frac{\partial u}{\partial y} + \frac{\partial v}{\partial x} \\ \epsilon_y &= \frac{\partial v}{\partial y} \quad \gamma_{yz} = \frac{\partial v}{\partial z} + \frac{\partial w}{\partial y} \\ \epsilon_z &= \frac{\partial w}{\partial z} \quad \gamma_{zx} = \frac{\partial w}{\partial x} + \frac{\partial v}{\partial z} \end{aligned}$$

(A. 5)

3. the equilibrium conditions

$$\begin{aligned} \frac{\partial \sigma_x}{\partial x} + \frac{\partial \tau_{xy}}{\partial y} + \frac{\partial \tau_{xz}}{\partial z} + X_b &= 0 \\ \frac{\partial \tau_{xy}}{\partial x} + \frac{\partial \sigma_y}{\partial y} + \frac{\partial \tau_{yz}}{\partial z} + Y_b &= 0 \\ \frac{\partial \tau_{xz}}{\partial x} + \frac{\partial \tau_{yz}}{\partial y} + \frac{\partial \sigma_z}{\partial z} + Z_b &= 0 \end{aligned}$$

(A. 6)

4. the compatibility conditions

$$\begin{aligned} \frac{\partial^2 \varepsilon_x}{\partial y^2} + \frac{\partial^2 \varepsilon_y}{\partial x^2} - \frac{\partial^2 \gamma_{xy}}{\partial x \partial y}, 2 \left(\frac{\partial^2 \varepsilon_x}{\partial y \partial z} \right) &= \frac{\partial}{\partial x} \left(-\frac{\partial \gamma_{yz}}{\partial x} + \frac{\partial \gamma_{xz}}{\partial y} + \frac{\partial \gamma_{xy}}{\partial z} \right) \\ \frac{\partial^2 \varepsilon_y}{\partial z^2} + \frac{\partial^2 \varepsilon_z}{\partial y^2} - \frac{\partial^2 \gamma_{yz}}{\partial z \partial y}, 2 \left(\frac{\partial^2 \varepsilon_y}{\partial x \partial z} \right) &= \frac{\partial}{\partial x} \left(\frac{\partial \gamma_{yz}}{\partial x} - \frac{\partial \gamma_{xz}}{\partial y} + \frac{\partial \gamma_{xy}}{\partial z} \right) \\ \frac{\partial^2 \varepsilon_x}{\partial z^2} + \frac{\partial^2 \varepsilon_z}{\partial x^2} - \frac{\partial^2 \gamma_{xz}}{\partial x \partial z}, 2 \left(\frac{\partial^2 \varepsilon_z}{\partial y \partial x} \right) &= \frac{\partial}{\partial x} \left(\frac{\partial \gamma_{yz}}{\partial x} + \frac{\partial \gamma_{xz}}{\partial y} - \frac{\partial \gamma_{xy}}{\partial z} \right) \end{aligned} \quad (A. 7)$$

5. the prescribed boundary conditions at the exterior surfaces of the body

Some simplification can be obtained by combining the different sets of equations. For example, eq. (A.4) & (A.6) can be combined to eliminate the six strain components.

Plane Stress Equations

Plane Stress conditions are obtained when $\sigma_z, \tau_{xz}, \tau_{yz}$ and all variations of stress with respect to z are zero, Thus for plane stress the stress strain relations as given by eq. (A.1), (A.3) reduce to the following :

$$\varepsilon_x = \frac{1}{E}(\sigma_x - \nu\sigma_y), \varepsilon_y = \frac{1}{E}(\sigma_y - \nu\sigma_x), \varepsilon_z = -\frac{\nu}{E}(\sigma_x + \sigma_y), \gamma_{xy} = \frac{\tau_{xy}}{G} \quad (A. 8)$$

also the strain-displacement in eq. (A.5), equilibrium conditions in eq. (A.6), and compatibility conditions in eq. (A.7) are, respectively

$$\varepsilon_x = \frac{\partial u}{\partial x}, \varepsilon_y = \frac{\partial v}{\partial y}, \gamma_{xy} = \frac{\partial u}{\partial y} + \frac{\partial v}{\partial x} \quad (A. 9)$$

$$\frac{\partial \sigma_x}{\partial x} + \frac{\partial \tau_{xy}}{\partial y} + \frac{\partial \tau_{xz}}{\partial z} + X_b = 0, \frac{\partial \tau_{xy}}{\partial x} + \frac{\partial \sigma_y}{\partial y} + \frac{\partial \tau_{yz}}{\partial z} + Y_b = 0 \quad (A. 10)$$

$$\frac{\partial^2 \varepsilon_x}{\partial y^2} + \frac{\partial^2 \varepsilon_y}{\partial x^2} - \frac{\partial^2 \gamma_{xy}}{\partial x \partial y} \quad (A. 11)$$

Substitution eq. (A.8) into eq.(A.11) gives

$$\frac{\partial^2}{\partial y^2}(\sigma_x - \nu\sigma_y) + \frac{\partial^2}{\partial x^2}(\sigma_y - \nu\sigma_x) = 2(1+\nu) \frac{\partial^2 \tau_{xy}}{\partial x \partial y} \quad (A. 12)$$

Differentiation of the first equilibrium equation with respect to x , and the second one with respect to y , and addition of these results gives

$$2 \frac{\partial^2 \tau_{xy}}{\partial x \partial y} = \frac{\partial^2 \sigma_x}{\partial x^2} - \frac{\partial^2 \sigma_y}{\partial y^2} - \frac{\partial X}{\partial x} - \frac{\partial Y}{\partial y} \quad (A. 13)$$

substitution of this equation into the preceding one gives

$$\left(\frac{\partial^2}{\partial x^2} + \frac{\partial^2}{\partial y^2} \right) (\sigma_x + \sigma_y) = -(1+\nu) \left(\frac{\partial X}{\partial x} - \frac{\partial Y}{\partial y} \right) \quad (A. 14)$$

If body forces are constant or zero, Eq (A.14) becomes

$$\left(\frac{\partial^2}{\partial x^2} + \frac{\partial^2}{\partial y^2} \right) (\sigma_x + \sigma_y) = 0 \quad (\text{A. 15})$$

There are three unknown stress components. The equations necessary to obtain a solution are the two equilibrium equations (A.10) and the compatibility equation (either A.14) or (A.15), together with the boundary conditions.

Plane Strain Equations

Simplification of elasticity problems also occurs when a state of plane strain or plane deformation exists. If the displacements of all points off a deformed body are in planes normal to the length of a body, a state of plane exists. It does not complicate the problem if a uniform extension in the direction of the axis of the body is superimposed upon the plane deformation. A good example of plane strain is a long horizontal tunnel at depth in a rock mass.

For plane strain to exist, γ_{xz} and γ must be zero throughout the body and the variation of ϵ_z with respect to z must be zero. Thus ϵ_z is zero or a constant. If ϵ_z is set equal to zero in the last equation (A.1), the result is

$$\sigma_x = \nu(\sigma_x + \sigma_y) \quad (\text{A. 16})$$

Thus the stress-strain relations for PLANE STRAIN with $\epsilon_z = 0$ become

$$\begin{aligned} \epsilon_x &= \frac{1}{E} [(1-\nu^2)\sigma_x - \nu(1+\nu)\sigma_y] \\ \epsilon_y &= \frac{1}{E} [(1-\nu^2)\sigma_y - \nu(1+\nu)\sigma_x] \\ \gamma_{xy} &= \frac{\tau_{xy}}{G} = \frac{2(1+\nu)}{E} \tau_{xy} \end{aligned} \quad (\text{A. 17})$$

The equilibrium conditions, the strain-displacement equations, and the compatibility conditions are the same for plane strain as for plane stress. Substitution of Eqs. (A.17) into Eq. (A. 11) gives

$$(1-\nu) \left[\frac{\partial^2 \sigma_x}{\partial y^2} + \frac{\partial^2 \sigma_y}{\partial x^2} \right] - \nu \left[\frac{\partial^2 \sigma_y}{\partial y^2} + \frac{\partial^2 \sigma_x}{\partial x^2} \right] = 2 \frac{\partial^2 \tau_{xy}}{\partial x \partial y}$$

Differentiating the equilibrium equations as before, adding the results, and substituting into the above equation gives

$$\left(\frac{\partial^2}{\partial x^2} + \frac{\partial^2}{\partial y^2} \right) (\sigma_x + \sigma_y) = -\frac{1}{1-\nu} \left(\frac{\partial X}{\partial x} + \frac{\partial Y}{\partial y} \right) \quad (\text{A. 18})$$

If the body forces are constant or zero, then Eq. (A. 18) becomes

$$\left(\frac{\partial^2}{\partial x^2} + \frac{\partial^2}{\partial y^2} \right) (\sigma_x + \sigma_y) = 0 \quad (\text{A. 19})$$

Thus, in the case of constant body forces, the compatibility equations in term of stress is the same for both plane strain and plane stress. Also it should be noted that neither the compatibility equation nor the equilibrium equations contain the elastic constants of the body. Hence the stress distribution is the same for all isotropic materials provided the state of stress or strain is two-dimensional. The equilibrium conditions and the compatibility condition together with the boundary condition provide the necessary equations for obtaining solutions to plane strain problems.

Stress-Displacement for circular opening in plane strain condition

The problem of a hole in an infinite plate is of special interest in the rock mechanics field because it corresponds to the problem of a long horizontal tunnel at depth in a uniform rock formation.

Consider an infinite plate of thickness t with a circular hole of radius a located at the origin as illustrated in Figure below. Let the applied stress in the x direction be S_x and in the y direction be S_y . At a large distance from the hole, the polar components of stress will be those resulting from applied stress only. Using Airy's stress function, the stress components in an infinite plate containing a circular hole when the applied-stress field at infinity is $\sigma_x = S_x$ and $\sigma_y = S_y$ are:

$$\begin{aligned}\sigma_r &= \left(\frac{S_h + S_v}{2}\right)\left(1 - \frac{a^2}{r^2}\right) + \left(\frac{S_h - S_v}{2}\right)\left(1 - 4\frac{a^2}{r^2} + 3\frac{a^4}{r^4}\right)\cos(2\theta) \\ \sigma_\theta &= \left(\frac{S_h + S_v}{2}\right)\left(1 + \frac{a^2}{r^2}\right) - \left(\frac{S_h - S_v}{2}\right)\left(1 + 3\frac{a^4}{r^4}\right)\cos(2\theta) \\ \tau_{r\theta} &= \left(\frac{S_v - S_h}{2}\right)\left(1 + 2\frac{a^2}{r^2} - 3\frac{a^4}{r^4}\right)\sin(2\theta)\end{aligned}\quad (A. 20)$$

The displacement that occur when a circular hole is subjected to a two-dimensional stress field under the condition of plane strain can be determined by integrating the stress-displacement equations for plane strain. The stress-displacement relations in polar coordinates are from Eq. (A. 17) and the equations:

$$\varepsilon_r = \frac{\partial u}{\partial r}, \quad \varepsilon_\theta = \frac{u}{r} + \frac{1}{r} \frac{\partial v}{\partial \theta}, \quad \gamma_{r\theta} = \frac{1}{r} \frac{\partial u}{\partial \theta} + \frac{\partial v}{\partial r} - \frac{v}{r} \quad (A. 21)$$

combining them gives

$$\begin{aligned}\frac{\partial u}{\partial r} &= \frac{1}{E} \left[(1 - \nu^2) \sigma_r - \nu(1 + \nu) \sigma_\theta \right], \quad \frac{u}{r} + \frac{1}{r} \frac{\partial v}{\partial \theta} = \frac{1}{E} \left[(1 - \nu^2) \sigma_\theta - \nu(1 + \nu) \sigma_r \right] \\ \frac{1}{r} \frac{\partial u}{\partial r} + \frac{\partial v}{\partial \theta} - \frac{v}{r} &= \frac{2(1 - \nu)}{E} \tau_{r\theta}\end{aligned}\quad (A. 22)$$

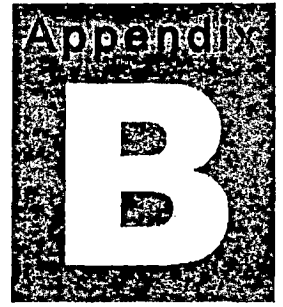
combining them with eqs. (A. 20) and integrating them give

$$\begin{aligned}u &= \frac{1 - \nu^2}{E} \left[\left(\frac{S_x + S_y}{2}\right) \left(r + \frac{a^2}{r}\right) + \left(\frac{S_x - S_y}{2}\right) \left(r - \frac{a^4}{r^3} + \frac{4a^2}{r}\right) \cos 2\theta \right] - \frac{\nu(1 + \nu)}{E} \\ &\quad \left[-\left(\frac{S_x + S_y}{2}\right) \left(r - \frac{a^2}{r}\right) - \left(\frac{S_x - S_y}{2}\right) \left(r - \frac{a^4}{r^3}\right) \cos 2\theta \right] \\ v &= \frac{1 - \nu^2}{E} \left[-\left(\frac{S_x - S_y}{2}\right) \left(r + \frac{2a^2}{r} + \frac{a^4}{r^3}\right) \sin 2\theta \right] - \frac{\nu(1 + \nu)}{E} \left[\left(\frac{S_x - S_y}{2}\right) \left(r - \frac{a^4}{r^3} + \frac{4a^2}{r}\right) \sin 2\theta \right]\end{aligned}\quad (A. 23)$$

When $r=a$,

$$\begin{aligned}u &= \frac{1 - \nu^2}{E} \left[a(S_x + S_y) + 2a(S_x - S_y) \cos 2\theta \right] \\ v &= -\frac{1 - \nu^2}{E} \left[2a(S_x - S_y) \sin 2\theta \right]\end{aligned}\quad (A. 25)$$

Equation (A. 25) differ from equation for plane stress only in the factor $1 - \nu^2$. Thus the displacements at the boundary of the circular hole, for the condition of plane strain, are approximately 94 % of the displacement for the condition of plane stress when poisson's ratio is 0.25.



DERIVATION OF STRUCTURAL MATRICES IN FINITE ELEMENT ANALYSIS

The principle of virtual work states that a virtual (very small) change of the internal strain energy must be offset by an identical change in external work due to the applied loads, or:

$$\delta U = \delta V \quad (B. 1)$$

where: U = strain energy (internal work) = U1+U2
V = external work = V1+V2+V3
δ = virtual operator

The virtual strain energy is:

$$\delta U_1 = \int_{vol} \{\delta \epsilon\}^T \{\sigma\} d(vol) \quad (B. 2)$$

Where: {ε} = strain vector
{σ} = stress vector
Vol = volume of element

U₁) Assuming linear materials and geometry, equation (A.4) and (B.2) are combined to give:

$$\delta U_1 = \int_{vol} \{\delta \epsilon\}^T [D] \{\epsilon\} d(vol) \quad (B. 3)$$

The strains may be related to the nodal displacements by:

$$\{\epsilon\} = [B] \{u\} \quad (B. 4)$$

it will be assumed that all effects are in the global cartesian system. Combining equation (B.3) and (B.4), and noting that {u} does not vary over the volume

$$\delta U_1 = \{U_1\}^T \int_{vol} [B]^T [D] [B] d(vol) \{u\} \quad (B. 5)$$

U₂) another form of virtual strain energy is when a surface moves against distributed resistance, as in a foundation stiffness. This may be written as:

$$\delta U_2 = \int_{area} \{\delta w_n\}^T \{\sigma\} d(area) \quad (B. 6)$$

Where: {w_n} = motion normal to the surface
{σ} = stress carried by the surface
area = area of the distributed resistance

Both {w_n} and {σ} will usually have only non-zero component. The point-wise normal displacement is related to the nodal displacement by

$$\{w_n\} = [N_n] \{u\} \quad (B. 7)$$

Where: [N_n] = matrix of shape functions for normal motions at the surface

The stress, {σ} is

$$\{\sigma\} = k [w_n] \quad (B. 8)$$

Where: k = the foundation stiffness in units of force per length per unit area

Combining equation (B.6) through (B.8), and assuming that k is constant over the area,

$$\delta U_2 = \{\delta u\}^T k \int_{area} [N_n]^T [N_n] d(area) \{u\} \quad (B. 9)$$

V₁) Next, the external virtual work will be considered. The initial effects will be studied first:

$$\delta V_1 = - \int_{vol} \{\delta w\}^T \frac{\{F^a\}}{vol} d(vol) \quad (B. 10)$$

Where: {w} = vector of displacements of a general point
{F^a} = acceleration force vector

according to Newton's second law;

$$\frac{F^a}{vol} = Q \frac{\partial^2}{\partial t^2} \{w\} \quad (B. 11)$$

Where: Q = density
 T = time

The displacement within the element are related to the nodal displacements by:

$$\{w\} = [N]\{u\} \quad (B. 12)$$

Where: $[N]$ = matrix of shape functions. Combining equations (B.10), (B.11), and (B.12) and assuming that Q constant over the volume,

$$\delta V_1 = -\{\delta u\}' \int_{vol} [N]^T [N] d(vol) \frac{\partial^2}{\partial t^2} \{u\} \quad (B. 13)$$

V₂) The pressure force vector formulation starts with:

$$\delta V_2 = \int_{area_p} \{\delta w_n\}'^T \{P\} d(area_p) \quad (B. 14)$$

Where: $\{P\}$ = applied pressure vector (normally contains only one non-zero component)

$area_p$ = area over which pressure acts

Combining equations (B.12) and (B.14),

$$\delta V_2 = -\{\delta u\}' \int_{area_p} [N_n]^T \{P\} d(area_p) \quad (B. 15)$$

unless otherwise noted, pressures are applied to the outside surface of each element and are normal to curved surfaces, if applicable.

V₃) Nodal forces applied to the element can be accounted for by:

$$\delta V_3 = \{\delta u\}' \{F_e^{nd}\} \quad (B. 16)$$

Where: $\{F_e^{nd}\}$ = nodal forces applied to the element

Finally equation (B.1), (B.5), (B.9), (B.13), (B.15), (B.16) may be combined to give:

$$\begin{aligned} & \{\delta U\}' \int_{vol} [B]^T [D][B] d(vol) \{u\} + \{\delta u\}' k \int_{area} [N_n]^T [N_n] d(area) \{u\} \\ & = -\{\delta u\}' \rho \int_{vol} [N]^T [N] d(vol) \frac{\partial^2}{\partial t^2} \{u\} + \{\delta u\}' \int_{area_p} [N_n]^T \{P\} d(area_p) + \{\delta u\}' \{F_e^{nd}\} \end{aligned} \quad (B. 17)$$

Note that the $\{\delta u\}'$ vector is a set of arbitrary virtual displacements common in all of above terms, the condition required to satisfy equation (B.17) reduce to:

$$([K_e] + [K_e^f])\{u\} = [M_e]\{u\} + \{F_e^{pe}\} + \{F_e^{nd}\} \quad (B. 18)$$

Where: $[K_e] = \int_{vol} [B]^T [D][B] d(vol)$ = element stiffness matrix

$[K_e^f] = k \int_{area} [N_n]^T [N_n] d(area)$ = element foundation stiffness matrix

$[M_e] = \rho \int_{vol} [N]^T [N] d(vol)$ = element mass matrix

$\{u\} = \frac{\partial^2}{\partial t^2} \{u\}$ = acceleration vector (such as gravity effects)

$\{F_e^{pr}\} = \int_{area} [N_n]^T \{P\} d(area)$ = element pressure vector

Equation (B.18) represents the equilibrium equation on a one element basis.



STEPWISE PROCEDURES

Example inputing data for model E01H

Model E01H

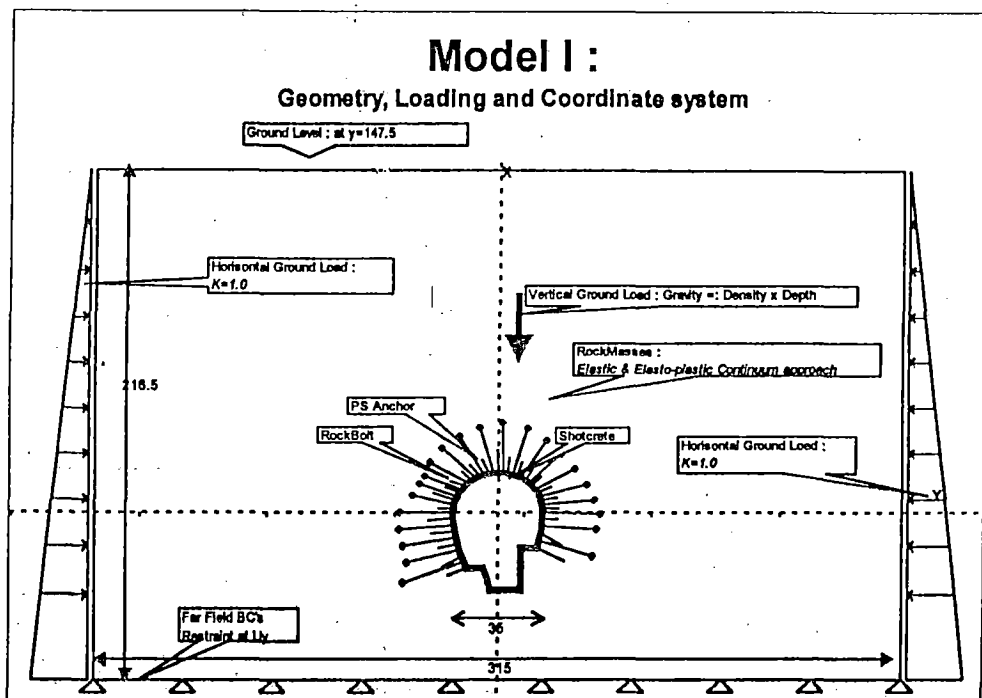
Stepwise Procedures for inputing data in Ansys (ver 5.4).

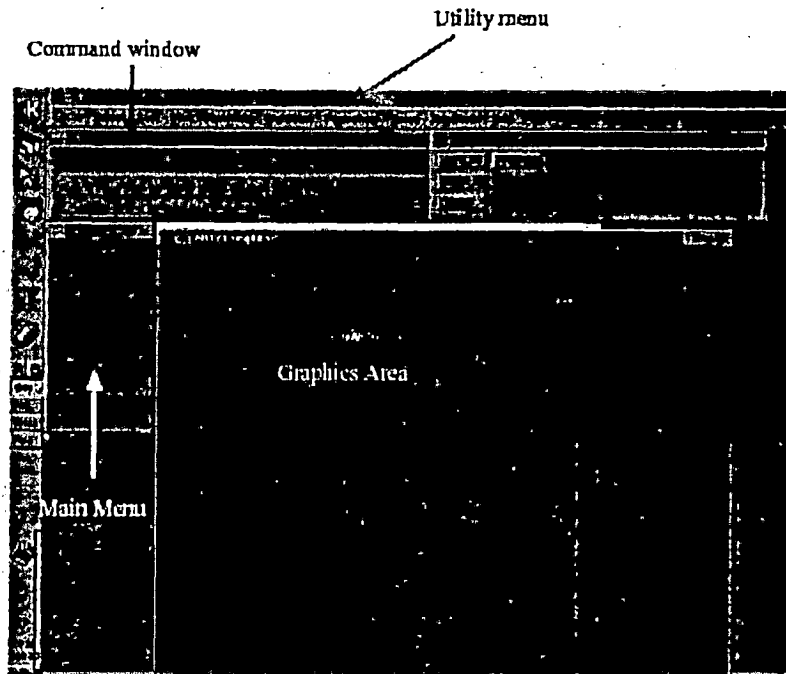
Problem Specification

1. Start-up and preliminary set-up
2. Specify element type and constants
3. Specify material properties
4. Specify geometry
5. Mesh geometry
6. Specify boundary conditions
7. Solve
8. Postprocess the results
9. Validate the results

Problem Specification

The finite element model considered here is the opening of rock cavern in Hydropower complex Cirata (Indonesia). The loading condition is rock medium gravity and horizontal/lateral ground stress at far-field boundary with $k=1.0$, support (shotcrete, rockbolts, PS anchor) not considered, since this example only have aim to introduce the stepwise procedures for solving the problem of underground opening in rock by finite element. The modeling is in 2-D plane strain condition, in elastic medium,





Step 1: Start-up and preliminary set-up

CREATE A FOLDER

Create a folder called *ERata* at a convenient location. This folder will be used to store files created during the session.

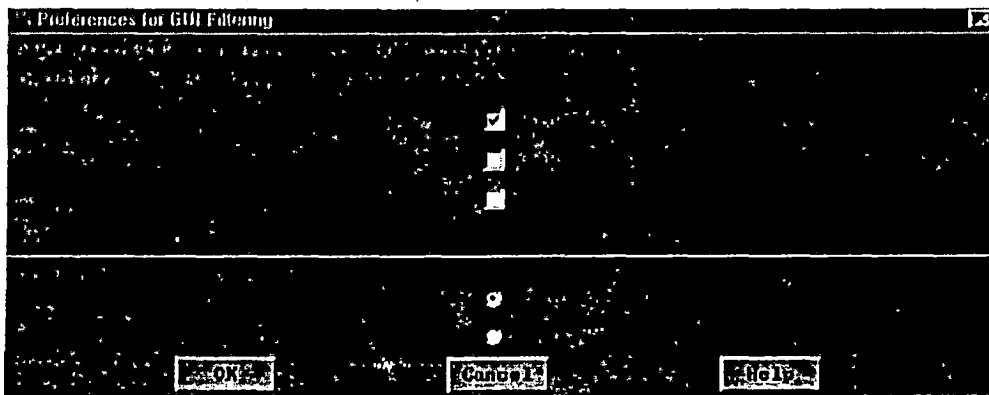
START ANSYS

Start > Programs > ANSYS Release 5.4 > ANSYS Interactive

Enter the location of the folder *ERata* as **Working directory** by browsing to it. Enter *E01H* as **Initial jobname**. So all files generated during this ANSYS session will have *E01H* as the prefix. Click on **Run**.

SET PREFERENCES

Main Menu > Preferences



In the *Preferences for GUI Filtering* dialog box, click on the box next to **Structural** so that a tick mark appears in the box.

Recall that this is an optional step that customizes the graphical user interface so that only the menu options valid for structural problems are made available.

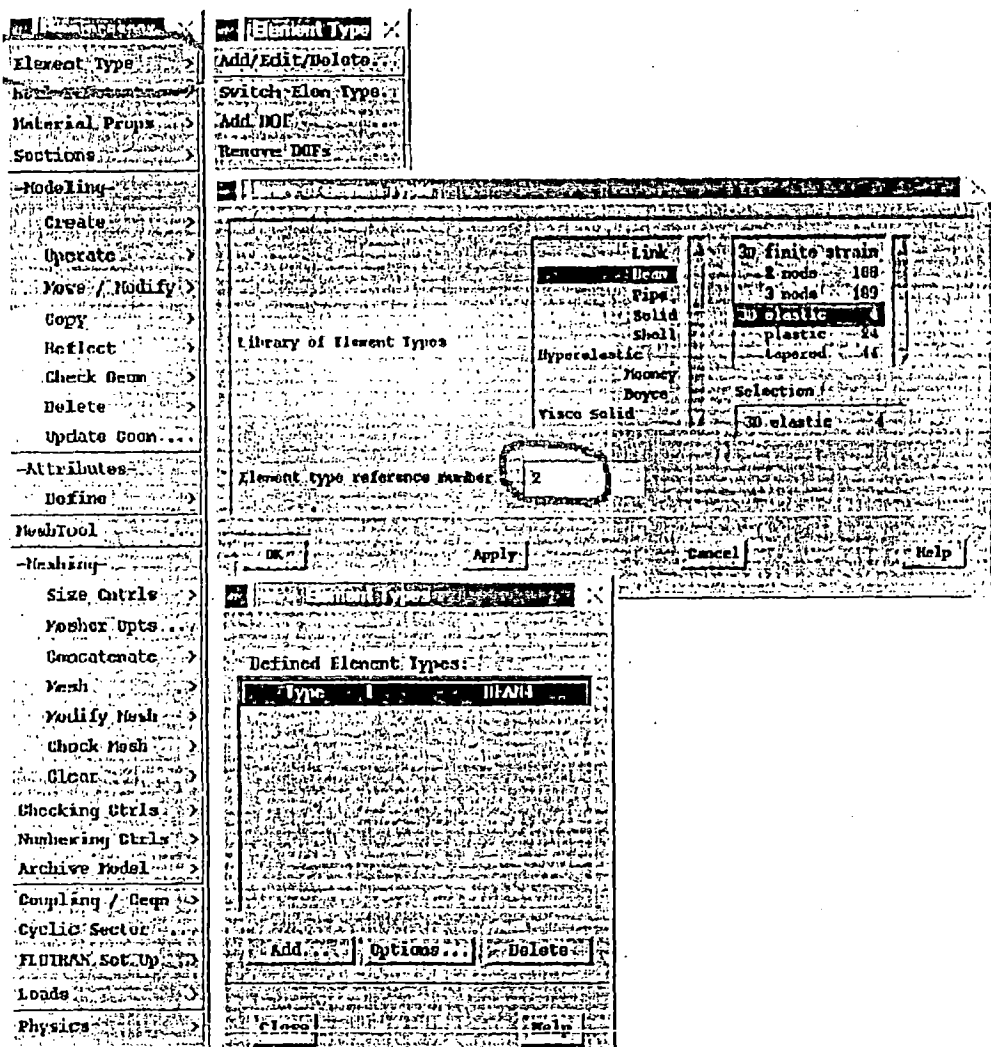
Step 2: Specify element type and constants

SPECIFY ELEMENT TYPE

In the Main Menu, click on *Preprocessor* to enter the preprocessor module in ANSYS. This is the module where we create the geometry, specify appropriate displacement constraints and loading, and mesh the geometry.

Main Menu > Preprocessor > Element Type > Add/Edit/Delete > Add...

Pick *Structural Solid* in the left field and *PLANE2* in the right field. Click *OK*. Repeat again for *BEAM3*.



Close the *Element Types* dialog box and also the *Element Type* menu.

SPECIFY ELEMENT CONSTANTS

Main Menu > Preprocessor > Real Constants > Add/Edit/Delete > Add...

This brings up the *Element Type for Real Constants* menu with a list of the element types defined in the previous step. We have two element types and we should select one by one, put appropriated real constant. For BEAM3, it will look like figure below. Click **OK**.

| | | |
|----------------------------|--------|--------|
| Element Type Reference No. | 2 | |
| Real Constant Set No. | 1 | |
| Cross-sectional area | AREA | 0.25 |
| Area moment of inertia | IZZ | 0.0013 |
| Total beam height | HEIGHT | 0.25 |
| Shear deflection constant | SHEARZ | 0 |
| Initial strain | ISTRN | 0 |
| Added mass/unit length | ADDMAS | 0 |

Close the *Real Constants* menu.

SAVE YOUR WORK

Toolbar > SAVE_DB

Step 3: Specify material properties

Main Menu > Preprocessor > Material Props > Constants Isotropic

| | | |
|----------------------------------|------|----------|
| Isotropic Material Properties | | |
| Properties for Material Number 1 | | |
| Young's modulus | EX | 21000000 |
| Density | DENS | 2.4 |
| Thermal expansion coeff | ALPH | |
| Reference temperature | REPT | |
| Poisson's ratio (minor) | NUXY | |
| Poisson's ratio (major) | PRXY | 0.17 |
| Shear modulus | GXY | |
| Friction coefficient | MU | |
| Damping multiplier | DAMP | |

Click **OK**. Repeat for PLANE2

| Isotropic Material Properties | | |
|----------------------------------|------|---------|
| Properties for Material Number 2 | | |
| Young's modulus | EX | 1400000 |
| Density | DENS | 2.6 |
| Thermal expansion coeff | ALPX | |
| Reference temperature | REFT | |
| Poisson's ratio (minor) | NUXY | |
| Poisson's ratio (major) | PRXY | 0.3 |
| Shear modulus | GHV | |
| Friction coefficient | FU | |
| Damping multiplier | DAMP | |
| OK | | Apply |
| Cancel | | Help |

Click OK. Close menu.

SAVE YOUR WORK : TOOLBAR > SAVE_DB

Step 4: Specify geometry

We'll first create keypoints corresponding to the points of the corner of far-field domain and points of joint of lines which connected to form cavern model and then generate lines from the keypoints, and area from lines. The keypoints will be created in the cartesian coordinate system.

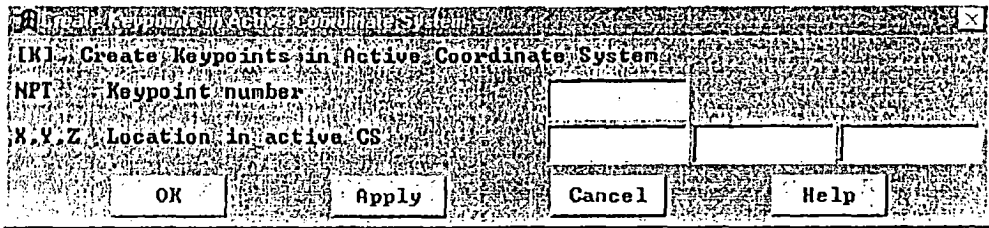
CREATE KEYPOINTS

Main Menu > Preprocessor > Modeling > Create > Keypoints > In Active CS

Enter the keypoint locations (think about where each one lies as you enter its coordinates):

LIST ALL SELECTED KEYPOINTS: DSYS= 0

| NO. | X | Y |
|-----|-----------|-----------|
| 1 | .0000000 | 17.50000 |
| 2 | -17.50000 | .0000000 |
| 3 | 17.50000 | .0000000 |
| 4 | -12.14488 | -23.10000 |
| 5 | 15.31100 | -15.00000 |
| 6 | 9.000000 | -15.00000 |
| 7 | 9.000000 | -32.10000 |
| 8 | -3.000000 | -32.10000 |
| 9 | -6.000000 | -23.10000 |
| 10 | 157.5000 | 147.5000 |
| 11 | -157.5000 | -69.00000 |
| 12 | 157.5000 | -69.00000 |
| 13 | -157.5000 | 147.5000 |



Save your work: Toolbar > SAVE_DB

CREATE LINES & AREA

We'll next generate lines from the 13 keypoints.

Main Menu > Preprocessor > Modeling > Create > Lines > Straight line

Main Menu > Preprocessor > Modeling > Create > Arcs > By Ends KP's & Rad

Create Far field Boundary
Connect KP 13-10,12-10,12-11,11-13
(by clicking the KP)

Create Opening
Connect KP 4-9,9-8,8-7,7-6,6-5

Create Arch
Pick KP 2&1, radius 17.5
Pick KP 1&3, radius 17.5
Pick KP 2&4, radius 52.5
Pick KP 5&3, radius 52.5

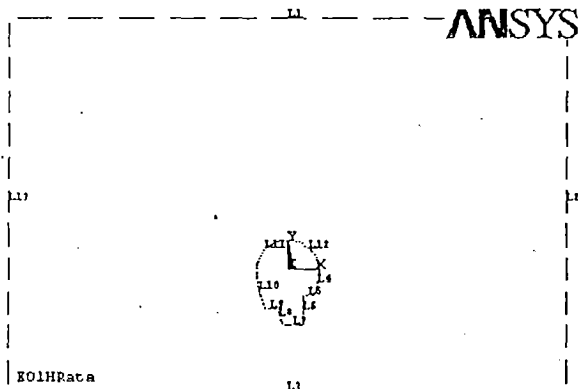
LIST ALL SELECTED LINES.

| NO. | KEYPOINTS | LENGTH | NDIV |
|-----|-----------|--------|------|
| 1 | 13 10 | 315.00 | 11 |
| 2 | 12 10 | 216.50 | 11 |
| 3 | 12 11 | 315.00 | 11 |
| 4 | 5 3 | 15.212 | 5 |
| 5 | 6 5 | 6.3110 | 2 |
| 6 | 7 6 | 17.100 | 4 |
| 7 | 8 7 | 12.000 | 2 |
| 8 | 9 8 | 9.4868 | 2 |
| 9 | 4 9 | 6.1449 | 2 |
| 10 | 2 4 | 23.919 | 9 |
| 11 | 2 1 | 27.489 | 15 |
| 12 | 1 3 | 27.489 | 15 |
| 13 | 11 13 | 216.50 | 11 |

PLOT LINES

Let's take a look at the lines that ANSYS generated in the Area creation process:

Utility Menu > Plot > Lines



CREATES AREAS

Save Your Work : Toolbar > SAVE_DB

Step 5: Mesh geometry

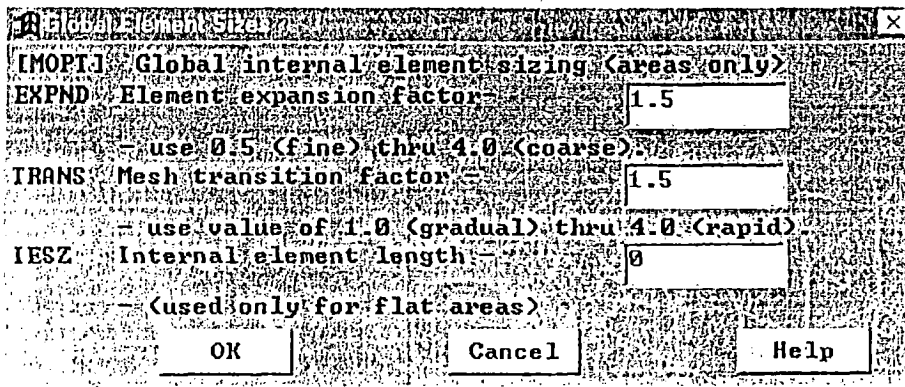
For Rock mass as area 1, the element type and material property set to be used in meshing should be selected by

Main Menu > Preprocessor > Attributes > Define

SET MESHING PARAMETERS

Main Menu > Preprocessor > Meshing > Size control

SET MESH SIZE



So as the lines using Picked lines and NDIV as in page 6 for each line.

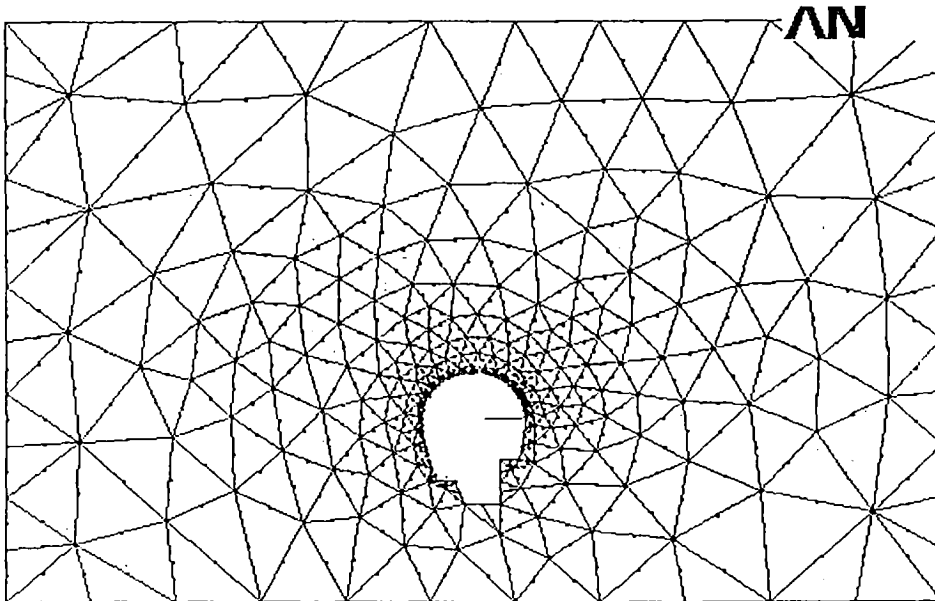
Main Menu > Preprocessor > Meshing > Size control > ManualSize > PickedLines

Example : Pick lines L1 and click *OK* in the pick menu. Enter 11 for *No. of element divisions* and click *Apply*. (The *Spacing Ratio* field can be left blank since the default value is one.) and so on.

SET MESH SIZE

Main Menu > Preprocessor > Meshing > Mesh > Area > free

The meshing will come like figure below :



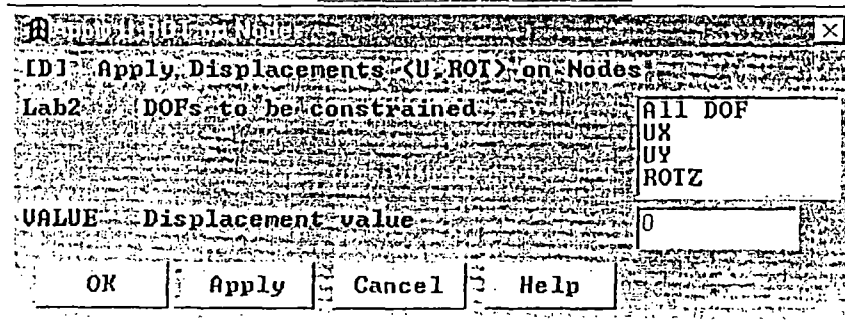
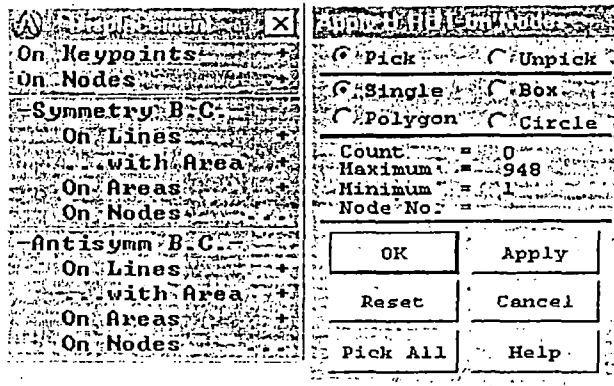
Save your work: Toolbar > SAVE_DB

Step 6: Apply Load

Apply Boundary condition : Displacement $U_Y = 0$ on bottom side

Main Menu > Preprocessor > Load > Apply > Structural Displacement > On

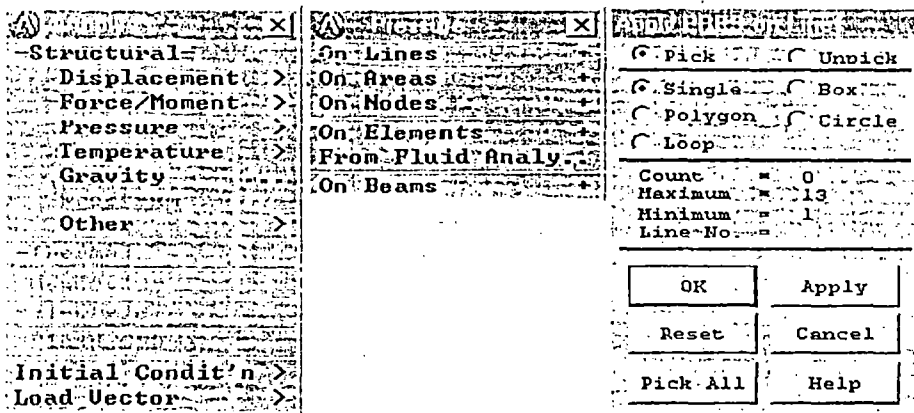
Nodes

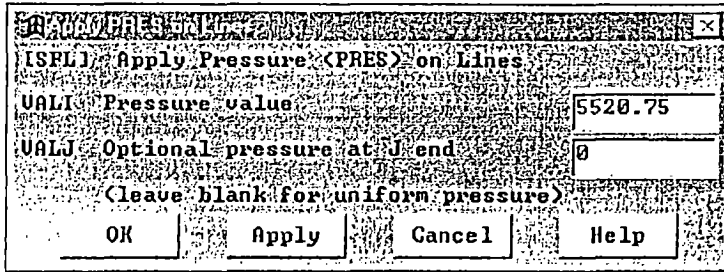


Select nodes at line in the bottom farfield boundary and click **OK** in the pick menu. Select **UY** for *DOFs to be constrained*. You can leave the *Displacement value* blank since the default is zero. Click **OK**. You'll see an arrow symbol in the *Graphics* window indicating that node is constrained in the radial direction.

Apply Horizontal ground pressure

Main Menu > Preprocessor > Loads > Apply > Structural > Pressure > On Lines

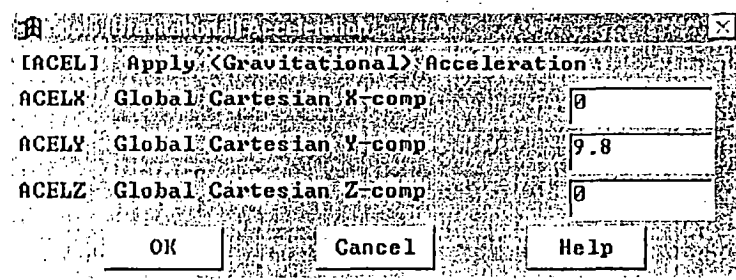




That value 5520.75 is for magnitude of horizontal pressure on bottom end of far-field boundary (left & right side).

Apply Gravity Load

Main Menu > Preprocessor > Loads > Apply > Structural > Gravity

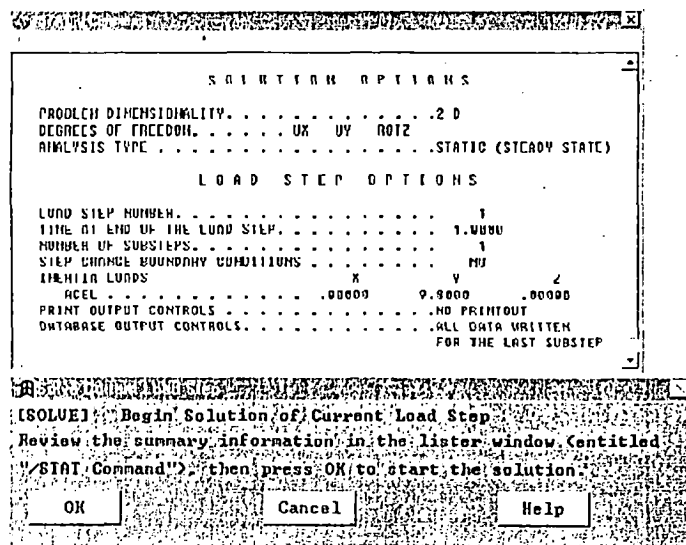


Step 7: Solve!

Main Menu > Solution

Enter check in the *Input* window. If the problem has been set up correctly, there will be no errors or warnings reported. If you look in the *Output* window, you should see the message: The analysis data was checked and no warnings or errors were found.

Main Menu > Solution > Solve > Current IS



Review the information in the /STATUS Command window. Close this window. Click **OK** in *Solve Current Load Step* menu. ANSYS performs the solution and a yellow window should pop up saying "Solution is done!". Close the yellow window. Verify that ANSYS has created a file called *Erata.rst* in your working directory. This file contains the results of the (previous) *solve*

Step 8: Postprocess the results

Enter the postprocessing module to analyze the solution.

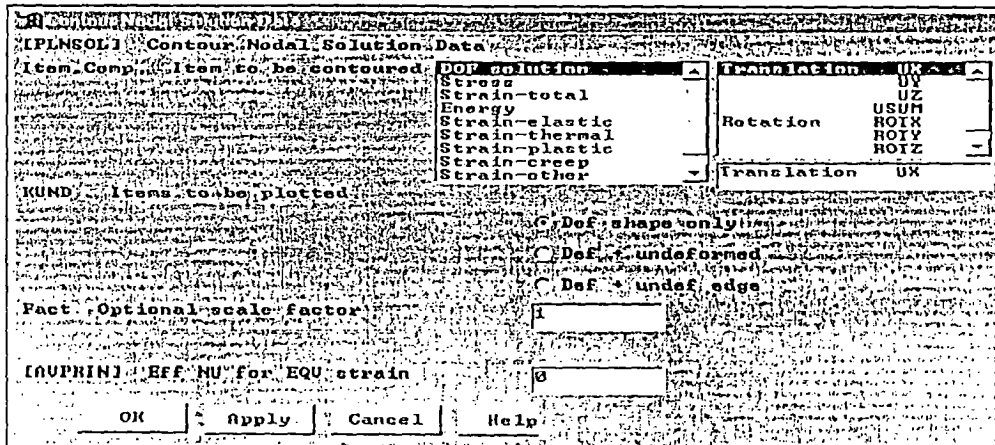
Main Menu > General Postproc

PLOT RESULTS

To display the results as *continuous* contours, select

Main Menu > General Postproc > Plot results > Contour Plot > Nodal Solu

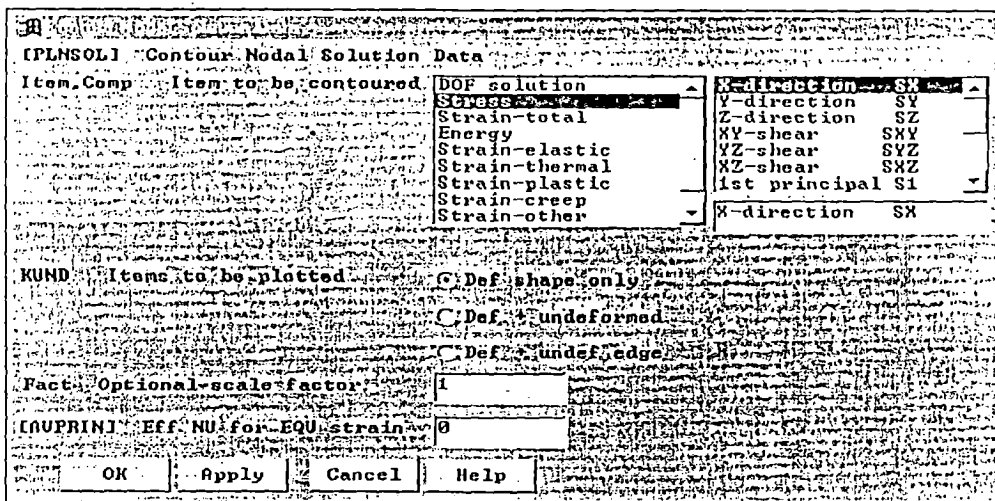
PLOT DISPLACEMENTS



Select *DOF* from the left list, *UX & UY* from the right list and click **OK**.

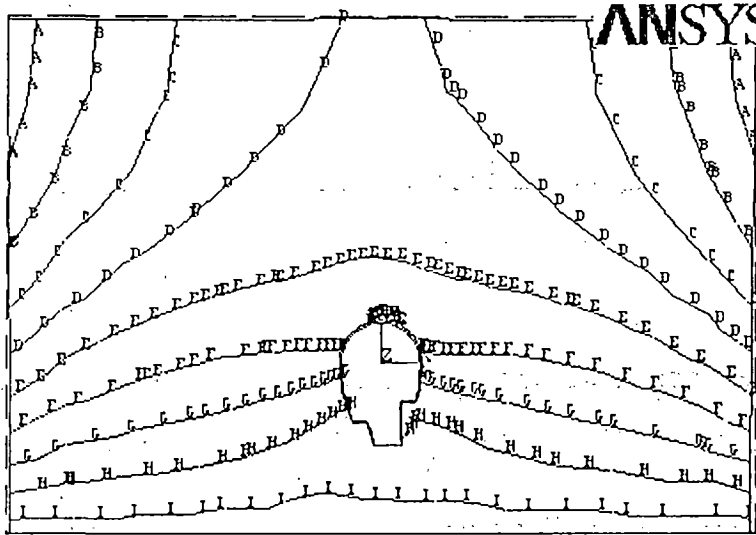
PLOT STRESS

Select *Stress* from the left list, *SX & S* from the right list and click **OK**.



Or you can choose other plot results, the plot result will be seen like figures below :

UY

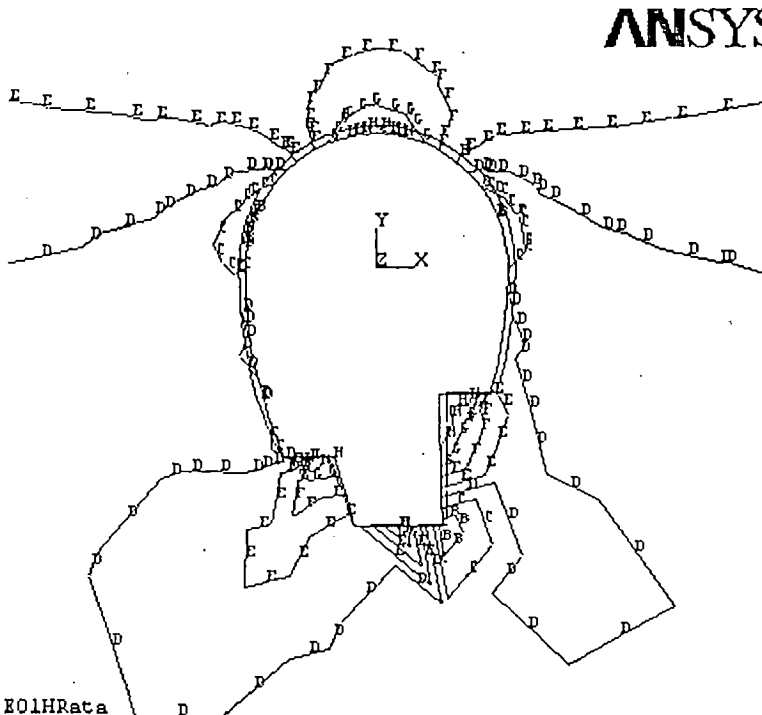


```

MAY 21 2004
22:34:07
NODAL SOLUTION
STEP=1
SUB =1
TIME=1
UY      (AVG)
RSYS=0
PowerGraphics
EFACET=1
AVRES=Mat
DMX =.105117
SMN =-.099461
A  =-.093936
B  =-.082884
C  =-.071833
D  =-.060782
E  =-.049731
F  =-.038679
G  =-.027628
H  =-.016577
I  =-.005526
    
```

EO1HRata

SY



```

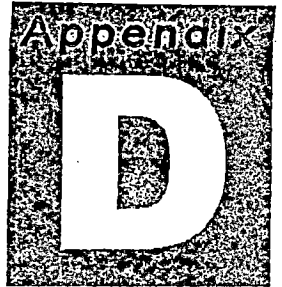
MAY 21 2004
22:37:01
NODAL SOLUTION
STEP=1
SUB =1
TIME=1
SY      (AVG)
RSYS=0
PowerGraphics
EFACET=1
AVRES=Mat
DMX =.105117
SMN =-7202
SMX =1044
A  =-6744
B  =-5827
C  =-4911
D  =-3995
E  =-3079
F  =-2162
G  =-1246
H  =-329.896
I  =586.347
    
```

EO1HRata

Save your work: Toolbar > SAVE_DB

Finish

File > Exit > Save Everything



EXPLANATION OF ELEMENTS

for modeling rock masses and shotcrete

C.1 General Element Features

The ANSYS program has a large library of element types. The ANSYS element library consists of more than 100 different element formulations or types. An element type is identified by a name (8 characters maximum), such as BEAM3, consisting of a group label (BEAM) and a unique identifying number (3). Not all element options are available in all ANSYS products. These restrictions are detailed in Section 4.11.4, "Product Restrictions," for each element.

Element Input

Many features are common to all ANSYS elements in the element library. These features are discussed in following paragraph:

C.1.1 Element Name

The ANSYS element library consists of more than 100 different element formulations or types. (Not all element types or features are available in all ANSYS products) An element type is identified by a name (8 characters maximum), such as BEAM3, consisting of a group label (BEAM) and a unique, identifying number (3).

C.1.2 Nodes

The nodes associated with the element are listed as I, J, K, etc. Elements are connected to the nodes in the sequence and orientation shown on the input figure for each element type. This connectivity can be defined by automatic meshing, or may be input directly by the user. The node numbers must correspond to the order indicated in the "Nodes" list. The I node is the first node of the element. The node order determines the element coordinate system orientation for some element types.

C.1.3 Degrees of Freedom

Each element type has a degree of freedom set, which constitute the primary nodal unknowns to be determined by the analysis. They may be displacements, rotations, temperatures, pressures, voltages, etc. Derived results, such as stresses, heat flows, etc., are computed from these degree of freedom results. Degrees of freedom are not defined on the nodes explicitly by the user, but rather are implied by the element types attached to them. The choice of element types is therefore, an important one in any ANSYS analysis.

C.1.4 Real Constants

Data which are required for the calculation of the element matrix, but which cannot be determined from the node locations or material properties, are input as "real constants." Typical real constants include area, thickness, inner diameter, outer diameter, etc. A basic description of the real constants is given with each element type.

C.1.5 Material Properties

Various material properties are used for each element type. Typical material properties include Young's modulus (of elasticity), density, coefficient of thermal expansion, thermal conductivity, etc. Each property is referenced by an ANSYS label - EX, EY, and

EZ for the directional components of Young's modulus, DENS for density, and so on. All material properties can be Input as functions of temperature.

Some properties for non-thermal analyses are called *linear* properties because typical solutions with these properties require only a single iteration. Properties such as stress-strain data are called *nonlinear* because an analysis with these properties requires an iterative solution. Some elements require other special data which need to be input in tabular form.

C.1.6 Surface Loads

Various element types allow surface loads. Surface loads are typically pressures for structural element types, convections or heat fluxes for thermal element types, etc.

C.1.7 Body Loads

Various element types allow body loads. Body loads are typically temperatures for structural element types, heat generation rates for thermal element types, etc. Body loads are designated in the "Input Summary" table of each element by a label and a list of load values at various locations within the element.

C.1.8 Special Features

The keywords in the "Special Features" list indicate that certain additional capabilities are available for the element. Most often these features make the element nonlinear and require that an iterative solution be done. The special feature are : "Plasticity,"; "Creep,"; "Swelling,"; "Large Deflection,"; "Large Strain,"; "Stress Stiffening,"; "Adaptive Descent,"; "Error Estimation,"; "Birth and Death,"; "Hyperelasticity,"; and "Viscoelasticity."

C.1.9 KEYOPTs

KEYOPTs (or key options) are switches, used to turn various element options on or off. KEYOPT options include stiffness formulation choices, printout controls, element coordinate system choices, etc. A basic description of the KEYOPTs is given with each element type. KEYOPTs are identified by number, such as KEYOPT(1), KEYOPT(2), etc., with each numbered KEYOPT able to be set to a specific value.

Note-The defaults for element key options are chosen to be most convenient for the ANSYS product you are using, which means that some of the defaults may be different in some of the ANSYS products. These cases are clearly documented under the "Product Restrictions" section of the affected elements. If you plan to use your input file in more than one ANSYS product, you should explicitly input these settings, rather than letting them default; otherwise, behavior in the other ANSYS product may be different.

C.2. ELEMENT TYPE FOR MODELING ROCKMASS

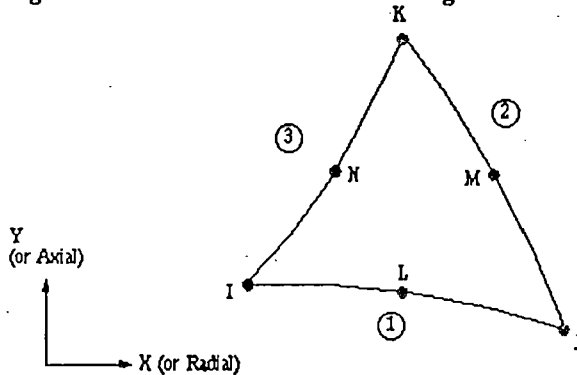
PLANE2 2-D 6-Node Triangular Structural Solid

| | |
|--------------|---|
| Multiphysics | ✓ |
| Mechanical | ✓ |
| Structural | ✓ |
| LS-DYNA | ✓ |
| LinearPlus | ✓ |
| Thermal | ✓ |
| Emag 3-D | |
| Emag 2-D | |
| FLOTRAN | |
| PrePost | ✓ |
| CD | ✓ |

PLANE2 is a 6-node triangular element compatible with the 8-node PLANE82 element. The element has a quadratic displacement behavior and is well suited to model irregular meshes (such as produced from various CAD/CAM systems).

The element is defined by six nodes having two degrees of freedom at each node: translations in the nodal x and y directions. You can use the element as a plane element (plane stress or plane strain) or as an axisymmetric element. The element also has plasticity, creep, swelling, stress stiffening, large deflection, and large strain capabilities. See Section 14.2 of the *ANSYS Theory Reference* for more details about this element.

Figure C.2-1 PLANE2 2-D 6-Node Triangular Structural Solid



The shape function for this element are:

$$u = u_I(2L_1 - 1)L_1 + u_J(2L_2 - 1)L_2 + u_K(2L_3 - 1)L_3 + u_L(4L_1L_2) + u_M(4L_2L_3) + u_N(4L_3L_1)$$

$$v = v_I(2L_1 - 1)L_1 + \dots \text{analogous to } u$$

$$w = w_I(2L_1 - 1)L_1 + \dots \text{analogous to } u$$

C.2.1 Input Data

Figure C.2-1 shows the geometry and node locations for this element.

Besides the nodes, the element input data includes a thickness (only if KEYOPT(3)=3) and the orthotropic material properties. Orthotropic material directions correspond to the element coordinate directions.

Section 2.7 describes element loads. Pressures may be input as surface loads on the element faces, shown by the circled numbers in Figure 4.2-1. Positive pressures act into the element. You can specify temperatures and fluences as element body loads at the nodes. The node I temperature T(I) defaults to TUNIF. If all other temperatures are unspecified, they default to T(I). If all corner node temperatures are specified, each midside node temperature defaults to the average temperature of its adjacent corner nodes. For any other input temperature pattern, unspecified temperatures default to TUNIF. Similar defaults occur for fluence except that zero is used instead of TUNIF.

Specify the nodal forces, if any, per unit of depth for a plane analysis (except for KEYOPT(3)=3) and on a full 360° basis for an axisymmetric analysis.

Table C.2-1 gives a summary of the element input.

Table C.2-1 PLANE2 Input Summary

| | |
|---------------------|---|
| Element Name | PLANE2 |
| Nodes | I, J, K, L, M, N |
| Degrees of Freedom | UX, UY |
| Real Constants | None, if KEYOPT (3) = 0, 1, 2 Thickness, if KEYOPT (3) = 3 |
| Material Properties | EX, EY, EZ, (PRXY, PRYZ, PRXZ or NUXY, NUYZ, NUXZ), ALPX, ALPY, ALPZ, DENS, GXY, DAMP |
| Surface Loads | Pressures: face 1 (I-J), face 2 (K-J), face 3 (I-K) |
| Body Loads | Temperatures: T (I), T (J), T (K), T (L), T (M), T (N) Fluences: FL (I), FL (J), FL (K), FL (L), FL (M), FL (N) |
| Special Features | Plasticity, Creep, Swelling, Stress stiffening, Large deflection, Large strain, Birth and death, Adaptive descent. |
| KEYOPT(3) | 0 - Plane stress 1 - Axisymmetric 2 - Plane strain (Z strain = 0.0) 3 - Plane stress with thickness input |
| KEYOPT(5) | 0 - Basic element printout 1 - Integration point stress printout 2 - Nodal stress printout |
| KEYOPT(6) | 0 - Basic element printout 3 - Nonlinear solution at each integration point also 4 - Surface printout for faces with nonzero pressure |

C.2.2 Output Data

The solution output associated with the element is in two forms:

- nodal displacements included in the overall nodal solution
- additional element output as shown in Table C.2-2

Figure C.2-2 illustrates several items.

The element stress directions are parallel to the element coordinate system. Surface stresses are available on any face having a nonzero pressure specification. Surface stresses are defined parallel and perpendicular to a face line (for example, line I-J) and along the Z axis for a plane analysis or in the hoop direction for an axisymmetric analysis.

Figure C.2-2 PLANE2 Stress Output

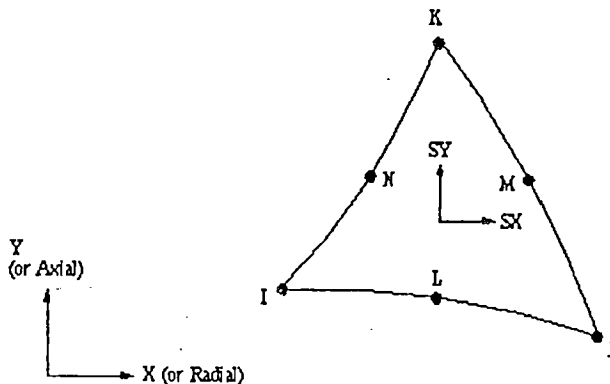


Table C.2-2 uses the following notation:

A colon (:) in the **Name** column indicates the item can be accessed by the Component Name method [**ETABLE**, **ESOL**]. The **O** and **R** columns indicate the availability of the items in the file *Jobname.OUT* (**O**) or in the results file (**R**), a **Y** indicates that the item is *always* available, a number refers to a table footnote which describes when the item is *conditionally* available, and a - indicates that the item is *not* available.

Table C.2-2 PLANE2 Element Output Definitions

| Name | Definition | O | R |
|-------------------|--|---|---|
| EL | Element number | Y | Y |
| NODES | Element corner nodes (I, J and K) | Y | Y |
| MAT | Material number for the element | Y | Y |
| THICK | Average thickness of the element | Y | Y |
| VOLU: | Element volume | Y | Y |
| CENT: X, Y | Global location of the element XC, YC | Y | Y |
| PRES | Pressures P1 at nodes J, I; P2 at K, J; P3 at I, L | Y | Y |
| TEMP | Temperatures - T(I), T(J), T(K), T(L), T(M), T(N) | Y | Y |
| FLUEN | Fluences - FL(I), FL(J), FL(K), FL(L), FL(M), FL(N) | Y | Y |
| S:INT | Stress intensity | Y | Y |
| S:EQV | Equivalent stress | Y | Y |
| EPEL: X, Y, Z, XY | Elastic strain | Y | Y |
| EPEL: 1, 2, 3 | Principal elastic strains | Y | Y |
| S: X, Y, Z, XY | Stresses (SZ=0.0 for plane stress elements) | Y | Y |
| S: 1, 2, 3 | Principal stresses | Y | Y |
| FACE | Face label | 1 | Y |
| EPEL(PAR, PER, Z) | Surface elastic strains (parallel, perpendicular, Z or hoop) | 1 | Y |
| TEMP | Surface average temperature | 1 | Y |
| S(PAR, PER, Z) | Surface stress (parallel, perpendicular, Z or hoop) | 1 | Y |
| SINT | Surface stress intensity | 1 | Y |
| SEQV | Surface equivalent stress | 1 | Y |
| EPPL: X, Y, Z, XY | Plastic strains | 2 | 2 |
| NL-EPEQ | Equivalent plastic strain | 2 | 2 |
| NL-SRAT | Ratio of trial stress to stress on yield surface | 2 | 2 |
| NL-SEPL | Equivalent stress on stress-strain curve | 2 | 2 |
| NL-HPRES | Hydrostatic pressure | - | 2 |
| EPCR: X, Y, Z, XY | Creep strains | 2 | 2 |
| EPSW: | Swelling strain | 2 | 2 |

1. Face printout if KEYOPT(6) = 4 and a nonzero pressure face.
2. Nonlinear solution, only if the element has a nonlinear material.

Table C.2-2a PLANE2 Miscellaneous Element Output

| Description | Names of Items Output | O | R |
|------------------------------------|---|---|---|
| Nonlinear Integration Pt. Solution | EPPL, EPEQ, SRAT, SEPL, HPRES, EPCR, EPSW | 1 | - |
| Integration Point Stress Solution | LOCATION, TEMP, SINT, SEQV, EPPL, S | 2 | - |
| Nodal Stress Solution | LOCATION, TEMP, S, SINT, SEQV | 3 | - |

1. Output at each integration point, if the element has a nonlinear material and KEYOPT(6)=3
2. Output at each integration point, if KEYOPT(5)=1
3. Output at each vertex node, if KEYOPT(5)=2

Table C.2-3 lists output available through the **ETABLE** command using the Sequence Number method. See [Chapter 5](#) of the *ANSYS Basic Analysis Procedures Guide* for more information. Table C.2-3 uses the following notation:

- Name - output quantity as defined in the Table C.2-2
- Item - predetermined *Item* label for **ETABLE** command
- E - sequence number for single-valued or constant element data
- I,J,...,N - sequence number for data at nodes I,J,...,N

Table C.2-3 PLANE2 Item and Sequence Numbers for the **ETABLE and **ESOL** Commands**

| Name | Item | E | I | J | K | L | M | N |
|------|-------|---|---|---|---|---|---|---|
| P1 | SMISC | - | 2 | 1 | - | - | - | - |
| P2 | SMISC | - | - | 4 | 3 | - | - | - |
| P3 | SMISC | - | 5 | - | 6 | - | - | - |

C.2.3 Assumptions and Restrictions

The area of the element must be positive. The element must lie in a global X-Y plane as shown in Figure C.2-1 and the Y-axis must be the axis of symmetry for axisymmetric analyses. An axisymmetric structure should be modeled in the +X quadrants. A face with a removed midside node implies that the displacement varies linearly, rather than parabolically, along that face. Surface stress printout is valid only if the conditions described in [Section 2.2.2](#) are met. See [Section 2.4.2](#) of the *ANSYS Modeling and Meshing Guide* for information on the use of elements with midside nodes.

C.2.4 Product Restrictions

When used in the product(s) listed below, the stated product-specific restrictions apply to this element in addition to the general assumptions and restrictions given in the previous section.

ANSYS/LinearPlus

- The DAMP material property is not allowed.
- Fluence body loads cannot be applied.
- The only special feature allowed is stress stiffening.
- KEYOPT(6)=3 does not apply.

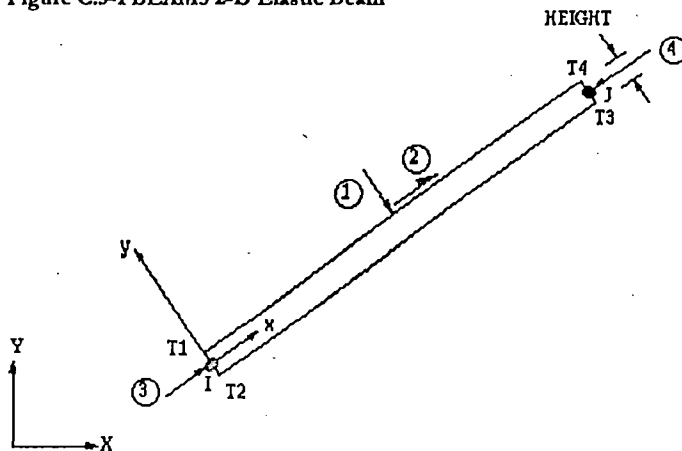
C.3 ELEMENT TYPE FOR MODELING SHOTCRETE

BEAM3 2-D Elastic Beam

| | |
|------------|---|
| Multibody | ✓ |
| Mechanical | ✓ |
| Structural | ✓ |
| LS-DYNA | ✓ |
| Linear | ✓ |
| Thermal | |
| Emag 3-D | |
| Emag 2-D | |
| FLTRAN | |
| PrePost | ✓ |
| ED | ✓ |

BEAM3 is a uniaxial element with tension, compression, and bending capabilities. The element has three degrees of freedom at each node: translations in the nodal x and y directions and rotation about the nodal z-axis. See Section 14.3 of the *ANSYS Theory Reference* for more details about this element. Other 2-D beam elements are the plastic beam (BEAM23) and the tapered unsymmetric beam (BEAM54).

Figure C.3-1 BEAM3 2-D Elastic Beam



C.3.1 Input Data

Figure C.3-1 shows the geometry, node locations, and the coordinate system for this element. The element is defined by two nodes, the cross-sectional area, the area moment of inertia, the height, and the material properties. The initial strain in the element (ISTRN) is given by δ/L , where δ is the difference between the element length, L (as defined by the I and J node locations), and the zero strain length. The initial strain is also used in calculating the stress stiffness matrix, if any, for the first cumulative iteration.

You can use the element in an axisymmetric analysis if hoop effects are negligible, such as for bolts, slotted cylinders, etc. The area and moment of inertia must be input on a full 360° basis for an axisymmetric analysis. The shear deflection constant (SHEARZ) is optional. You can use a zero value of SHEARZ to neglect shear deflection. The shear modulus (GXY) is used only with shear deflection. Properties you do not input default as described in Section 2.4. You can specify an added-mass-per-unit-length with the ADDMAS value.

Node and Element Loads. Section 2.7 describes element loads. You can specify pressures as surface loads on the element faces, shown by the circled numbers in Figure C.3-1. Positive normal pressures act into the element. You specify lateral pressures as a force per unit length. End "pressures" are input as a force. KEYOPT(10) allows tapered lateral pressures to be offset from the nodes. KEYOPT(9), used to request output at intermediate locations, is not valid if

- stress stiffening is turned on [SSTIF,ON]
- more than one component of angular velocity is applied [OMEGA]
- any angular velocities or accelerations are applied with the CGOMGA, DOMEGA, or DCGOMG commands.

Table C.3-1 summarizes the element input. Section 2.1 contains a general description of element input.

Table C.3-1 BEAM3 Input Summary

| | |
|---------------------|--|
| Element Name | BEAM3 |
| Nodes | I, J |
| Degrees of Freedom | UX, UY, ROTZ |
| Real Constants | AREA, IZZ, HEIGHT, SHEARZ, ISTRN, ADDMAS |
| Material Properties | EX, ALPX, DENS, GXY, DAMP |
| Surface Loads | Pressure: face 1 (I-J) (-Y normal direction), face 2 (I-J) (+X tangential direction), face 3 (I) (+X axial direction), face 4 (J) (-X axial direction) (use a negative value for loading in the opposite direction) |
| Body Loads | Temperatures: T1, T2, T3, T4 |
| Special Features | Stress stiffening, Large deflection, Birth and death |
| KEYOPT(6) | 0 - No printout of member forces and moments 1 - Print out member forces and moments in the element coordinate system |
| KEYOPT(9) | Used to control additional output between ends I and J N - Output at N intermediate locations (N = 0, 1, 3, 5, 7, 9) |
| KEYOPT(10) | Used only for tapered surface loads with the SFBEAM command. 0 - Offset for load placement is in terms of length units 1 - Offset is in terms of a length ratio (0.0 to 1.0) |

Note-SHEARZ goes with the IZZ. If SHEARZ=0, there is no shear deflection in the element Y direction.

C.3.2 Output Data

The solution output associated with the element is in two forms:

- nodal displacements included in the overall nodal solution
- additional element output as shown in Table C.3-2.

Figure C.3-2 illustrates several items. Section 2.2 gives a general description of solution output. See the *ANSYS Basic Analysis Procedure Guide* for ways to view results.

Figure C.3-2 BEAM3 Stress Output

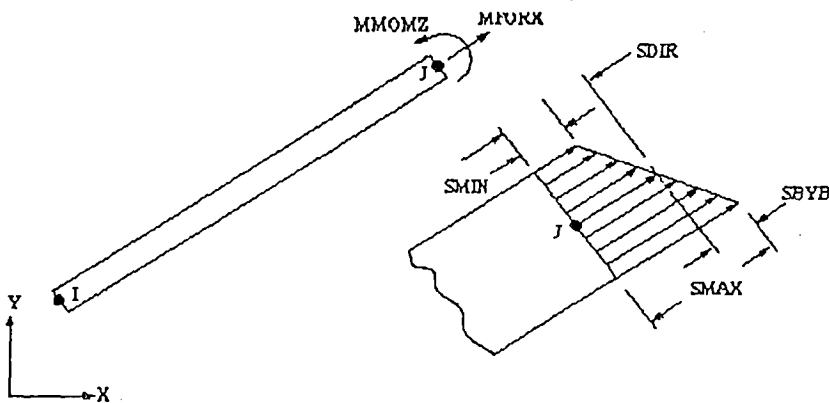


Table C.3-2 uses the following notation:

A colon (:) in the **Name** column indicates the item can be accessed by the Component Name method. The **O** and **R** columns indicate the availability of the items in the file *Jobname.OUT* (**O**) or in the results file (**R**), a **Y** indicates that the item is *always* available, a number refers to a table footnote which describes when the item is *conditionally* available, and a - indicates that the item is *not* available.

Table C.3-2 BEAM3 Element Output Definitions

| Name | Definition | O | R |
|------------|---|---|---|
| EL | Element number | Y | Y |
| NODES | Element nodes - I, J | Y | Y |
| MAT | Element material number | Y | Y |
| VOLU: | Element volume | N | Y |
| CENT: X,Y | Center location of the element XC, YC | N | Y |
| TEMP | Temperatures T1, T2, T3, T4 | Y | Y |
| PRES | Pressure P1 at nodes I,J; OFFST1 at I,J; P2 at I,J; OFFST2 at I,J; P3 at I; P4 at J | Y | Y |
| SDIR | Axial direct stress | 1 | 1 |
| SBYT | Bending stress on the element +Y side of the beam | 1 | 1 |
| SBYB | Bending stress on the element -Y side of the beam | 1 | 1 |
| SMAX | Maximum stress (direct stress + bending stress) | 1 | 1 |
| SMIN | Minimum stress (direct stress - bending stress) | 1 | 1 |
| EPELDIR | Axial elastic strain at the end | 1 | 1 |
| EPELBYT | Bending elastic strain on the element +Y side of the beam | 1 | 1 |
| EPELBYB | Bending elastic strain on the element -Y side of the beam | 1 | 1 |
| EPTHDIR | Axial thermal strain at the end | 1 | 1 |
| EPTHBYT | Bending thermal strain on the element +Y side of the beam | 1 | 1 |
| EPTHBYB | Bending thermal strain on the element -Y side of the beam | 1 | 1 |
| EPINAXL | Initial axial strain in the element | 1 | 1 |
| MFOR(X, Y) | Member forces in the element coordinate system X and Y direction | 2 | Y |
| MMOMZ | Member moment in the element coordinate system Z direction | 2 | Y |

1. The item repeats for end 1, intermediate locations (see KEYOPT(9)), and end J.
2. If KEYOPT(6)=1.

The following tables list output available through the **ETABLE** command using the Sequence Number method. Tables C.3-3 through C.3-3e all use the following notation:

- Name - output quantity as defined in the Table C.3-2
- Item - predetermined *Item* label for **ETABLE** command
- E - sequence number for single-valued or constant element data
- I, J - sequence number for data at nodes I and J
- IL*n* - sequence number for data at Intermediate Location *n*

Table C.3-3 BEAM3 (KEYOPT(9)=0) Item and Sequence Numbers for the **ETABLE and **ESOL** Commands**

| KEYOPT(9)=0 | | | | |
|-------------|-------|---|---|---|
| Name | Item | E | I | J |
| SDIR | LS | - | 1 | 4 |
| SBYT | LS | - | 2 | 5 |
| SBYB | LS | - | 3 | 6 |
| EPELDIR | LEPEL | - | 1 | 4 |
| EPELBYT | LEPEL | - | 2 | 5 |
| EPELBYB | LEPEL | - | 3 | 6 |
| EPTHDIR | LEPTH | - | 1 | 4 |
| EPTHBYT | LEPTH | - | 2 | 5 |
| EPTHBYB | LEPTH | - | 3 | 6 |
| EPINAXL | LEPTH | 7 | - | - |
| SMAX | NMISC | - | 1 | 3 |
| SMIN | NMISC | - | 2 | 4 |

| | | | | | |
|--------|-------|-------------|----|----|---|
| MFORX | SMISC | - | 1 | 7 | |
| MFORY | SMISC | - | 2 | 8 | |
| MMOMZ | SMISC | - | 6 | 12 | |
| P1 | SMISC | - | 13 | 14 | |
| OFFST1 | SMISC | - | 15 | 16 | |
| P2 | SMISC | - | 17 | 18 | |
| OFFST2 | SMISC | - | 19 | 20 | |
| P3 | SMISC | - | 21 | - | |
| P4 | SMISC | - | - | 22 | |
| | | Pseudo Node | | | |
| | | 1 | 2 | 3 | 4 |
| TEMP | LBFE | 1 | 2 | 3 | 4 |

Table C.3-3a BEAM3 (KEYOPT(9)=1) Item and Sequence Numbers for the ETABLE and ESOL Commands

| KEYOPT(9) = 1 | | | | | | |
|---------------|-------|-------------|----|-----|----|--|
| Name | Item | E | I | IL1 | J | |
| SDIR | LS | - | 1 | 4 | 7 | |
| SBYT | LS | - | 2 | 5 | 8 | |
| SBYB | LS | - | 3 | 6 | 9 | |
| EPELDIR | LEPEL | - | 1 | 4 | 7 | |
| EPELBYT | LEPEL | - | 2 | 5 | 8 | |
| EPELBYB | LEPEL | - | 3 | 6 | 9 | |
| EPTHDIR | LEPTH | - | 1 | 4 | 7 | |
| EPTHBYT | LEPTH | - | 2 | 5 | 8 | |
| EPTHBYB | LEPTH | - | 3 | 6 | 9 | |
| EPINAXL | LEPTH | 10 | - | - | - | |
| SMAX | NMISC | - | 1 | 3 | 5 | |
| SMIN | NMISC | - | 2 | 4 | 6 | |
| MFORX | SMISC | - | 1 | 7 | 13 | |
| MFORY | SMISC | - | 2 | 8 | 14 | |
| MMOMZ | SMISC | - | 6 | 12 | 18 | |
| P1 | SMISC | - | 19 | - | 20 | |
| OFFST1 | SMISC | - | 21 | - | 22 | |
| P2 | SMISC | - | 23 | - | 24 | |
| OFFST2 | SMISC | - | 25 | - | 26 | |
| P3 | SMISC | - | 27 | - | - | |
| P4 | SMISC | - | - | - | 28 | |
| | | Pseudo Node | | | | |
| | | 1 | 2 | 3 | 4 | |
| TEMP | LBFE | 1 | 2 | 3 | 4 | |

Table C.3-3b BEAM3 (KEYOPT(9)=3) Item and Sequence Numbers for the ETABLE and ESOL Commands

| KEYOPT(9) = 3 | | | | | | | |
|---------------|------|---|---|-----|-----|-----|----|
| Name | Item | E | I | IL1 | IL2 | IL3 | J |
| SDIR | LS | - | 1 | 4 | 7 | 10 | 13 |
| SBYT | LS | - | 2 | 5 | 8 | 11 | 14 |

| | | | | | | | | |
|---------|-------|----|----|----|----|----|----|----|
| SBYB | LS | - | 3 | 6 | 9 | 12 | 15 | |
| EPELDIR | LEPEL | - | 1 | 4 | 7 | 10 | 13 | |
| EPELBYT | LEPEL | - | 2 | 5 | 8 | 11 | 14 | |
| EPELBYB | LEPEL | - | 3 | 6 | 9 | 12 | 15 | |
| EPTHDIR | LEPTH | - | 1 | 4 | 7 | 10 | 13 | |
| EPTHBYT | LEPTH | - | 2 | 5 | 8 | 11 | 14 | |
| EPTHBYB | LEPTH | - | 3 | 6 | 9 | 12 | 15 | |
| EPINAXL | LEPTH | 16 | - | - | - | - | - | |
| SMAX | NMISC | - | 1 | 3 | 5 | 7 | 9 | |
| SMIN | NMISC | - | 2 | 4 | 6 | 8 | 10 | |
| MFORX | SMISC | - | 1 | 7 | 13 | 19 | 25 | |
| MFORY | SMISC | - | 2 | 8 | 14 | 20 | 26 | |
| MMOMZ | SMISC | - | 6 | 12 | 18 | 24 | 30 | |
| P1 | SMISC | - | 31 | - | - | - | - | 32 |
| OFFST1 | SMISC | - | 33 | - | - | - | - | 34 |
| P2 | SMISC | - | 35 | - | - | - | - | 36 |
| OFFST2 | SMISC | - | 37 | - | - | - | - | 38 |
| P3 | SMISC | - | 39 | - | - | - | - | - |
| P4 | SMISC | - | - | - | - | - | - | 40 |

| | | | | | |
|------|------|-------------|---|---|---|
| | | Pseudo Node | | | |
| | | 1 | 2 | 3 | 4 |
| TEMP | LBFE | 1 | 2 | 3 | 4 |

Table C.3-3c BEAM3 (KEYOPT(9)=5) Item and Sequence Numbers for the **ETABLE** and **ESOL** Commands

| KEYOPT(9) = 5 | | | | | | | | | |
|---------------|-------|----|----|-----|-----|-----|-----|-----|----|
| Name | Item | E | I | IL1 | IL2 | IL3 | IL4 | IL5 | J |
| SDIR | LS | - | 1 | 4 | 7 | 10 | 13 | 16 | 19 |
| SBYT | LS | - | 2 | 5 | 8 | 11 | 14 | 17 | 20 |
| SBYB | LS | - | 3 | 6 | 9 | 12 | 15 | 18 | 21 |
| EPELDIR | LEPEL | - | 1 | 4 | 7 | 10 | 13 | 16 | 19 |
| EPELBYT | LEPEL | - | 2 | 5 | 8 | 11 | 14 | 17 | 20 |
| EPELBYB | LEPEL | - | 3 | 6 | 9 | 12 | 15 | 18 | 21 |
| EPTHDIR | LEPTH | - | 1 | 4 | 7 | 10 | 13 | 16 | 19 |
| EPTHBYT | LEPTH | - | 2 | 5 | 8 | 11 | 14 | 17 | 20 |
| EPTHBYB | LEPTH | - | 3 | 6 | 9 | 12 | 15 | 18 | 21 |
| EPINAXL | LEPTH | 22 | - | - | - | - | - | - | - |
| SMAX | NMISC | - | 1 | 3 | 5 | 7 | 9 | 11 | 13 |
| SMIN | NMISC | - | 2 | 4 | 6 | 8 | 10 | 12 | 14 |
| MFORX | SMISC | - | 1 | 7 | 13 | 19 | 25 | 31 | 37 |
| MFORY | SMISC | - | 2 | 8 | 14 | 20 | 26 | 32 | 38 |
| MMOMZ | SMISC | - | 6 | 12 | 18 | 24 | 30 | 36 | 42 |
| P1 | SMISC | - | 43 | - | - | - | - | - | 44 |
| OFFST1 | SMISC | - | 45 | - | - | - | - | - | 46 |
| P2 | SMISC | - | 47 | - | - | - | - | - | 48 |
| OFFST2 | SMISC | - | 49 | - | - | - | - | - | 50 |
| P3 | SMISC | - | 51 | - | - | - | - | - | - |

| | | | | | | | | | | |
|----|-------|---|---|---|---|---|---|---|---|----|
| P4 | SMISC | - | - | - | - | - | - | - | - | 52 |
|----|-------|---|---|---|---|---|---|---|---|----|

| | | | | | |
|------|------|-------------|---|---|---|
| | | Pseudo Node | | | |
| | | 1 | 2 | 3 | 4 |
| TEMP | LBFE | 1 | 2 | 3 | 4 |

Table C.3-3d BEAM3 (KEYOPT(9)=7) Item and Sequence Numbers for the ETABLE and ESQL Commands

| KEYOPT(9) = 7 | | | | | | | | | | | |
|---------------|-------|----|----|-----|-----|-----|-----|-----|-----|-----|----|
| Name | Item | E | I | IL1 | IL2 | IL3 | IL4 | IL5 | IL6 | IL7 | J |
| SDIR | LS | - | 1 | 4 | 7 | 10 | 13 | 16 | 19 | 22 | 25 |
| SBYT | LS | - | 2 | 5 | 8 | 11 | 14 | 17 | 20 | 23 | 26 |
| SBYB | LS | - | 3 | 6 | 9 | 12 | 15 | 18 | 21 | 24 | 27 |
| EPELDIR | LEPEL | - | 1 | 4 | 7 | 10 | 13 | 16 | 19 | 22 | 25 |
| EPELBYT | LEPEL | - | 2 | 5 | 8 | 11 | 14 | 17 | 20 | 23 | 26 |
| EPELBYB | LEPEL | - | 3 | 6 | 9 | 12 | 15 | 18 | 21 | 24 | 27 |
| EPTHDIR | LEPTH | - | 1 | 4 | 7 | 10 | 13 | 16 | 19 | 22 | 25 |
| EPTHBYT | LEPTH | - | 2 | 5 | 8 | 11 | 14 | 17 | 20 | 23 | 26 |
| EPTHBYB | LEPTH | - | 3 | 6 | 9 | 12 | 15 | 18 | 21 | 24 | 27 |
| EPINAXL | LEPTH | 28 | - | - | - | - | - | - | - | - | - |
| SMAX | NMISC | - | 1 | 3 | 5 | 7 | 9 | 11 | 13 | 15 | 17 |
| SMIN | NMISC | - | 2 | 4 | 6 | 8 | 10 | 12 | 14 | 16 | 18 |
| MFORX | SMISC | - | 1 | 7 | 13 | 19 | 25 | 31 | 37 | 43 | 49 |
| MFORY | SMISC | - | 2 | 8 | 14 | 20 | 26 | 32 | 38 | 44 | 50 |
| MMOMZ | SMISC | - | 6 | 12 | 18 | 24 | 30 | 36 | 42 | 48 | 54 |
| P1 | SMISC | - | 55 | - | - | - | - | - | - | - | 56 |
| OFFST1 | SMISC | - | 57 | - | - | - | - | - | - | - | 58 |
| P2 | SMISC | - | 59 | - | - | - | - | - | - | - | 60 |
| OFFST2 | SMISC | - | 61 | - | - | - | - | - | - | - | 62 |
| P3 | SMISC | - | 63 | - | - | - | - | - | - | - | - |
| P4 | SMISC | - | - | - | - | - | - | - | - | - | 64 |

| | | | | | |
|------|------|-------------|---|---|---|
| | | Pseudo Node | | | |
| | | 1 | 2 | 3 | 4 |
| TEMP | LBFE | 1 | 2 | 3 | 4 |

Table C.3-3e BEAM3 (KEYOPT(9)=9) Item and Sequence Numbers for the ETABLE and ESQL Commands

| KEYOPT(9) = 9 | | | | | | | | | | | | | |
|---------------|-------|----|---|-----|-----|-----|-----|-----|-----|-----|-----|-----|----|
| Name | Item | E | I | IL1 | IL2 | IL3 | IL4 | IL5 | IL6 | IL7 | IL8 | IL9 | J |
| SDIR | LS | - | 1 | 4 | 7 | 10 | 13 | 16 | 19 | 22 | 25 | 28 | 31 |
| SBYT | LS | - | 2 | 5 | 8 | 11 | 14 | 17 | 20 | 23 | 26 | 29 | 32 |
| SBYB | LS | - | 3 | 6 | 9 | 12 | 15 | 18 | 21 | 24 | 27 | 30 | 33 |
| EPELDIR | LEPEL | - | 1 | 4 | 7 | 10 | 13 | 16 | 19 | 22 | 25 | 28 | 31 |
| EPELBYT | LEPEL | - | 2 | 5 | 8 | 11 | 14 | 17 | 20 | 23 | 26 | 29 | 32 |
| EPELBYB | LEPEL | - | 3 | 6 | 9 | 12 | 15 | 18 | 21 | 24 | 27 | 30 | 33 |
| EPTHDIR | LEPTH | - | 1 | 4 | 7 | 10 | 13 | 16 | 19 | 22 | 25 | 28 | 31 |
| EPTHBYT | LEPTH | - | 2 | 5 | 8 | 11 | 14 | 17 | 20 | 23 | 26 | 29 | 32 |
| EPTHBYB | LEPTH | - | 3 | 6 | 9 | 12 | 15 | 18 | 21 | 24 | 27 | 30 | 33 |
| EPINAXL | LEPTH | 34 | - | - | - | - | - | - | - | - | - | - | - |

| | | | | | | | | | | | | | |
|--------|-------|---|----|----|----|----|----|----|----|----|----|----|----|
| SMAX | NMISC | - | 1 | 3 | 5 | 7 | 9 | 11 | 13 | 15 | 17 | 19 | 21 |
| SMIN | NMISC | - | 2 | 4 | 6 | 8 | 10 | 12 | 14 | 16 | 18 | 20 | 22 |
| MFORX | SMISC | - | 1 | 7 | 13 | 19 | 25 | 31 | 37 | 43 | 49 | 55 | 61 |
| MFORY | SMISC | - | 2 | 8 | 14 | 20 | 26 | 32 | 38 | 44 | 50 | 56 | 62 |
| MMOMZ | SMISC | - | 6 | 12 | 18 | 24 | 30 | 36 | 42 | 48 | 54 | 60 | 66 |
| P1 | SMISC | - | 67 | - | - | - | - | - | - | - | - | - | 68 |
| OFFST1 | SMISC | - | 69 | - | - | - | - | - | - | - | - | - | 70 |
| P2 | SMISC | - | 71 | - | - | - | - | - | - | - | - | - | 72 |
| OFFST2 | SMISC | - | 73 | - | - | - | - | - | - | - | - | - | 74 |
| P3 | SMISC | - | 75 | - | - | - | - | - | - | - | - | - | - |
| P4 | SMISC | - | - | - | - | - | - | - | - | - | - | - | 76 |

| | | | | | |
|------|------|-------------|---|---|---|
| | | Pseudo Node | | | |
| | | 1 | 2 | 3 | 4 |
| TEMP | LBFE | 1 | 2 | 3 | 4 |

C.3.3 Assumptions and Restrictions

The beam element can have any cross-sectional shape for which the moment of inertia can be computed. However, the stresses are determined as if the distance from the neutral axis to the extreme fiber is one-half of the height. The element height is used only in the bending and thermal stress calculations. The applied thermal gradient is assumed linear across the height and along the length. The beam element must lie in an X-Y plane and must not have a zero length or area. The moment of inertia may be zero if large deflections are not used.

C.3.4 Product Restrictions

When used in the product(s) listed below, the stated product-specific restrictions apply to this element in addition to the general assumptions and restrictions given in the previous section.

ANSYS/LinearPlus

- The DAMP material property is not allowed.
- The only special features allowed are stress stiffening and large deflections.

References:

I. Books

1. Brady, BHG, Brown, ET.(1993), "*Rock Mechanics for underground mining, (2nd Ed)*", Chapman & Hall.
2. Brown, ET (Ed) (1987)"*Analytical and Computational methods in Engineering Rock Mechanics*", Allen & Unwin.
3. Chen. WF, Baladi GY (1985) '*Soil Plasticity, theory and Implementation*', Elsevier
4. Hoek, Evert (2000),"*Practical Rock Engineering*", www.rocscience.com
5. Jaeger, Charles (1979),"*Rock Mechanics and Engineering*", Cambridge University Press
6. LAPI ITB (1995),"*Stability analysis of Underground powerhouse Cirata*", unpublished
7. Obert & Duvall (1967),"*Rock Mechanics and The Design of Structures*", John Wiley & Sons
8. Potts, D, (Ed.) (2002),"*Guidelines for the use of advanced numerical analysis*", Thomas Telford
9. Romana, (Ed) (1988),"*Rock Mechanics and Power Plant*", Proceeding of ISRM Symposium, Vol. I, A.A.Balkema
10. Sinha, RS (1989),"*Underground Structures, Design and Instrumentation*", Elsevier
11. TNO Building & Construction Research (2002),"*Diana-8.1 user manual-material library*", www.dianasoftware.com

II. Papers/Dissertations/Theses

1. B. DasGupta et al (1995),"*Numerical Analysis of Large Underground Cavern for Hydropower*, in Conference on Design and Construction of Underground Structures, pg 251-260 ISRMTT
2. Bouvard A. (1986),"*FEM analysis for Underground powerhouse at Maung Indonesia*", in Large Rock Cavern symposium, Finland, A.A. Balkema
3. Dhawan, KR, et.al. (2002),"*2D and 3D finite element analysis of underground opening in an inhomogeneous rock mass*, in Int. J. of Rock Mech & Min. Sci. 39 (2002) pg 217-227, www.elsevier.com
4. G. Reik et. Al (1986),"*Influence of Geological Condition on Design and Construction of Cirata Powerhouse Cavern*, in Large Rock Cavern symposium, Finlandia", A.A. Balkema
5. Jing, L (2003),"*A review of Techniques, advances and outstanding issues in numerical modeling for rock mechanics and rock engineering, a journal review article*", in In. J. of Rock Mech & Min. Sci 40 (2003) pg 283-353, www.elsevier.com
6. Kamemura, K et al (1986),"*Observational methods for design and construction of Underground Powerhouse*", in Large Rock Cavern Symposium Finland, A.A. Balkema
7. Kalkani, E.C. (1988), '*Finite-element stress analysis in underground powerhouse-cavern and support measures design*' in Proceeding of ISRM symposium on Rock Mechanics and Power Plants, Madrid page 187-194 A.A. Balkema
8. Kovari, K, et. al. (1976),"*Parametric studies as a design aid in tunneling*, in Numerical Methods in Geomechanics Vol II pg 773-790, ASCE.
9. Liu et al (1988),"*Design of Mingtan power cavern*, in Proceeding of ISRM symposium on Rock Mechanics and Power Plants, Madrid pg. 199 -208 A.A.Balkema
10. NK Samadhiya (1998),"*Influence of Anisotropy and Shear Zones on Stability of Cavern*", PhD thesis, University of Roorkee
11. RS Arya et al (1995),"*Finite Element Analysis of Underground twin-cavities-a study*", in Conference on Design and Construction of Underground Structures, pg 251-260 ISRMTT